



HAL
open science

Role of the phosphatases over the erythrocytic cycle of the malaria parasite *Plasmodium falciparum*

Alexandra Victoria Miliu

► **To cite this version:**

Alexandra Victoria Miliu. Role of the phosphatases over the erythrocytic cycle of the malaria parasite *Plasmodium falciparum*. Human health and pathology. Université Montpellier, 2018. English. NNT : 2018MONTT029 . tel-01947777

HAL Id: tel-01947777

<https://theses.hal.science/tel-01947777>

Submitted on 7 Dec 2018

HAL is a multi-disciplinary open access archive for the deposit and dissemination of scientific research documents, whether they are published or not. The documents may come from teaching and research institutions in France or abroad, or from public or private research centers.

L'archive ouverte pluridisciplinaire **HAL**, est destinée au dépôt et à la diffusion de documents scientifiques de niveau recherche, publiés ou non, émanant des établissements d'enseignement et de recherche français ou étrangers, des laboratoires publics ou privés.



THÈSE

Pour obtenir le grade de
Docteur

Délivré par L'UNIVERSITÉ DE MONTPELLIER

Préparée au sein de l'école doctorale Sciences
Chimiques et Biologiques pour la Santé (CBS2)

Et de l'unité de recherche UMR 5235 CNRS
Dynamique des Interactions Membranaires Normales
et Pathologiques (DIMNP)

Spécialité : **Parasitologie**

Présentée par **Alexandra Victoria MILIU**

**Role of the phosphatases over the
erythrocytic cycle of the malaria
parasite *Plasmodium falciparum***

Soutenue le 29 Novembre 2018 devant le jury composé de

M. Jamal KHALIFE, DR CNRS, Institut Pasteur, Lille

Rapporteur

M. Hans-Peter BECK, Professor, Swiss TPH, Basel

Rapporteur

Mme Marie-France CESBRON-DELAUW, DR CNRS,
Université Grenoble 1

Examinatrice

Mme Mauld LAMARQUE, MC, Université de Montpellier

Directrice de thèse

Mme Catherine BRAUN-BRETON, Professor, Université de
Montpellier

Co-directrice de thèse



Table of contents

Abbreviations.....	9
INTRODUCTION	
Chapter 1: Malaria and the <i>P. falciparum</i> life cycle	15
1.1 Apicomplexa - phylogeny and ultrastructure	15
1.2 Malaria.....	16
1.2.1 Malaria epidemiology and human <i>Plasmodium</i> species	16
1.2.2 Malaria control strategies	18
1.3 <i>P. falciparum</i> life cycle	20
1.3.1 Mosquito stages	20
1.3.2 Liver stages	21
1.3.3 Intraerythrocytic development	21
1.4 Insight into 3 key events of <i>P. falciparum</i> RBC cycle.....	22
1.4.1 Invasion	22
1.4.2 Cell cycle and schizogony	27
1.4.3 Exit from the host cell: egress	32
Chapter 2: Phosphorylation in <i>Plasmodium</i>.....	36
2.1 General aspects of protein phosphorylation	36
2.1.1 Generalities	36
2.1.2 <i>Pf</i> kinome.....	36
2.2 Phosphoproteomic studies: phosphorylation is a widespread post-translational modification during <i>P. falciparum</i> intraerythrocytic growth.....	38
2.3 Phosphorylation as an important regulator of <i>P. falciparum</i> RBC cycle	41
2.3.1 Phospho-signaling and secretory organelle discharge	42
2.3.1.1 Phospho-signaling leading to egress: PKG and CDPK5	43
2.3.1.2 Phospho-signaling leading to invasion: PKA and CDPK1	45
2.3.2 Phosphorylation of adhesins and invasion.....	47
2.3.3. Phosphorylation of the glideosome machinery	49
2.3.4 Phosphorylation as a regulator of <i>P. falciparum</i> cell cycle	50
2.4 Phosphorylation in the host RBC during <i>P. falciparum</i> development.....	55
Chapter 3: Plasmodium phosphatases.....	61
3.1 Phosphatase groups/ classification.....	61
3.1.1 Serine/Threonine phosphatases.....	61
3.1.1.1 PPP superfamily: mechanism and inhibitors	62
3.1.1.2. PPM family.....	66
3.1.1.5 FCP/ SCP family.....	68
3.1.2 Phospho-tyrosine phosphatases	70

3.2 Regulation of phosphatases	72
3.2.1. PPP regulation	72
3.2.2. PPM regulation.....	74
3.2.3. PTP regulation	75
3.3 Phosphatases in Plasmodium	76
3.3.1 The Plasmodium phosphatome – <i>In silico</i> studies	76
3.3.2 PPs which function in the mosquito stages.....	80
3.3.3 PPs important for liver stage development.....	81
3.3.4 PPs important in the parasite erythrocytic cycle.....	83
4. Objectives of this thesis	87
<u>RESULTS</u>	
Chapter 1: Functional characterization of the phosphatase Shelph2.....	93
1.1 Introduction.....	93
1.2 Shelph2, a bacterial-like phosphatase of the malaria parasite <i>Plasmodium falciparum</i> , is dispensable during asexual blood stage.....	93
1.3 Conclusion and perspectives	109
Chapter 2: GlmS ribozyme strategy and characterization of PP4 and PP7	110
2.1 Introduction.....	110
2.2 Setting up the <i>glmS</i> ribozyme system for getting inducible PP knockdown parasites	112
2.3 Subcellular localization of PP4 and PP7.....	115
2.4 Generating inducible knockout (iKO) of PP7	116
2.5 Conclusion and perspectives	118
Chapter 3: Characterization of PfPP1 phosphatase	119
3.1 Introduction and Strategy	119
3.2 Article: PP1 has essential functions in <i>P. falciparum</i> erythrocytic schizogony and egress	120
Introduction.....	120
Results	122
Discussion	128
Experimental procedures	130
Supplementary Data.....	133
3.3 Conclusions and perspectives	134
MATERIAL & METHODS	137
<u>DISCUSSION</u>	<u>148</u>
References	153

Summary

Plasmodium falciparum, the etiologic agent of malaria, is an obligate intracellular parasite of the Apicomplexa phylum that is responsible for 445000 deaths annually. *Plasmodium* development in human red blood cells (RBCs) corresponds to the symptomatic phase of the disease. It starts by the active penetration of the host cell by the invasive form named merozoite, followed by the parasite multiplication in a process called schizogony to form 16-32 new merozoites that are released from the RBC (egress step) and start a new cycle. During its 48h intra-erythrocytic development, this parasite uses reversible protein phosphorylation to regulate invasion, schizogony as well as egress, but our current knowledge on the contribution of parasite phosphatases in these cellular events is still very poor.

The objective of my thesis was to identify and functionally characterize phosphatases potentially involved in egress or invasion during *P. falciparum* RBC cycle. I focused my work on 4 of them, namely PP1, PP4, PP7 and Shelph2, on the basis of their late transcriptional expression profile during the intra-erythrocytic cycle, as this profile matches the timing of these two essential events. The first part of this study is dedicated to the functional characterization of Shelph2, a phosphatase of bacterial origin. By reverse genetics using CRISPR-Cas9 strategy, we endogenously tagged the gene, and showed that Shelph2 is stored in apical vesicles in the developing merozoites. We also demonstrated that it is dispensable for parasite RBC development, as the deletion of the gene did not affect invasion, parasite multiplication nor egress, suggesting possible functional redundancy with other parasite phosphatases.

In the second part of this work, we aimed to describe the roles of PP1, PP4 and PP7. As they were described as likely essential, we set up in the laboratory a conditional knock-down strategy named the glmS ribozyme, with the idea of destabilizing the mRNA following self-cleavage of the ribozyme upon metabolite addition, here glucosamine. We successfully introduced the *glmS* sequence in 3' of the genes of interest for PP4 and PP7 but we did not observe any significant protein depletion upon glucosamine addition, thus preventing us to use these lines to study PP4 and PP7 functions. Yet, these engineered parasite lines were used to analyze the subcellular localization of these phosphatases. As an alternative to the ribozyme, we used an inducible knock-out (iKO) approach based on a dimerizable Cre recombinase (DiCre system) that excises DNA fragments located between two *loxP* sites. We established two parasite lines, the iKO-PP7 that has not been further characterized and the iKO-PP1 strain. Using the iKO-PP1 parasites, we showed that PP1 is predominantly a cytosolic phosphatase mostly expressed during schizogony. Furthermore, the inducible excision of PP1 gene at two different time points of *P. falciparum* RBC cycle permitted us to reveal that PP1 plays two essential roles, one during schizogony and the other one at the time of parasite egress. This is to our knowledge the first description of a parasite phosphatase required for these developmental steps.

Key words: Malaria, *Plasmodium falciparum*, phosphatases, egress, schizogony

Résumé

Plasmodium falciparum, l'agent étiologique du paludisme, est un parasite intracellulaire obligatoire du phylum des Apicomplexa, responsable de 445 000 décès par an. Le développement de *Plasmodium* dans les globules rouges (GRs) humains correspond à la phase symptomatique de la maladie. Il commence par la pénétration active de la cellule hôte par la forme invasive nommée mérozoïte, suivie par la multiplication du parasite dans un processus appelé schizogonie pour former 16 à 32 nouveaux mérozoïtes qui sont alors libérés des GRs (étape de sortie) et peuvent alors initier un nouveau cycle. Au cours de son développement intra-érythrocytaire de 48h, ce parasite utilise la phosphorylation réversible de protéines pour réguler les étapes d'invasion, de schizogonie et de sortie du GR, mais nos connaissances actuelles sur la contribution des phosphatases parasitaires dans ces mécanismes demeurent très incomplètes.

L'objectif de ma thèse était d'identifier et de caractériser des phosphatases potentiellement impliquées dans la sortie ou l'invasion des GRs par *P. falciparum*. J'ai centré mon travail sur 4 d'entre elles, à savoir PP1, PP4, PP7 et Shelph2, sur la base de leur profil d'expression transcriptionnelle tardive au cours du cycle intra-érythrocytaire, qui correspond à ces deux événements cellulaires. La première partie de cette étude est consacrée à la caractérisation fonctionnelle de Shelph2, une phosphatase d'origine bactérienne. Par génétique inverse utilisant la stratégie CRISPR-Cas9, nous avons étiqueté le gène au locus endogène et montré que Shelph2 est stockée dans des vésicules apicales des mérozoïtes en formation. Nous avons également démontré que cette phosphatase n'est pas essentielle pour le développement intra-érythrocytaire du parasite dans les GRs car la délétion du gène n'affecte pas les étapes d'invasion, de multiplication des parasites ou de leur sortie des GRs, ce qui suggère la possibilité d'une redondance fonctionnelle avec d'autres phosphatases parasitaires.

Dans la deuxième partie de ce travail, nous avons cherché à décrire les rôles de PP1, PP4 et PP7. Les gènes codant pour ces enzymes étant décrits comme probablement essentiels, nous avons mis en place au laboratoire une stratégie de knock-down conditionnel (ribozyme *glmS*), avec l'idée de déstabiliser l'ARNm après auto-clivage du ribozyme lors de l'addition d'un métabolite, ici la glucosamine. Nous avons introduit avec succès la séquence *glmS* en 3' des gènes d'intérêt pour *PP4* et *PP7*, mais nous n'avons pas observé de déplétion protéique significative lors de l'addition de glucosamine, empêchant d'utiliser ces lignées pour étudier les fonctions de *PP4* et *PP7*. Cependant, ces lignées parasitaires modifiées ont été utilisées pour analyser la localisation subcellulaire de ces phosphatases. Comme alternative au ribozyme, nous avons utilisé une approche de knock-out inductible (iKO) basée sur une recombinase Cre dimérisable (système DiCre) qui excise des fragments d'ADN situés entre deux sites *loxP*. Nous avons établi deux lignées de parasites, iKO-*PP7* qui n'a pas encore été caractérisée et la souche iKO-*PP1*. En utilisant les parasites iKO-*PP1*, nous avons montré que *PP1* était principalement une phosphatase cytosolique majoritairement exprimée au stade schizontes. De plus, l'excision inductible du gène *PP1* à deux moments différents du cycle érythrocytaire de *P. falciparum* nous a permis de révéler que *PP1* joue deux rôles essentiels, l'un pendant la schizogonie et l'autre au moment de la sortie du parasite. A notre connaissance, ce travail représente la première description d'une phosphatase parasitaire requise pour ces étapes du développement asexué de *P. falciparum*.

Mots clés : Paludisme, *Plasmodium falciparum*, phosphatases, egress, schizogonie

Remerciements

Parasites are a very heterogenous group of beasts. They come in different sizes, and different lifestyles, “with the king of Spain being a remarkably big and very parasitic specimen” (JABB). That is why throughout my thesis I had problems explaining my friends and whoever was interested, what the hell parasitology is. I believe my educating efforts came to no end, as after 3 years of talking about my parasites, and even showing them in the microscope, the above cited person still was convinced about the existence of the “Malaria virus”. Not to talk about that Ivorian friend who assured me that Abidjan is Malaria-free, because the fevers he experienced were just – fevers, what else.

For this thesis, first and foremost, I must thank Mauld Lamarque for her goodwill, her support, her guidance and for her fairness during these three years. Thanks you for all that time you have taken and your infinite positive energy, for your dynamics in changing approaches from today to tomorrow, for introducing me into the marvelous world of Plasmodium, for explaining, for letting me develop ideas and approaches. You were always present and helping, even during your baby break, you were guiding and criticizing the necessary amount but at the same time left me the necessary freedom. I doubt a better and more understanding PhD supervisor exists, also on the personal level.

Thanks to Catherine Braun-Breton for co-directing and wisely guiding this thesis, and for her kindness. Thanks to Maryse Lebrun for doing my PhD in her team, for her scientific feedback, her consideration and support. Thanks to Georges Lutfalla for cordially receiving and accompanying me in the DIMNP.

Many thanks to the Jury members Jamal Khalife, Hans-Peter Beck and Marie-France Cesbron-Delauw for making themselves available, for taking their time reading this manuscript and for going on a train journey to my defense in Montpellier.

I thank epigenmed for their funding that made this thesis possible, as well as the scientific exchange they provided in the famous epigenmed days.

I want to thank all the DIMNP, and especially to team 1 for their scientific stimulation, for their kindness and support, I would have spent a less great time without all of you. To Caty the Mistress of Plasmodium techniques who always has an open ear and a helping hand, in any respect, Mother Theresa who performs miracles to integrate just everybody in the lab. To our “mum” Diana, who was there buzzing around in her projects, her PhD babies Marga and Justine, her real babies, but always with humour, wisdom and a good heart. Thanks Margarida for your generosity to share your pipets, and to talk about the sense of life while we were pipetting the correct stuff into the wrong tubes. To Justine for her great sarcasm, discussions and her practicality of taking things. To Eleonora, for bringing some movement to the lab. To Ana Rita, who became a great colleague, always helpful, and asking for advice at eye level. To our former dream team Juliette and Wassim, to Juliette for being a kind, honest, helpful and artistic neighbor. To Seb, always with scientific feedback, a lot of wisdom and consideration. To Marjo for bringing some great craziness to the lab. Great that you came to Montpellier, Rakhee, you are just the kindest and most open-minded person I ever met, like from another planet, not just another continent. Thanks to Mila and Maude. Thanks to Kai, Sharon and Rachel, and to Eliane who prepared 1001 LB plates for all of us. To Michel and Anne, les inseparables, who always cared. To Laurence for sharing some of her expertise from the great universe of microscopy.

Thanks to the Bacteriology team, thanks to Marianita for el gato Simon and other moments. Enchantée te connaitre Malika, for being always kind, forgiving and connecting. To Preeti who always has time for

a smile and a chat. To the JJ team for their stimulating scientific input. To Yann for his FACS expertise, his exceptional kindness and always an open ear to help, for Philippe for his expertise with qPCR.

For Veronique, Nathalie, Gael, Christine who helped with good mood, coffee and their organizing skills, to Christian who saved our dying computers, and Luc who always was there when there is a screw to turn or good mood to spread.

Thanks to all my friends who made these three years of my life in Montpellier. To Leentje for bringing Speculoos, Chimay, interesting conversations and much fun. To Julija, Eastern Grace and Eastern dwarf who connected the dark and the light side (us of course) of the lab. To Les Bibiches who were just everything. "La vie est une baguette, faut la manger." малинка, thanks for bringing the laughter to the lab, the craziness, and freedom just to do everything that was on our minds, everywhere at every moment. Thanks for sharing everything. Thanks to Annabelle interesting conversations and for her great sense of justice. Thanks to Rafa for his positive vibes at home, you are right, jamais tout est perdu;).

Finally a big thanks to my family who were there at 1300 km from here, aber eigentlich nur einen Katzensprung entfernt de la mare la Janni Capidani. Danke an Heng, den nichts außer Fassung bringen kann, der immer mitlacht, der mir nie sauer ist, selbst wenn ich Mist baue. Multumesc Papa, tu ești eroul vieții mele. Danke Mama Karla Kolumna, für 28 Jahre eines Weges, mich auf zwei Beine zu stellen, um vielleicht mal erwachsen zu sein. Thanks to my parents who made all my life journey till here possible.

Infinitas gracias a Juan por las tonterías, las absurdidades, las genialidades, por distraerme hacia las cosas importantes de la vida, por descubrir nuevos caminos y nuevas filosofías, por mucha risa y por compartir estos tres años, desde Valencia, Namur, Mouscron, Paris y Barcelona, y sobre todo, desde el corazón.

Dedicated to all those that follow their dreams and that risk their lives for being free, to my dad, and to all the Hashims, Hamids, Mamadous and Oumars of these days

Abbreviations

ACT	Artemisinin-based combination therapy
Act-1	Actin 1
Ark	Aurora-related kinase
At	<i>Arabidopsis thaliana</i>
BIPPO	5-benzyl-3-isopropyl-1H-pyrazolo[4,3-d]pyrimidin-7(6H)-one (a PDE inhibitor)
BSG	Basigin
C1, C2	Compound 1/2 (PKG inhibitors)
CA	Carbonic anhydrase
CaM	Calmodulin
cAMP	Cyclic adenosine monophosphate
CalA	Calyculin A
CDK	Cyclin-dependent protein kinase
CMG	Cdc45/MCM2-7/GINS (DNA replication complex)
CR1	Complement receptor 1
CRK	Cdk/Cdc2-related protein kinase
Cn	Calcineurin
CnA	Calcineurin catalytic subunit A
CDS	Coding sequence
CAPTPase	<u>C</u> old- <u>a</u> ctive <u>p</u> rotein <u>t</u> yrosine- <u>p</u> hosphatase (the Shelph prototype from <i>Shewanella</i> species)
Cdk	Cyclin-dependent kinase
cGMP	Cyclic guanosine monophosphate
CK	Casein kinase
Cn	Calcineurin
CnA	Calcineurin subunit A (catalytic)
CnB	Calcineurin subunit B (regulatory)
CP	Centriolar plaque
CPC	Chromosomal passenger complex
CRK	CDK-related kinase
CTD	C-terminal domain (of RNAP II)
Cyc	Cyclin
DAG	Diacylglycerol
DD	Destabilization domain
DDK	Dbf4-dependent kinase
DNA Pol	DNA Polymerase
dsRNA	Double-stranded RNA
EBA	Erythrocyte binding antigen
EBL	Erythrocyte binding-like
EMP1	Erythrocyte membrane protein 1
EXP1	Exported protein 1
FCP	F-cell production 1, a member of NLI-interacting family of phosphatases
GAP40, 45, 50, ...	Glideosome-associated proteins
GlcN	Glucosamine
GlcN6P	Glucosamine-6-phosphate
glmS	Ribozyme encoded by the <i>glmS</i> operon
GO	Gene ontology
GPA	Glycophorin A
GPC	Glycophorin C
GPI	Glycosyl phosphatidylinositol

gRNA	Guide RNA
H bonds	Hydrogen bonds
hpi	Hours post invasion
HR	Homology region
hsp	Heat shock protein
I1, I2, I3	Inhibitors 1, 2, 3 of PP1 activity
IFA	Immunofluorescence assay
iKD	Inducible knockdown
iKO	Inducible knockout
IP ₃	Inositol (1,4,5) triphosphate
ISR	Integrated stress response
iRBC	Infected red blood cell
KD	knockdown
KO	knockout
MAPK	Mitogen-activated protein kinase
MC	Maurer's clefts
MCM	Mini-chromosome maintenance protein
MJ	Moving junction
MLC	Myosin light chain
MS	Mass spectrometry
MSP	Merozoite surface protein
MTIP	MyoA tail domain-interacting protein
MTOC	Microtubule organising center
MyoA	MyosinA
Nek	NIMA (never in mitosis gene A)-related kinase
OA	Okadaic acid
ORC	Origin recognition complex
P55/MPP1	RBC membrane palmytoylated protein 1
<i>Pb</i>	<i>Plasmodium berghei</i>
<i>Pb</i> DT-3'	<i>Plasmodium berghei dihydrofolate reductase-thymidylate synthase 3'</i> -transcription terminator sequence
<i>Pf</i> DHFR-TS	<i>P. falciparum</i> dihydrofolate reductase-thymidylate synthase
PCR	Polymerase Chain Reaction
PDE	Cyclic nucleotide phosphodiesterase
PEXEL	<i>Plasmodium</i> export element
Pf	<i>Plasmodium falciparum</i>
<i>p</i> NPP	<i>Para</i> -Nitrophenylphosphate
PIP	PP1-interacting protein
PIP ₂	Phosphatidylinositol 4,5,-bisphosphate
PK	Protein kinase
PKA	cAMP-dependent protein kinase
PKB	Protein kinase B
PKG	cGMP-dependent protein kinase
PLC	Phospholipase C
PM	Plasma membrane
PP	Protein phosphatase
PP1, 2, ...	Members of PPP group
PP1c	Catalytic subunit of PP1
PPEF	Protein phosphatase with EF-hand domains
PPKL	Protein phosphatase with <u>K</u> elch- <u>L</u> ike domains
PPM	Metal-dependent protein phosphatases
PPP	Phosphoprotein phosphatases family of PPs
PRL	Phosphatase of regenerating liver

PTP	Phospho-Tyrosine-phosphatase
PTPLA/B	PTP-like phosphatase, member A/B
PV	Parasitophorous vacuole
PVM	Parasitophorous vacuole membrane
qRT-PCR	Quantitative real-time PCR
Rapa	Rapamycin
RBL	Reticulocyte binding like
Rh	Reticulocyte binding homologue
RBC	Red blood cell
RNAi	RNA interference
RON	Rhoptry neck protein
RH	Reticulocyte binding-like
RNAP II	RNA Polymerase II
ROS	Reactive oxygen species
Sc	<i>Saccharomyces cerevisiae</i>
SCP	Small RNAP II CTD phosphatase
SERA	Serine repeat/rich antigen
Shelph	<i>Shewanella</i> -like phosphatase
SP	Signal peptide
SRS	SAG1-related sequence
STP	Serine/Threonine phosphatase
SUB1	Subtilisin-like protease 1
STP	Protein-Serine/Threonine phosphatase
TF	Transcription factor
TRAP	Thrombospondin-related anonymous protein
WB	Western Blot
WHO	World Health Organization
Y2H	Yeast two-hybrid screening

INTRODUCTION

Chapter 1: Malaria and the *P. falciparum* life cycle

1.1 Apicomplexa - phylogeny and ultrastructure

Apicomplexa constitutes a phylum that comprises more than 5000 species, of which most have an obligate parasitic lifestyle, and causing important diseases in humans and animals. These include notably the etiologic agent of malaria and toxoplasmosis, respectively *Plasmodium* and *Toxoplasma gondii*. Together with Ciliates and Dinoflagellates, Apicomplexa belong to the Alveolata, characterized by a set of sacs, named alveoli, beneath their plasma membrane (Figure 1). In Apicomplexa, these alveoli form a system of flattened membrane cisternae that are stabilized by a protein meshwork underneath, and named the Inner Membrane Complex (IMC), which together with the plasma membrane is referred to as the pellicle. The pellicle, along with the subpellicular microtubules, maintains the shape and the ultrastructure of the parasite, but importantly, it is also the location of the cell locomotion machinery known as the glideosome. This machinery allows the parasite to glide and thus cross biological barriers actively penetrate a host cell.

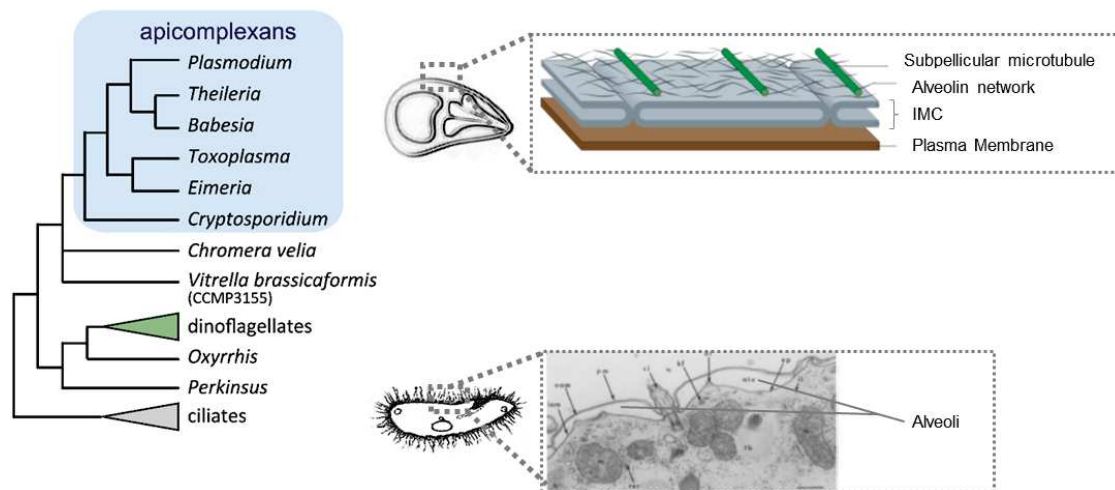


Figure 1: Consensus phylogenetic tree of Alveolata and ultrastructure of the pellicle. The Apicomplexan pellicle consists of the PM and the IMC, built up of several flattened vesicle sacs^{1,2}.

Besides the IMC, Apicomplexans are characterized by the presence of the apicoplast, a non-photosynthetic plastid acquired by secondary endosymbiosis of a red algae¹. Although the apicoplast has its origin in the chloroplast, throughout evolution this plastid has lost its photosynthetic machinery. However, it has maintained anabolic pathways, such as fatty acid, isoprenoid and heme biosynthesis¹. The presence of this plastid makes Apicomplexans sensitive to antibiotics that target bacterial DNA replication, transcription or translation³.

Apicomplexa furthermore share a common ultrastructure within the invasive forms called zoites: these highly polarized cells bear a set of specific organelles at their apical tip, namely the micronemes and the rhoptries, that are exocytosed precisely at the time of their egress from and invasion into their host cell (Figure 2). Micronemes are the smallest of the secretory organelles and contain proteins that once released from their compartments relocate at the parasite surface where they are ideally positioned to bind host cell receptors, thereby promoting irreversible attachment. Rhoptries on the other hand are large and elongated organelles divided into a thin apical duct named the neck and a posterior bulbous part known as the bulb. Rhoptries are secreted after the micronemes and allow the parasite (i) to establish a direct contact with the plasma membrane of its host cell, known as the moving-junction, that moves rearward along the parasite powered by the glideosome as the parasite

enters the cell; (ii) to manipulate host cell gene expression upon infection, at least in *T. gondii*. In the case of *P. falciparum*, rhoptries were also reported to contain a set of adhesins required for RBC attachment/invasion.

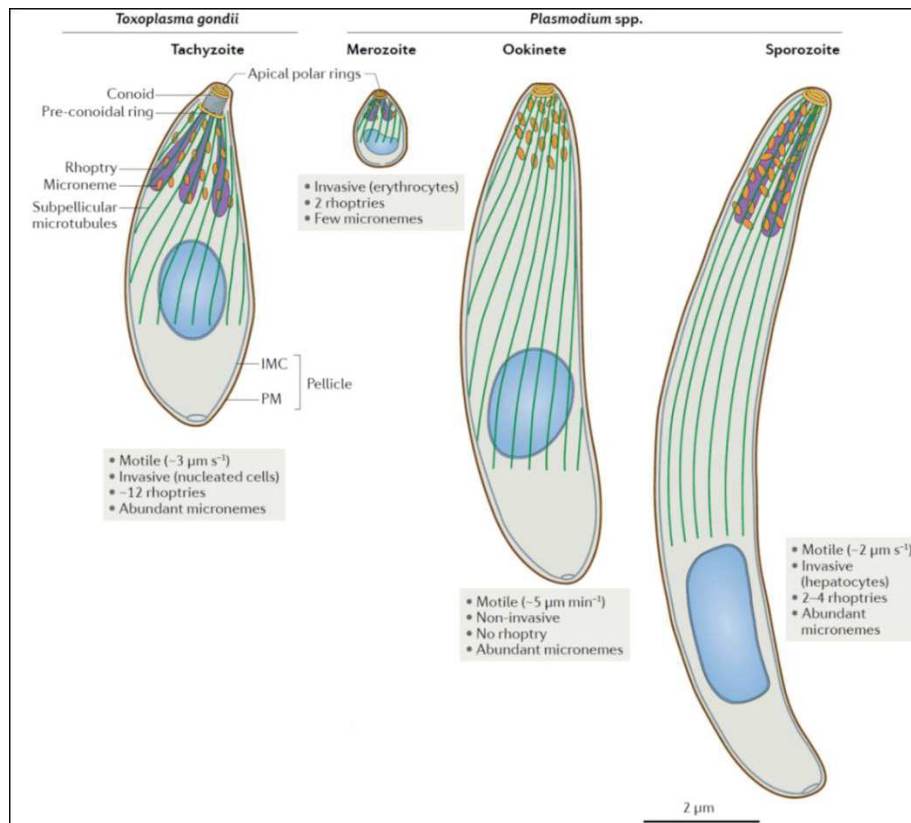


Figure 2: Secretory organelles and cytoskeleton of invasive stages of *T. gondii* and *Plasmodium*².

1.2 Malaria

1.2.1 Malaria epidemiology and human *Plasmodium* species

Malaria is one of the deadliest infectious diseases worldwide, with almost half of the world population living in regions with risk of malaria transmission⁴. Malaria is caused by different species of Apicomplexan parasites of the genus *Plasmodium*. This disease is prevalent in tropical and subtropical areas, due to the ecology of its insect vector *Anopheles* *ssp.*

In 2016, Malaria accounted for 216 million cases worldwide, out of which the great majority was caused by *Plasmodium falciparum*, and only 4% of cases due to *P. vivax*. 90% of Malaria cases occur in sub-Saharan Africa. Most Malaria cases occur in 15 countries classified as endemic with high Malaria incidence, out of which 14 countries in Sub-Saharan African and India, which bears 50% of all infections by *P. vivax*. Malaria caused an estimated of 445 000 deaths in 2016 worldwide⁵.

The WHO set up an ambitious global technical strategy for the period from 2016 till 2030, with several objectives to improve accessibility to prevention, diagnosis and treatment of malaria. These measures aim at decreasing the worldwide malaria incidence and mortality by 40% by 2020, and by 90% by 2030. Progress was already achieved from 2010 till 2015, with malaria incidence rates reduced by 54% in South-East Asia (SEA), and 21% in Africa, and mortality rates decreasing by 46% and 31%, respectively. Although advances in malaria control can be seen in percentage of the population, the WHO global

aims are difficult to achieve because exactly the regions at high Malaria risk experience a strong population growth, resulting in increasing population densities in malaria endemic regions. Therefore the absolute case and mortality numbers of the last years do not show a big improvement with 237 million cases in 2010 and 211 million cases in 2015.

Plasmodium species have a vertebrate as well as a blood-sucking invertebrate host. Vertebrate hosts include birds, reptiles and mammals. The invertebrate hosts are mainly mosquitoes of different genera but human *Plasmodium* species are transmitted only by female *Anopheles* mosquitoes.

Five *Plasmodium* species commonly infect humans, out of which *P. falciparum* and *P. vivax* are the predominant species. *P. malariae* and *P. ovale* cause only minor malaria incidence, with *P. malariae* showing a spotty geographical distribution in the world and *P. ovale* mainly present at the African West Coast. *P. knowlesi* in Southeast Asia primarily infects macaques, but can infect humans occasionally.⁶

P. falciparum is believed to have been transmitted to humans from gorillas in Western Africa 10 000 to 100 000 years ago⁷. Since then it expanded world-wide, following human migration routes, and reaching the Americas only in the 16th century by slave trade⁸. *P. falciparum* is spread in tropical and subtropical areas around the world, but mainly found in Sub-Saharan Africa. The worldwide distribution of infections due to *P. falciparum* reflects mostly the ecology of its Anopheline vector, and whether a certain urban, rural or natural environment is suitable for the mosquito. Figure 3 shows the world map of its prevalence, depicting an estimation of the parasite rate (PfPR), and thus the percentage of infected individuals at a certain time. The map shows alarmingly high parasite rates, with 40 to 70% of children infected in many areas of tropical Africa.

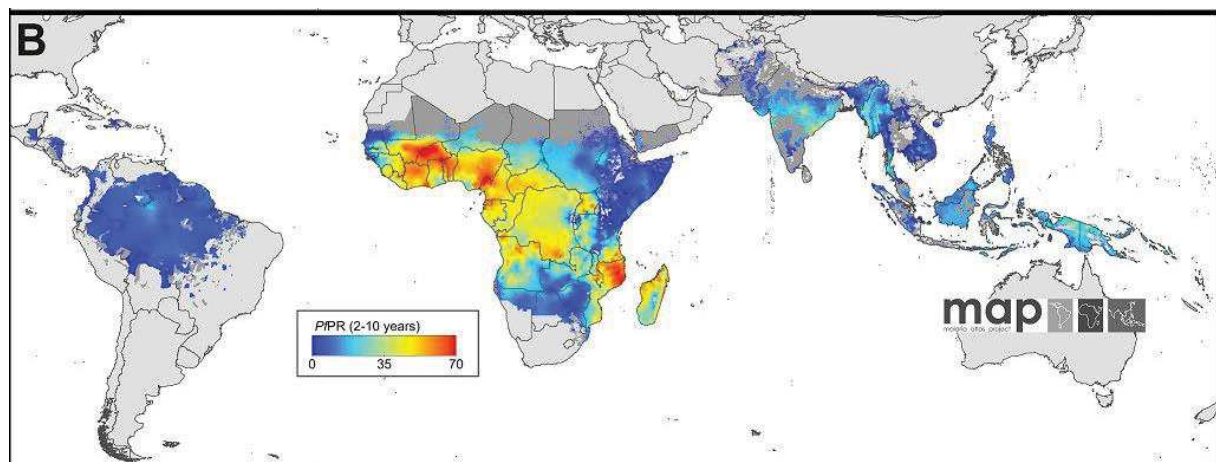


Figure 3: Worldwide distribution of *P. falciparum* endemicity in 2010. The parasite rate (PfPR) describes the proportion of individuals infected at a given time. Available data from parasite rate surveys worldwide were used for modeling PfPR for different regions on every 5 x 5 km pixel. PR was age-standardized, representing here the percentage of 2-10 year-old children infected by Pf.

P. falciparum has the unique ability to confer cytoadherent properties to the infected RBC (iRBC). Pf erythrocyte membrane protein 1 (PfEMP1) is a parasite protein exported to the RBC surface and that mediates attachment to endothelial cells in small and medium-size blood vessels, allowing the parasite-infected cells to escape splenic clearance. Cytoadherence is responsible for the major complications in Pf malaria pathogenesis, namely for cerebral and placental malaria⁶. When parasites adhere to microvasculature in the brain, a massive pro-inflammatory immune response is mounted, which can break down the blood-brain barrier. Once the integrity of the blood-brain barrier is disrupted, cytokines, chemokines and soluble parasite components enter the brain and activate microglia and astrocytes thus causing neuroinflammation¹⁰. This is why cerebral malaria has such a high case fatality: 10-20% of cases - when treated. Placental malaria is caused when iRBCs sequester

in the intervillous space of the placenta, the interface of exchange between mother and embryo with high vascularization. This leads to maternal anemia, low birth weight, premature labor and increased risk of abortion. Besides, the adherent properties of iRBCs make them sequester uninfected RBCs (rosetting) and thrombocytes, which contributes to the development of anemia, thrombocytopenia and microvascular obstruction⁶.

P. vivax is mainly found in Southeast Asia and Latin America, and in Africa its distribution overlaps with *P. falciparum* occurrence. The evolutionary history and origin of *P. vivax* is complex and not clear yet. *P. vivax* likely evolved from a primate *Plasmodium* species which was transmitted to humans. However, it is not sure whether this transmission and the further evolution of *P. vivax* occurred in Africa or Asia⁸. Nowadays, in Asia and Oceania, *P. falciparum* and *P. vivax* cause similar case numbers, but in tropical America, *P. vivax* causes most infections⁶. However, in Africa, *P. vivax* malaria is much less common because the human population is in majority negative in Duffy-binding antigen, the reticulocyte-specific receptor that *P. vivax* uses for blood stage invasion⁶. The specificity of *P. vivax* for reticulocytes, an erythroid precursor stage is the reason why long-term *in vitro* culture of this parasite has not been achieved yet. *P. vivax* has the peculiarity to form dormant liver stages, so-called hypnozoites. Hypnozoites can reactivate to form liver stage schizonts and establish malaria recurrent infections in the infected person. Hypnozoite reactivation displays different dynamics depending on the geographical area, with parasite strains in temperate and subtropical regions having longer dormant periods (8–10 months or longer) and those in tropical regions exhibiting shorter relapse intervals (around 3-6 weeks). No *in vitro* model exists for *P. vivax* liver infection, and the molecular mechanisms underlying hypnozoite reactivation are not understood¹¹.

As *P. falciparum* is the major and most virulent human *Plasmodium* species, it is the main focus of worldwide research on malaria.

1.2.2 Malaria control strategies

Malaria control integrates both strategies targeting the Anopheline vector as well as the parasite in the infected human.

Targeting the vector

Malaria prevention by vector control is an effective measure driven forward by the WHO and local governments in the endemic regions. Insecticide-treated bed nets (ITNs) and indoor residual insecticide spraying are applied for diminishing host-vector contact. Insecticides are also used for fumigation in the outside areas for controlling vector density⁵. However, the massive use of insecticides is accompanied by the advent of mosquito resistances to the main classes of insecticides used against *Anopheles* spp¹².

Targeting the parasite

Malaria comes in two presentations of the disease, uncomplicated and severe. While the symptoms of uncomplicated malaria are unspecific (fevers, body-ache, chills and diarrhea), the most common manifestations of severe malaria are cerebral malaria, lung injury and kidney injury⁶. Malaria treatment at an early, unspecific phase can prevent later complications. The main classes of antimalarial compounds include artemisinin, antifolates (e.g. pyrimethamine) and quinoline drugs^{6,13}. The first quinoline drug quinine was extracted from the bark of the Cinchona tree in South America and used for almost 300 years as antimalarial. Nowadays, a variety of quinolone drugs are used efficiently as antimalarials: 4-aminoquinolines such as chloroquine, amodiaquine or piperazine, 8-aminoquinoline

such as primaquine, and 4-quinolinemethanols including mefloquine. The quinoline moiety is responsible for the antimalarial properties of these compounds, but the precise mode of their action remains unclear. Quinolines affect the heme catabolism of the erythrocytic stages of *Plasmodium* species, and lead to the accumulation of toxic heme intermediates in the parasite's food vacuole. Moreover, chloroquine and primaquine exhibit efficacy against liver stages, and therefore must possess additional targets in parasite biology¹³.

The current standard chemotherapy of *Pf* malaria are artemisinin-based combination therapies (ACT), which are recommended by the WHO and widely used to prevent the development of drug resistances in a parasite population. ACTs contain an artemisinin derivative, which rapidly reduces parasitaemia, and an additional more stable partner drug for full parasite clearance over a longer time. The partner drugs used at the moment are quinoline drugs (mefloquine, amodiaquine, piperaquine), lumefantrine or sulfadoxine-pyrimethamine⁶. ACT are used for the treatment of uncomplicated as well as severe malaria, and the choice of drug mixture depends on the occurrence of drug resistance in the respective region. Unfortunately, parasite resistance to most antimalarials, including chloroquine, artemisinin and sulfadoxine/primaquine has emerged over time¹⁴, making research for new antimalarials a future priority^{6,12}. For treating *P. vivax* malaria, primaquine, an 8-aminoquinoline antimalarial agent, is the agent of choice, despite of its hemolytic effect, especially in people with glucose-6-phosphate dehydrogenase (G6PD) deficiency. It is the only drug that can kill all liver stages (schizonts as well as hypnozoites) and can in this way prevent relapse¹¹.

As malaria prevention strategy, chemoprophylaxis is recommended for pregnant women and children, as they are most vulnerable to the disease, and for travelers. Therefore one major WHO strategy is intermittent preventive treatment in pregnancy (IPTp) and infants with sulfadoxine-pyrimethamine. The proportion of women receiving IPTp has constantly increased in Sub-Saharan Africa, and in 2015 half of women received at least one dose of IPTp¹².

Vaccine

To date there are no clinically approved malaria vaccines available, but different strategies are being followed for Malaria vaccine development. Many vaccine strategies aim at mounting a strong immune response against sporozoites in the human body, the parasite form injected by the mosquito during a bite, thereby permitting to fight the parasite from the moment it enters the human host. The vaccine that is most advanced in development is RTS,S/AS01, a subunit vaccine based on *Pf* circumsporozoite protein. In phase 3 clinical trials with African children, it provided only protection to one third of vaccinated infants. Besides, it was not equally efficacious against different parasite strains. The second well developed vaccine strategy is intravenous application of radiation-attenuated whole sporozoites, the so-called *Pf*SPZ vaccine⁶. Irradiated sporozoites can invade hepatocytes and initiate liver stage development including protein and antigen expression. However, radiation induces DNA breakage in the parasites, so liver stage development of parasites with damaged genomes gets arrested during nuclear divisions¹⁵. The *Pf*SPZ vaccine is now entering clinical trials in Africa⁶. So all in all, there is no vaccine yet available that would provide a broad and efficacious protection from different *Pf* strains.

In conclusion, *P. falciparum* malaria can lead to severe clinical symptoms. The fact that case fatality is high for severe malaria, even when treated, demonstrates that treatment at this stage is too late or not effective enough. Apart from this, resistances arise against different classes of antimalarials, as well as against the insecticides used for vector control. The only reliable solution to prevent disease, morbidity and almost half a million deaths per year would therefore be a vaccine that efficiently protects the more than 3.2 billion people living in regions of risk⁴.

1.3 *P. falciparum* life cycle

P. falciparum has a complex life cycle, with parasite stages adapted to different environments in the mosquito and human hosts (Figure 4). In the following, parasite development in the mosquito, as well as liver and blood stages in the human host are described, with a specific focus on intraerythrocytic development.

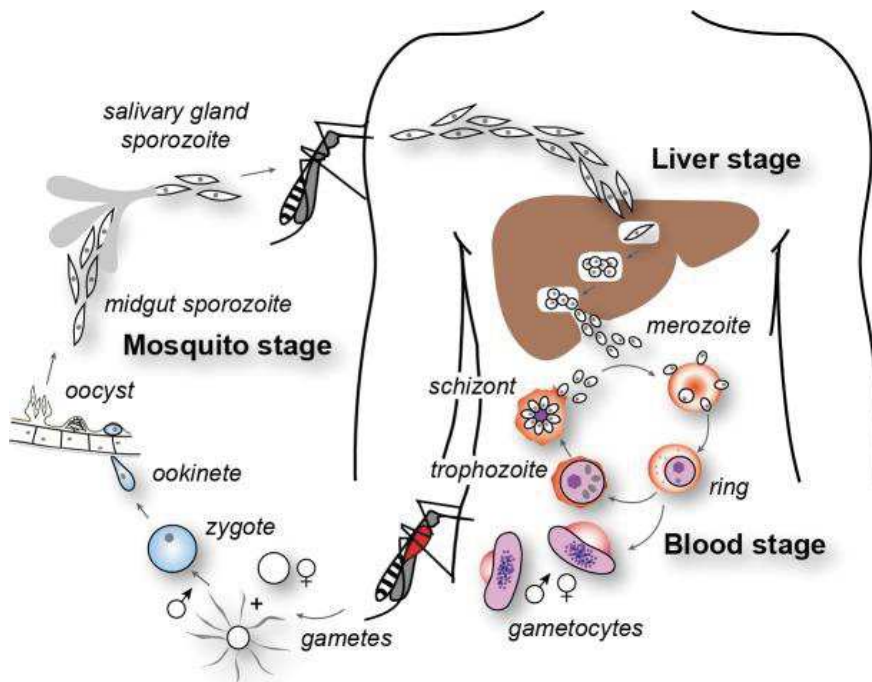


Figure 4: The life cycle of *P. falciparum*. The *Anopheles* mosquito bites a human and injects sporozoites that migrate to the liver. Asexual replication of the parasite takes place first inside the hepatocyte, and later, in RBCs. Gametocytes are formed from the asexual blood stages, and can establish infection in the mosquito upon the next blood meal. Sexual parasite development in the mosquito involves gametocyte activation to gametes, fertilization, zygote maturation to motile ookinetes and the oocyst giving rise to thousands of sporozoites that migrate to the salivary glands¹⁶.

1.3.1 Mosquito stages

The sexual development of *Plasmodium* species takes place in different compartments of the mosquito body and involves a series of parasite transitions. The Anopheline mosquito taking a blood meal from an infected human host ingests male and female gametocytes. The first developmental step of *Plasmodium* in the mosquito is the maturation of gametocytes into gametes, which takes place in the mosquito midgut. Gametogenesis is triggered by stimuli in the mosquito environment (xanthurenic acid and a drop in temperature) that activate Ca^{2+} -signaling that induces male microgametocytes to undergo three rounds of DNA synthesis and mitosis to generate an 8n polyploid cell, which divides to give rise to eight haploid (1n) axoneme-containing motile microgametes. The same activation signaling then leads to the egress of the male and female gametes from erythrocytes¹⁷.

Fusion of the male and female gametes generates the zygote, which develops into a motile ookinete over approximately 18 hours.

The ookinete in the midgut lumen must traverse the peritrophic matrix in order to reach the midgut epithelial cells. The peritrophic matrix is a thick chitin-based layer that is built up in 24 hours after mosquito blood ingestion and coat the luminal side of the midgut epithelium. The ookinete then migrates through the epithelial cell to the intracellular space between the epithelial surface and basal lamina, where it differentiates into an oocyst. The oocyst matures during 10 days, where many rounds

of nuclear replication create a sporoblast with thousands of nuclei. Upon sporozoites individualization and sporoblast rupture, thousands of sporozoites are released into the mosquito hemocoel. They migrate to and invade the salivary glands lumen and can be transmitted to the human when the mosquito takes another blood meal¹⁸.

1.3.2 Liver stages

Malaria transmission to the human occurs when an infected mosquito takes a blood meal and injects crescent-shape sporozoites with its saliva into the skin connective tissue. The sporozoites need to cross the epidermis and dermis, during which they transmigrate cells. Some of them leave the skin via a blood vessel or the lymphatic system, until they reach liver blood vessels and adhere to the endothelium. Sporozoites then cross the endothelial barrier either by transmigration of endothelial or Kupffer cells, or by squeezing through the space between endothelial cells in order to enter the liver¹⁹.

Once a sporozoite has invaded a hepatocyte, it develops inside a vacuole formed by the parasite and thus named the parasitophorous vacuole, into a spherical liver stage also called a liver stage trophozoite. The trophozoite then undergoes liver stage schizogony, consisting of 13 to 14 rounds of DNA replication and mitosis. Several thousand merozoites are thus formed in the resulting syncytial schizont. These merozoites are released from the hepatocyte as merosomes, vesicles budding from the infected hepatocyte and containing a variable number of merozoites released from the parasitophorous vacuole and surrounded by the plasma membrane of their host cell; merozoites are then released from the merosomes into the blood stream, where they start infection of red blood cells (RBCs)²⁰.

1.3.3 Intraerythrocytic development

Repetitive cycles of parasite development in RBCs are responsible for the clinical symptoms of malaria. The parallels between liver stage and blood stage development are obvious, including the intracellular parasite growing inside a parasitophorous vacuole (PV) and the process of schizogony that gives rise to a syncytial cell from which infectious merozoites are released.

As the merozoite moves into the RBC, the MJ moves as a ring around the parasite until invasion is complete. While the parasite pushes itself inside the RBC, a compartment inside the RBC is formed, the PV. The PV is delimited by the parasitophorous vacuole membrane (PVM) which was formed by the invagination of the host cell plasma membrane, but gets modified by incorporation of parasite proteins as well as parasite phospholipids²¹. The PVM is the interaction interface of the parasite with its host cell. From the beginning of RBC infection, *Plasmodium* restructures the host RBC for assuring parasite survival in many ways. This remodeling is carried out by parasite proteins exported to the PVM, to specific sites in the RBC cytosol or to the RBC membrane (RBCM). Some exported parasite factors facilitate the access to nutrients, and others help the infected RBC (iRBC) to survive in the blood circulation, such as the variant immune-adhesin *PfEMP1* that is inserted into the iRBC membrane. For exporting proteins to the host cell, *P. falciparum* builds up a secretory pathway from the PV to the RBCM. Maurer's clefts (MCs) are Golgi-like stacks that are formed in the RBC cytosol upon *Pf* infection, and that form part of this protein trafficking machinery²².

After invasion, the ring stage parasite takes 18-22 hours post invasion (hpi) to develop into trophozoites, and at this transition the nucleus rounds up while the parasite prepares for DNA replication. Trophozoites then undergo several rounds of DNA replication, mitosis and nuclear division, resulting in a syncytial schizont. A last synchronous round of mitosis and nuclear division is followed by cytokinesis of an average of 16 to 22 daughter merozoites²³. Once daughter cell segmentation is

complete, parasite signaling mediates sequential rupture of the PVM and RBCM in a short time frame to release the merozoites into the blood stream and start another round of replication in RBCs.

A subpopulation of intraerythrocytic parasites switches to sexual development, giving rise to female and male gametocytes, which can establish infection in the mosquito. Depending on the parasite strain and the development of the disease, 5 to 20 % of blood stage parasites undergo gametocytogenesis. Environmental stresses on the parasite, such as drugs treatment or a high host parasitaemia, increase the ratio of parasites committing to sexual maturation. Gametocytogenesis proceeds in five phases (phase I to V), with phase I gametocytes resembling trophozoites, and then acquiring more and more a crescent shape and specific structures²⁴. However, the common laboratory strain 3D7 used in our lab forms only very few gametocytes, unless it is stressed by drugs or starvation. In the following sections, the major steps of RBC development are described in molecular detail.

1.4 Insight into 3 key events of *P. falciparum* RBC cycle

1.4.1 Invasion

Invasion is a highly regulated sequence of molecular interactions and signaling events between the merozoite and the host RBC, with Figure 5 showing a schematic overview. Egress triggers the discharge of adhesins from micronemes, which are then deposited onto the merozoite apical end. Then merozoite establishes a primary reversible contact using merozoite surface proteins and host cell receptors. Then the parasite re-orientates to face the RBC with its apical tip, aided by waves of deformation in the RBC. Apical adhesins of the EBL and Rh families now establish an irreversible binding to the RBC, which permits the translocation of the RON complex into the host membrane. RON-AMA1 interactions sustain the Moving Junction (MJ) between parasite and RBC, and the parasite starts entering the host cell²⁵.

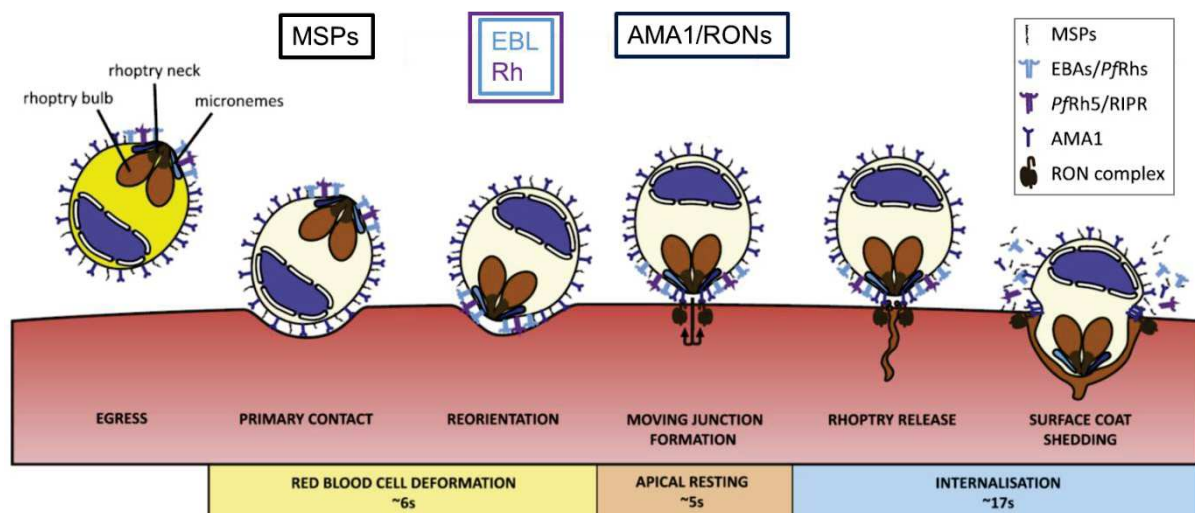


Figure 5: Overview of the host-parasite interactions important for merozoite invasion. Primary contact is achieved via GPI-anchored MSP proteins (black). Following re-orientation, specific interactions are carried out by micronemal EBL (light blue) as well as Rhoptry neck Rh proteins (purple). This permits the translocation of a RON complex (brown) into the RBC membrane. RON complex binding of merozoite AMA1 (dark blue). Adapted from ²⁵.

Primary contact

The first step of merozoite invasion is the primary attachment to the RBC. This attachment is dynamic, with the merozoite repeatedly attaching and detaching, and is believed to occur *via* the reversible interaction of merozoite surface proteins (MSPs), anchored to the plasma membrane by a glycosyl phosphatidylinositol (GPI)-anchor, to RBC receptors. To date, there are 11 GPI-anchored proteins that are known or potential erythrocyte ligands (Table 1)²⁶.

The most important parasite ligand in this primary attachment is MSP1²⁷. MSP1 is proteolytically processed by parasite protease SUB1 during schizogony. The cleavage products remain non-covalently attached and form a multimeric complex with MSP6 and MSP7 that covers the whole merozoite surface²⁸. The corresponding RBC receptors for MSP1/6/7 are likely Band 3 as well as glyophorin A (GPA) and Heparin-like proteins, as they were found to interact with MSP1^{29–31}. The current model is that MSP1 interacts with both GPA and Band 3 that associate in the RBC membrane: the 83kDa fragment of MSP1 binds GPA, while the C-terminal fragment MSP1_{42kDa} interacts with Band3, forming a receptor/co-receptor complex as depicted in Figure 6. After fulfilling its role in attachment to the host RBC, the MSP1/6/7 complex is shed from the merozoite surface by the parasite protease SUB2 secreted onto the merozoite surface³².

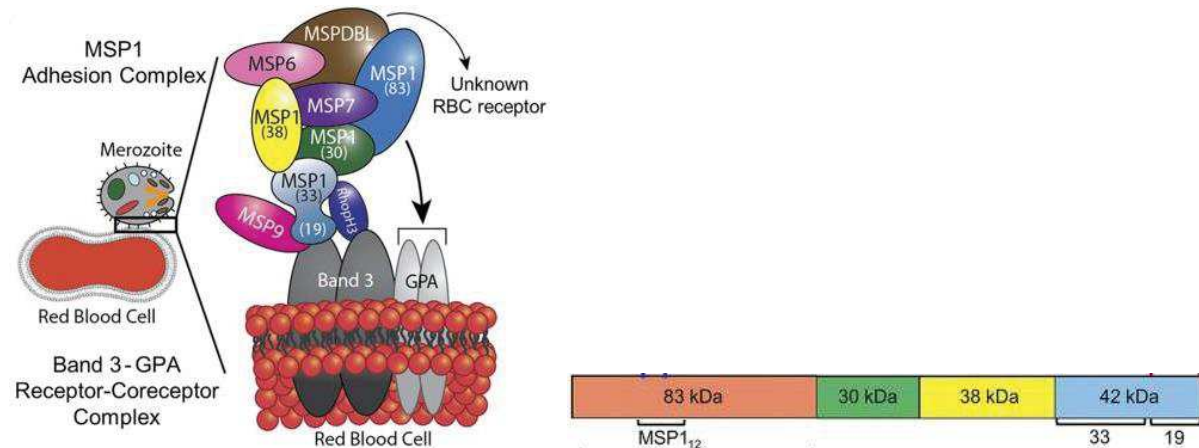


Figure 6: Model of the MSP1-RBC receptor complex. The left panel shows a model of the MSP1/6/7 complex that associates by non-covalent interactions. Only the N-terminal part of MSP1, MSP1_{33kDa} is attached to the merozoite surface by a GPI anchor. Additional bound proteins are MSP9, RhopH3 and MSPDBL1 and 2. Band 3 and GPA in the host RBC membrane associate in close proximity. While MSP1_{83kDa} interacts with GPA, MSP1_{19kDa} binds Band3. On the right panel, the SUB1 cleavage sites are shown, generating the 83kDa, 30kDa, 38kDa and 42kDa fragments. After MSP1 complex interaction with the host receptors Band3 and GPA, the complex is shed from the merozoite surface by SUB2 which cleaves inside the 42kDa fragment, leaving only the 19kDa fragment bound to the merozoite surface via its GPI anchor³⁰.

Apart from the MSPs, the GPI-anchored adhesion molecules include proteins possessing a 6-Cys-motif, also called s48/45 domain (see Table 1)³³. The s48/45 domain is a homologue of the SAG1-related sequence (SRS) fold found in *T. gondii*. *T. gondii* SRS proteins localize on the parasite surface and are involved in reversible attachment, out of which TgSAG1 is the immunodominant antigen^{33,34}. *P. falciparum* encodes 12 members of the s48/45 family, most of which are located on the parasite surface and are involved in host cell contact in different phases of the parasite development³³. Pf12, Pf38, and Pf41 were shown to localize to lipid rafts in the merozoite membrane³⁵.

Table 1: The invasion-related GPI-anchored proteins of the *P. falciparum* merozoite²⁶

Name	Accession No.	Function/Features	Structure
GPI-Anchored MSP ^a			
MSP-1	PF3D7_0930300	required for merozoite egress through binding spectrin, major surface antigen and may bind Band 3; forms major complex on merozoite surface	two epidermal growth factor (EGF) domains in side-by-side arrangement at C terminus
MSP-2	PF3D7_0206800	not known	
MSP-4	PF3D7_0207000	not known	
MSP-5	PF3D7_0206900	not known	
MSP-8	PF3D7_0502400	not known	
MSP-10	PF3D7_0620400	not known	two EGF domains in side-by-side arrangement at C terminus
P12	PF3D7_0612700	member of 6-cys family, binds to Pf41	6-cys domains with similarity to <i>T. gondii</i> surface protein SAG1; P12 structure reveals two juxtaposed 6-cys domains
P38	PF3D7_0508000	member of 6-cys family	6-cys domains with similarity to <i>T. gondii</i> protein SAG1
P41		member of 6-cys family, binds to P12	P41 requires an interdomain insertion for interaction with P12
P92	PF3D7_1364100	cys-rich surface protein; binds factor H and involved in complement evasion	
P113	PF3D7_1420700	member of <i>Plasmodium</i> translocon for exported proteins (PTEX); also reported to bind the amino terminus of PFRh5	

Reorientation and attachment

Following the first attachment to the RBC, the merozoite re-orientates so its apical end faces the host cell. This ensures that the adhesins secreted from the apical tip of the parasite can interact with their host receptors. The molecules mediating this irreversible attachment belong to two protein families, namely the Erythrocyte Binding Like (EBL) and the Reticulocyte binding protein Homolog (Rh) families (Figure 5 Figure 7), localizing to the micronemes and the rhoptry neck respectively^{36,37}. EBA175, EBL1 and EBA140 bind to glycoporphin A (GPA), B and C respectively^{38,39}, while Rh4 and Rh5 interact with Complement Receptor 1 (CR1) and Basigin (BSG) respectively^{40,41} (Figure 7). The receptors of EBA181, Rh2a, Rh2b have not been identified yet. This extensive repertoire of ligand-receptor allows the parasite to use alternate invasion pathways and adapt to RBC polymorphisms²⁵.

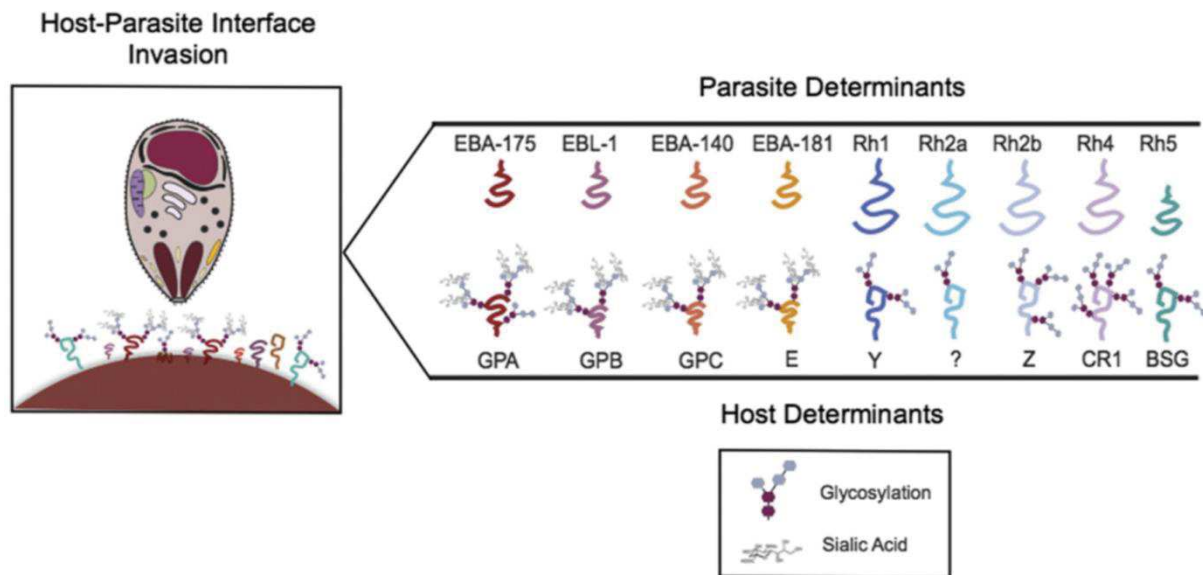


Figure 7: Pairs of host receptors and parasite ligands on the interface between the merozoite and the RBC. Host receptor modifications (glycosylation, sialic acid) are depicted⁴².

Of all the parasite ligands cited above, Rh5 is unique as it is the only member to be essential for all the *P. falciparum* strains tested^{43,44}. In the recent years, the Rh5/BSG interaction has attracted tremendous interest for several reasons: (i) antibodies against Rh5 potentially block invasion of laboratory as well as field *P. falciparum* strains known to exhibit diverse invasion phenotypes^{41,45}; (ii) Rh5 is a major determinant of *P. falciparum* host cell tropism^{46,47}. Therefore, Rh5 appears as an essential determinant of *P. falciparum* invasion and represents today a lead candidate in vaccination studies.

Besides enabling attachment between the parasite and the host cell surface, the engagement of parasite ligands with their receptors also fulfills some signaling function. Indeed, it was shown that the interaction between EBA175 and its receptor GPA triggered the secretion of rhoptry proteins, likely by inducing restoration of basal intracellular calcium concentrations in the parasite⁴⁸.

Moving-junction formation

Following attachment, the parasite then establishes a molecular bridge at the interface between host and parasite plasma membranes, known as the moving junction (MJ). This structure takes the form of a ring surrounding the parasite and is maintained during the whole invasive process, moving from the apical tip to the rear of the parasite as it penetrates the host (Figure 8).

Its molecular composition has been first elucidated in *Toxoplasma* and results from the cooperative secretion of micronemes and rhoptries: the micronemal protein AMA1 in the parasite plasma membrane interacts with a complex of rhoptry neck proteins RON2/4/5/8 injected on the host side, with RON2 being the receptor for AMA1⁴⁹⁻⁵². In contrast to the adhesins that are clearly distinct between Apicomplexan parasites, the MJ components are conserved in Apicomplexa, with the exception of RON8 that is coccidian specific^{53,54}. Consistent with this observation, formation of the MJ was shown to be essential for invasion, likely by providing a strong grip for the parasite to withstand the shear forces of the invasive process. Indeed, inhibitory antibodies or peptides targeting the AMA1-RON2 interaction drastically impair invasion⁵⁵. Likewise, genetic disruption or down-regulation of AMA1 or RON2 affects the invasive capacity of the parasite^{56,57}. In *Toxoplasma* the capacity of the AMA1 or RON2 mutants to retain some residual invasion allowed the identification of AMA-like and RON2-like homologues that can interact to partially compensate for the loss of AMA1-RON2 pair⁵⁷. Whether this is also true for *Plasmodium* has not been investigated for the moment.

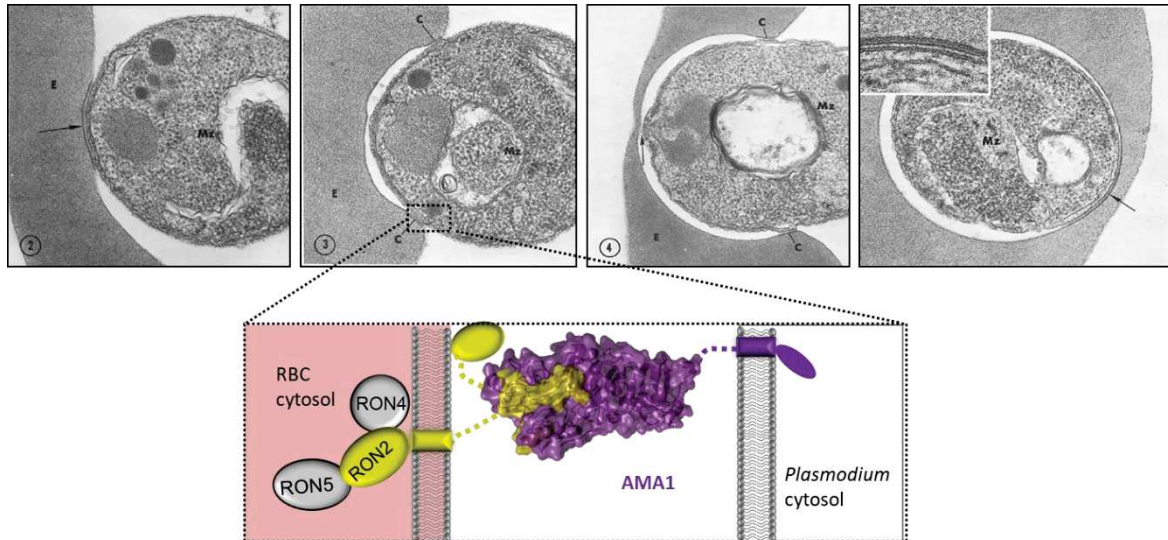


Figure 8: A MJ is formed upon merozoite invasion. TEM picture from ⁵⁸. Molecular composition of the MJ from *M. Lamarque*

In addition to providing an anchor during host cell penetration, the MJ is thought to act as a molecular sieve that selectively filters host transmembrane proteins from the nascent PV⁵⁹. This process would be crucial for the establishment of a non-fusogenic PV that could not fuse with host cell lysosomes⁶⁰.

Motility-driven penetration

Apicomplexan parasites use a common actin-myosin based machinery called the glideosome to move on substrates, notably allowing active penetration of a host cell by a zoite. The parasite glideosome is located at the pellicle, i.e. in the space between the PM and the IMC, and generates the force that drives parasite motility. The glideosome has been intensively investigated in *T. gondii*, mostly by the knockout or inducible KD of a single gene, by multiple knockouts, and by co-immunoprecipitation (co-IP) studies that characterized direct and indirect interaction partners⁶¹. The glideosome seems to be largely conserved among the Apicomplexa, including *Plasmodium*.

The key conserved components of the *Plasmodium* glideosome are short actin fibers, the myosin heavy chain MyoA, associated to the Myosin Tail Interacting Protein (MTIP) in *Plasmodium* (or Myosin light chain (MLC) in the other genus), and three Glideosome Associated Proteins, namely GAP40, GAP45 and GAP50⁶²⁻⁶⁵ (**Figure 9**). Conditional depletion of MyoA, MTIP or GAP45 affects motility of zoites, consistent with their role in gliding⁶⁶⁻⁶⁸. Gliding motility also requires actin polymerization as treatment of zoites with cytochalasin D, an inhibitor of actin polymerization, prevents gliding and invasion⁶⁹. These actin filaments are thought to be formed between the plasma membrane and the IMC⁷⁰. The gliding motility relies on the rearward traction of these microfilaments by MyoA, MyoA being anchored to the IMC via GAP50 and GAP45. The myosin stroke is transmitted to the surface bound adhesins by the binding of their cytoplasmic tails to the actin filaments via the Glideosome Associated Connector (GAC)⁷¹. Therefore, the rearward displacement of such parasite-RBC interaction complexes pushes the parasite forward. In *Plasmodium* merozoites, filamentous actin was specifically detected associated with the MJ^{70,72} (Figure 9B and C).

Apart from this “classical” MyoA-glideosome containing the GAP40/45/50 complex, different glideosome complexes are described in *T. gondii* which can partially compensate for each other⁶¹. Gene knockout studies demonstrated the flexibility of glideosome assembly: when TgMyoA is depleted, the parasites manage to achieve 25% invasion efficiency. Whereas the classical MyoA glideosome is assembled by GAP45, GAP80 recruits a MyoC-based glideosome at the basal polar ring of the tachyzoite. Upon MyoA-KO, this MyoC-ELC1-GAP80-GAP40-GAP50-IAP1 complex partially

relocates to the apical tip to assure invasion⁷³. For *Plasmodium*, no study has so far been conducted on the possible redundancy of glideosome complexes.

Besides, different models exist for the topology of the glideosome, meaning the spatial and functional organization of the key components and how they generate force⁷⁴. The currently most accepted model is the “fixed linear motor model” represented in Figure 9, where MyoA is stably linked to the IMC via the GAP complex and actin is connected to PM adhesins by linker proteins, such as the glideosome-associated connector (GAC)⁷¹. GAP45 is inserted into the parasite PM by acylation, and thereby plays an important role for assembly and anchoring of the glideosome between the IMC and the PM. When the merozoite is attached to the host RBC by ligand-receptor interactions, the actomyosin motor will displace these ligand receptor complexes and the whole parasite membrane relative to the IMC, which results in a gliding movement that pushes the parasite into the host cell (see Figure 9).

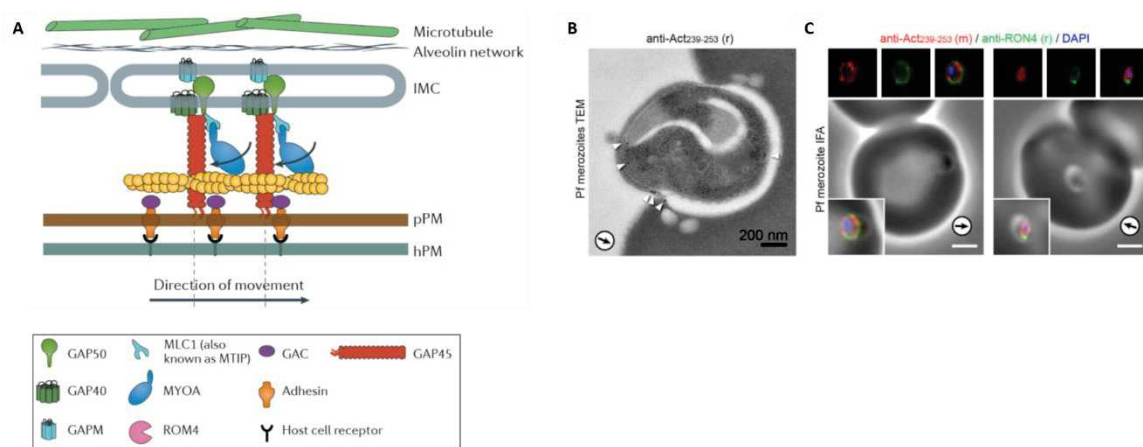


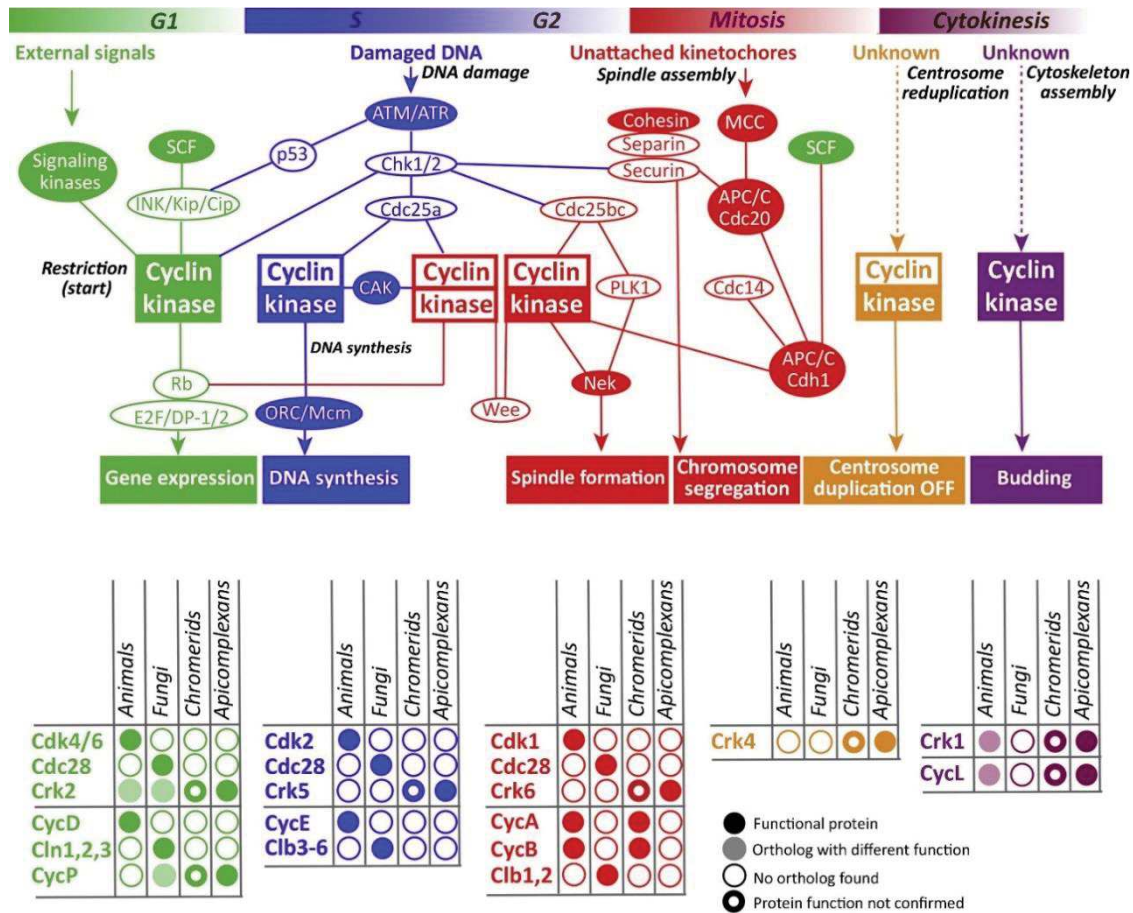
Figure 9: Glideosome architecture and localization of actin filaments². (B) TEM of an invading merozoite. Actin is labelled by gold-particle-coupled antibodies (arrowheads). (C) IFA of invading merozoites, labelled with α -actin red, α -RON4 green and DAPI nuclear staining⁷⁰.

1.4.2 Cell cycle and schizogony

In *Plasmodium* schizogony, three to four rounds of DNA replication and nuclear division give rise to a syncytial schizont, which undergoes a synchronous mass cytokinesis only at the end of schizogony. Although this mode of cell division differs from classical eukaryotic cell division, it can be described in the classical phases of the cell cycle: a G₁ phase (growth and preparation for DNA replication), S phase for DNA replication and finally mitosis (M) phase, but G₂ phase is short or absent. The G₁ phase was found to proceed in *Toxoplasma* the same as in animal cells, with the first half of G₁ dedicated to protein and RNA biosynthesis, followed by a switch to DNA synthesis in the second half⁷⁵. The Apicomplexan cell cycle can be described as a growth phase, followed by one synchronous budding phase when daughter cells are formed.

The mechanisms regulating the onset of schizogony are still poorly understood. In metazoans, various cell cycle “checkpoints” assure that every step of DNA replication and mitosis is correctly completed before the cell can proceed in development. Many factors control cell cycle progression, including Cyclins and Cyclin-dependent kinases (CDKs). In *Plasmodium* however, evidence that such cell cycle checkpoints exist is scarce. The conservation of cell cycle regulators in Apicomplexa compared to animals and fungi are summarized in Figure 10. Some cell cycle regulators are conserved between Apicomplexa and other eukaryotes (cohesins, APC/C), whereas others were lost in the Apicomplexan

lineage (Separins, Securins, canonical cyclins Cyc D, E, A). This generated a need for new cell cycle regulators which evolved specifically in Apicomplexa, such as Cyc P/U and Apicomplexa-specific CDKs PK6 and Crk5⁷⁶. Chapter 2 will describe in detail current knowledge of how *Plasmodium* CDKs and phosphorylation control the parasite cell cycle.



Trends in Parasitology

Figure 10: The eukaryotic cell cycle and conserved mechanisms in *Plasmodium*. Chromatids are the Apicomplexan ancestor. All eukaryotic lineages can be tracked back to the last common ancestor of eukaryotes (LECA)⁷⁶.

DNA replication

During ring stage at the beginning of RBC development, parasites are in G₁ phase. The end of G₁ is marked by a transition from the “ring” morphology to a spherical nucleus at ~18 to 22hpi, when parasites prepare for chromosome replication. DNA synthesis, meaning S phase, starts in a mature trophozoite at 24 to 26hpi. The *Plasmodium* genome consists of 14 chromosomes plus one mitochondrial and one apicoplast genome that get replicated independently of the nuclear genome.

The basic principles and major players for the initiation and the progression of DNA replication are well conserved among eukaryotes, and are best described in yeast. The so-called pre-initiation complex (pre-IC), which starts DNA replication, is formed by the sequential assembly and activation of various intermediate protein complexes (see Figure 11). The first step is the recognition of origins of replication by heterohexameric ORC (origin recognition complex) complexes, which serve as a platform for the recruitment of Cdc6, Cdt1 and mini-chromosome maintenance proteins (MCM 2-7), giving rise to an initial helicase loading intermediate, the OCCM complex. Once the OCCM complex is well installed on the DNA, Cdc45 and GINS factors associate to form the OCM complex, on ATP hydrolysis and Cdt1 release. The ORC then dissociates, and assembly of PCNA (proliferating cell nuclear antigen) and many other factors form the pre-IC. The activated MCM hexamer is the catalytic core of the replicative

helicase, forming a channel inside of which the double-stranded DNA is unwound to give rise to the replication fork. Different DNA Polymerases (DNA Pol) are recruited to the replication fork. While the MCM complex unwinds the DNA, DNA Pol α primes DNA synthesis, and DNA Pol ϵ and δ catalyze leading and lagging strand synthesis, respectively⁷⁷.

The basic components of pre-replicative complexes and of the catalytically active replisome are conserved in *Plasmodium*, while some factors such as Cdc45, Cdc6 and the MCM-phosphorylating kinase DDK (Dbf4-dependent kinase) seem to be absent. *Plasmodium* homologues have been identified and validated for PCNA, DNA polymerases, ORC and MCM proteins⁷⁸. While classical eukaryotic ORC consists of ORC1 to 6 proteins, it is not sure whether *Plasmodium* ORC has the same composition, as only PfORC1, PfORC2 and PfORC5 have been characterized, and homologues for ORC3 and 4 have been proposed in *P. berghei*^{78,79}. MCM 2 to 7 are conserved in *Plasmodium*, and likely form a hexameric helicase complex, as MCM2, 6 and 7 were shown to interact in the parasite⁸⁰. For some other components of the pre-IC and replication machinery, such as Cdt1 and GINS, putative homologues have been identified *in silico*, but functional validations are still missing⁷⁸.

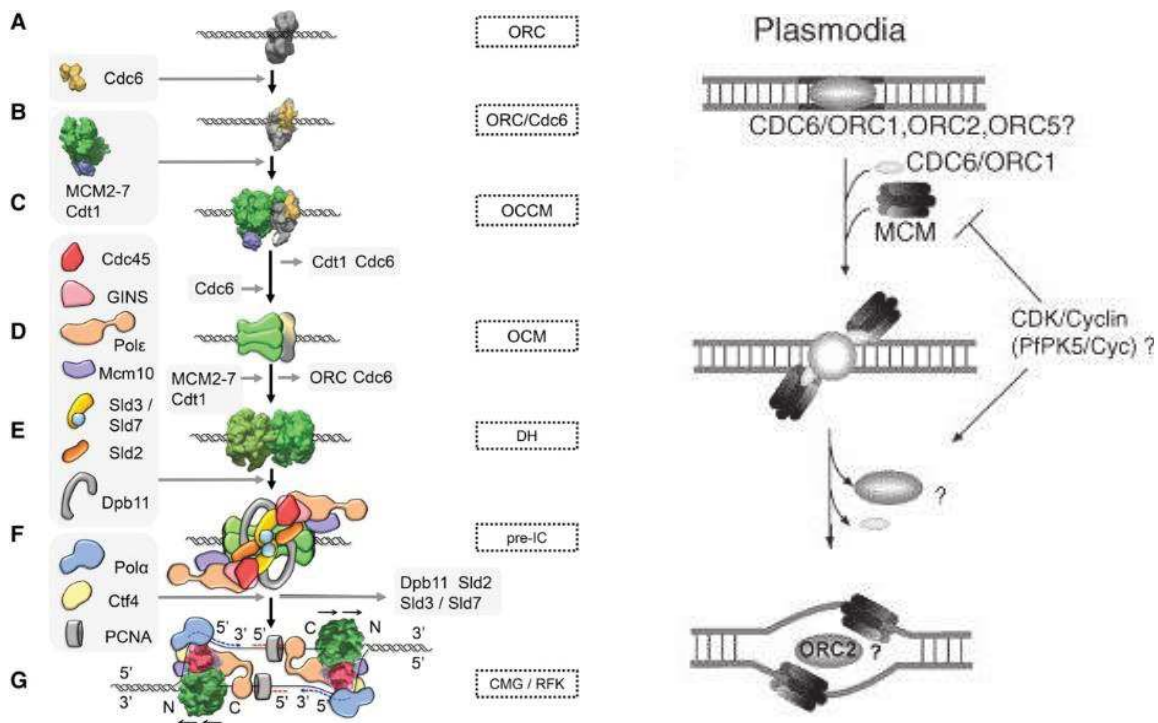


Figure 11: Model for DNA replication initiation in Eukaryotes and Plasmodium. In Eukaryotes ORC1 to 6 proteins form the ORC recognizing the origins of replication. For *Plasmodium* the composition of the ORC complex is not sure, as only PfORC1, PfORC5 and PfORC2 have been characterized to date. CDKs/Cyclins regulate assembly and protein turnover of components of the pre-IC. *Plasmodium* Cdk homologue PfPK5 was shown to phosphorylate PfOrc1, but might regulate also other components of the pre-IC⁷⁹. Eukaryotic DNA replication is driven by helicase activity of the MCM complex that opens the replication fork, a function conserved in *Plasmodium*⁸⁰. DNA Polymerases are recruited to the replication fork to catalyze DNA synthesis. Models from^{77,80}.

DNA synthesis is initiated at many replication origins simultaneously to assure the rapid and complete replication of eukaryotic genomes⁷⁷. In *Plasmodium* a technique using pulses of synthetic nucleotide labeling, followed by immunodetection of *de novo* DNA synthesis permitted to investigate the distribution of active replication forks during the erythrocytic S phase. The replication forks are scattered along the *Plasmodium* genome at a mean distance of 65kb. Interestingly, the replication speed is not constant and decreases as schizogony proceeds, perhaps due to limitation in nucleotide availability or in space⁸¹.

So all in all, *Plasmodium* likely uses conserved eukaryotic mechanisms of DNA replication, but future studies are necessary for the understanding of how the parasite regulates DNA replication.

Mitosis

Simultaneously with DNA replication, the nucleus prepares for mitosis by centrosome duplication. In most eukaryotes, centrosomes are the microtubule-organizing centers (MTOC) of the mitotic spindle, and mark the poles of the mitotic spindle. Mammalian centrosomes consist of a pair of cylinder-shaped centrioles surrounded by a pericentriolar matrix. Transmission electron microscopy showed that *Plasmodium* lacks centrioles, but possesses electron-dense plaques that seem to be embedded in the nuclear membrane, facing the nuclear interior as well as the cytoplasm⁸². These structures also consist of typical centrosomal proteins such as centrin 1. These MTOC structures found in *Plasmodium* are therefore termed centriolar plaques (CPs)⁸³.

The 2n trophozoite then undergoes nuclear division by mitosis. Mitosis in *Plasmodium* differs from traditional mitosis in three main aspects, as seen in Figure 12. A major hallmark of *Plasmodium* is that it undergoes a “closed mitosis”, which takes place inside the intact nuclear envelope, whereas the nuclear envelope disassembles in most other eukaryotic cells. Second, *Plasmodium* chromosomes do not condense for mitosis to happen, but get segregated in their uncondensed state. Another difference is that in most mammalian cells mitosis is directly followed by cytokinesis, whereas *Plasmodium* generates a cell containing many nuclei, which get distributed to separate daughter cells only at the end of schizogony⁸⁴.

Figure 12 schematically shows all phases of *Plasmodium* mitosis as reviewed in Gerald *et al.* (2011)⁸⁴. The best observations of *Plasmodium* mitosis were generated by TEM, but light microscopy also contributed, for example by the use of the MTOC marker Centrin3⁸⁵. In *Plasmodium* prophase, the mitotic spindle starts to assemble inside the nucleus, starting from the duplicated CPs embedded in the nuclear envelope⁸². In metaphase, the spindle microtubules contact the centromeres of the uncondensed chromosomes via a protein structure called kinetochore, which is deposited on top of the centromeres. The *Plasmodium* chromosomes align on the equatorial plate, and each kinetochore gets bound by two microtubules, emerging from opposite CPs⁸⁶. TEM studies show that *Plasmodium* spindles are remarkably short, starting from lengths of 0.5µm until an average of 1 µm from pole to pole, indicating that the spindle poles often localize close to each other, and not on opposite sides of the nucleus⁸⁶.

Segregation of sister chromatids towards the spindle poles is the main hallmark of anaphase, and can be blocked by microtubule-stabilizing agents⁸⁷. Once the chromosomes are entirely segregated, the nuclear membrane divides to form around both daughter genomes, which are now ready for a new round of DNA replication and mitosis.

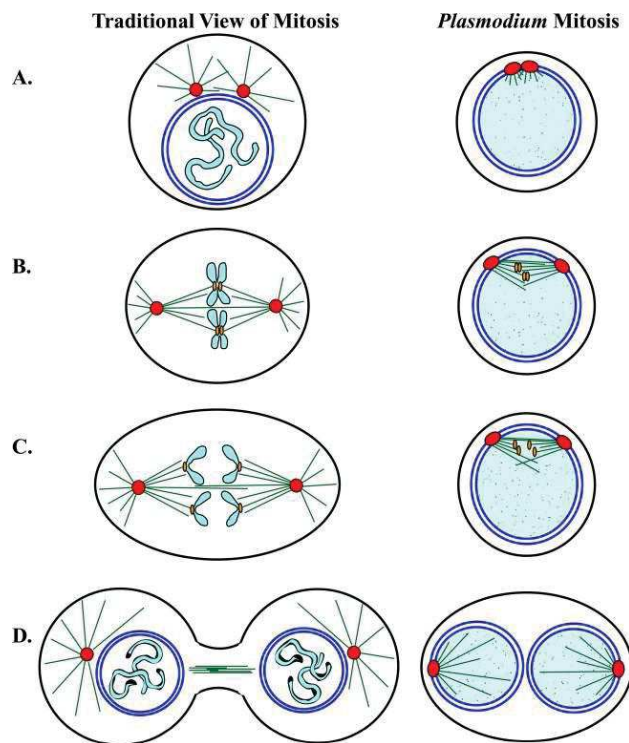


Figure 12: Scheme comparing traditional mitosis to mitosis in *Plasmodium* blood stage schizogony. The plasma membrane is shown in black and the nuclear membrane in blue, the MTOC is depicted as red circle, microtubules are green lines and the kinetochores are shown as orange ovals. (A) Prophase in traditional mitosis is characterized by chromosome condensation and nucleation of cytoplasmic microtubules by the two cytoplasmic MTOCs. In *Plasmodium* chromosomes do not condense. The duplicated MTOCs are embedded in the nuclear membrane, and the mitotic spindle begins to form inside the nucleus. (B) In traditional metaphase, the condensed chromosomes are arranged in the metaphase plate and connected to the mitotic spindle microtubules attached through the kinetochores. In *Plasmodium* metaphase, the uncondensed chromosomes are also attached via the kinetochore to the mitotic spindle inside the intact nuclear membrane. (C) In Anaphase, sister chromatids migrate to the opposite poles of the mitotic spindle. (D) Telophase. Traditionally, the nuclear membrane is formed around each daughter genome, chromosomes start to decondense and the cell starts division. In *Plasmodium* telophase the nuclear membrane gets distributed to both daughter genomes which start new rounds of DNA replication and mitosis before cytokinesis occurs⁸⁴.

At some moment the schizont stops all asynchronous nuclear divisions, and undergoes one last synchronous mitosis that runs over into cytokinesis.

Cytokinesis

The multinucleate schizont needs to distribute each nucleus to a daughter cell that is formed by a process called internal budding or segmentation. To achieve this, the parasite must make sure that every forming merozoite is equipped with one nucleus and all necessary organelles and intracellular structures. The pellicle, consisting of the IMC and scaffold microtubules, was shown to spatially coordinate the correct segmentation of daughter cells in *T. gondii* endodyogeny and in *Plasmodium* schizogony^{88,89}. The pellicle serves as the scaffold for the forming cell where the other cellular components are transported to and the membrane is built around it eventually.

Although most insights into cytokinesis come from *T. gondii* endodyogeny, the basic mechanisms are believed to be conserved in *P. falciparum* schizogony⁸³. An ultrastructural study showed that the pellicle starts forming at the future merozoite apex, just where the spindle pole bodies were located in the precedent mitosis. At the same time, a Golgi-like compartment is established at the future merozoite apex, and secretory organelle proteins are synthesized *de novo*, which leads to the formation of dense granules, rhoptries and micronemes. Meanwhile the IMC is growing towards the distal end, supported by its subpellicular microtubules⁸⁹.

Besides, the two organelles of symbiont origin, mitochondrion and apicoplast, divide independently and migrate into the newly forming merozoite. Cytoskeletal elements, such as actin, might serve as tracks for their migration. PfActin-1 (Act-1) depletion using the DiCre system resulted in abrogated apicoplast segregation to the newly forming merozoite, with the apicoplast forming aggregates in the schizont⁹⁰. Interestingly, mitochondrial segregation to the daughter cells was not affected in the Act-1 iKO. Act-1 fulfils additional functions in cytokinesis: upon conditional depletion of PfAct-1, daughter merozoites formed that could not separate from each other, as scission of the common membrane enclosing the budding cells and the food vacuole was not complete. PfAct-1-iKO merozoites were able to egress, but stayed attached even after release, demonstrating a role of Act-1 in merozoite formation or segregation⁹⁰.

However, the understanding of molecular networks that organize merozoite budding is patchy in *Plasmodium*, with only some regulators known that take part in distinct processes during cytokinesis. The GTPases Rab11a and Rab11b for example were shown to direct vesicular trafficking during IMC biogenesis in budding, directing IMC proteins to the growing IMC⁹¹. Another protein discovered to control cytokinesis is merozoite-organizing protein (MOP). In PfMOP-depleted parasites, a proportion of daughter merozoites remain attached together or to the food vacuole, with the IMC and the overlying membrane not covering the whole merozoite. MOP localizes to the apical tip of the forming merozoites at the very beginning of cytokinesis, in close proximity to where the rhoptry neck of the future merozoites is formed. From this apical position, MOP might control IMC biogenesis and daughter cell segmentation⁹².

During the synchronous round of mitosis, the IMC scaffold is guided by centrosomes to build up at the apical end of the daughter cell⁹³. In *T. gondii*, the apical and basal part of the forming IMC are capped by two different complexes of specialized proteins and cytoskeletal structures. The basal complex forms a contractile ring at the basal end of the forming parasite. While budding progresses, the ring moves gradually to the posterior end of the forming daughter cell, probably driven by Myosin motor proteins. This movement promotes the construction of the daughter cell, and the ring constricts just when budding is complete. The major basal complex protein MORN1 has a homologue in Pf that also localizes to the basal end of budding daughter cells, and is thought to have conserved functions across different Apicomplexan species⁹⁴. The final step of cytokinesis is when every daughter cell gets covered with a new plasma membrane (PM) around the fully formed IMC. This starts by invagination of the schizont PM and then ingression to coat every merozoite⁹³. Basal complex transmembrane protein 1 (BTP1) is thought to coordinate the synchrony between IMC and PM formation, and thus to assure convergent parasite assembly⁹³. Soon after cytokinesis is completed, the egress of the fully formed merozoites starts.

1.4.3 Exit from the host cell: egress

Merozoite egress from the RBC proceeds as a series of highly orchestrated events. Merozoite egress requires disruption of the PVM, modifications of the RBC sub-membrane cytoskeleton and finally RBC membrane rupture (RBCM) (see Figure 13). The underlying signaling pathways have only partially been unraveled. However, it is consent that cyclic nucleotides, Ca²⁺ and phosphate signaling orchestrate different steps of egress. This includes the release of egress-specific secretory organelles called exonemes, leading to the activation of PV-resident proteases that are important mediators of egress⁹⁵⁻⁹⁷.

PVM rupture

At the end of schizogony, the cytokinesis of the daughter merozoites is completed, and the segmented schizont is ready for egress. *Plasmodium* exits the RBC via an inside-out mode, with the PVM being the first membrane to rupture in egress. The first morphological change observed in egress is the rounding up of the PVM, which can be blocked by the Ca^{2+} chelator BAPTA-AM⁹⁸. Activity of cGMP-dependent protein kinase (PKG) then is essential for triggering the next step, PVM rupture⁹⁹. However, molecular events already induce PVM leakage long before PKG activation. Hale *et al.* employed video microscopy, electron tomography and X-ray tomography to show that the PVM is partially permeabilized already 10-30min prior to egress. As there are no major membrane disruption visible by electron tomography, the membrane is likely permeabilized by small perturbations, such as pores, but no molecular actors have been identified for such a process¹⁰⁰. Biophysical analysis confirmed that permeabilization of the PVM is likely important for its final rupture, as it permits osmotic swelling. Analysis of infected RBCs compared to non-infected RBCs constructed a model in which osmotic swelling is the major driving force of PVM rupture and for the later rupture of the RBCM (Figure 13)¹⁰¹.

Ten minutes before PVM ruptures, activation of PKG leads to the release of the subtilisin-like serine protease SUB1 from exonemes into the lumen of the PV¹⁰². Once inside the PV, SUB1 cleaves and activates a number of parasite proteins, including MSP1, MSP6, MSP7 and the serine repeat antigen proteases SERA4, SERA5 and SERA6⁹⁵. These downstream events finally conduct to PVM rupture 1 min before final egress¹⁰⁰. PVM rupture can be experimentally blocked by selective PKG inhibitors: compound 1 and 2 (c1 and c2) reversibly inhibit PVM rupture in egress, and give rise to a similar phenotype as parasites depleted of SUB1^{96,103}.

P. falciparum encodes nine SERA proteases, which possess a central papain-like protease domain. SERA proteins are produced to accumulate mainly inside the PV in schizont stage, where they can get activated by proteolytic processing⁹⁵. Although SERA and MSP proteins get activated by the action of SUB1, they are not required for PVM rupture, but rather in opening the RBCM: SERA5, SERA6 as well as MSP1 were found to participate in modifications of the linkage between the RBC's sub-membrane skeleton and the RBCM^{96,97,104}.

Till date, the exact effectors mediating PVM lysis are not identified. Putative lytic factors are Perforin-like proteins (PLP), which possess a membrane attack complex/perforin (MACPF) domain that can insert into membranes and form pores upon oligomerization¹⁰⁵. PfPLP1 is a micronemal protein that gets inserted into the PVM and RBCM, following its Ca^{2+} dependent discharge from micronemes. When adding recombinant PLP1 to RBCs, the protein bound to RBC membranes, oligomerized and led to membrane permeabilization, a mechanism common to perforins¹⁰⁶. So Ca^{2+} signaling could activate PLP1-mediated pore formation in the PVM, but no reverse genetic study has proven this role of PLP1 *in vivo* yet.

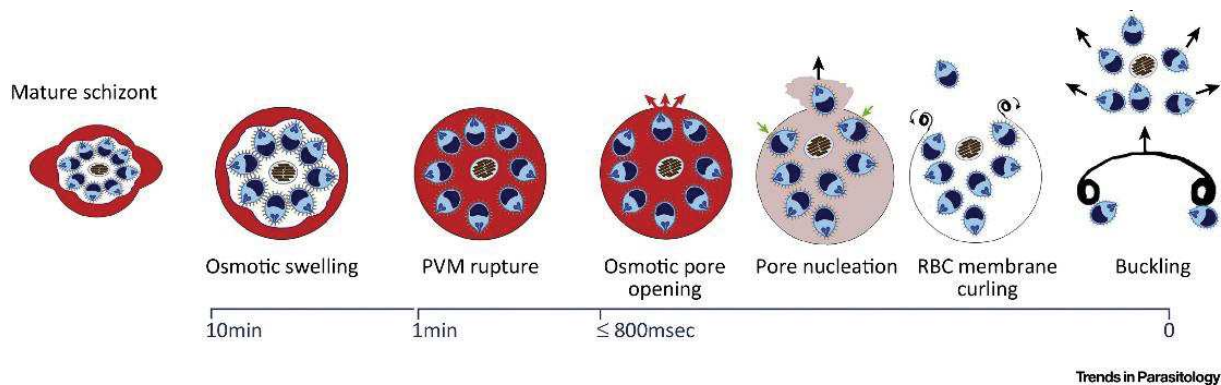


Figure 13: Model for the main steps in merozoite release. The major morphological changes of the infected RBC prior to egress are depicted. Osmotic swelling of the schizont is observed ca. 10min before egress, and later the PVM ruptures 1min before final egress. The RBCM becomes permeabilized, leading to an osmotic pore opening and pore nucleation that ejects a part of merozoites. The remaining intracellular merozoites are discharged by the buckling and curling of the RBCM¹⁰⁷.

Breakdown of the RBC skeleton and membrane

When merozoites are released from the PV, they are still encased by the RBC sub-membrane cytoskeleton and the RBCM. The parasite needs to find ways to weaken these host barriers for getting out of the host cell. Electron and X-ray tomography enabled the observation of major changes in RBC structure just after PVM rupture: the RBCM partially loses its structural scaffold and collapses upon the parasites¹⁰⁰. This change in RBCM structure is likely caused by the modification and partial digestion of the RBC cytoskeleton, a process likely performed by proteases⁹⁶. The subsequent opening of the RBCM, occurs only seconds before egress. According to the biophysical model (Figure 13), this pore opening initiates merozoites release, followed by RBC membrane curling and buckling to expulse the remaining merozoites. The authors claim that parasite-induced modifications of the RBC skeleton are a prerequisite for this curving and buckling to happen¹⁰¹.

The importance of proteases for RBCM breakdown can be experimentally shown using E64, a broad-spectrum cysteine protease inhibitor. E64 treatment of late schizonts permits PVM rupture, but prevents the final RBCM rupture, likely by inhibition of the responsible proteases¹⁰⁸. As E64-treated schizonts display the same phenotype as SERA6-iKO parasites trapped inside the RBCM after PVM rupture, SERA6 was proposed to be the major target of E64 (Figure 14A)⁹⁶.

SERA6 is the only protease proven to mediate the final RBCM opening, as parasites depleted of SERA6 develop till schizont stage and lyse the PVM, but are not capable to open the RBCM (Figure 14A). The mode of action of SERA6 is its processing of RBC cytoskeleton β -spectrin⁹⁶. $\alpha_2\beta_2$ -spectrin tetramers form filaments that connect the junctional complexes which link the cytoskeleton to the RBCM. Therefore SERA6 activity likely initiates partial dissociation of the spectrin network which could facilitate RBCM destabilization (Figure 14B)⁹⁶.

Besides SERA6, MSP1 is another SUB1 target that plays a role in destabilizing the RBC skeleton and membrane¹⁰⁴. SUB1 cleaves the primary MSP1 into four fragments that remain non-covalently attached and are translocated to the merozoite surface where they remain membrane-linked via a GPI anchor on MSP1₄₂ and MSP1₁₉ (see Figure 6)¹⁰⁹. SUB1-mediated cleavage, and especially the cleavage site generating the 38 and 42kDa fragments was found to be important for egress, as egress was delayed in parasites depleted of the 38/42 cleavage site. Protein structure analysis and protein binding assays suggest that the 38/42 processing exposes heparin and spectrin binding sites on these MSP1 fragments. Furthermore, parasites lacking the N-terminal GPI anchor of MSP1, and therefore lacking the MSP1 complex on their surface, present defective egress, with merozoites staying trapped in incompletely ruptured membranes. These results highlight the importance of the SUB1-mediated

processing for MSP1 function, and that the tetrameric MSP1 complex deposited on the merozoite surface has two distinct roles, one in egress and one in invasion^{28,97}.

SERA5 on the other hand was found to be a factor that slows down merozoite egress, and which is important, but not essential for egress⁹⁷. In absence of SERA5 parasite re-invasion efficiency gets reduced by 50%, which was due to premature inefficient egress. However, egress of the SERA5-iKO was defective in many cases, with the merozoites not properly dispersed as many of them were trapped in incompletely ruptured membranes. SERA5 therefore is believed to delay RBCM rupture until other effectors have properly destabilized the RBC cytoskeleton and membrane⁹⁷.

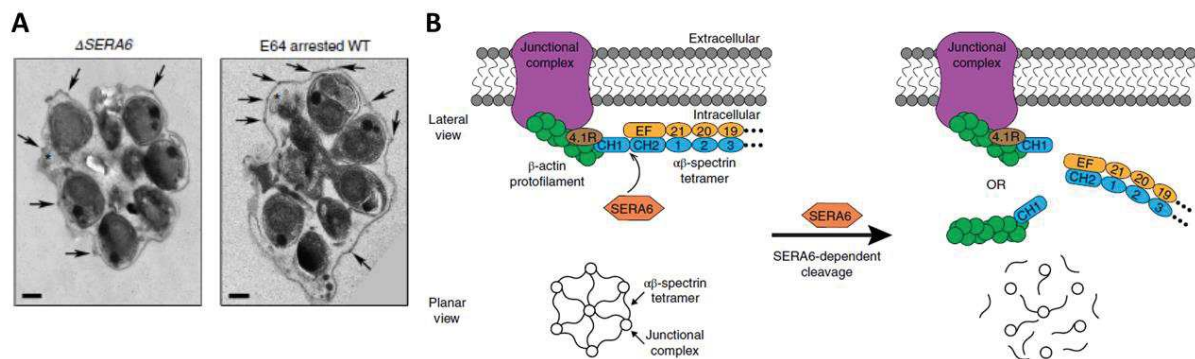


Figure 14: SERA6 functions in egress by breaking down the RBC submembrane skeleton. (A) TEM micrographs of arrested SERA6-iKO schizonts, which show a similar phenotype as E64-arrested schizonts. Both show remnants of ruptured PVM (asterisks) close to the trapped merozoites. Knobs (arrows) are visible on the undamaged RBCM. Scale bars 500nm. (B) Model of SERA6-mediated processing of β -spectrin, leading to the breakdown of the RBC submembrane skeleton⁹⁶.

PLPs might be effectors for the final RBCM permeabilization, as they were found to translocate to the RBCM after their discharge from micronemes¹⁰⁶, analogous to the reported PLP-mediated permeabilization of the host cell membrane in *T. gondi*¹¹⁰.

In conclusion, egress requires the controlled discharge of egress-specific apical organelles, such as exonemes. Micronemes on the other hand have been strongly associated with invasion, as they store the adhesins of the EBL family and AMA1, as well as the merozoite surface sheddase SUB2^{32,37,49}, but the CDPK5-dependent AMA1 secretion has recently also been described to be essential for egress¹¹¹. On the other hand, PfPLP1 and PfPLP2 are secreted from micronemes and might function in egress by mediating membrane permeabilization¹⁰⁶. PfPLP2 was shown to play a similar role in egress of the sexual blood stages, although it is dispensable in the asexual stages: PLP2 is also released from micronemes in a Ca^{2+} -dependent manner, and is required for RBCM rupture when activated gametocytes egress from the host RBC¹¹². So finally a subset of micronemes might also play egress-specific functions. This would imply PLP discharge to be triggered specifically prior to PVM or RBCM rupture, and regulation of secretion might involve action of a CDPK.

Chapter 2: Phosphorylation in *Plasmodium*

2.1 General aspects of protein phosphorylation

2.1.1 Generalities

Reversible protein phosphorylation is one of the most essential mechanisms to control cellular functions. In eukaryotic cells, phosphorylation occurs on three major hydroxyl-containing amino acids, serine (Ser), threonine (Thr) and tyrosine (Tyr), resulting in the formation of stable phosphomonoesters.

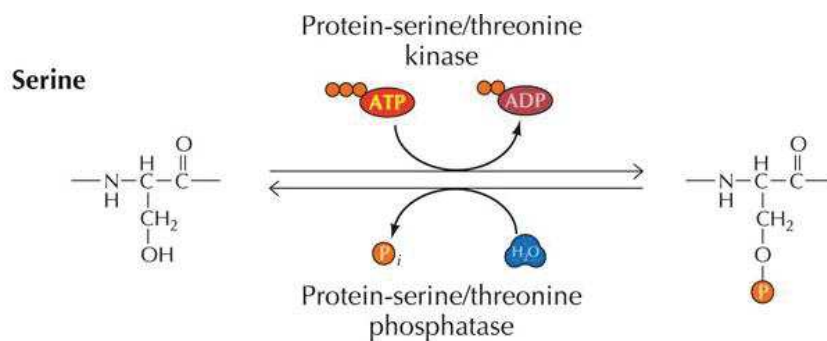


Figure 15: Scheme of reversible protein phosphorylation by kinases and phosphatases¹¹³

From these three amino acids, serine is by far the most common residue to be phosphorylated, as exemplified by a phosphoproteomic analysis in human cells: the relative abundance of phosphoserine, phosphothreonine and phosphotyrosine are 86.4%, 11.8% and 1.8%, respectively¹¹⁴. Apart from these major targets of phosphorylation, the amine group of arginine, lysine and cysteine can also be reversibly modified by eukaryotic protein kinases and phosphatases. This leads to the formation of acid-labile phosphoramidates, which play important roles in signal transduction and other regulatory processes¹¹⁵.

2.1.2 *Pf* kinome

Two independent *in silico* analyses of *P. falciparum* genome allowed the identification of genes encoding 86 or 99 putative protein kinases (PKs) depending on the stringency of the analysis^{116,117}. Strikingly, *P. falciparum* has much more kinases with the conserved ePK catalytic sites than *P. berghei*, with 86 compared to 66 predicted kinases, respectively (Figure 16). From these, 64 kinases are orthologous pairs.

The large superfamily of ePKs is defined by a conserved domain structure and catalytic site residues: 12 sub-domains termed I to XII fold to form the catalytic core structure¹¹⁸. Three catalytic residues are present in an active ePK: an ATP-binding Lys, an Asp in the catalytic loop and a DFG motif where Asp chelates the Mg²⁺ ion. The ePK superfamily includes serine/threonine kinases (STKs) as well as tyrosine kinases (TKs). TKs evolved from STKs and are characterized by an additional catalytic loop motif that discriminates them from all STKs. However, some STK can also phosphorylate tyrosine residues. TKs are subdivided into transmembrane receptor TKs that function as dimers (e.g. growth factor receptors: EGF receptor), and cytoplasmic TKs (JAK, FAK, Syk) on the other hand¹¹⁹. *Plasmodium* possesses no TKs, but only Tyrosine kinase-like (TKL) proteins, which despite their similarity to TKs display Ser/Thr kinase activity. Other major ePK families that are conserved between eukaryotes and *Plasmodium* are

cyclic nucleotide and Ca²⁺/phospholipid-dependent kinases (AGC), Calmodulin-dependent kinases (CamK), Casein kinase 1 (CK 1) and CMGCs, a group that contains CDKs, CDK-like and mitogen-activated (MAPK) kinases¹¹⁶, as shown in Figure 16. However, other kinase families are divergent between *Plasmodium* and most eukaryotes, such as the Apicomplexan-specific FIKK kinases and the Calcium-dependent protein kinases (CDPKs) found in plants and Apicomplexa. Apart from ePK family kinases (Figure 16), *Plasmodium* encodes so-called “atypical protein kinases”, among others two RIO kinases, and two putative members of ABC1 kinases. RIO family kinases are found in organisms from Archaea to humans and were shown to mediate rRNA processing and ribosome biogenesis in yeast¹¹⁶.

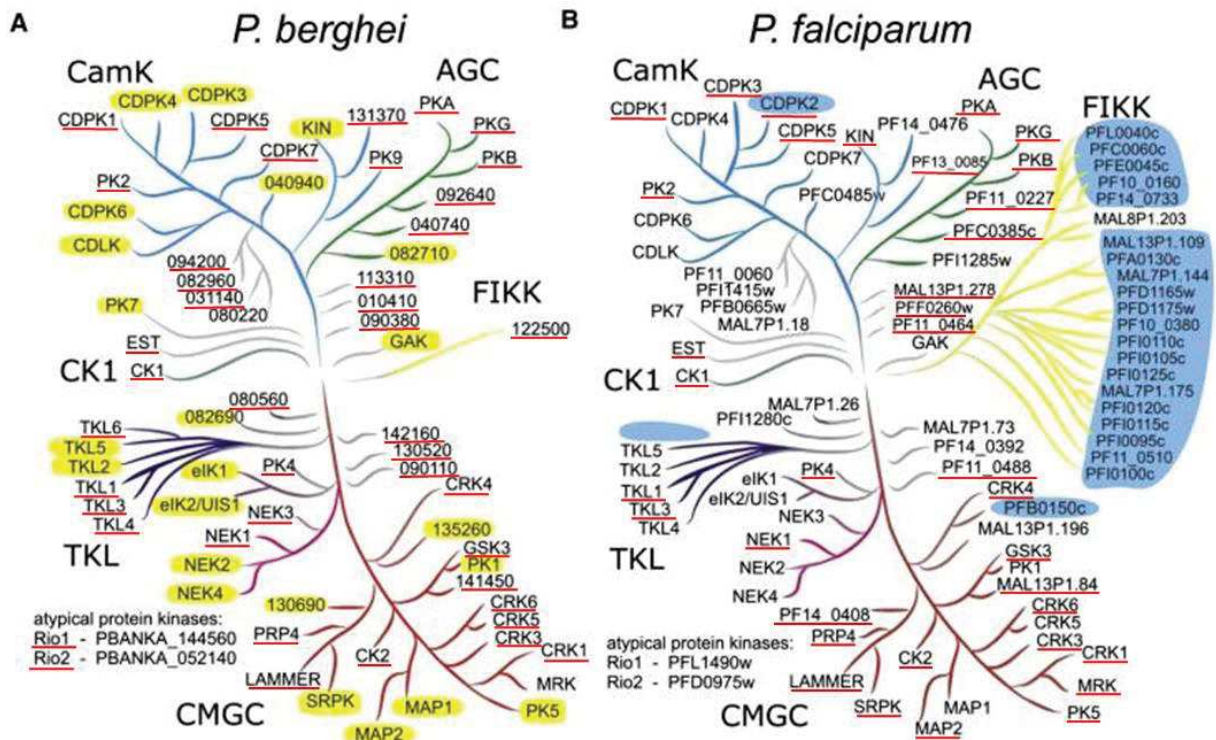


Figure 16: Phylogenetic tree of *Plasmodium* ePKs. Likely essential kinases are underlined in red^{120,121}. (A). The ePK family kinases of *P. berghei* are depicted. Kinases with homology to human kinases are highlighted in yellow. (B) *P. falciparum* proteins containing ePK domains. Highlighted in blue are kinases that differ between *P. falciparum* and *P. berghei*¹²⁰.

The surplus of kinases in *Pf* compared to *Pb* can be merely attributed to the expansion of an Apicomplexa specific group of ePK-related proteins namely the FIKK kinase family comprising 20 members¹²². The FIKK family was termed on the basis of the conserved Phe-Ile-Lys-Lys amino acid motif. Only *P. falciparum* and *P. reichenowi* have an expanded repertoire of FIKKs, whereas all other *Plasmodium* species have only one member. They possess a C-terminal catalytic domain with conserved motifs involved in phosphotransfer, amino acid targeting and catalysis, but they lack a glycine-rich loop for ATP anchoring in subdomain I, and therefore have restricted homology to described ePK groups⁶. *P. falciparum* FIKKs display an N-terminal signal sequence followed by an export motif known as the PEXEL motif that targets proteins outside the PV, and accordingly, most of them were shown to be exported in the RBC^{123,124}.

Another feature of *Plasmodium* kinome is the presence of a family of calcium-dependent protein kinases or CDPKs, that are found in great diversity in plants, but also in Alveolata¹²⁵. Canonical CDPKs are composed of an N-terminal Ser/Thr kinase domain and four EF hand domains. However, there are several CDPK families that are characterized by a slightly variant domain structure. A short inhibitory domain links the EF hand domains to the kinase domain. Ca²⁺ activates CDPKs by binding to the EF-

hands. This results in a conformational change of the whole protein, which will activate kinase activity. CDPKs are likely sensors of Ca^{2+} frequency modulation. However, they also sense the amplitude of Ca^{2+} signals: different isoforms possess different Ca^{2+} activation thresholds, which also depend on the substrate. Therefore, CDPK activity towards diverse substrates is differentially regulated by Ca^{2+} ¹²⁶. *Plasmodium* encodes 6 or 7 CDPKs, depending on the species. *Plasmodium* CDPKs are important Ca^{2+} effectors and were shown to regulate translational control, microneme secretion, egress from the erythrocyte, ookinete and liver stage motility, as described in details in the following sections^{127,128}.

Reverse genetic studies highlighted the importance of kinases in *P. falciparum*¹²¹ and *P. berghei*¹²⁰. In an attempt to knock out the 65 ePKs of *P. falciparum*, 36 ePKs were found likely essential for the asexual parasite stages¹²¹ (highlighted in Figure 16B). For *Pb* on the other hand, 43 kinases could not be knocked out in the erythrocytic stages and are therefore likely essential. The 23 remaining kinases are dispensable in blood stages, but 8 of them are essential for the completion of the parasite development in the mosquito¹²⁰.

2.2 Phosphoproteomic studies: phosphorylation is a widespread post-translational modification during *P. falciparum* intraerythrocytic growth

Protein phosphorylation is important for *Plasmodium* to regulate cellular processes, as nearly half of parasite kinases are essential¹²¹.

Several global phosphoproteomic analyses have been conducted for *P. falciparum* asexual stages that differ in the parasite stage analyzed, and also in technical aspects such as sample preparation and data processing. Here we aim to summarize the most important findings. Every phosphoproteome study revealed different subsets of phosphoproteins, with some degree of overlap. The combined data on the schizont phosphoproteome reported a total of 12 525 phosphosites¹²⁹.

The phosphoproteome of 3 stages of *P. falciparum* intra-erythrocytic development

To understand how the parasite regulates its asexual development within RBC, Pease *et al.* performed a global quantitative phosphoproteomic analysis at 3 stages of its asexual growth, i.e. ring, trophozoite and schizont and analyzed the phosphorylation changes associated with parasite maturation. They detected 2767 proteins of parasite origin, which represent 55% of the predicted proteome. Half of those were phosphorylated at some stage of the intraerythrocytic development, giving 6293 phosphosites from 1337 proteins. Next the group analyzed how phosphorylation sites develop over the intra-erythrocytic cycle. 34% of the identified proteins and 75% of phosphosites show changes in abundance as the erythrocytic cycle progresses, and only 19% of phosphosites were identical in all three stages. The absolute number of phosphosites decreases from rings to trophozoites, and then peaks in schizont stage¹³⁰.

Tyrosine phosphorylation in the parasite

Pease *et al.* found that the majority of phosphorylations occurred on Ser residues (82%), followed by Thr (13.5%) and Tyr (4.5%)¹³⁰. This proportion of Tyr phosphorylation is higher than the ~1% reported in other studies. It is curious that no protein tyrosine kinase was found *in silico* in the *Plasmodium* genome. This raises the question if *Plasmodium* codes for a yet unidentified Tyrosin kinase, or if the parasite's dual specificity kinases (DYRKs) are responsible for the Tyr phosphorylations observed. DYRK proteins are defined as dual-specificity protein kinases because they have phosphorylation activity on tyrosine, serine, and threonine residues, although the tyrosine phosphorylation activity is restricted to

autophosphorylation¹³¹. So the presence of phospho-Tyr does not necessarily imply the presence of a parasite strict Tyr kinase activity¹²¹.

Another possibility is that host kinases are responsible for Tyr phosphorylations on parasite proteins. Host kinases could be activated or recruited by parasite-induced signaling.

Several studies have demonstrated PTK activity in *Plasmodium*. A membrane-bound PTK activity was detected in all RBC stages, with increasing activity from ring to trophozoite stage. PTK activity then decreased during transition from schizonts to merozoites¹³². In a later study Kumar *et al.* used an *in vitro* kinase assay to confirm a PTK activity in asexual *P. falciparum* extracts that was inhibited by PTK inhibitors. Furthermore, the group searched for Tyr-phosphorylated proteins in *Pf* extracts using metabolic labeling and α -Phospho-Tyr immunoblot detection. Two major Tyr-phosphorylated proteins were detected, at 52 and 58 kDa, and those proteins were hyper-phosphorylated in presence of the PTP-inhibitor vanadate¹³³.

Solyakov *et al.* found that most Tyr phosphorylated substrates are parasite kinases, such as PfGSK3 and PfCLK3. Nevertheless, Tyr phosphorylation on GSK3 and CLK is likely the result of Tyr autophosphorylation activity of these Ser/Thr kinases, because such activity was demonstrated for the mammalian GSK orthologue. CLK3 is phylogenetically related to the DYRKs family¹¹⁶. Tyrosine phosphorylation is less frequent in extracellular merozoites (0.4 % of phosphosites) than in schizonts (2.4 %)¹³⁴. This suits the model in which host Tyr kinases are responsible for parasite protein Tyr phosphorylation. Host TK activity is not present anymore in the extracellular merozoites, while parasite PTPs take charge of removing the phosphate groups from tyrosine residues, thereby reducing the amount of Phospho-Tyr.

The schizont phosphoproteome

Three independent studies investigated the phosphoproteome of the schizont stage^{121,129,135}. They differ in technical aspects such as sample preparation and data processing, as well as in the synchrony of the parasites collected for the analyses. Yet, enrichment of proteins involved in specific functional classes was reported:

- Among the parasite phosphoproteins, many invasion-related proteins and proteins of the apical complex were found¹²⁹, such as AMA1, MSP1, MSP7 and rhoptry proteins like CLAG3.1, RhopH3 and RAP-1¹²¹. If phosphorylation is important for the correct functioning of these adhesins, they likely get phosphorylated shortly after they get synthesized, or while they are inside their secretory organelles. For CLAG3.1 for example the phosphorylated protein was detected via an antibody in the rhoptries of budding merozoites inside schizonts. CLAG3.1 was proposed to have functions in adherence and invasion as well as nutrient import, and its phosphorylation might be crucial for protein function¹²¹.
- Many parasite kinases were found to be phosphorylated on Thr or Tyr residues^{129,135}. Some of these phosphorylation events occurred in the activation loop of the respective kinase, such as T¹⁸⁹ of PKA or Y²²⁹ of glycogen synthase kinase (GSK), which in the respective mammalian kinase orthologues was shown to be essential for full kinase activity¹²¹. This suggests that many kinases are regulated by phosphorylation, which seems important specifically in schizont stage. Several kinases were shown to be functionally important during schizogony, so it is consistent that kinases are a major target of regulation by phosphorylation in this stage.
- Another group of proteins highly phosphorylated in schizonts are parasite proteins exported to the host cell (see Figure 17)^{121,135}. *Plasmodium* exports proteins for parasite survival, particularly for having access to nutrients or enabling egress. The importance of

phosphorylation for the function of exported proteins has not been investigated yet, but would be interesting to study.

- “Cell cycle and DNA processing” proteins were found phosphorylated. Lasonder *et al.* confirmed that proteins involved in DNA replication initiation and chromosome packing are highly phosphorylated¹³⁶. These phosphorylations are therefore specifically relevant for schizogony, as schizogony comprises DNA replication and mitosis.
- One last category of proteins was found enriched in schizonts: motility and locomotion¹³⁶. So it seems the schizont is already “priming” its motor machinery for the future functions in merozoites.

In summary, proteins belonging to the following parasite functions are linked to extensive phosphorylation in schizonts: invasion, gliding and motility, exportome, cell cycle and DNA processing and pathogenesis.

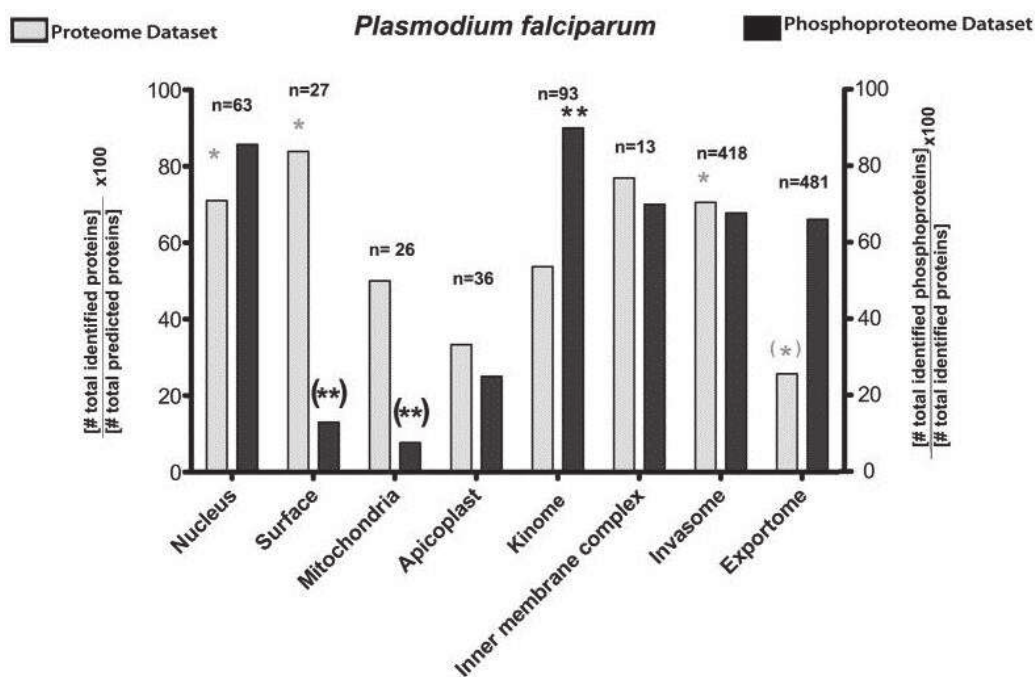


Figure 17: Functional protein groups detected in the Pf proteome and phosphoproteome by Treeck *et al.* The total number of predicted proteins *n* is indicated. * means over/underrepresentation, ** means significant over/underrepresentation within the total predicted proteome¹³⁷

The merozoite phosphoproteome

The Holder group analyzed how the phosphoproteome changes when late intraerythrocytic parasites develop into extracellular merozoites^{134,136}. They found 740 merozoite proteins phosphorylated on 1765 phosphosites. Comparison to the schizont phosphoproteome previously investigated by the group showed that 44.5% of phosphosites were unique to merozoites. MSP1 and EBA181 for example are exclusively phosphorylated in extracellular merozoites, whereas SUB2 S₁₂₄₀ is specifically phosphorylated in schizonts. MSP1 and EBA181 are adhesins important for merozoite invasion, and SUB2 is a protease secreted prior to egress, so the timely specific phosphorylation of these proteins seem to be important for their respective functions.

Some protein classes were specifically phosphorylated in merozoites compared to schizonts, as demonstrated by gene ontology (GO) enrichment, and presented in Figure 18. Proteins of the autophagy machinery, such as protease activities, the proteasome and ubiquitylation were found

enriched in the merozoite phosphoproteome. Protein degradation could be an important biological process in merozoites and regulated by phosphorylation, as the morphological changes from schizont to merozoites might be accompanied by the degradation of schizont-specific proteins. Also proteins involved in locomotion and movement, as well as in the cellular response to stress were specifically enriched among merozoite phosphopeptides¹³⁴. As merozoites in the blood are exposed to stress and starvation, and need to invade a host cell, likely aided by their actomyosin motor, it seems that proteins regulating these functions are specifically regulated by phosphorylation at this stage.

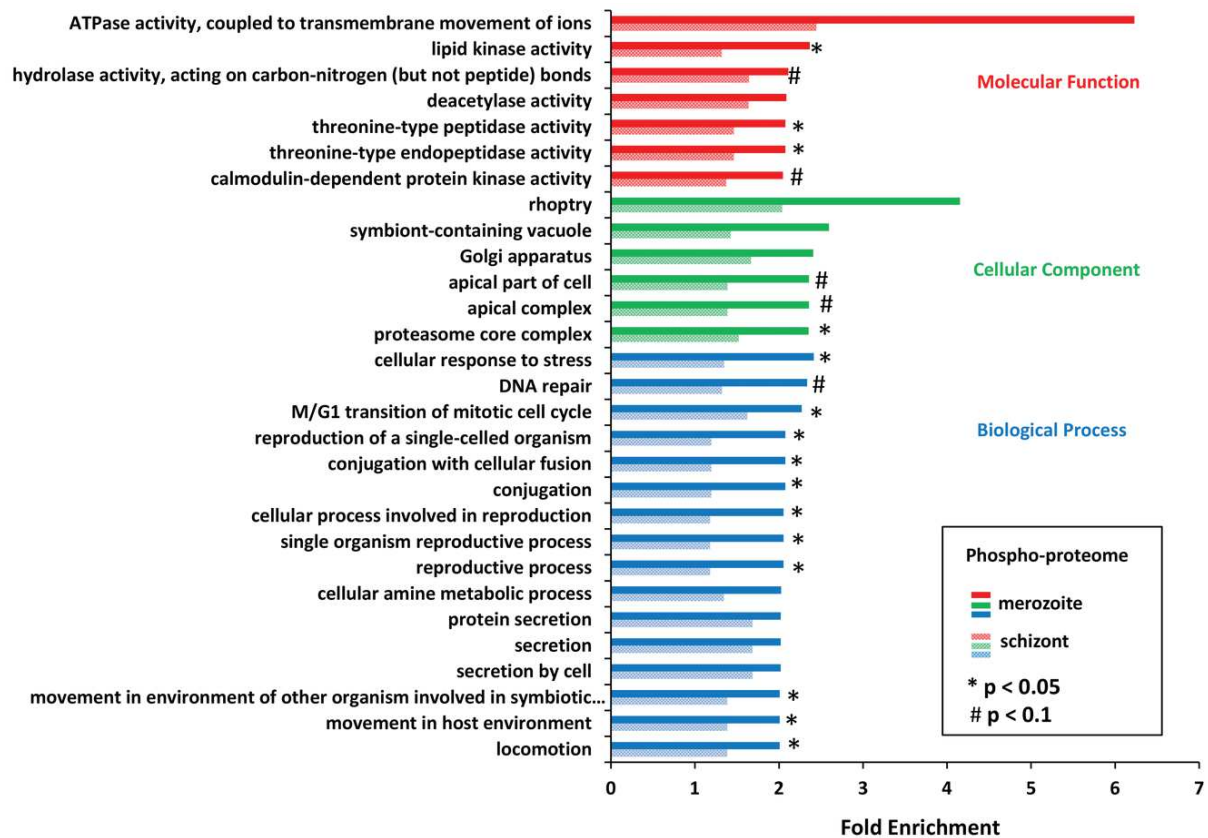


Figure 18: GO functional annotation and enrichment of phosphoproteins, comparing schizonts and merozoites by Lasonder et al. Comparative GO enrichment analysis between schizonts and merozoites. Fold enrichment was calculated relative to all 5500 *P. falciparum* proteins¹³⁴.

So overall the phosphoproteomic studies in *Plasmodium* have generated a valuable list of phosphosites all over the parasite's proteome. These studies additionally have shown that specific protein functions are regulated by phosphorylation in a stage-specific manner. The phosphoproteome is the basic database, and the challenge is now to validate and functionally characterize the reported phosphorylations on a single protein level.

The current knowledge of those phosphorylations... that were already demonstrated to be crucial for parasite invasion, schizogony and egress, are presented in the following subchapters.

2.3 Phosphorylation as an important regulator of *P. falciparum* RBC cycle

Phosphoproteomic studies revealed which parasite and host proteins are phosphorylated at specific stages. However, single protein approaches are necessary for uncovering the responsible kinases and understanding the function of a specific phosphorylation for the parasite cycle. In the following

subchapters, the current knowledge about specific protein phosphorylations and their role in *Plasmodium* development are presented. Figure 19 gives an overview about kinases essential for different steps of RBC development.

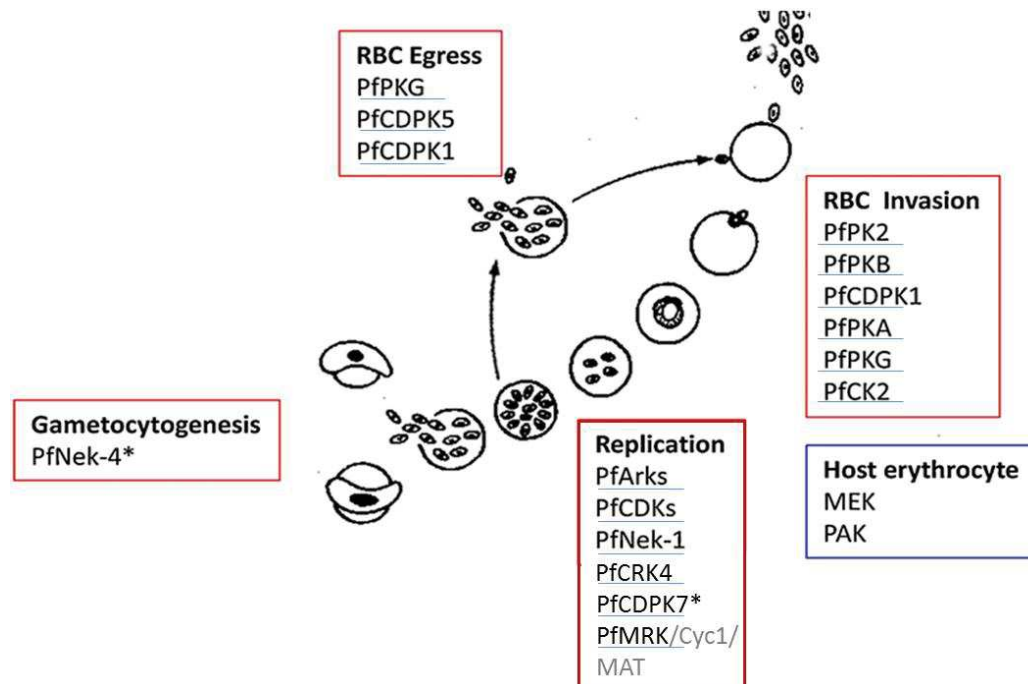


Figure 19: Plasmodium (red boxes) and host (blue box) kinases essential for different steps of the parasite's intraerythrocytic development. All kinases that could not be deleted in *Pb* are underlined in blue^{120,138}. Kinases with a * are not essential for blood stage: *PfNek-4* is highly expressed in gametocytes, but not essential for their development. *PfCDPK7* deletion impairs schizogony, but does not completely ablate parasite development. The complex of the kinase *PfMRK* with *Cyc1* and *MAT* was shown to be essential for cytokinesis, and *PfMRK* could not be deleted neither in *Pf* nor in *Pb*^{120,121,139}. Both *MRK* and *CRK4* belong to the CDK-related kinases. This scheme was adapted from¹²⁸.

Phosphorylation plays a role in egress and invasion by different mechanisms. First, phospho-signaling involving key parasite kinases is central to secretory organelles discharge required for egress and invasion to take place. Second, the gliding machinery known as the glideosome was shown to be differentially phosphorylated, suggesting a mode of controlling the merozoite acto-myosin motor necessary for invasion, although the precise function of these phosphorylation events is still not fully understood. Third, the phosphorylation of the cytoplasmic tails of merozoite surface adhesins has been shown to be required for proper invasion, which might be part of intracellular signaling or simply regulate adhesion.

2.3.1 Phospho-signaling and secretory organelle discharge

In Apicomplexan parasites, the discharge of specialized apical organelles is critical for parasite egress and invasion, and is controlled by phospho-signaling. The first apical organelles to be discharged in late schizonts are exonemes, and their release of SUB1 is controlled by PKG^{95,99}. Next, a subset of micronemes containing AMA1 and EBA175 is secreted, triggered by the PKG and CDK5 kinases prior to egress. Once the merozoite is egressed, the secretion of other subsets of micronemes is induced⁴⁸. Adhesins essential for invasion indeed, are stored in micronemes, and therefore the timely translocation of these adhesins is necessary for the merozoite's ability to invade a new RBC. Rhoptries and dense granules discharge is induced in the merozoite attached to the RBC, and is necessary for establishing successful invasion⁷².

2.3.1.1 Phospho-signaling leading to egress: PKG and CDPK5

Once the merozoites are fully formed, they need to rupture first the PVM, and then the RBCM to egress. This requires a highly regulated series of events involving signaling via second messengers, and phosphorylation cascades to activate the proper effectors in a coordinated manner. PKG and CDPK5 activate signaling pathways that are indispensable for parasite egress, leading to microneme and exoneme secretion prior to egress^{99,111}.

PKG

Investigating *Pf*PKG function experimentally largely benefited from the availability of two small-molecule inhibitors, compound 1 (c1) and compound 2 (c2). They specifically inhibit Apicomplexan PKG in a competitive and reversible manner¹⁴⁰. Taylor *et al.* treated infected RBC with c1 or c2 and observed a complete block of egress and thus showed the essentiality of PKG for egress¹⁰³. As control, a parasite line was engineered to express c1-insensitive PKG. These c1-insensitive parasites showed no growth or egress defect upon c1 or c2 treatment, but were inhibited by the broad-spectrum kinase inhibitor staurosporine¹⁰³.

Based on these findings, the Blackman group set out to understand the molecular mechanisms of the PKG inhibitor-mediated egress block¹⁰². They found that PKG activity is necessary for microneme secretion as well as for the discharge of the serine protease SUB1 into the PV from exonemes at the time of egress. This would allow SUB1 to access its substrates, among which cysteine proteases of the SERA family. Processing of SERA5 and SERA6 are necessary for efficient egress. Next, they artificially increased the cGMP level by Zaprinast, a cyclic nucleotide phosphodiesterase (PDE) inhibitor. Interestingly, Zaprinast treatment led to rapid MSP1 and SERA5 processing and premature merozoite egress. Zaprinast induced egress even in young schizonts, and the released merozoites were not invasion-competent.

Apart from PKG, Ca^{2+} signaling plays an important role in egress and parasite treatment with the Ca^{2+} chelator BAPTA-AM prevents egress. Surprisingly, BAPTA-AM could not reverse the effect of Zaprinast, suggesting that either PKG downstream signaling leads to increases of cytoplasmic Ca^{2+} or that PKG alone is sufficient to induce egress in a Ca^{2+} -independent manner¹⁰².

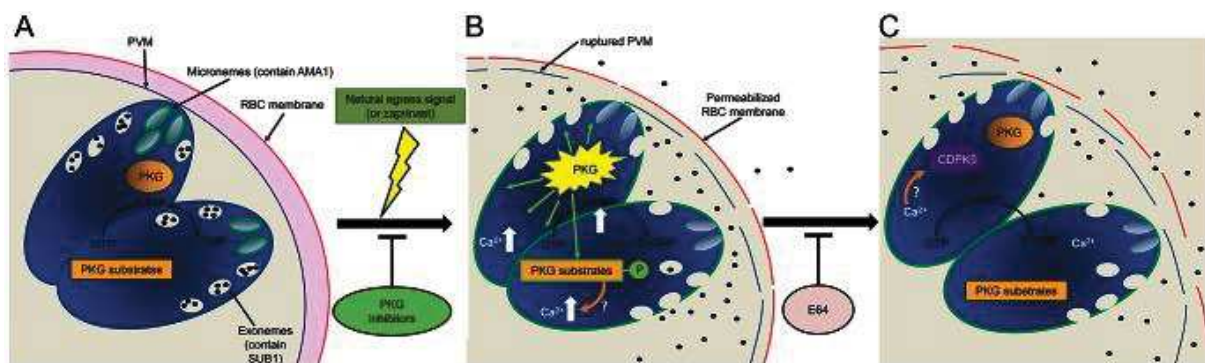


Figure 20: Model of PKG function in egress, according to ⁹⁹. (A) AMA1 is stored in micronemes and SUB1 in exonemes prior to PKG activation. (B) Cellular signaling leads to an increase of intracellular cGMP, which in turn activates PKG. PKG activity induces AMA1 and SUB1 release, possibly by Ca^{2+} signaling. AMA1 is deposited onto the merozoite surface (green). The PVM is ruptured shortly after. (C) The Ca^{2+} peak activates CDPK5 which collaborates to assure the final steps of egress. A more recent study suggested another model with CDPK5 action being required already at earlier steps of egress (Figure 21)

cGMP and Ca^{2+} signaling are connected via phosphoinositide metabolism, as was recently shown in *P. berghei* ookinete gliding motility as well as *P. falciparum* merozoite egress¹⁴¹. PKG acts upstream of Ca^{2+} -signaling as c2-mediated PKG inhibition leads to a drop of intracellular Ca^{2+} , which renders ookinetes nearly immobile. PKG activity leads to an increased production of the second messenger

inositol (1,4,5) triphosphate (IP₃), followed by the mobilization of Ca²⁺ from intracellular stores¹⁴¹. IP₃ is generated by hydrolysis of the membrane lipid phosphatidylinositol (4,5) bisphosphate (PIP₂) by phospholipase C (PLC) activity. PLC is likely a downstream target of PKG, as PDE inhibition in schizonts results in the stimulation of PIP₂-hydrolysis accompanied by a Ca²⁺ peak¹⁴¹.

Besides, PKG was shown to control the enzymes responsible for the phospholipid synthesis pathway which generates PIP₂ and IP₃. Membrane-resident PIP₂ is synthesized in two reactions from phosphatidylinositol (PI) by lipid kinases. PKG inhibition changed the lipid composition in the ookinete's membranes, accumulating the non-phosphorylated precursor PI whereas the amount of PI₄P and PIP₂ decreased. So PKG controls IP₃ synthesis and release, and can generate a downstream Ca²⁺ signal, which activates diverse CDPKs.

Indeed, Ca²⁺ is the trigger to activate CDPK5, the second major kinase in egress signaling, as described in the next section^{111,127} (see Figure 20).

CDPK5

CDPK5 was shown to be essential for merozoite egress from the RBC¹²⁷. Conditional knockdown of CDPK5 resulted in parasites that developed normally until the late schizont stage, but that were completely blocked in egress. One of the earliest events in egress, PVM rupture was prevented in the CDPK5-KD, but could be induced by PKG stimulation with the PDE inhibitor BIPPO^{111,127}. In order to understand the mechanism how CDPK5 participates in egress, SUB1 discharge and SUB1-mediated processing of SERA5 and MSP1 were monitored, showing that SUB1 secretion occurred normally in the CDPK5-KD¹²⁷. Still, the downstream protease processing of SERA5 and MSP1 was slowed down in absence of CDPK5¹¹¹. The major defect of the CDPK5-KD schizonts was their incapability to secrete AMA1 and EBA175 from micronemes prior to egress. However, the block of both AMA1 and EBA175 translocation in the CDPK5-KD could be overcome by BIPPO-mediated PKG stimulation¹¹¹. So it seems that an increase in PKG activity can partially substitute for or complement CDPK5 function. Absalon *et al.* made another interesting observation: mechanical release of merozoites from egress-blocked CDPK5-KD schizonts induced AMA1 discharge onto the surface of merozoites, which were able to re-invade. They suggest that the physical shearing force or contact of the merozoite with the extracellular medium induced a PKG-dependent translocation of AMA1 to the merozoite surface, rendering the merozoites invasion-competent. AMA1 and EBA175 are merozoite surface adhesins required for invasion, and no study has shown a function of these molecules in egress^{38,49}. Therefore the egress block in CDPK5-KD schizonts could indicate that CDPK5 functions in the secretion of additional, not yet described micronemal proteins specific for egress, such as PLP1¹⁰⁶.

So all in all, CDPK5 and PKG have complementary or overlapping functions in microneme secretion, PVM rupture and egress. A model integrating CDPK5 and PKG functions in egress is depicted in Figure 21.

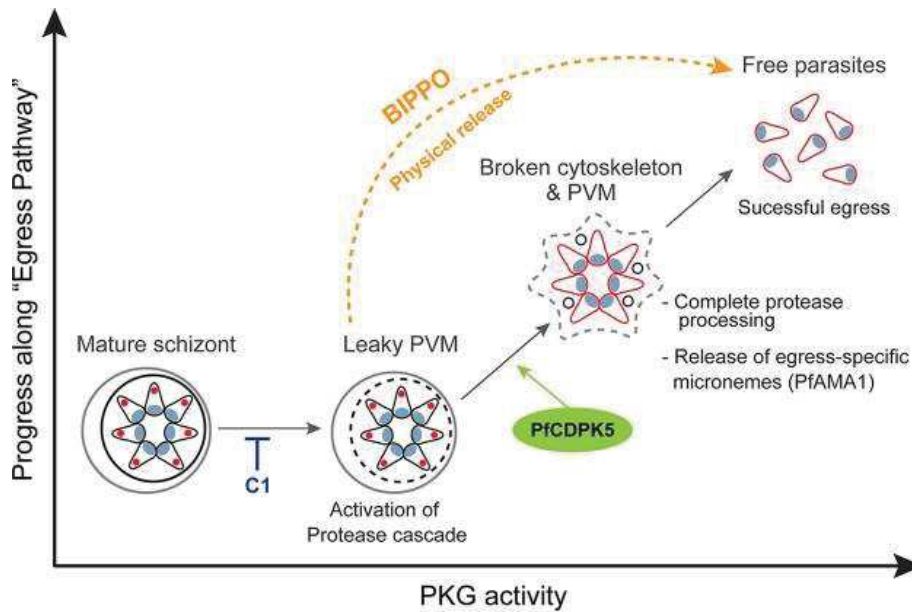


Figure 21: Model for the cooperative action of CDPK5 and PKG required for merozoite egress¹¹¹. PKG activity increases when egress is approaching, and activates CDPK5. CDPK5 then is required for AMA1 release from micronemes. Both CDPK5 as well as PKG are required for successful egress. BIPPO, a PDE inhibitor, artificially increases PKG activity to accelerate parasite egress.

Interestingly, phosphorylation also controls protease activity, as was shown for SERA5: CDPK1 is activated prior to egress by a peak in intracellular Ca^{2+} , and was shown to phosphorylate SERA5. This phosphorylation, most likely on T₅₄₉, then activates protease activity and is essential for egress to occur¹⁴².

2.3.1.2 Phospho-signaling leading to invasion: PKA and CDPK1

The parasite signaling pathways that regulate parasite invasion were first deciphered in *T. gondii*, and were later found conserved in *Plasmodium* merozoites⁴⁸. Microneme discharge in *T. gondii* tachyzoites is induced by a sequence of molecular events, beginning with the sensing of a low extracellular K^{+143} that is translated into the release of Ca^{2+} from intracellular stores¹⁴⁴, and which induces downstream effects via CDPKs and other Ca^{2+} effectors¹⁴⁵.

Merozoite surface adhesins needed for attachment to the host cell are stored in micronemes and rhoptries. Cyclic nucleotides and Ca^{2+} take part in the signaling that leads to the discharge of these secretory organelles. Merozoites get already prepared for invasion before they egress: AMA1 and EBA175 secretion from micronemes is induced just prior to egress both by PKG and CDPK5, thus depositing the major adhesins onto the merozoite surface in preparation for invasion^{99,111}. Not all micronemes are discharged before egress, but additional secretion is induced in the extracellular merozoite.

Once the merozoites are released in the extracellular medium, they are being exposed to a low K^{+} environment⁴⁸, which increases HCO_3^- and H^+ production by carbonic anhydrase (CA) to maintain the intracellular pH. These HCO_3^- ions then stimulate adenylate cyclase β ($\text{Ac}\beta$) activity, resulting in a peak of intracellular cAMP (Figure 22)¹⁴⁶. The second messenger cAMP then activates PKA, which was found necessary for the secretion of the micronemal proteins EBA175 and AMA1. Interestingly, cAMP and Ca^{2+} signaling are both necessary for microneme secretion and are even interconnected: cAMP functions through an additional response element, Epac, to induce an intracellular Ca^{2+} peak: cAMP activates Epac, a guanine nucleotide exchange factor for Rho GTPase 1 (Rap1). The activated Rap1-GTP leads to phospholipase C (PLC) stimulation, and PLC activity cleaves PIP_2

phospholipid from the parasite PM, releasing diacylglycerol (DAG) and inositol-3-phosphate (IP₃). IP₃ functions as second messenger that induces the release of Ca²⁺ from intracellular stores^{146,147}. PKG is another key player in invasion, which contributes to a peak in Ca²⁺ via stimulation of PLC¹⁴⁸. By this means signaling by cyclic nucleotides, phosphoinositides, phosphorylation and Ca²⁺ are interconnected for coordinating invasion.

One of the downstream effector of the Ca²⁺ signal is CDPK1¹⁴⁹. The function of PfCDPK1 was studied using an inducible KD strategy. The CDPK1-KD parasites showed a 40% reduction in attachment and invasion, meaning that the defect in invasion could be only attributed to an attachment defect. As described previously, merozoites attachment is mediated by different classes of adhesins. In the CDPK1-KD, discharge of EBA175 from micronemes was significantly decreased¹⁵⁰. Another study using CDPK1 inhibitors found that AMA1 secretion as well was reduced when CDPK1 activity was blocked¹⁴⁹. So CDPK1 controls the secretion of AMA-1 and EBA-175 from micronemes, which is an important step for successful invasion.

In *Toxoplasma*, a molecular mechanism upstream of Ca²⁺ and cAMP signaling was found which ultimately leads to microneme secretion. In particular, PLC is thought to be the sensor that gets activated in contact with the extracellular medium. PLC activity releases DAG and IP₃ from the parasite PM. IP₃ promotes the release of Ca²⁺ from intracellular stores, whereas DAG activates another pathway: DAG is transformed into phosphatidic acid (PA) which is sensed by an acylated pleckstrin-homology (APH) receptor on micronemes. PA binding to APH1 is thought to enable microneme fusion with the parasite PM. It remains to be studied whether this mechanism is conserved in *Plasmodium*¹⁵¹.

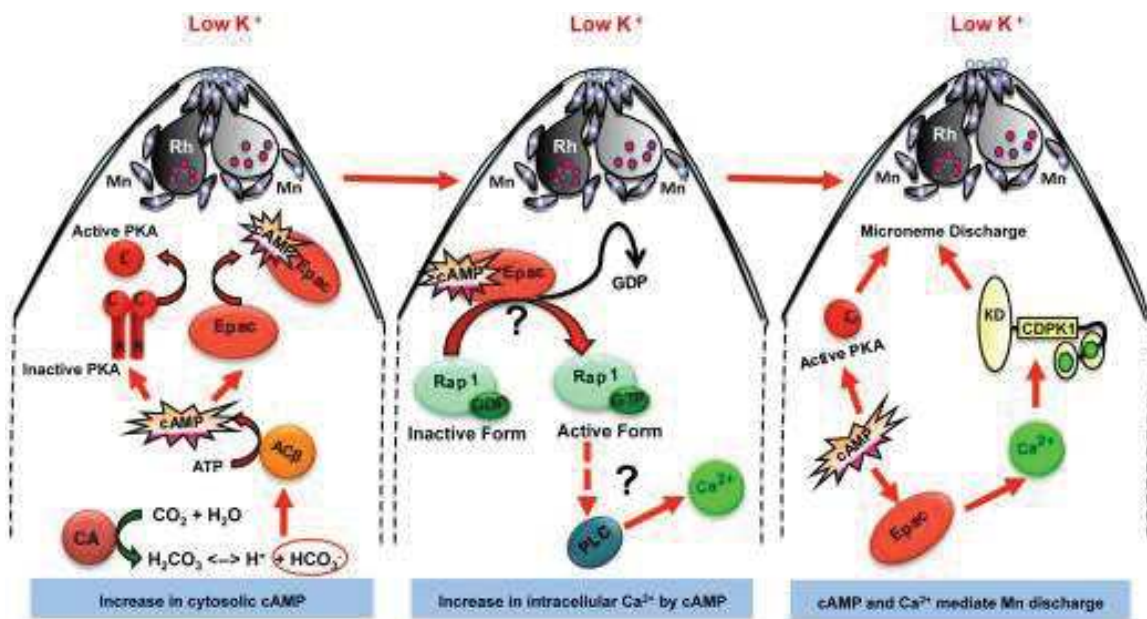


Figure 22: Model for the cAMP and Ca²⁺-mediated signaling pathways involved in microneme (Mn) and release during merozoite invasion. When merozoites encounter the extracellular low K⁺ milieu, carbonic anhydrase (CA) increases production of HCO₃⁻ and H⁺. HCO₃⁻ ions activate the soluble Adenylyl cyclaseβ (ACβ). cAMP activates PKA as well as Epac proteins that lead to an increase of Ca²⁺ via PLC activation. Microneme secretion then is induced by CDPK1 and PKA, depositing AMA1 and EBL-type adhesins (white ovals) onto the merozoite apical tip. Rhoptries (Rh) are secreted posterior to micronemes¹⁴⁶.

Interestingly, the role of cAMP in invasion seems to be conserved across different life stages of the parasite: cAMP not only is important for microneme secretion in RBC invasion by merozoites, but also for the apical organelle exocytosis necessary for sporozoite entry into hepatocytes¹⁵². *Plasmodium* sporozoites migrate through host hepatocytes until they establish an infection in a final hepatocyte. During their contact with the host cell cytosol in transmigration, the discharge of apical organelles is

triggered, leading to the deposition of the adhesin TRAP (thrombospondin-related anonymous protein) on the apical end of the sporozoites. TRAP family members link the parasite actomyosin motor to the parasite surface and host cell, and were shown to be important in sporozoites for motility and invasion. In order to understand if cAMP signaling is involved in TRAP apical exocytosis, a knockout of the transmembrane adenylyl cyclase α (AC α) was generated in *P. berghei*. The PbAC α -KO sporozoites had a defect in apical exocytosis and were less infective¹⁵². Apical exocytosis of TRAP from sporozoites is comparable to merozoite microneme discharge, as both processes are initiated by the extracellular K⁺ and depend on intracellular Ca²⁺ signals. However, it is interesting that in liver stages the transmembrane-located AC α is important. This enzyme is dispensable in RBC stages where only the soluble AC, AC β , provides the necessary cAMP peak for microneme secretion.

In conclusion, the secretion of different subsets of micronemes necessary for invasion is controlled by the cooperative action of CDPK1 and PKA.

2.3.2 Phosphorylation of adhesins and invasion

Merozoites take only 1 to 2 minutes to recognize and to invade a host RBC, so invasion needs to proceed as a series of tightly regulated events¹⁵³, most likely implicating phosphorylation and dephosphorylation processes.

As mentioned in the previous section, global phosphoproteomic studies indicated that some merozoite adhesins were specifically phosphorylated, at the schizont and merozoite stages. The first micronemal adhesin for which the role of its cytoplasmic tail phosphorylation was analyzed in detail is AMA1¹⁵⁴. In this study, the authors used an elegant complementation assay to link the cytoplasmic tail of AMA1 and invasion. The interaction between AMA1 and RON2 required for MJ formation can be inhibited in the 3D7 line by the inhibitory peptide R1, while AMA1 from W2 strain is resistant to this inhibition due to AMA1 polymorphisms. By complementing the invasion defect of a 3D7 line treated with R1 with different AMA1 constructs from the W2 line, it was demonstrated that the cytoplasmic tail of AMA1 is required to rescue the invasion defect of 3D7. The authors further showed that replacing the six predicted phosphorylated residues (Y₅₇₆, Y₅₈₅, S₅₉₀, S₆₁₀, T₆₁₃ and Y₆₂₂) in alanine (AMA1-PM) also abrogated AMA1 function (Figure 23). From these, S₅₉₀ and S₆₁₀ phosphorylations were reported in the previous phosphoproteomic studies, with the highest phosphorylation found in rings compared to trophozoites and schizonts^{121,130,136}. Therefore, AMA1 tail phosphorylation might be important either for RON2 binding or for downstream signaling within the parasite. Of these 6 residues, S₆₁₀A mutation alone was sufficient to abrogate AMA1 function. This residue was shown to be phosphorylated in a calcium- and cAMP-dependent manner by PKA¹⁵⁵. Thus, the PKA-mediated AMA1 phosphorylation is required but not necessarily sufficient to make AMA1 fully functional for RBC invasion.

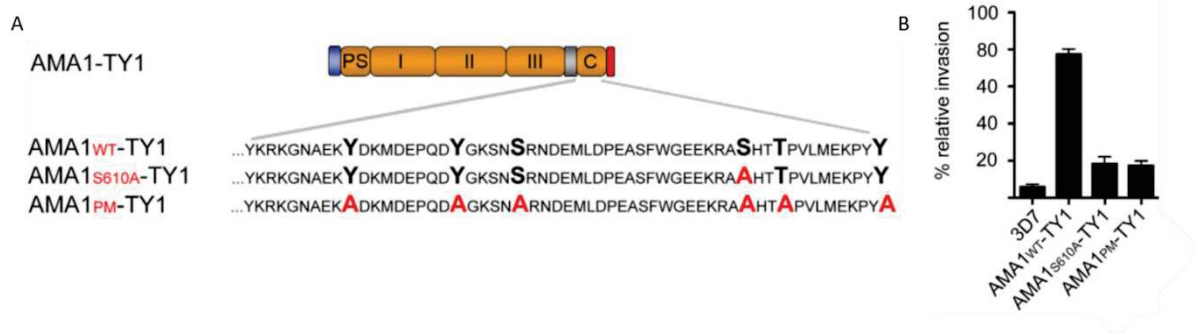


Figure 23: PfkA-mediated phosphorylation of AMA1 Ser610 is required for efficient merozoite invasion. (A) Scheme of the TY1-tagged AMA1 that was ectopically expressed. The positions of introduced phosphoablative mutations in the cytoplasmic tail (C) are indicated. Signal peptide (blue), prosequence (PS), ectodomains I, II and III, transmembrane domain (grey) and tag (red). (B) Invasion assay using the wt or mutated AMA1-expressing parasite strains. Assays were performed in presence of R1 peptide which binds to and neutralizes the endogenously expressed AMA1. Adapted from¹⁵⁵.

Interestingly, PKA-mediated Ser₆₁₀ phosphorylation enables downstream phosphorylation of AMA1 T₆₁₃ by GSK3 *in vitro*. Phospho-ablative mutation of both Ser₆₁₀ and T₆₁₃ resulted in a 80% inhibition of invasion, indicating that AMA1 is sequentially phosphorylated on Ser₆₁₀ and T₆₁₃, assuring its proper function in invasion¹⁵⁶. Additional phosphosites Ser₅₈₈ and Ser₅₉₀ were reported on AMA1, but they were shown not to be involved in invasion^{130,156}. In *Toxoplasma*, S₆₁₀ is replaced by D₅₅₈ and mutation of this residue does not alter tachyzoite invasion efficiency¹⁵⁷. However, TgAMA1 C-tail is phosphorylated on another residue (S₅₂₇)¹³⁷ and binding of a recombinant RON2 protein to TgAMA1 leads to a decrease of this phosphorylation, a pre-requisite for full invasion efficiency¹⁵⁷. Whether similar dephosphorylation of *Plasmodium* AMA1 tail is also important at some stage of the invasion process is currently unknown.

Apart from AMA1, the cytoplasmic tails of EBA-140, EBA-175, EBA-181, Pfrh2a, Pfrh2b and Pfrh4 were shown phosphorylated *in vitro* by kinases present in parasite extracts. Consistent with the presence of predicted casein kinase 2 phosphorylation sites in the C-tail of these adhesins, recombinant CK2 can phosphorylate the six tested adhesins in an *in vitro* kinase assay¹⁵⁸. Besides, CK2 has been proven to phosphorylate the Pfrh2 cytoplasmic tail on Ser₃₂₃₃ prior to host cell egress. Rh2 phosphorylation *in vivo* likely happens inside the rhoptries before Rh2 is translocated to the plasma membrane¹⁵⁹. The conditional depletion of CK2 blocks parasite growth, presumably by affecting invasion, suggesting that CK2-mediated phosphorylation of adhesins might be essential for merozoite invasion. This hypothesis has been further tested *in vivo* by substituting independently or in combination 4 C-tail residues of Pfrh4 targeted by CK2. The invasion data indicated that similarly to AMA1 C-tail phosphorylation, the phosphosites Ser₁₆₆₇, Tyr₁₆₈₀ and Tyr₁₆₈₄ are key amino acids for Rh4 function during invasion¹⁵⁸.

While phosphorylation of EBL and Rh family adhesins likely plays a functional role for *Plasmodium* invasion, it is not clear whether MSP proteins are phosphorylated in merozoites. Two studies indicate that MSP proteins are not phosphorylated in schizonts^{121,137}. However, two other studies detected 6 putative phosphorylation sites on MSP1^{130,134,136}. So further studies are needed to validate the predicted MSP1 phosphosites and to understand if this modification has importance for MSP1 function in invasion.

The importance of phosphorylation for merozoite attachment to the RBC is also illustrated by the role of the parasite phosphatase calcineurin (Cn)¹⁶⁰. Using an inducible knockdown strategy of the regulatory subunit of Cn (CnB), Paul *et al.* showed that CnB depletion has a drastic impact on *P. falciparum* asexual growth that could be attributed to a defect in invasion, independent of microneme secretion. By treating the parasites with cytochalasin D, that allows attachment but not invasion to proceed, the authors observed a 60% decrease in the capacity of the mutant to adhere to RBCs (Figure

24), thus establishing that Cn is primarily involved in the merozoite attachment step. Because of the synergistic effect of Cn depletion with inhibition of Rh- or EBL-Receptor interactions, the authors concluded that Cn is required for the function of ligand-host receptor interactions. Importantly, the function of Cn is also conserved in *Toxoplasma*.

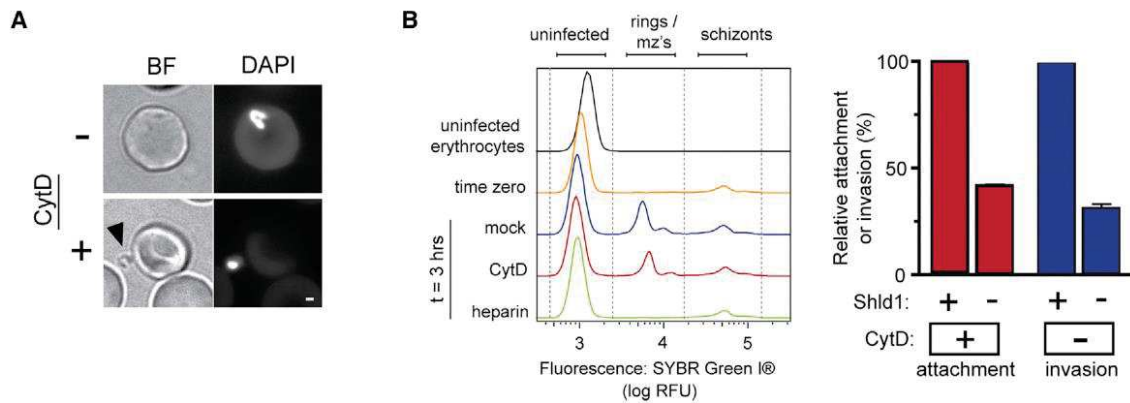


Figure 24: PfCalcineurin specifically regulates merozoite attachment to erythrocytes. (A) Cytochalasin D (CytD) permits attachment, but blocks invasion of Calcineurin-expressing parasites (PfCnB-DD parasite + Shield in both conditions). (B) Measurement of merozoite attachment to RBCs by flow cytometry. The left panel shows histograms of SYBR-green treated samples treated with different drugs. Heparin inhibits merozoite attachment. Relative fluorescence units (RFU). On the right side, invasion and attachment was quantified using the histogram data¹⁶⁰.

All these studies shed light on an additional role of parasite adhesins that not only serve as ligands for RBC receptors via their ectodomain, but also fulfills another crucial role via the phosphorylation of their C-tail domain, yet this second function needs to be defined. It is possible that the cytoplasmic domains bind to components of the motor complex, and that they mediate motor complex activation upon receptor binding. Alternatively, they could just stabilize the motor complex. The cytoplasmic tails of EBL and Rh adhesins might also mediate the signaling inside the parasite that induces rhoptry secretion and invasion. In any case, future studies need to investigate the precise role of the cytoplasmic tails, and how their phosphorylation contributes to invasion.

2.3.3. Phosphorylation of the glideosome machinery

The gliding motility of Apicomplexa parasites is provided by a protein complex, whose components and organization are reminded in Figure 9A.

Several studies support a role of Ca^{2+} and phosphorylation to regulate gliding motility upon invasion¹⁶¹. GAP45 indeed, is phosphorylated on different residues by CDPK1 in response to PLC and Ca^{2+} signaling¹⁶². GAP45 is only expressed in schizonts, but is differentially phosphorylated at different schizont stages: S_{149} phosphorylation by CDPK1 for example was high from 39 to 45hpi, whereas S_{103} became heavily phosphorylated by CDPK1 only at 45hpi. It is possible that a phosphorylation that appears just prior to the moment of egress and invasion might be important for glideosome function in invasion. However, in *T. gondii* GAP45 is also phosphorylated, but its phosphorylation is not important for protein function: parasites expressing GAP45 with phospho-ablative mutations do not have defects in glideosome assembly or motility¹⁶³.

PfPKB was shown to be essential for merozoite invasion. Interestingly, this kinase co-localizes with the glideosome, and phosphorylates GAP45 *in vitro*¹⁶⁴. PKB is activated by Calmodulin (CaM) binding, and

hence in response to Ca^{2+} signals. A pull-down assay in search for PKB function in invasion and PKB substrates, completed by *in vitro* and *in vivo* phosphorylation assays demonstrated that PKB phosphorylates GAP45. The authors hypothesize that the function of PKG for merozoite invasion consists in the regulation of the motor complex¹⁶⁴. At the same time, GAP45, GAP40 and MyoA are likely substrates of PKG, as was shown in a study using a PKG inhibitor and phosphoproteomics¹⁶⁵.

Another phosphoproteomic study showed that MTIP is phosphorylated on S₁₀₇ or S₁₀₈ in schizonts, so Douse, et al. aimed to analyze which effect this MTIP phosphorylation has on the structure of the protein and its interaction with MyoA¹³⁷. Using NMR structural analysis of MTIP wild type and phosphomimetic mutants, this group found out that phosphorylation of S₁₀₇ and S₁₀₈ weakens the tight clamp of MTIP around the MyoA tail¹⁶⁶. Therefore this phosphorylation of MTIP could serve as a means of regulation of the motor complex. Additional phosphosites were found on MTIP, such as S₈₅ phosphorylated by PKA and S₄₇ phosphorylated by CDPK1 in merozoites, but not in schizonts^{134,136,167}. S₄₇ phosphorylation was experimentally validated by *in vivo* metabolic labeling and immunoblotting: MTIP S₄₇ is highly phosphorylated in merozoites, but not phosphorylated in schizonts¹³⁴. It is tempting to speculate that MTIP activates myosin movement for parasite invasion, analogous to the function of mammalian MLC1 for striated muscle contraction. Mammalian MLCs are regulatory proteins phosphorylated upon a Ca^{2+} signal in the muscle fiber. Phosphorylation of MLC1 triggers the myosin heavy chain (MHC) to bind to the actin filament, which enables subsequent contraction. In a similar way, a Ca^{2+} signal might activate the parasite motor complex via CDPK1 and MTIP, thereby triggering merozoite invasion¹⁶⁷.

As described in the previous section, existing studies indicate that the primary role of CDPK1 in invasion is the control of microneme secretion. Nevertheless, MTIP, MyoA, GAP45 and several IMC proteins were shown to be phosphorylated by CDPK1, indicating that this kinase could also control the actomyosin motor¹⁵⁰. CDPK1 might therefore act as a 'master regulator', coordinating different steps of invasion.

2.3.4 Phosphorylation as a regulator of *P. falciparum* cell cycle

During Plasmodium intra-erythrocytic development, this parasite uses complex protein phosphorylation cascades to regulate its development.

In parasite schizogony the parasite replicates to form up to 32 new daughter cells. This implicates several rounds of DNA replication and mitosis. Nuclear division is asynchronous in *Plasmodium falciparum*, with only the last round of DNA replication and segregation being synchronous and coordinated with daughter cells budding. In eukaryotes, the cell cycle is controlled by complexes of cyclins and CDKs, which regulate critical "checkpoints" of its progression. Plasmodium encodes 6 enzymes related to the CDK family, but no homologues to canonical cell cycle cyclins^{116,168}. Besides, the three Plasmodium Cyclins Cyc1, Cyc3 and Cyc4 do not demonstrate a typical "cycling" pattern during the cell cycle, but are rather ubiquitously expressed. Therefore, it is thought that the Plasmodium cell cycle is not controlled by the conventional periodic Cyclin-Cdk activities, but also by other regulatory mechanisms such as Aurora-related kinases (Arks), NIMA kinases (Neks) or even CDPKs⁷⁸.

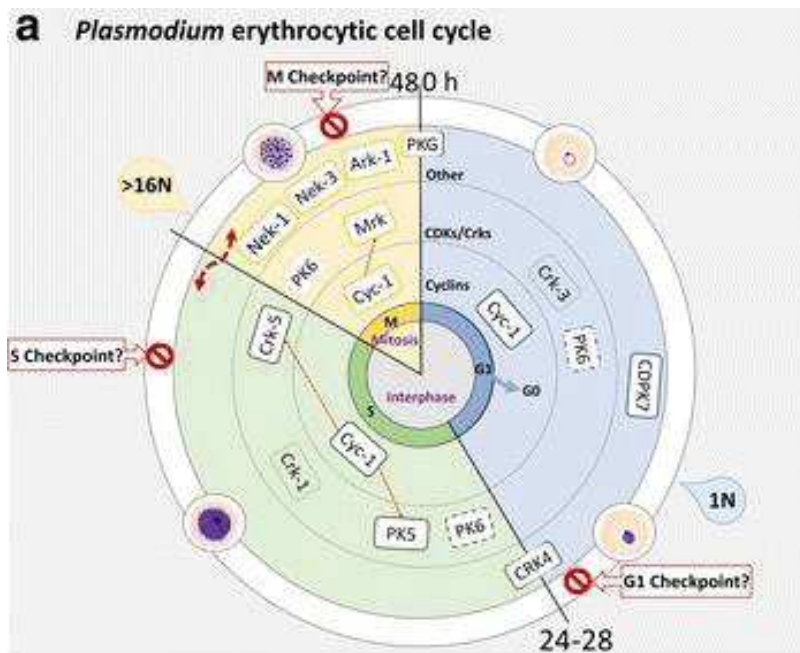


Figure 25: The putative involvement of Cyclins, CDKs and other kinases in the erythrocytic cell cycle⁷⁸.

Some recent data point towards a role of kinases in cell cycle regulation, and are schematically depicted in Figure 25. To identify regulators of schizogony, Ganter *et al.* engineered conditional knockdown lines of 23 kinases whose expression peaks in schizont stage and may therefore participate in the control of this process¹⁶⁹. Except for *crk4*, none of the kinase genes with homology to CDK genes (*pk5*, *pk6*, *crk1*, *crk3*, *mrk*) was included in the screen because their expression shows no clear peak in schizogony^{168,170}. This strategy allowed the group to identify Cdc2-related protein kinase 4 (CRK4) and PKG as essential kinases. It is to be noted that the partial depletion of the other kinases due to the conditional system used may undermine the essentiality of some of the other enzymes tested. Another study used polyamines depletion to induce a cell cycle arrest at the G₁/S phase transition, which is at ~ 15hpi¹⁷¹. This arrest is reversible and addition of polyamines allows the parasite to resume their asexual replication. This tool allowed for tight synchronization of the parasites, and was used to analyze changes in gene expression patterns between G₁ and S phase, with the aim to identify potential “master regulators”. Numerous ApiAP2 transcription factors as well as several kinase genes were found to be differentially expressed between G₁ and S phase, including *ark3*, *crk4*, *crk5*, *cdpk4*, *pk2*, *pk5*, *ark2* and *nek*¹⁷¹.

Although the exact molecular mechanism is not clear, these results suggest that kinases and protein phosphorylation take part in regulating the *Plasmodium* cell cycle.

DNA replication

In late trophozoite stage the parasite enters S phase to duplicate its haploid DNA. During schizogony, sequential rounds of S and M phase give rise to up to 32 daughter cells. DNA replication and the switch to the ensuing mitosis need to be tightly regulated on the level of each nucleus, and the components of the replication machinery are starting to be investigated as putative targets of regulation.

DNA replication in metazoans is initiated when a heterohexameric ORC complex recognizes origins of replication on the DNA, and serves as platform for the stepwise assembly of the pre-initiation complex (pre-IC). The pre-IC furthermore consists of MCMs that act as helicase and contribute to DNA replication licensing. In yeast, the assembly and activation of the pre-IC depends on the phosphorylation of various subunits, such as MCM phosphorylation by Dbf4-dependent kinase (DDK)⁷⁷.

In *Plasmodium* however, neither MCM2 nor MCM6 or MCM7 were found to be phosphorylated, which can be explained by the absence of a DDK homologue⁸⁰.

ORC proteins are regulated by CDKs and by ubiquitinylation in many eukaryotes, and similarly, PfOrc1 was found to be regulated by the *Plasmodium* CDK-related kinase PK5⁷⁹. PfORC1 localizes to the nuclear periphery in trophozoites, but is found mostly in the cytoplasm of late schizonts, where the protein amount is decreasing rapidly after 40hpi. PfORC1 is composed of a C-terminal putative DNA-binding domain, a central ATPase domain and an N-terminal domain that might serve in regulation, as it is likely phosphorylated on Thr₂ and Ser₂₀. This N-terminal domain is phosphorylated by recombinant PK5 in presence of Ringo, homologue to the Ringo *Xenopus* protein shown to activate mammalian CDKs, as well as by a kinase activity that is highest in *Plasmodium* schizont stage lysates, and probably corresponds to PK5. Interestingly, ORC1 phosphorylation leads to its dissociation from DNA. The authors propose a model in which ORC1 initiates DNA replication and controls *var* gene expression in the nucleus. After DNA replication is complete, ORC1 is phosphorylated, dissociates from the DNA, and gets translocated to the cytoplasm and degraded by the proteasome⁷⁹.

Phosphorylation may play a part in regulating DNA replication, and the kinase CRK4 is a likely regulator. PfCRK4 was found to localize to the nucleus and to be expressed from 28hpi onwards¹⁶⁹. An inducible knockdown line using the DD strategy (CRK4-KD) demonstrated that CRK4 depletion led to a drastic block in DNA replication during schizogony (Figure 26B, C, D). Consequently, mitosis did not proceed normally, and enlarged hemispindle structures were visible as nuclei stopped dividing (Figure 26D). Quantitative phosphoproteomic profiling of the CRK4-KD parasites indicated that 220 proteins showed a ≥ 2 fold decrease in phosphorylation upon CRK4 depletion. Of these, GO enrichment identified processes related to “DNA replication” and “nucleus” (Figure 27), thereby suggesting that CRK4 directly phosphorylates components of the DNA replication machinery¹⁶⁹.

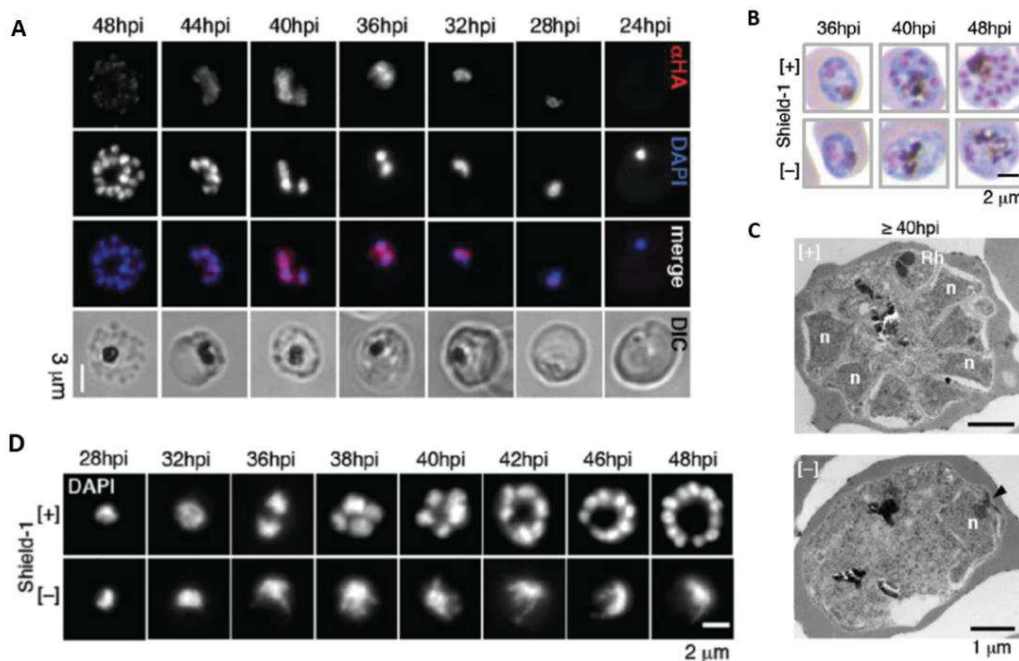


Figure 26: Nuclear Crk4 is essential for schizogony. (A) IFAs of PfCRK4-HA-DD parasites in presence of Shield-1 through intra-erythrocytic development show a nuclear localization of CRK4. (B) Giemsa blood smears of parasites development of CRK4-depleted versus CRK4-expressing parasites (C) TEM images show that nuclei (n) stop dividing and secretory organelles such as rhoptries (Rh) are not synthesized in the CRK4-depleted parasites. A spindle pole body in the dividing (+)Shield parasites is marked by arrowhead. (D) Nuclear development during schizogony in the PfCRK4-DD parasites shown by DAPI staining¹⁶⁹.

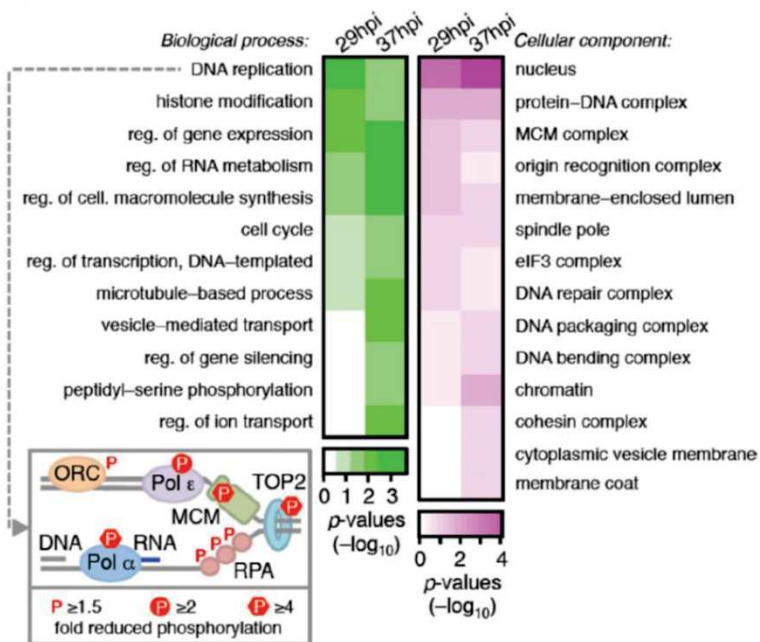


Figure 27: Phosphoproteomic profiling of CRK4-depleted parasites, ensued by GO term enrichment, suggests a role of CRK4 in S phase. The box highlights *P. falciparum* homologues of yeast factors needed for initiation of DNA replication, found to be likely phosphorylated by CRK4¹⁶⁹.

Another gene that is possibly involved in the initiation of DNA replication encodes the MAPK phosphatase 1 (MKP1). This gene was identified in *Pf* by a genome-wide PiggyBac insertional mutagenesis study. *mkp1* disruption led to a retarded intracellular growth phenotype, but the number of merozoites per schizont was not affected. When analyzing in details the growth phenotype, Balu *et al.* observed that pre-S-phase was abnormally prolonged in the *mkp1*-mutant, whereas the other phases of intraerythrocytic growth were not delayed. So it seems that MKP1 is somehow involved, although not essential, in the initiation of DNA replication. However, MKP1 might exert its functions as pseudophosphatase, as the *mkp1* gene has an insertion in the Dual specificity PP domain, which might render the protein enzymatically inactive¹⁷².

Further hints that reversible protein phosphorylation controls DNA replication came from a transcriptome analysis of S phase parasites, compared to cell-cycle G1 arrested parasites. The transcriptome of cell cycle-arrested and re-activated parasites matched with the transcriptomes of quiescent and non-quiescent yeasts for conserved mechanisms in DNA replication. Interestingly, PP1 and a PP2A regulatory subunit were found up-regulated in S phase after cell cycle reactivation in both *Plasmodium* and yeast, together with factors associated with DNA replication, as shown in Table 2¹⁷¹. This suggests that these two phosphatases might play a role in the initiation or progression of DNA replication, or in the switch between S phase and mitosis in *Plasmodium*.

Table 2: Matched cell cycle orthologues in Plasmodium and yeast that get up-regulated in S phase. *P. falciparum* transcripts that were up-regulated in S phase compared to G1-arrested parasites were matched with cell cycle related transcripts from non-quiescent versus quiescent yeast¹⁷¹.

S phase (8/21 orthologues in re-initiated dataset)			
pf3d7_1319700	Protein phosphatase PP2A regulatory subunit A, putative	YAL016W	Protein phosphatase PP2A regulatory subunit A
pf3d7_1241700	Replication factor C subunit 4, putative	YOL094C	Replication factor C subunit 4
pf3d7_1361900	Proliferating cell nuclear antigen (PCNA)	YBR088C	Proliferating cell nuclear antigen (PCNA)
pf3d7_0630300	DNA polymerase epsilon, catalytic subunit a, putative	YNL262W	DNA polymerase epsilon catalytic subunit A
pf3d7_1414400	Serine/threonine protein phosphatase PP1 (PP1)	YER133W	Serine/threonine-protein phosphatase PP1-2
pf3d7_1211700	DNA replication licensing factor MCM5, putative (MCM5)	YLR274W	Minichromosome maintenance protein 5 (MCM5)
pf3d7_0411900	DNA polymerase alpha	YNL102W	DNA polymerase alpha catalytic subunit A
pf3d7_0910900	DNA primase large subunit, putative	YKL045W	DNA primase large subunit
pf3d7_1437200	Ribonucleoside-diphosphate reductase, large subunit, putative	YER070W	Ribonucleoside-diphosphate reductase large chain 1

Mitosis

Eukaryotic mitosis is regulated by the coordinated activation of kinases and phosphatases that together induce the signaling required for mitotic entry, progression and exit¹⁷³. Canonical mitosis is in first place regulated by waves of Cyclin-CDK activities. Besides CDKs, NIMA-related kinases (Nek) and Aurora-related kinases (Ark) are known to regulate eukaryotic cell cycle progression. Metazoan Aurora A family members control spindle formation and mitosis, whereas Aurora B proteins ensure chromosome condensation, segregation, and cytokinesis as part of the chromosomal passenger complex (CPC). Eukaryotic CPCs control the proper attachment of spindle microtubules to the kinetochores, thus ensuring that every daughter nucleus obtains exactly the correct set of chromosomes. A CPC consisting of TgArk1/INCEP1/INCEP2 (Inner centromere proteins 1 and 2) has been recently identified in *T. gondii*¹⁷⁴. Conditional knockdown of TgArk1 or the expression of a catalytically dead Ark1 resulted in defects in nuclear division, as seen by the presence of parasites with giant multi-lobed nuclei as well as of nuclei devoid of DNA. Besides, the TgArk-mutant or TgArk-KD parasites showed a cytokinesis defect, as multiple IMCs formed within one mother cell, but could not elongate and complete budding, thus resembling Russian dolls. So the catalytically active TgArk1 is essential for nuclear segregation and cytokinesis, whereas INCEP1 is believed to be a scaffold protein, and INCEP2 to assure the correct localization of the CPC¹⁷⁴.

In *Plasmodium*, three Ark sequences with closest similarity to Aurora A were identified, and PfArk1 expression was characterized. IFA of PfArk1-GFP showed the protein to localize as two dots to a subset of nuclei in each schizont. Co-localization with α -Tubulin indicated that Ark1 dots were only found at nuclei that had duplicated the centriolar plaques (CP) and started to form a mitotic spindle. The authors therefore suggest that Ark1 is recruited to the duplicated CPs at the entry to M phase, indicating that Ark1 only stains nuclei that are about to divide¹³⁸. Generating Ark1-KO parasites failed, suggesting an essential function of the gene. So, based on its localization to *Plasmodium* CPs, PfArk1 might regulate spindle formation and mitosis in the parasite. Future functional studies will hopefully help understand if a CPC containing Ark also exists in *Plasmodium*, and whether they control chromosome segregation and cytokinesis, as was shown for *T. gondii*¹⁷⁴.

Besides the Ark family members, *Plasmodium* also encodes four Nek proteins, out of which only PfNek1 is expressed in the blood stages. PfNek1 is likely essential for parasite development, and localizes near the nuclei in rings and schizonts. Interestingly, PfNek1 is highly expressed in male gametocytes, but not in female ones¹⁷⁵. Apart from its essentiality in blood stage, Nek1 function in both asexual stages

as well as in male gametocytes is still unknown. *PbNek2* and *PbNek4* on the other hand are produced in the female gametocyte, and transmitted to the zygote where they fulfill functions in the DNA replication and meiosis needed for ookinete conversion¹⁷⁶.

Cytokinesis

After nuclear divisions are complete, each nucleus is equipped with the entire set of subcellular organelles to form daughter merozoites. Daughter cell budding is initiated and spatially controlled on the level of the IMC that is built up around the merozoite from the apical to the basal end^{83,89}.

If *Plasmodium* possesses several CDKs, it should also encode cyclins to regulate the activity of these CDKs. The *Plasmodium* genome does not encode any genes with sequence similarity to conventional G₁, M or S-phase cyclins identifiable by *in silico* screening. However, *PfCyc1* was identified based on homology to yeast atypical Cyclin H¹³⁹. Cyclin H in metazoans and yeast assembles into a complex Cdk7/CycH/MAT1 known to act as transcription factor TFIIH for RNA Pol II, but in some cells, this complex functions as a cell cycle regulator. Also in *Plasmodium* *PfCyc1* forms a complex with MAT1 and MRK (MO15-related protein kinase), a member of the CMCG/CDK family of kinases. *Cyc1*-depleted parasites display normal DNA replication and nuclear division, but daughter cell segmentation is defective (see Figure 28)¹³⁹. The model is that *Cyc1* assembles with MAT1 and MRK, leading to the activation of the MRK kinase and the phosphorylation of substrates necessary for cytokinesis.

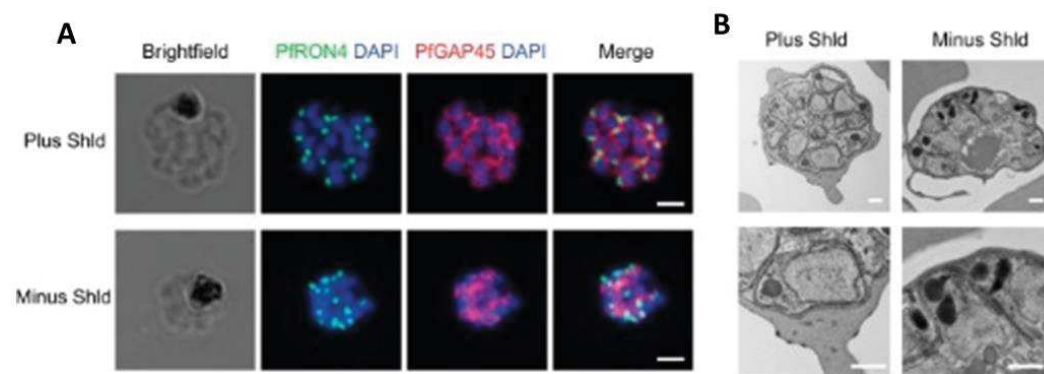


Figure 28: *PfCyc1* is required for cytokinesis. An inducible KD strategy was used by generating *PfCyc1*-DD parasites. Late schizont stage parasites were blocked in E64 to take IFA pictures or TEM sections. (A) IFAs using GAP45 IMC marker and rhoptry protein RON4. The IMC is not correctly forming around each daughter nucleus in the *Cyc1*-depleted parasites. Rhoptries are formed normally in both Shield (+) and (-). (B) TEM of the *Cyc1*-DD parasites. The *Cyc1*-depleted parasites show an abnormal merozoite morphology, although the nuclei and rhoptries look normal. Scale bars are 500nm¹³⁹.

In this section, available data on CRK4, Ark1 and *Cyc1* were summarized to demonstrate examples of how kinases can regulate *Plasmodium* DNA replication, mitosis and daughter cell replication, respectively. Future work is necessary to shed more light on these yet very poorly understood regulation networks.

2.4 Phosphorylation in the host RBC during *P. falciparum* development

Phosphoproteomic studies of infected RBCs revealed that numerous RBC proteins change their phosphorylation status upon Pf infection, and that (de)phosphorylation is one mechanism how Plasmodium modulates the host RBC. The parasite can interfere with the phosphorylation of host proteins either directly by secreting parasite kinases and phosphatases into the RBC, or indirectly by regulation of host kinases or phosphatases.

The RBC has a specific morphology and a particular sub-membrane skeleton, which renders the RBC membrane (RBCM) elastic when the RBC undergoes deformations while passing through narrow blood vessels. A spectrin skeleton combined with a meshwork of actin filaments maintain RBC morphology and flexibility. The major component of the skeleton are dimers of α - and β -spectrin, which form a heterotetrameric functional unit. This spectrin network is connected to the membrane by immobilized Band 3 at spectrin-ankyrin binding sites and at actin junctional complexes via the membrane protein glycophorin-C (GPC) or -D (see Figure 29)¹⁷⁷. Apart from membrane-bound p55/MPP1 (membrane palmytoylated protein 1), junctional complexes contain actin and its associated proteins: Dematin, protein 4.1, tropomyosin, tropomodulin, and a heterodimer of α -Adducin and β -Adducin serve as connectors and/or regulate actin filament dynamics (see Figure 30)¹⁷⁸. All these proteins are responsible for RBC mechanical deformability and membrane integrity.

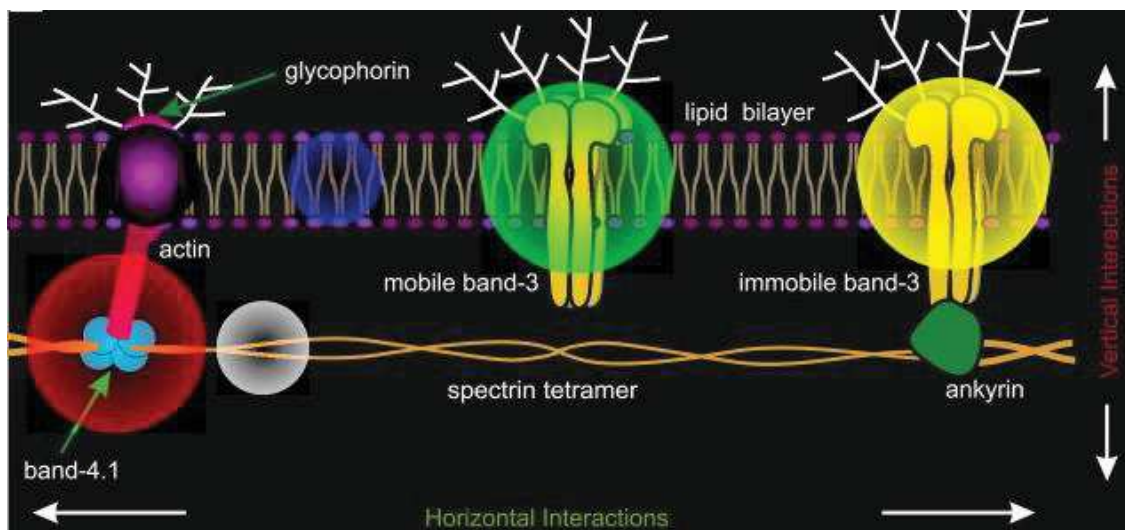


Figure 29: Scheme of the RBC membrane¹⁷⁷. The blue sphere represents a lipid particle and the red sphere signifies an actin junctional complex. The gray sphere represents a spectrin particle and the black sphere represents a glycophorin particle. The yellow and green circles correspond to a band-3 complex connected to the spectrin network and a mobile band-3 complex, respectively. A mesoscale detailed membrane model.

Various skeletal proteins can be reversibly phosphorylated by erythrocyte kinases and phosphatases, which were shown to alter RBC membrane properties. One example is Band 4.1 phosphorylation by PKC on Ser₃₁₂, which reduces its ability to form ternary complexes with spectrin and actin. PKC stimulation and subsequent Band 4.1 phosphorylation decreases membrane mechanical strength, as was measured in resealed RBC ghosts¹⁷⁹. What is stimulating RBC kinases or phosphatases in physiological conditions to phosphorylate RBC skeletal proteins, is not known. Interestingly, *Plasmodium* infection triggers additional specific phosphorylations in these RBC proteins, as will be described in the next sections.

Phosphorylations induced during parasite invasion

During *Plasmodium* invasion (de)phosphorylation events are not only triggered in the parasite, but also in the host cell. Zuccala *et al.* characterized the phosphoproteome of freshly invaded ring parasites after 1.5min of invasion¹⁸⁰. They confirmed previous findings that parasite invasion specifically induces changes in the phosphorylation of RBC membrane and submembrane proteins: They found 13 phosphopeptides enriched in iRBCs compared to RBCs in at least 2 out of 4 experiments. Those phosphosites were located in GPC, PIEZO1, β -Spectrin, protein 4.1, Ankyrin and also eIF4B (see **Table 3**). As control, they performed the invasion assays in presence of different inhibitors: Heparin blocks attachment, and R1 specifically hinders AMA1-dependent adhesion. Surprisingly, most of the phosphosites were found in the absence and presence of these inhibitors¹⁸⁰. So probably, merely the

contact of the merozoite to the RBC is sufficient to induce phosphorylation of RBC surface proteins, and these phosphorylations take place before successful parasite invasion.

It is possible that the phosphorylation of these RBC surface proteins facilitates parasite entry. However, many of these modifications upon invasion had been previously reported by Bouyer *et al.* for late schizonts as well¹⁸¹. So these phosphorylations are likely induced upon invasion, but might not have (exclusively) invasion-specific functions. This implies that these modifications would not be specific to invasion, and that they do not serve a specific function upon invasion. In this case, modification of these RBC membrane and sub-membrane skeleton proteins could weaken membrane stability to enable both parasite invasion and egress.

Table 3: Shortlisted RBC phosphopeptides specifically phosphorylated upon merozoite invasion. 13 phosphopeptides were detected as outlier phosphopeptides in at least 2 experiments. Abbreviations: Y, yes peptide is an outlier. N, no. ND, not detected. Hep, Invasion conducted in the presence of Heparin. R1, Invasion with R1 treatment. Inv, uninhibited Invasion assay

Protein	Peptide	Mapped	Experiment 1			Experiment 2			Experiment 3			Experiment 4		
			Hep.	R1	Inv.									
Beta-spectrin	LLTSQDVSYDEAR	S1301	Y	Y	Y	Y	Y	Y	ND	ND	Y	ND	ND	ND
Beta-spectrin	LLTSQDVSYDEAR	Y1302	ND	ND	ND	ND	ND	ND	ND	ND	ND	ND	ND	Y
PIEZO1	SGsEEAVTDPGER	S1621	Y	Y	Y	Y	Y	Y	ND	ND	ND	ND	ND	ND
PIEZO1	SGSEEAVtDPGER	T1626	ND	ND	ND	ND	ND	ND	Y	Y	Y	Y	Y	Y
Glycophorin C	GTEFAEsADAALQGDPALQDAGDSSR	S104	N	N	N	ND	ND	ND	Y	Y	Y	Y	Y	Y
EIF4B	SQSSDTEQQsPTSGGGK	S504	N	N	N	ND	ND	ND	Y	Y	Y	Y	Y	Y
EIF4B	SQSSDtEQQSPTSGGGK	T500	ND	ND	ND	ND	ND	ND	ND	ND	ND	N	N	N
Protein 4.1	TQTVtISDNANAVK	T738	ND	ND	ND	ND	ND	ND	ND	ND	Y	ND	ND	ND
Protein 4.1	TQTVTIIsDNANAVK	S740	ND	ND	ND	ND	ND	ND	ND	ND	ND	Y	Y	Y
Ankyrin	RQDDATGAGQDsENEVSLVSGHQR/ GDDATGAGQDsENEVSLVSGHQR	S1666	N	N	N	N	N	N	Y	N	N	Y	Y	Y
Ankyrin	ITHSptVsQVTER	S1686, T1688	N	Y	Y	N	N	N	N	N	N	ND	ND	ND
Ankyrin	ITHSptVsQVTER	T1688, S1690	ND	ND	ND	N	N	N	ND	ND	ND	Y	N	N
Glucose 1,6-bis-phosphate synthase	AVAGVmITAsHNR	M171, S175	ND	ND	ND	ND	ND	ND	Y	N	N	Y	Y	N

Phosphorylation of a major erythrocyte membrane protein, Band 3, was suggested to be important for invasion. Band 3 is the major Tyr-phosphorylated protein in the RBC membrane in schizonts. Its hyperphosphorylation was shown to decrease Band 3 affinity to ankyrin¹⁸². Fernandez-Pol *et al* proposed a model in which Band 3 hyperphosphorylation is necessary for merozoite invasion, with the decreased interaction of Band 3 and Ankyrin destabilizing the RBC sub-membrane skeleton and by this means favoring merozoite invasion¹⁸³. The phosphatase Shelp2 is then secreted into the RBC and restores low levels of Band3 phosphorylation after successful merozoite invasion¹⁸³.

Phosphorylation of the host RBC over the whole *Pf* cycle

As early as in 1994 it was demonstrated that the maturation of malaria parasites in human RBCs is accompanied by protein 4.1 phosphorylation. *In vivo* metabolic labeling revealed that Band 4.1 is phosphorylated only in the trophozoite/schizont stage, while it is not phosphorylated in uninfected RBCs and ring stages. The next aim was to identify the kinase responsible for protein 4.1 phosphorylation. Band 4.1 phosphorylation was shown to be blocked *in vivo* by CKI-7, a specific casein kinase (CK) inhibitor. So the responsible kinase is either parasite CK1 or CK2, or one of the RBC CKs¹⁸⁴.

In 2010, the first global approach was undertaken to analyze the impact of *Pf* infection on the RBC proteome. 2-D electrophoresis, combined with Western blots using anti-phosphoserine and anti-phosphotyrosine antibodies and mass spectrometry (MS)¹⁸⁵, revealed changes in phosphorylation of RBC membrane proteins upon *Pf* infection. Following this study, three phosphoproteomic studies analyzed the RBC phosphoproteome of *Pf*-infected cells in schizont stage by liquid chromatography tandem MS of tryptic peptides¹⁸¹, following phosphopeptide enrichment in two studies^{121,136}.

All phosphoproteomic studies came to similar results, revealing that most of the proteins phosphorylated upon *Plasmodium* infection are cytoskeletal proteins, RBC membrane proteins (most of which transporters), and membrane associated proteins. Figure 30 schematically depicts the cytoskeletal proteins phosphorylated in schizonts, as found by Bouyer *et al.*¹⁸¹. GO term analysis confirmed that proteins associated to cytoskeleton organization and regulation are highly enriched in the phosphoproteome of infected RBCs, but are also enriched in RBCs to a lesser degree. Phosphoproteins associated to the spectrin cytoskeleton for example, are enriched 170 fold in infected RBCs and 115 fold in normal RBCs, relative to all RBC proteins¹⁸⁶. Table 4 summarizes the phosphoproteomic findings of these RBC membrane and cytoskeletal proteins.

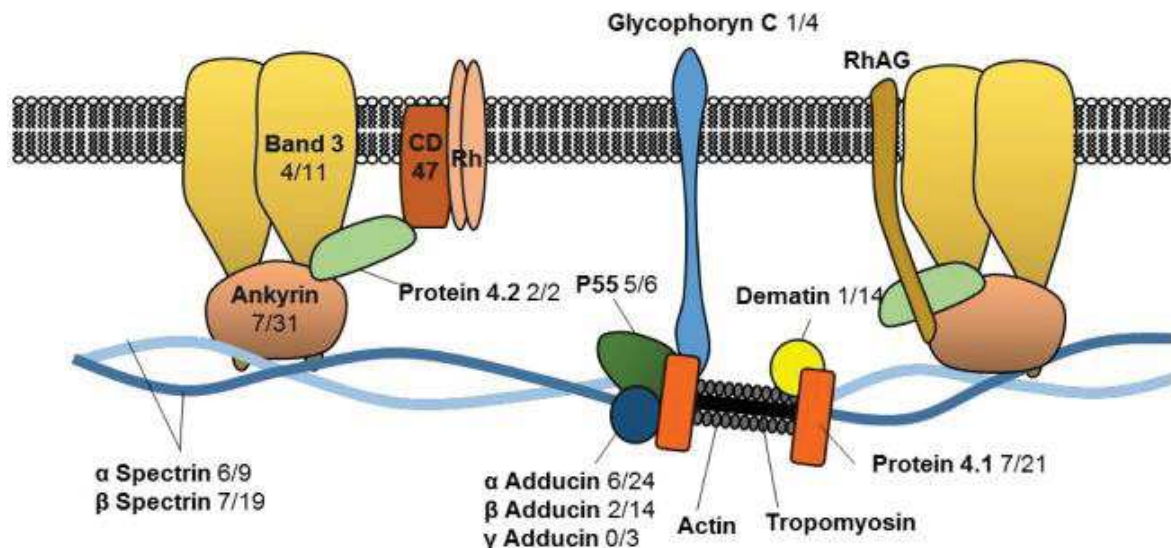


Figure 30: Proteins of the RBC membrane and sub-membrane skeleton found to be specifically phosphorylated in *Plasmodium* infection. Phosphoproteins as found by Bouyer *et al.* 2016 in schizont stage. The numbers indicate counts of phosphorylation sites found specifically in schizonts compared to total phosphorylation sites (infected and non-infected RBCs)¹⁸¹.

The major skeletal protein β -spectrin was found to be differentially phosphorylated upon *Plasmodium* infection^{181,185}, just as band 4.1 and ankyrin^{181,184,185}, which help anchor the spectrin network to the membrane. The phosphorylation of these cytoskeletal components could alter the binding strength among components of the skeleton and thereby modify skeleton stability. α -adducin, β -adducin, tropomyosin and dematin are differentially phosphorylated in trophozoites and schizonts^{121,181,185}. Different isoforms of α - and β -Adducin as well as dematin and tropomyosin participate in regulating the dynamics of polymerization and depolymerization of the actin fibers at the junctional complexes^{136,178}. Their phosphorylation status might therefore regulate the dynamics of actin filament assembly, which finally influence the strength of the submembrane skeleton.

The membrane proteins phosphorylated upon *Plasmodium* infection are Band 3, GPC, p55/MPP1 and flotillin 1^{121,181,185}, which take part in anchoring the sub-membrane skeleton. Surprisingly, membrane proteins that are not linked to the RBCM skeleton, were also found phosphorylated in iRBCs: among others a glucose transporter, GLUT-1, and a nucleoside transporter, as well as CD44 immunoantigen^{121,181}. One could hypothesize that phosphorylation of RBCM transporters could increase nutrient uptake into the RBC necessary for parasite growth. Apart from those protein functional groups, Hsp90 β , Hsp70 and proteins involved in ubiquitinylation/ proteasomal degradation^{121,136} are phosphorylated by *Plasmodium* kinases or parasite activated RBC kinases.

Table 4: List of RBC membrane and sub-membrane skeletal proteins that are specifically phosphorylated or dephosphorylated in *Plasmodium* infection. This table gives an overview of phosphoproteomic data or experimental validations for RBC membrane and cytoskeletal proteins whose phosphorylation status is modified upon *Plasmodium* infection.

Most sites are phosphorylated upon infection, except for the sites indicated to be dephosphorylated in iRBCs. "young rings" refers to rings 2 min after invasion¹⁸⁰

RBC protein	Phosphosites	Putatively responsible kinase	Parasite stage and reference
RBC sub-membrane skeleton			
Spectrin β chain	S ₁₃₀₁		schizonts ¹²¹
	S ₁₃₀₁ , Y ₁₃₀₂		young rings ¹⁸⁰
	S ₁₄₄₄ S ₈₁₇ dephosphorylated upon infection		schizonts ¹⁸¹
Ankyrin	S ₁₆₆₆ , S ₁₆₈₆		schizonts ¹²¹
	S ₁₆₆₆ , S ₁₆₈₆ , T ₁₆₈₈		young rings ¹⁸⁰
	S ₈₅₆		trophozoite ¹⁸⁵
Protein 4.1	nd	casein kinase : PfCK1 or PfCK2 or one of the RBC casein kinases	¹⁸⁴
	S ₄₆₁ , S ₆₆₄		trophozoite ¹⁸⁵
	S ₅₄₂ , S ₅₅₁ , S ₅₅₅ , S ₆₈₄ , S ₇₁₂ , S ₈₄₉		schizonts ¹²¹
	T ₇₃₈ , S ₇₄₀		young rings ¹⁸⁰
	S ₅₄₂ S ₁₀₄ , S ₉₅ de-phosphorylated upon infection		schizonts ¹⁸¹
Actin-binding proteins			
α -Adducin	S ₅₉ , S ₇₂₆	S ₅₉ likely by PKA	schizonts ¹⁸¹
	S ₄₀₈		trophozoite ¹⁸⁵
	S ₃₅₈ , S ₅₈₆		schizonts ¹²¹
β -Adducin	S ₇₁₃		trophozoite ¹⁸⁵
	S ₅₃₂ , S ₅₉₂ , S ₆₂₁		schizonts ¹²¹
Tropomyosin 3	Y ₂₁₄		trophozoite ¹⁸⁵
Dematin	S ₄₀₃		trophozoite ¹⁸⁵
	S ₂₈₉		schizonts ¹⁸¹
RBC transmembrane proteins that anchor the spectrin skeleton			
Band 3	S ₃₄₉ , S ₃₅₆		schizonts ¹²¹
	Y ₈ , Y ₂₁ , Y ₃₅₉ , Y ₉₀₄	RBC Syk and Lyn kinases ¹⁸⁷	Higher phosphorylation in trophozoites than in rings ¹⁸⁵
	S ₃₄₉ , Y ₃₅₉		schizonts ¹⁸¹
Glycophorin-C			schizonts ¹²⁹
	S ₁₂₂		schizonts ¹²¹
RBC membrane proteins, transporters and membrane-associated proteins			
Piezo 1	S ₁₆₂₁ , T ₁₆₂₆		young rings ¹⁸⁰
Flotillin	Y ₂₀₃		trophozoite ¹⁸⁵
P55/ MPP1	S ₂₄₃ , Y ₄₂₉		trophozoite ¹⁸⁵
	S ₄₀₉		schizont ¹⁸¹
CD44	S ₇₀₆		schizonts ¹²¹
			schizont ¹⁸¹
Carbonic Anhydrase I	S ₁₉₈		trophozoite ¹⁸⁵
			schizont ¹⁸¹
GLUT-1			schizont ¹⁸¹
	T ₂₃₈ , S ₄₉₀		schizonts ¹²¹
Equilibrative nucleoside transporter 1	S ₂₅₄		schizonts ¹²¹
			schizont ¹⁸¹

Although the phosphosites were identified, the responsible kinases have not been validated for most of them. Phosphorylation motif analysis allows for predicting RBC kinases involved in the phosphorylations, suggesting a prominent role of CK2, PKA and PKC in phosphorylating RBC targets upon *Plasmodium* infection. One of the few experimentally validated phosphosites is α -adducin Ser₅₉, which was confirmed to be specifically phosphorylated in schizonts, most likely by PKA¹⁸¹.

Although the great majority of *Plasmodium*-induced phosphomodifications occur on RBC Ser and Thr residues, some proteins such as Band 3 are specifically Tyr phosphorylated¹⁸¹. Complex phosphoserine protein patterns appear in the later trophozoite stage, as was shown by protein 2D electrophoresis and MS¹⁸⁵.

Band 3 was shown to be hyperphosphorylated on specific Tyr residues in ring and trophozoite stage, and gets dephosphorylated when maturing into schizonts. Phosphorylation augments from ring to trophozoite stage, where four phospho-Tyr sites (Y₈, Y₂₁, Y₃₅₉, Y₉₀₄) were identified¹⁸⁵. As *Pf* does not possess any Tyr kinase, the parasite likely modulates the activity of RBC Syk and Lyn kinases to modify Band 3. This is supported by the finding that treatment of iRBCs with Syk inhibitors reduces the parasite-induced Band 3 hyperphosphorylation¹⁸⁸. In uninfected RBCs, these phosphosites can be phosphorylated by RBC Tyr kinases Syk and Lyn in a sequential phosphorylation process: Syk phosphorylates Tyr 8 and 21, which in turn will allow other, yet unknown PPs to access Band 3^{182,187}. Interestingly, Syk inhibitor treatment impedes parasite egress. The current model is that parasite-induced Band 3 phosphorylation reduces its affinity for the spectrin/actin cytoskeleton, which results in RBCM destabilization necessary for merozoite egress¹⁸⁸.

In summary, phosphoproteomic and single-protein approaches have compiled much evidence that *Plasmodium* infection modulates the phosphorylation of various RBC proteins, notably of membrane and cytoskeleton structural proteins. As the RBC sub-membrane skeleton poses a physical barrier to parasite invasion and egress, one can speculate that the parasite modifies the structural properties of this barrier by phosphorylation for establishing a successful infection.

Plasmodium interferes with host signaling

Many pathogens interfere with host signaling to ensure proper infection. This is the case for *P. falciparum* mosquito stages, where the parasite has an interest in modulating the host immune response. However, the erythrocyte as a host cell lacks a nucleus and therefore lacks several signal response pathways regulating gene expression and cell proliferation. Till date, knowledge on to which degree *Plasmodium* interferes with RBC signaling pathways is scarce. It was shown that *Plasmodium* infection stimulates the erythrocyte PAK1 \rightarrow MEK1 pathway through a still uncharacterized mechanism. PAK1 is a kinase upstream of MEK1 in the MAPK (mitogen-activated protein kinase) signal cascade. The MAPK cascade is composed of three kinases that vertically activate one another, with MAPK as the most downstream effector. MAPK signaling in RBCs was proposed to regulate transport across the RBC membrane, thereby facilitating nutrient uptake into the iRBC necessary for the parasite. Alternatively, MAPK-mediated phosphorylation could alter the mechanical properties of the membrane, and destabilize the membrane for facilitating parasite egress. PAK1 and MEK1 kinases have no orthologue in *Plasmodium*, and their inhibition by drugs has parasitocidal effects on *P. berghei* liver and blood stages *in vitro*¹⁸⁹.

This chapter has described and demonstrated that phosphorylation and kinases are important for almost all aspects of the parasite life. The following chapter will focus on *Plasmodium* phosphatases, still much less understood than the kinases, and current knowledge about their function in parasite development.

Chapter 3: Plasmodium phosphatases

3.1 Phosphatase groups/ classification

Protein phosphatases (PPs) are classified according to their substrate specificity, as well as to the conservation of the catalytic domain and the mechanism of catalysis.

Based on their amino acid specificity, we can discriminate protein serine/threonine phosphatases and tyrosine phosphatases.

3.1.1 Serine/Threonine phosphatases

The serine/threonine phosphatases (STPs) can be further classified into three independent groups: the phosphoprotein phosphatases (PPPs) and the metallo-dependent phosphatases (PPM) both require the presence of metal ions for catalysis. The third group of STPs includes the aspartate-based phosphatases, which comprise the TFIIIF-associating carboxy-terminal domain (CTD) phosphatases (FCP) and small CTD phosphatases (SCP), both of which specifically dephosphorylate the CTD of RNA Polymerase II (see Figure 31).

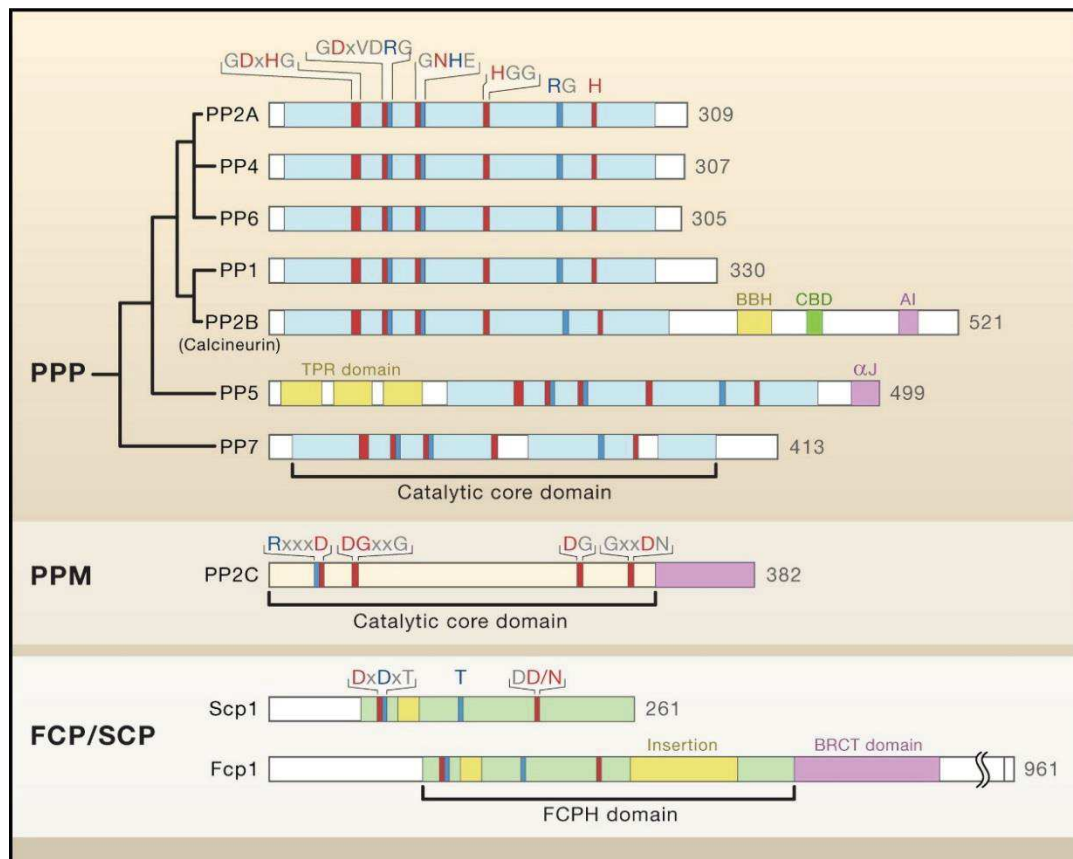


Figure 31: The three families of Ser/Thr phosphatases PPP, PPM and FCP/SCP. The catalytic core domain with signature sequence motifs of every phosphatase group is shown. Residues involved in metal coordination are depicted in red, residues for phosphate binding are blue. For the PPP family, the subfamilies PP1 to PP7 are presented.¹⁹⁰

3.1.1.1 PPP superfamily: mechanism and inhibitors

The PPP family comprises a vast array of different PP activities. Most eukaryotes possess seven subfamilies of PPPs: the PP1, PP2A, PP2B, PP4, PP5, PP6 and PP7, that are defined by sequence variation in their catalytic domain, and the presence of additional regulatory domains for PP2B and PP5. Additional distinction is made on the basis of sensitivity to different small molecule PP inhibitors. Figure 32 shows schematically the phylogeny of PPP subgroups. Among PPPs, PP2A, PP4 and PP6 form a separate sub-cluster, as they share structural features and regulatory mechanisms¹⁹¹. In eukaryotic cells, PP1 and PP2A are the major players, and together they are responsible for 90% of phosphatase activity¹⁹². Together with PP2B (PP3/Calcineurin) and PP2C, they account for the majority of protein serine/threonine activity in eukaryotic cells *in vivo*¹⁹⁰.

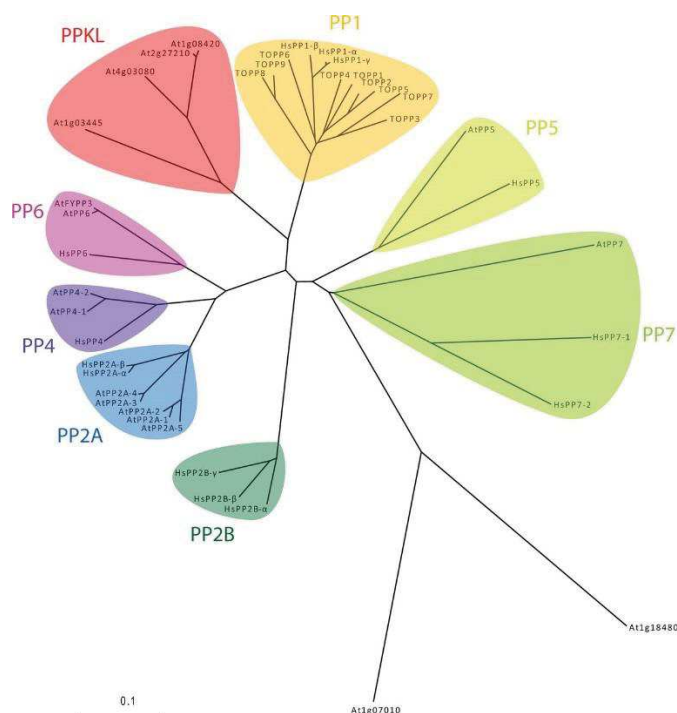


Figure 32: Phylogenetic tree of the PPP family in plants and animals. The tree was generated by phylogenetic analysis of the catalytic domains of *H. sapiens* and *A. thaliana* enzymes using ClustalW¹⁹³.

The catalytic subunit of PPPs adopts a conserved fold, with a β -sandwich placed between two α -helical domains, as shown exemplarily for PP1 (A). The substrate-binding site and catalytic residues are placed in the interface between these three domains. Three highly conserved motifs are found in the PPP catalytic domain, the GDXHG, GDXDRG and GNH(E/D) motifs, as depicted in Figure 31. This so called “phosphoesterase” motif is even conserved among STPs from bacteria, bacteriophage γ and archaea¹⁹⁴. These PPP signature motifs are important for the binding of metal ions and the substrate in the active center, as well as for catalysis (Figure 33B). Six conserved residues bind the two metal ions Mn^{2+} and Fe^{2+} in octahedral coordination in the enzyme catalytic site¹⁹⁰. Metal ions stabilize negative charges, which enables them to make a phosphoester more susceptible to nucleophilic attack and to stabilize the transition state phosphate in the PPP active site.

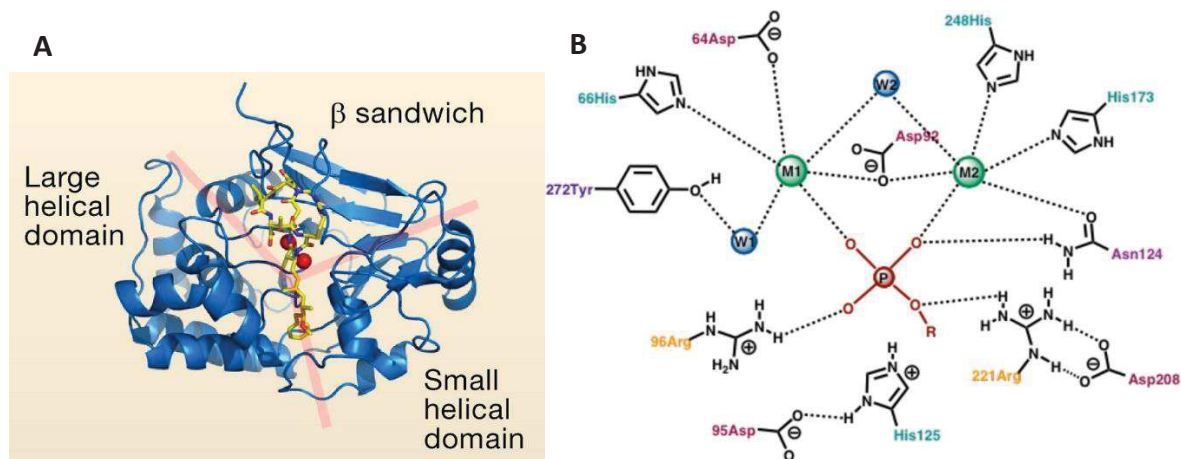


Figure 33: PP1 structure and catalytic site. (A) Structure of HsPP1 bound to okadaic acid (yellow). A Y-shaped surface groove (pink) is formed by the three domains of PP1. The two metal ions (red spheres) are Mn^{2+} and Fe^{2+} .¹⁹⁰ (B) Scheme of the HsPP1 active site.¹⁹⁵

Catalysis follows a general acid-base mechanism, which starts by the deprotonation of a water molecule. The resulting hydroxyl molecule is bound and its charge is stabilized by the two metal ions that are coordinated by water molecules and highly conserved residues in the active site, namely three His, two Asp and one Asn residue (indicated in Figure 33B)¹⁹⁶. The hydroxyl molecule then initiates the nucleophilic attack on the phosphoester substrate, and the dephosphorylated substrate is released from the active site. The crystalline structure of PP1 suggests the involvement of two active site Arg residues, R₉₆ and R₂₂₁, for the hydrogen bonding of the substrate, and this could stabilize the reaction transition states¹⁹⁵.

In order to check this hypothetical function of R₉₆ and R₂₂₁, these residues were mutated into Lys in the human PP1 enzyme, and enzymatic activity was tested using distinct non-physiological substrates. The mutant recombinant enzymes had different activities towards different substrates, confirming a function of R₉₆ and R₂₂₁ in substrate binding and in determining the specificity of the reaction¹⁹⁵.

Calcineurin

PPPs are usually encoded on a single polypeptide. One exception is PP3 which functions only as heterodimer, and which will be shortly presented here. PP3, also known as PP2B or Calcineurin (Cn), is a special PPP member, which is regulated by Ca^{2+} signaling. Cn is a heterodimeric protein composed of the large catalytic domain CnA which binds the small calcium-binding regulatory unit CnB¹⁹⁷. A rise of the intracellular Ca^{2+} -level induces activation of the Cn heterodimer in two steps. First, Ca^{2+} ions bind CnB, which then induces conformational changes that expose the Calmodulin (CaM)-binding site on CnA. Ca^{2+} /CaM binding to CnA then activates enzymatic activity by displacing the autoinhibitory region from the CnA catalytic domain¹⁹⁸. Cn in mammals is predominantly important for diverse neuronal processes¹⁹⁸.

PPP inhibitors

Various inhibitors have been described and used to study PP function, as well as resolving PP three dimensional structure: Okadaic acid (OA), calyculins and microcystin-LR are selective inhibitors of the PPP family and do not bind to PPMs or other phosphatases^{199,200}. These inhibitors are natural products, originating from the secondary metabolism of marine organisms: calyculins have been first isolated from the marine sponge *Discodermia calyx*, OA is produced by dinoflagellates and microcystin-LR is synthesized by blue algae²⁰¹. In their natural environment, these cytotoxins often act as biological

defense mechanisms to protect their host organism. The mechanism of how the host organisms get resistant to or regulates activity of these toxins is closely linked to symbiont ecology, and is poorly understood²⁰². One interesting mechanism was revealed for calyculin A (calA): CalA is produced by symbiotic bacteria of *Discodermia*, and stored in an inactive phosphorylated form in the sponge. Only upon tissue damage to the sponge, phosphocalyculin is dephosphorylated, activated and released²⁰³.

Calyculins, OA and microcystins are potent inhibitors of PP1 and PP2A-activities, but differ in their PP1/PP2A selectivity. Cal A inhibits both PP1 and PP2A at similar IC₅₀ values (0.4 – 2.0 nM for PP1 and 0.25 – 3 nM for PP2A¹⁹⁹), whereas OA inhibits PP2A at a much lower IC₅₀ and is therefore considered as a selective PP2A-inhibitor²⁰⁴. In fact, OA and calA inhibit all members of the type 2A group of phosphatases (PP2A, PP4, and PP6). Both OA and calA show similar inhibitory effects on PP2A, PP4 and PP6, but the exact IC₅₀ values vary depending on the substrate molecule used for the PP activity assay²⁰⁵. OA inhibits PP1, PP2A, PP4, PP6 and even PP5, but shows the highest inhibitory effect against PP2A and PP4^{205–207}.

The structure of the complex of calA bound to the PP1 catalytic subunit was resolved by X-ray crystallography²⁰⁴. This structure showed that calA binds to the hydrophobic and the acidic surface grooves of the PP1 catalytic subunit (Figure 34A), which corresponds to the substrate binding site. The calA molecule consists of a phosphate moiety, a polyketide and a hydroxyl C₁₃ tail, and the crystal structure demonstrated that it binds PP1 in a similar position as the endogenous substrate, with active site residues and the two metal ions involved in binding (Figure 34B)¹⁹⁹. Several residues of PP1 interact with the inhibitor molecule in the active center of the enzyme, with Arg₉₆ and Arg₂₂₁ forming salt bridges and Tyr₂₇₂ forming a hydrogen bond to calA²⁰⁴. Mutagenesis studies have demonstrated that a Y₂₇₂F mutated enzyme is 100 times less sensitive to calA, while phosphatase activity is almost unaffected²⁰⁸.

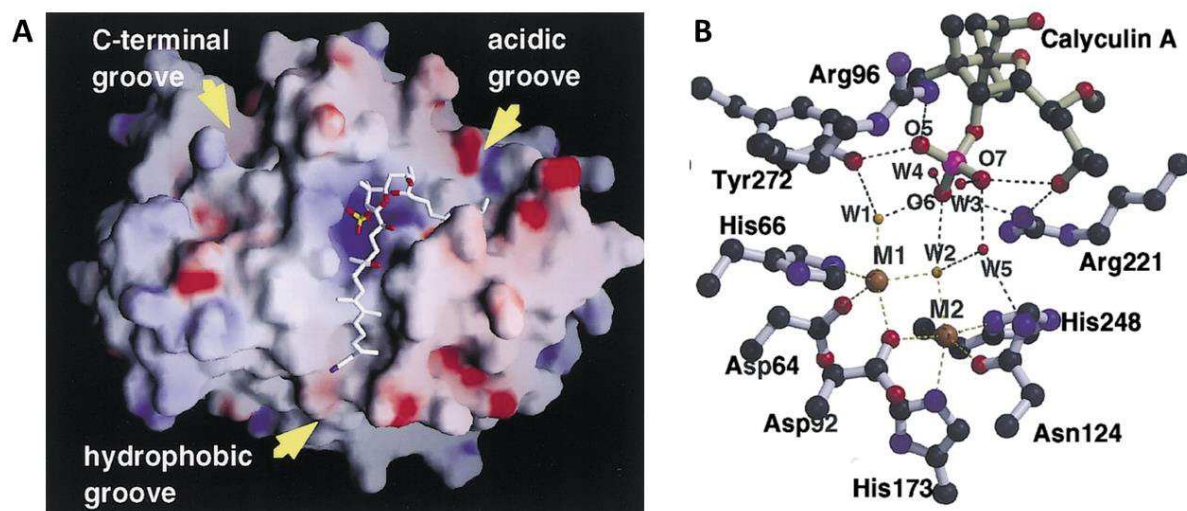


Figure 34: Calyculin A binding to PP1 γ , as determined by X-ray crystallography²⁰⁴. (A) The molecular surface of the PP1 γ -Calyculin A complex. (B) Scheme depicting the interactions between residues of PP1 γ and calA. Metal ions (M), metal-bound water oxygen atoms- orange, other water oxygen atoms – red. The dashed lines indicate bonds between atoms. Only Tyr₂₇₂, Arg₉₆ and Arg₂₂₁ bind to CalA directly.

Plant-like phosphatases

Phylogenetic analysis of the PPP family in animals and plants revealed a unique subgroup only present in *Viridiplantae* and *Alveolata*: Protein phosphatase with kelch-like domains (PPKL), as shown in Figure 32. PPKLs form a PPP subfamily that contains kelch-tandem repeats at the N-terminus. The kelch motif can be implicated in various cellular functions, especially in actin-based cytoskeleton formation and transcriptional regulation²⁰⁹. The first PPKL to be studied is *A. thaliana* Bsu1 (*bri1* suppressor1). AtBsu1

acts as an antagonist of brassinosteroid hormone signaling²¹⁰. Brassinosteroids are plant steroid hormones, involved in growth, stem elongation and vascular development, and act by binding to a membrane-associated receptor kinase that activates BZR1 and BES1 transcription factors (TFs) that accumulate in the nucleus. *AtBsu1* functions as Brassinosteroid counterplayer by decreasing the phosphorylation of these TFs in the nucleus²¹⁰.

Sequence similarity of the catalytic domain shows that PPKL and PP1 are closely related. The current hypothesis regarding the origin of PPKLs is that this group evolved from a PP1/PPKL-like ancestral enzyme present in the progenitor organism of algae and plants, which gave rise to PPKL as well as PP1 in plants. A PPKL gene was probably acquired by Alveolata during their evolution, through secondary endosymbiosis of red and green algae and subsequent nuclear gene transfer¹⁹³.

Bacterial-like phosphatases

Among the PPPs present in eukaryotes, phosphatases are found that have high similarity to groups of bacterial proteins: the *Shewanella*-like phosphatases (Shelphs), the Rhizobiales-like phosphatases (RLPHs) and the ApaH-like phosphatases (ALPHs)²¹¹. These sequences have been incorporated into eukaryotic genomes by way of the original mitochondrial endosymbiosis (Shelphs, RLPHs) or donation by an archaeal ancestor²¹².

➤ **Phylogeny of *Shewanella*-like phosphatases**

The group of *Shewanella*-like phosphatases (Shelphs) is found in bacteria as well as diverse eukaryotes, including plants, red algae, fungi, apicomplexans and kinetoplastids²¹¹. Interestingly, they are absent from animals, making them attractive putative drug targets. In plants, Shelphs phylogenetically cluster into two groups with different sub-cellular localization. The Shelph1 lineage is chloroplastic, while Shelph2 members are cytoplasmic²¹³. Since their transfer to eukaryotes by the original mitochondrial endosymbiosis, Shelphs seem to have taken a different evolutionary path in photosynthetic eukaryotes versus in the lineage that developed into pathogenic organisms²¹⁴. Shelphs of photosynthetic organisms are cytoplasmic, plastid- or mitochondrial-resident proteins. In contrast, Shelphs of Apicomplexans, Excavata and Oomycetes, often possess a predicted N-terminal signal peptide (SP), which would target them to the ER co-translationally. *Plasmodium* proteins bearing a SP enter the ER and, depending on the presence of additional protein sorting motifs, they are further trafficked to different localizations, such as the parasite apicoplast and mitochondrion^{215,216}, or even beyond the parasite limits, secreted into the host organism²¹⁴.

➤ **Shelph structure and enzymatic properties**

The prototypic Shelph phosphatase was first isolated from the psychrophilic γ -proteobacterium *Shewanella* by Tsuruta *et al.*²¹⁷ in 1998, and was named cold-active protein tyrosine-phosphatase (CAPTPase). The same group extensively investigated CAPTPase structural and catalytic properties, with a special focus on its adaptation to cold temperatures. The “local flexibility/rigidity” concept proposes that the catalytic center of a cold-active enzyme is unstructured and flexible, whereas rigid regions of the same protein are responsible for the high activity at low temperatures. This model proves true for CAPTPase, as the rigidity of one of the Zn-binding centers due to bulky amino acids was shown to be crucial for the thermostability and catalytic efficiency at low temperatures²¹⁸.

Tsuruta *et al.* published a first crystal structures of CAPTPase in 2005 (PDB IV73)²¹⁹ and one with higher resolution (1.1 Å) in 2008 (PDB 2Z72)²¹⁸. *Shewanella* CAPTPase is constructed of 3 β -sheets (Sheet I, Sheet I' and Sheet II) and 14 α -helices, connected by loop structures (Figure 35A). A narrow groove lies along the surface of the enzyme, and in the deepest part of this groove the two metal ions, the phosphate and one solvent molecule are bound²¹⁹. CAPTPase possesses a variant of the

phosphoesterase signature motifs, namely DXH, GDXXDR and GNHE²¹⁸. Those conserved residues lie within loop structures that connect the βαβαβ-fold to form the catalytic site with a di-nuclear metal center, which is conserved from PPP enzymes. Metal analysis of CAPTPase showed that the active center of the enzyme contains two Zn²⁺ ions, each of which is coordinated by five ligands (Figure 35B)²¹⁸.

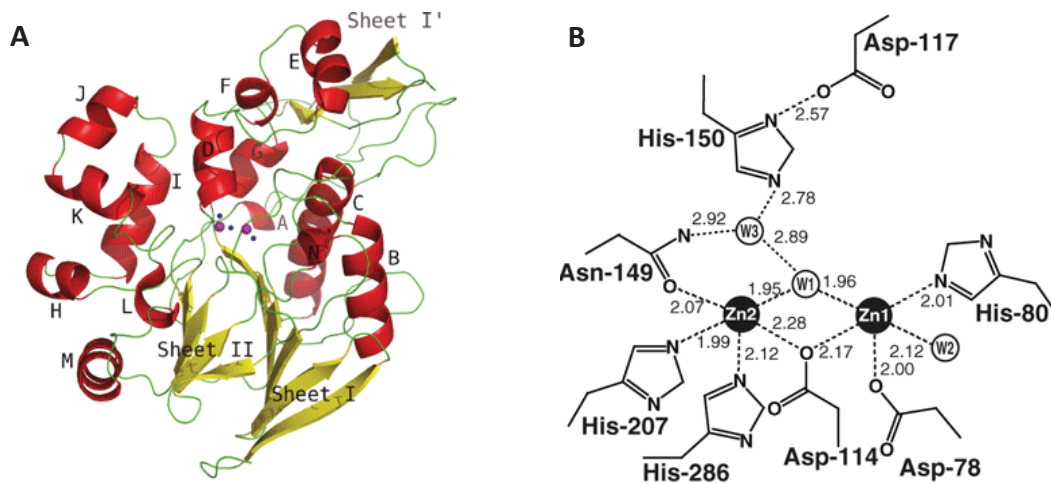


Figure 35: CAPTPase overall protein structure and active site from *Shewanella*²¹⁸. (A) Large and small spheres represent metal ions and water molecules at the catalytic site, respectively. α -helices, β -sheets and loop structures are represented by red ribbons, yellow arrows and green strands. (B) Schematic representation of the CAPTPase active site. Inter-atomic distances are indicated.

Site-directed mutagenesis studies identified several residues essential for the enzymatic activity of CAPTPase²²⁰, which were confirmed by the crystal structure analysis (Figure 35B²²¹). His₁₅₀ can function as acid catalyst at neutral pH and forms the catalytic dyad together with Asp₁₁₄²²², whereas the other residues are part of the binuclear metal center. The very same architecture of the catalytic site is found in other PPP members, e.g. in human Calcineurin^{218,223}.

A striking feature of *Shewanella* CAPTPase is a strict specificity for phospho-Tyr²²⁴, although it exhibits the conserved active site architecture of PPPs, but neither biochemical nor structural studies could explain this unusual activity^{221,222}. Furthermore, the physiological roles and native substrates of this PP in *Shewanella* bacteria have not been identified yet.

In conclusion, Shelpfs are atypical members of the PPP family, as they have the same conserved phosphoesterase motifs and catalytic residues, but possess strict Tyr specificity. They differ completely in their structural and enzymatic properties from the PTP family^{219,225}, with which they share only the specificity for Phospho-Tyr.

3.1.1.2. PPM family

Phylogenetic analysis suggest that PPMs originated in bacteria and entered the eukaryotic lineage by the endosymbiosis which gave rise to mitochondria²¹⁴. The PPM family are protein phosphatases dependent on manganese/magnesium ions (Mn²⁺/Mg²⁺), and comprises the PP2C group and the pyruvate dehydrogenase phosphatases.¹⁹⁰ In mammalian cells at least 18 PP2C family members are present, whose main function is the regulation of stress signaling, aside from cell differentiation, growth, survival and metabolism²²⁶. The PP2C family is characterized by the conserved motifs RxxxED, DGxxG, DGxWD and DN, that are responsible for metal coordination and phosphate binding (see Figure 31)²²⁷. Mammalian PPMs have their active site residues arranged around two central metal ions, which are Mn²⁺ in the case of human PP2C α (Figure 36)²²⁸.

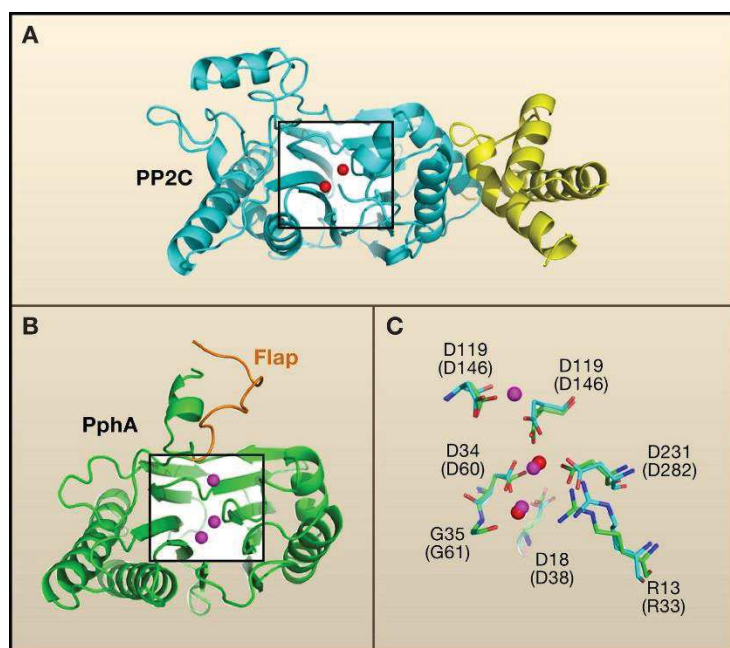


Figure 36: PP2C structure and catalytic site. (A) Architecture of the human PP2C protein. Two metal ions are bound in the catalytic site. (B) and (C) PP2C homologue PphA from *Thermosynechococcus elongates* has three metal ions in the active site and an additional loop structure, indicated as Flap. The conserved active site residues of PphA are shown in green, the homologues of the human enzyme(cyan) are indicated in brackets²²⁹.

Bacterial PPM homologues share the same conserved residues, but all bacterial PPM crystal structures contain three metal ions and an additional loop structure named “Flap”. However, recent biochemical and mutational studies suggest that not only bacterial, but also plant and human PP2C require a third metal ion for catalysis. This third metal ion was not detected in the crystal structure by Das, *et al.* 1996 (Figure 37B) due to the low pH of the crystallization conditions²³⁰. The residues that would bind this ion (D₁₄₆, D₂₃₉) are highly conserved, and their ablation severely affects catalysis²³¹. So the active center of the human enzyme likely looks like the bacterial one more than believed till date, and the structure and enzymatic mechanism of the active center need to be reinvestigated.

Figure 37 shows the position and functions of the conserved residues during catalysis. Three metal ions are coordinated by water molecules and conserved active site amino acids in an octahedral conformation. They function in the stabilization of negative charges generated during the reaction, both for nucleophile generation and binding of the released phosphate group. In the well-studied bacterial enzymes, a conserved Asp (D₂₂₃ in MspP) as part of the GxxDN motif in the catalytic center serves as base to activate a water molecule, and the resulting negative charge is stabilized by the two metal ions. The resulting hydroxide ion serves as the nucleophile to attack the phosphorous atom in a nucleophilic substitution, type 2 (S_N2)-like reaction, which releases the dephosphorylated substrate (see Figure 37A). In the resulting transition state the free phosphate is stabilized by hydrogen bonds and electrostatic interactions before it is released and the enzyme can start a new cycle of catalysis (see Figure 37B). Arg₁₇ residue in MspP (Arg₃₃ in the human PP2C, Figure 37B) in the RxxxD motif plays an essential role for substrate binding and stabilization of phosphate in the transition state²³².

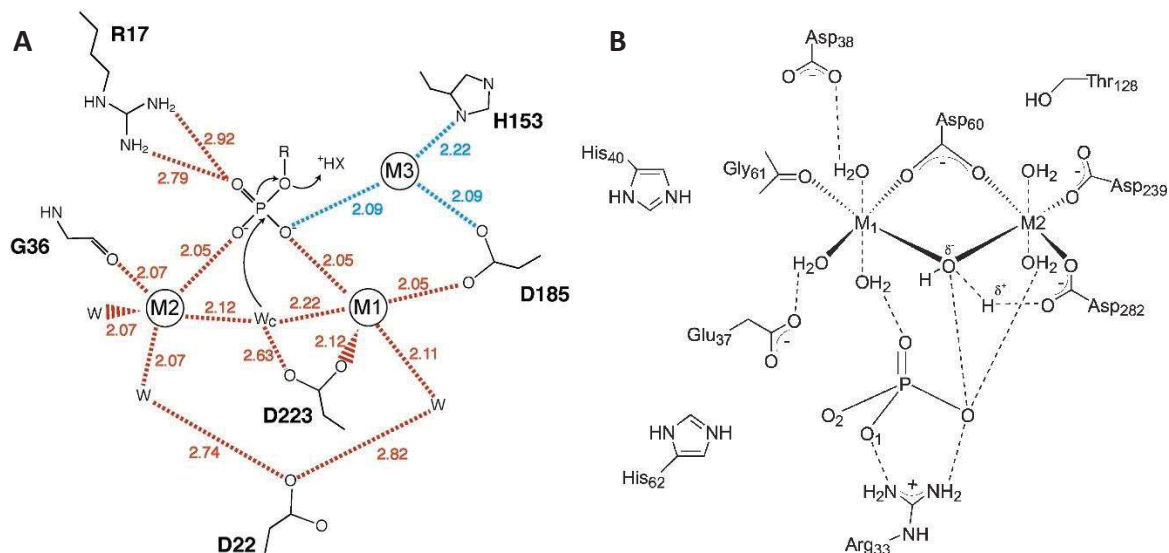


Figure 37: Catalytic mechanism of the PP2C active site (A) Initiation of the nucleophilic attack in *MspP* from *Mycobacterium smegmatis*. Interatomic distances are depicted in Å. Proposed PPM catalytic mechanism²³² (B) SN2 transition state in the human PP2C isoform α that has two metal ions in this crystal structure. The phosphate is stabilized by hydrogen bonding to H_2O and electrostatic interactions with Arg₃₃^{228,233}. However, PP2C was found to have a third metal ion in its active center, which likely does not appear in the structure by Das et al. due to the low pH of the crystallization conditions^{230,231}.

So all in all, the PPM and PPP families of phosphatases possess similarities regarding their catalytic mechanism and architecture of the active site. PPMs as well as PPPs have a conserved metal ion active center that is essential for catalysis^{228,230}. Metal ions are required for both groups to activate a water molecule to initiate the nucleophilic attack in an S_N2 -like reaction that leads to the release of the phosphate group¹⁹⁰. Nevertheless, these similarities have arisen from convergent evolution, as PPP and PPM sequences phylogenetically distinct.

3.1.1.5 FCP/SCP family

The third major group of Ser/Thr phosphatases is composed of the SCP and FCP groups, both of which have the CTD of RNA Polymerase II (RNAP II) as only known substrate²³⁴. The CTD of RNAP II is conserved among eukaryotes and consists of multiple heptapeptide repeats with the consensus sequence YSPTSPS. The number of repeats varies from 26 in yeast to 52 in mammals. Ser₂ and Ser₅ in the consensus repeat are the major phosphosites in the CTD, but Ser₅, Thr₄ and Tyr₁ can be phosphorylated as well²³⁵.

The progression of RNAP II through the transcription cycle and the recruitment of RNA processing enzymes are tightly regulated by sequential phosphorylation and dephosphorylation on its CTD. Phosphorylation is required for recruitment and assembly of RNAP II to the DNA, and the later dephosphorylation is necessary for recycling the complex for a new transcription cycle. Hypophosphorylated RNAP II enters the preinitiation transcription complex at the promoter. Then, Ser₅ in the CTD of RNAPII is phosphorylated by the Cyclin dependent kinases Cdk7 or Cdk12 and transcription is initiated. Ser₅ phosphorylation enables the recruitment of the 7-methyl-G RNA capping enzyme. While Ser₅ phosphorylation is necessary for transcription initiation, Ser₂ is phosphorylated only later by Cdk9 and phospho-Ser₂ is characteristic for the transcriptional elongation activity of RNAP II²³⁵. Meanwhile, phosphorylation of Ser₅ is gradually removed by SCP1 and other phosphatases^{235,236}. When transcription is completed, FCP1 takes charge of dephosphorylating Ser₂, thereby regenerating RNAP II for a new cycle²³⁵.

The conserved structural core of SCP and FCP is the FCP homology domain (FCPH) (Figure 31). In the human Scp1 protein, the FCPH domain is connected to a three-stranded beta sheet, termed the insertion domain (Figure 38A). The active site contains a single Mg^{2+} ion and is located in a cleft between the FCPH and the insertion domain. FCP has an additional BRCT domain (BRCA1 C-terminal domain like), which is absent from SCPs (see Figure 31)¹⁹⁰. The BRCT domain is known as dimerization domain, but it can also mediate the interaction with proteins not containing a BRCT domain, such as RNA helicase A²³⁷.

FCP/SCP are characterized by the conserved DXDX(T/V) motif, and the cluster of two Asp residues is required for Mg^{2+} coordination and catalysis. Besides this motif, other conserved residues in the active site participate in the coordination of the Mg^{2+} ion and the catalytic residues involved in phosphoryl-transfer. The catalytic mechanism of FSP/SCP follows a two-step mechanism and is described in Figure 38B: the nucleophilic attack on the phosphate is conducted by the catalytic Asp residue (Asp₉₆ in HsSCP1), the first Asp in the DXDX (T/V) motif. In the second step, a water molecule mediates hydrolysis of the phosphoryl-enzyme intermediate. The function of the Mg^{2+} ion during catalysis is merely to neutralize negative charges of the phosphate group²³⁸.

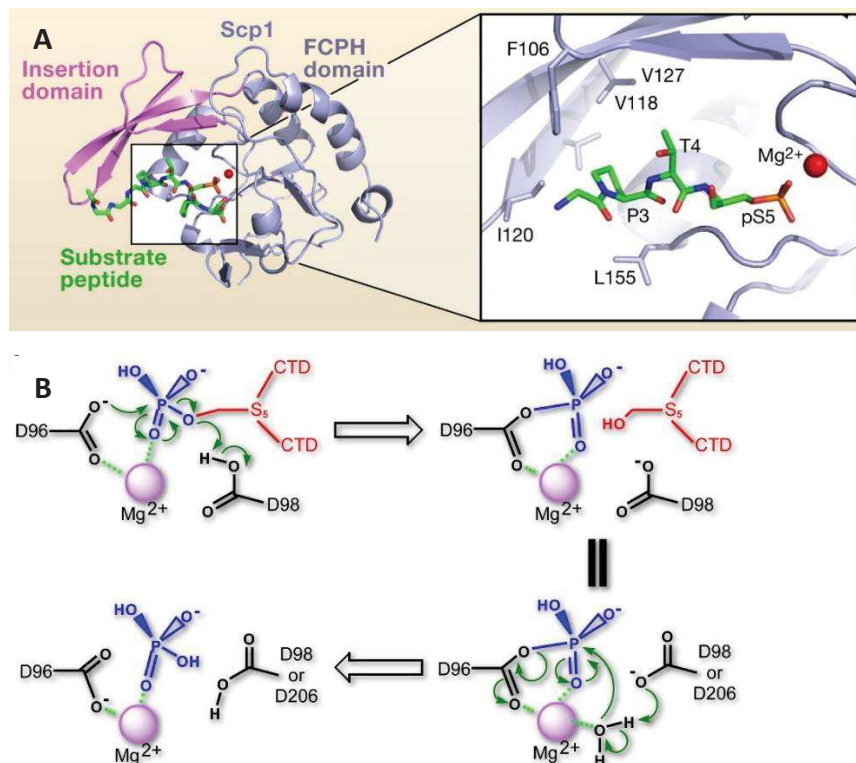


Figure 38: Structure, substrate binding and catalytic mechanism of human SCP1. (A) The crystal structure of HsScp1 is schematically shown. The SCP1 active site forms a groove into which a portion of the CTD repeat, Ser₂-Pro₃-Thr₄-Ser₅ is bound. A hydrophobic pocket is formed by Scp1 residues Phe₁₀₆, Val₁₁₈, Ile₁₂₀, Val₁₂₇, and Leu₁₅₅, which sequesters the Pro₃ ring of the substrate. B) Scp1-mediated catalysis following a two-step mechanism^{190,238}.

In summary, FCP/SCP are essential for ensuring correct transcription and mRNA processing of all cellular genes transcribed by RNAP II.

3.1.2 Phospho-tyrosine phosphatases

Proteins phosphorylated on Tyr residues are dephosphorylated by protein-tyrosine phosphatases (PTPs). The PTP superfamily consists of three evolutionary unrelated groups that developed the same catalytic mechanism by convergent evolution: classic PTPs, dual-specificity PTPs and the low molecular weight PTPs (LMW-PTPs)²³⁹. Classic PTPs can be further sub-divided into cytoplasmic PTPs and receptor-like PTPs that possess trans-membrane domains. Receptor-like PTPs have important functions in signaling, e.g. in developmental processes in animals, but are absent from protozoans^{239,240}. PTP activities are inhibited by Zn^{2+} , vanadate and molybdate.

PTPs share a common fold where one central β -sheet is surrounded by six α -helices, and the active site is usually placed in a groove of the enzyme, the size of which determines substrate specificity²⁴¹. The active site of classical PTPs is formed by the phosphate-binding loop (P-loop), a glutamine-bearing loop (Q-loop), a general acid loop (WPD-loop), and a substrate binding (recognition) loop (Figure 39). It is delimited by a conserved catalytic P-loop (H/V)C(X)5R(S/T), also referred to as the CX₅R motif, and an aspartate serving as general base catalyst.

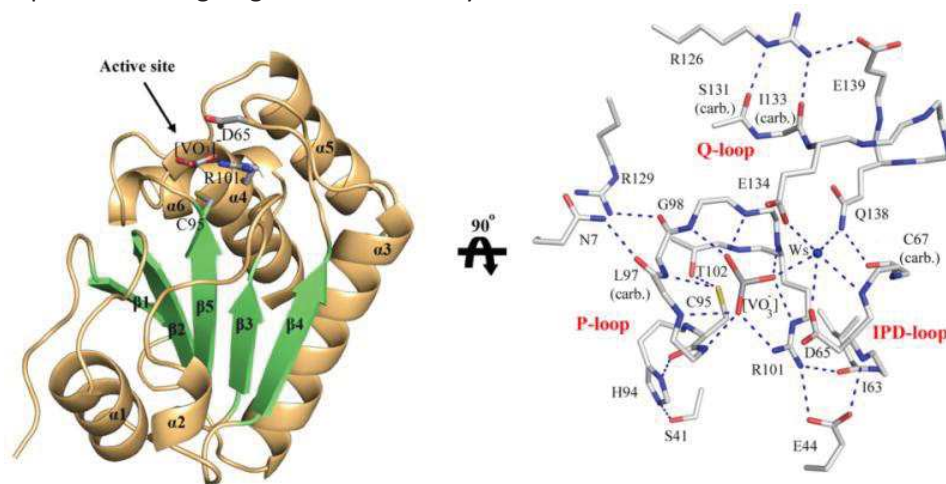


Figure 39: Structure of a PTP, human VHZ. VHZ is one of the smallest PTPs that contain all minimal structural elements of PTPs. Cartoon presentation of VHZ in complex with the PTP inhibitor orthovanadate (VO_3^-) shows the classical PTP α/β fold. The central β -sheet (green) is surrounded by six α -helices (brown). The right panel shows the important active site residues forming H bonds (dashed lines) to the inhibitor. Classical PTPs have an additional N-terminal substrate binding loop which lacks in VHZ²⁴².

The CX₅R motif recognizes the phosphorylated substrate and contains the catalytic cysteine that initiates the nucleophilic attack and subsequently forms a thiophosphate intermediate with the substrate. In the second reaction step, the aspartate serves as base to deprotonate a water molecule which will then be the nucleophile and cause the release of the enzyme and inorganic phosphate²⁴³. The reaction scheme for PTP catalysis is presented in Figure 40.

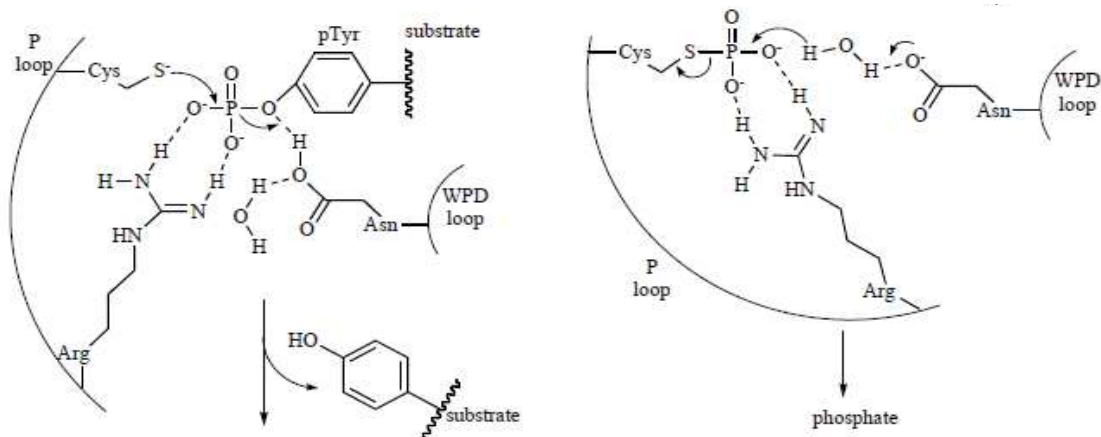


Figure 40: Scheme of the catalytic mechanism of the PTP family. Dephosphorylation of Tyr-phosphorylated proteins succeeds in a two-step mechanism: first the catalytic Cys performs a nucleophilic attack on the phosphate group, releasing the dephosphorylated substrate. The phosphate is covalently linked to the enzyme in the reaction intermediate. Then the conserved Asp residue activates a water molecule to serve as nucleophile in the following hydrolysis of the phosphoenzyme intermediate and release of the enzyme²⁴¹.

The catalytic mechanism of PTPs has the striking feature that phosphate is covalently bound as reaction intermediate. This is fundamentally different from catalysis of PPPs and PPMs: in the PPP/PPM S_N2 transition state the free phosphate is bound by hydrogen-bonding and electrostatic interactions in the active site²²⁸. So PTP inhibitors should potentially be more effective than PPP or PPM inhibitors: the PTP inhibitor molecule mimics a phosphorylated substrate and will completely block the enzyme when catalytic residues irreversibly form a covalent bond to the inhibitor. However, it is complicated to develop a selective PTP inhibitor for a particular PTP, as the active site is highly conserved among the whole family²⁴¹.

Dual-specificity phosphatases (DSP) are unique as they are capable of dephosphorylating phospho-Ser/P-Thr as well as phospho-Tyr residues. Although DSPs and PTPs share little sequence identity, both groups have a similar overall structure and catalytic mechanism, including the conserved catalytic core and the same catalytic mechanism²⁴⁴.

Interestingly, among PTPs some groups of inactive enzymes are known, such as PTP-like A/B proteins (PTPLA/B). These inactive phosphatases are nonetheless well conserved in many organisms. Inactive PTPs possess the protein domain structure of PTPs, but have some essential catalytic residues mutated. The PTPL group for example has a substitution of the essential Arg in the catalytic center (see Figure 40). Investigation of several inactive PTP members suggests that these proteins have lost their catalytic activity and evolved to fulfill other functions like phospho-Tyr recognition, which can support scaffolding and protein targeting¹⁹³.

3.2 Regulation of phosphatases

3.2.1. PPP regulation

Phosphatases of the PPP group have a broad range of substrates and their functions are often redundant with other PPs²⁴⁵. Moreover, the protein serine/Thr kinases outnumber the Ser/Thr phosphatases. This suggests that the evolution of Ser/Thr phosphatase diversity was rather driven by interaction with other proteins than by gene duplication and subsequent diversification events²⁴⁶. Therefore PPs have been recognized only later to have high substrate specificity important for controlling the equilibrium between the phosphorylated and dephosphorylated states of a protein.

PPs play a dynamic role in signaling, as they can be turned on and off by a tight regulation of their subunit composition and selective targeting. PP regulatory subunits can either facilitate or ablate binding of specific substrates, or direct the phosphatase to a specific subcellular localization¹⁹².

➤ PP1

PP1 is a key enzyme playing essential roles in transcription and cell cycle progression, but also in glycogen metabolism, protein synthesis and apoptosis in most eukaryotes¹⁹². PP1 exemplarily shows to which level PPP phosphatases can be regulated by interacting proteins named PP1-interacting proteins (PIPs). The highly conserved catalytic subunit (PP1c) is associated to one or two variable regulatory subunits, to form what is called a PP1 holoenzyme. From an evolutionary point of view, PP1 has gradually expanded its repertoire of functions by the acquisition and evolution of new regulatory subunits, while the catalytic subunit remained well conserved²⁴⁶. PIPs can either be substrates, targeting subunits, substrate specifiers or endogenous inhibitors of PP1c activity, as depicted in Figure 41¹⁹². The regulation by PIPs explains how PP1 can dephosphorylate different substrates with high specificity *in vivo*, although the apo-PP1 (PP1c) has low substrate specificity²⁴⁷.

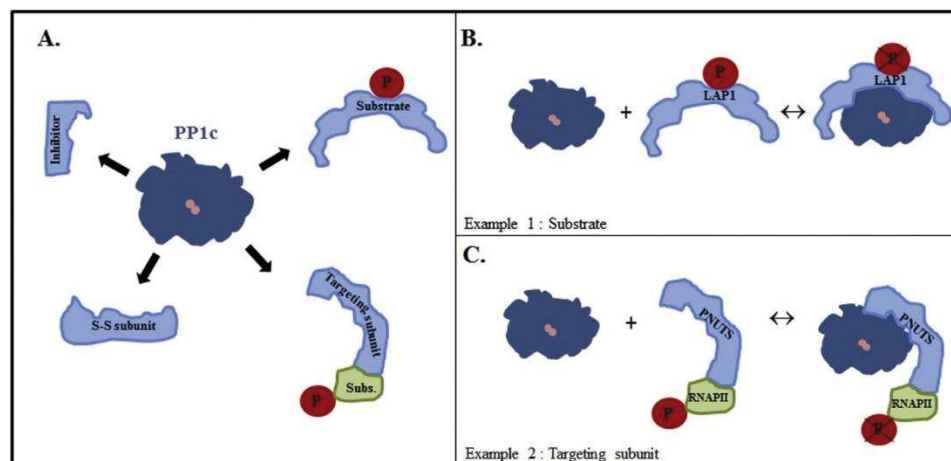


Figure 41: Different types of PP1 regulatory proteins. (A) PP1 regulatory proteins can be substrates, targeting subunits, inhibitors of the catalytic activity and substrate-specifiers. (B) LAP1 is an example of a PP1 substrate. (C) PNUTS is a PP1 targeting subunit and the PNUTS:PP1 complex is able to promote the dephosphorylation of Ser₅ of the CTD of RNAPII¹⁹².

In mammals, about 200 putative PIPs have been identified that might act as regulatory subunits of PP1c²⁴⁷. Structural analysis of the PP1-PIP complexes helps to understand at the protein level how a PIP redefines PP1 substrate specificity. The actual model is the following: every PIP binds to PP1 in a different way. PIP binding modifies the three surface grooves of PP1 (Figure 42B), which is thought to create a new surface for interactions with the substrate or to modify access to the active site^{190,248}. So

the question arises if there is a common binding mode or motif in PP1 involved in PIPs binding. The second question is if different PIPs are structurally related and can be divided into subclasses.

In search for a consensus PP1 docking motif, early studies found that a majority of PIPs contain a variant of the "RVxF" motif that binds to a hydrophobic channel on the surface of PP1c. This binding motif is a degenerate consensus sequence [R/K](X)0-1[V/I](p)[F/W], where X can be any amino acid and (p) any residue except proline²⁴⁹. A recent study combined structure analysis, molecular modeling and biochemical validation to refine the consensus motif to [H/K/R][A/C/H/K/M/N/Q/R/S/T/V][V][C/H/K/N/Q/R/S/T][F/W]. Val at position 3 and a bulky hydrophobic amino acid (Phe/Trp) at position 5 are invariant and essential for PP1 binding: these residues are accommodated in two hydrophobic pockets on the surface of PP1 and establish very strong, hydrophobic interactions (Figure 42A-B)²⁵⁰.

Apart from this conserved motif that mediates primary interaction, every PIP binds different parts of PP1 protein and thus has different domains to establish additional binding interactions. The substrate specifier MYPT1 (Myosin phosphatase targeting subunit) for example wraps halfway around PP1. MYPT1-PP1 interaction regulates Myosin II-dependent movement of smooth muscle cells. MYPT1 assembles with the δ isoform of PP1 and with M20, a protein of unknown function, to form the Myosin phosphatase holoenzyme in smooth muscle cells. Myosin phosphatase is targeted by MYPT1 to specifically dephosphorylate Ser₁₉ of Myosin Light chain (MLC), a process that triggers smooth muscle relaxation²⁵¹. Three motifs in MYPT1 ensure PP1 binding: the MyPhoNE motif (myosin phosphatase N-terminal element) located in the MYPT1 N-terminal α -helix, the RVxF motif and a folded ankyrin-repeat region (Figure 42C). Interestingly, the MyPhoNE consensus sequence of RxxQ[VIL][KR]x[YW] is also present in other unrelated PP1 targeting proteins, and therefore is a PP1 docking motif. Another common secondary PP1 docking motif is the SILK motif with a [GS]IL[RK] consensus sequence, which is involved in PP1 binding by the endogenous protein Inhibitor-2²⁴⁹.

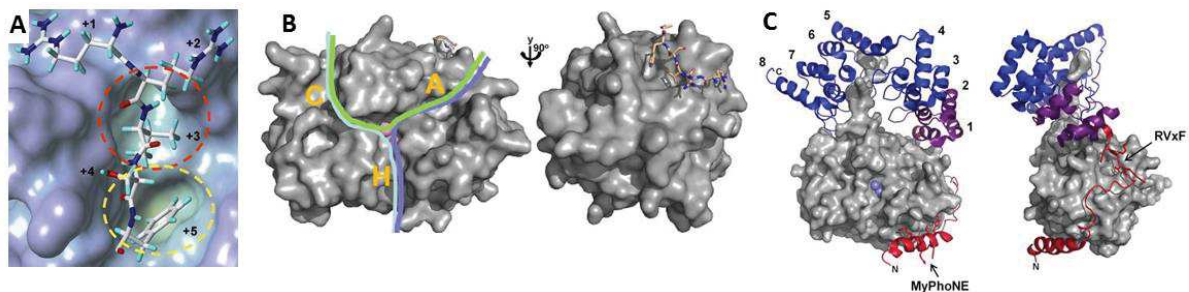


Figure 42: PP1 binding by regulatory subunits. (A) View of the two PP1 hydrophobic pockets that accommodate invariant Val +3 and Trp/Phe +5 of the PP1 docking consensus peptide²⁵⁰. (B) Surface presentation of the PP1 catalytic subunit bound to a RVxF peptide, shown in a stick representation. The pink metal sphere is the metal ion in the active center. The C-terminal (C), hydrophobic (H) and acidic (A) substrate binding grooves are indicated²⁴⁸. (C) PP1 in complex with the targeting subunit MYPT1. MYPT1 has three regions that establish interaction with PP1: the RVxF motif, the Ankyrin-repeat region (purple) and an N-terminal α -helix (red) that contains the MyPhoNE motif²⁵¹.

➤ PP2A

PP2A, PP4 and PP6 form a distinct phylogenetic group among PPPs (Figure 32). Their catalytic subunits are present as heterodimeric or trimeric complexes and they are regulated in a similar way¹⁹¹. As an example, the complex regulatory mechanism of PP2A will be described. The PP2A holoenzyme is composed of different subunits that are encoded by separate genes. The PP2A core is composed of a catalytic (C) as well as a scaffold subunit (A), which can bind an additional regulatory subunit (B) to form the heterotrimeric holoenzyme. Humans possess two isoforms of subunits A and C each, as well as four unrelated families of regulatory subunits (B, B', B'' and B'''). The function of the regulatory subunit is to refine PP2A substrate specificity¹⁹¹.

The four different regulatory subunit families adopt different structures and bind to different regions of the A and C subunits (Figure 43). Importantly, each group of B subunits has a distinct interface to interact with the substrate protein, which explains how different B subunits ensure different PP2A substrate specificity. An example is that any member of the B subunit family, but not B' or B'', mediate PP2A recognition of the microtubule-binding protein Tau²⁵². Hyperphosphorylated Tau polymerizes into intracellular neurofibrillary tangles in the brain and is thought to be involved in the onset of Alzheimer's disease. PP2A is one of the key players for the dephosphorylation of hyperphosphorylated Tau, and as such PP2A is probably controlling Tau function *in vivo*²⁵³. Additional regulation is achieved on the level of different isoforms and splice variants, and tissue- or cell type specific expression of selected subunits. Therefore each PP2A holoenzyme with its unique composition has a specific substrate specificity and function in a cell.

While the regulatory subunit defines substrate selectivity, there is an additional level of regulation mediated by the reversible methylation of the Leu₃₀₉ residue found in a TPDYL motif on the C subunit that activates the enzyme, probably by favoring the assembly of the holoenzyme. At the same time, methylation modulates the affinity of C for some regulatory subunits, and is therefore regulating the specificity of holoenzyme assembly¹⁹⁰.

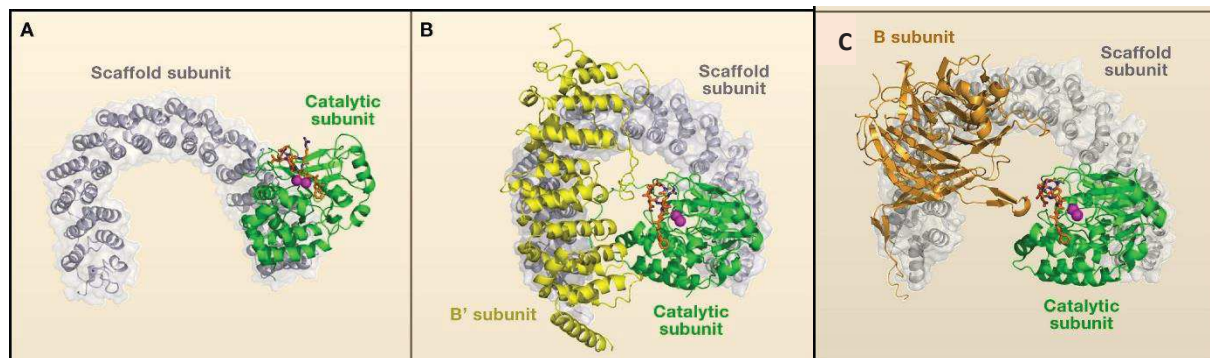


Figure 43: PP2A assembly and structure. (A) Structure of the heterodimeric PP2A core composed of the catalytic (green) and the scaffold subunit (grey). (B) and (C). Structure of the heterotrimeric PP2A holoenzyme, containing the regulatory subunit of the B' or B family. B or B' subunits have different architectures. They bind to different regions of the scaffold subunit and have different interactions with the catalytic subunit¹⁹⁰.

➤ Other PPPs

Not all PPP members are controlled by interacting proteins. PP5 contains a tetratricopeptide (TRP) regulatory domain at its N-terminus that acts as ligand-dependent allosteric PP5 regulator. In absence of stimuli, the TRP domain blocks the PP5 active site and maintains the phosphatase in an autoinhibited conformation. However, binding of polyunsaturated fatty acids or Hsp90 to TRP leads to its conformational change and to activation of the enzyme²²⁹.

3.2.2. PPM regulation

In contrast to the PPP family, PPMs are presumably monomeric functional entities and do not assemble with regulatory interaction partners. Instead, the PPM catalytic domain can be paired with a multitude of regulatory domains and sequence motifs in the same protein (Figure 44A). Depending on the regulatory domain, every PPM has a specific activity, substrate specificity or regulatory mechanism¹⁹⁰.

Mammalian PPM enzymes are not well understood on the structural and enzymatic level, but bacterial enzymes are much better characterized, also regarding protein regulation. The investigation of *Bacillus subtilis* SpoIIIE revealed a conserved molecular mechanism of how phosphatase activity is regulated by a structural switch: the catalytic domain of SpoIIIE contains two α -helices that act as allosteric regulator

of enzyme activity. Upon dimerization of two SpoIIE monomers, the α -helical switch rotates 45° and is shifted towards the active site (Figure 44B-C). This shift places the carbonyl oxygen of G₆₂₉ and the side chain of D₆₂₈ into the position where they can coordinate the two Mn²⁺ ions in the active site. By this structural rearrangement, SpoIIE is switched from its inactive to its active state. In the case of SpoIIE, the switch leads to dimerization required for activity. However, this α -helical switch was found broadly conserved in other PP2C enzymes, for example in human pyruvate dehydrogenase phosphatase 1. Therefore the authors suggest that this α -helical switch is a conserved mechanism of how PP2C enzymes can be activated by different input signals²⁵⁵.

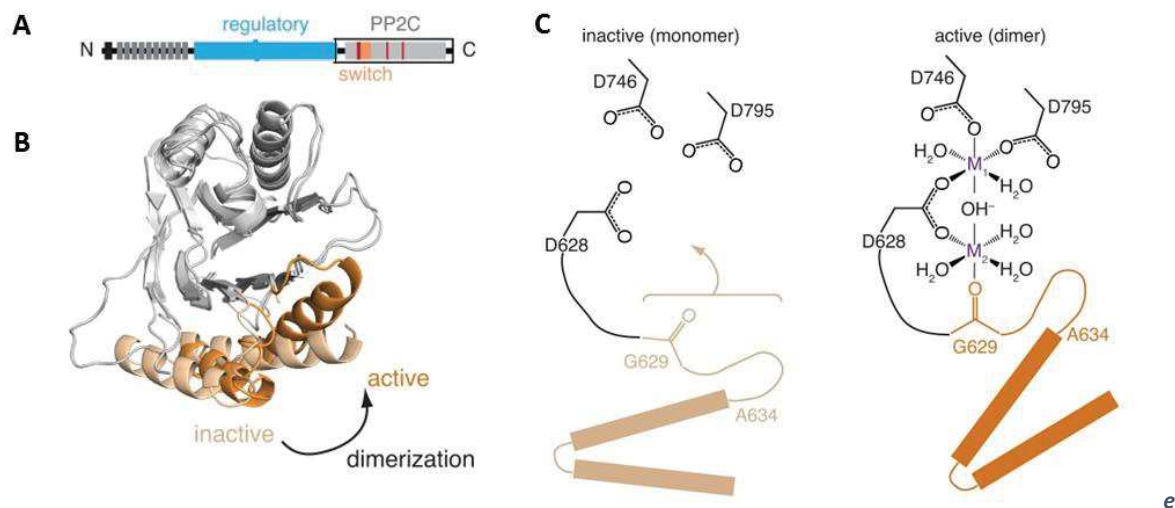


Figure 44: Regulation of a PP2C from *B. subtilis*, SpoIIE, by α -helical switch. (A) is a scheme of the SpoIIE primary structure with its N-terminal cytoplasmic degradation tag in black, the 10 trans-membrane segments in dark grey, the regulatory domain in blue, and the PP2C catalytic domain shown in light grey. The switch helices are depicted in orange and the metal-coordinating residues within the active site in red. The black box shows the part of the protein that was crystallized for (B). (B) Ribbon diagram of the SpoIIE catalytic domain structure and comparison of the monomer and dimer. Dimerization leads to repositioning of the α -helical switch. (C) Model of how repositioning of the switch leads to phosphatase activation. The two Mn²⁺ ions are likely coordinated by the side-chain of D₆₂₈ and the carbonyl oxygen of G₆₂₉ in the active SpoIIE²⁵⁵.

3.2.3. PTP regulation

The PTP group of PPs also displays specific mechanisms of regulation. Besides the catalytic domain, PTP genes often encompass additional domains that control specificity, regulation and activity. So the ancestral PTP phosphatase domain is thought to have further evolved by fusion to additional domains with regulatory functions. This is in contrast to STP catalytic domains, which expanded their repertoire by interaction with new protein partners²⁵⁶.

Besides, PTPs can be regulated by post-translational modifications such as phosphorylation or oxidation. The catalytic Cys residue is prone to reversible oxidation, and oxidation inhibits the catalytic properties of the enzyme²⁵⁷. PTP1B is one of the most studied PTPs. This PP down-regulates insulin and leptin signaling and also plays a role in signaling associated to breast tumorigenesis²⁵⁶. Apart from the N-terminal catalytic domain, PTP1B has a regulatory domain and a C-terminal hydrophobic segment that directs the protein to the cytoplasmic face of the endoplasmic reticulum²⁵⁸. This targeting to the ER surface is an example of how PTPs are regulated by specific subcellular localization, which restricts the spectrum of possible substrates²⁵⁹. The regulatory domain down-regulates PTP1B activity, but neither the upstream signals nor the exact mechanism is known. However, regulation of PTP1B catalytic activity by reversible thiol oxidation is well studied, and depicted in Figure 45A. Locally produced ROS, in particular H₂O₂, induce oxidation of the active site Cys to form a singly oxidized, reversible sulphenic acid, which renders PTP1B temporarily inactive²⁶⁰. A subsequent condensation

reaction converts the sulfenic acid to a cyclic sulphenamide, which can then be accessed by reducing systems in the cell. PTP1B then is regenerated and reactivated by the cellular glutathion and thioredoxin (reaction mechanism shown in Figure 45B)²⁵⁹. This reversible oxidation provides a means to temporarily turn off or on PTP1B activity, as was reported for example in response to insulin *in vivo*²⁶¹.

Receptor-PTPs can be additionally activated or inactivated by dimerization²⁶².

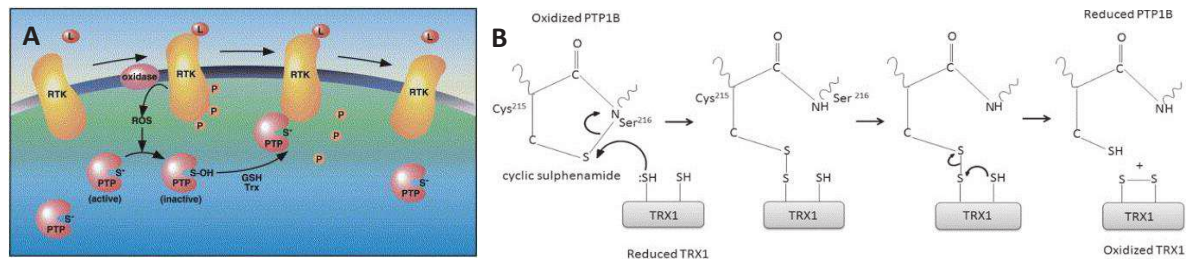


Figure 45: Reversible oxidation transiently inactivates PTP1B enzyme. (A) Free electrons generated in the cell are transferred to NADP. NADPH oxidases then recycle NADP and produce ROS. ROS in turn can transiently inactivate the PTP1B active site by thiol oxidation. The enzyme is reduced and regenerated by Glutathion (GSH) and Thioredoxin-1 (Trx)²⁵⁹ (B) Proposed mechanism for reduction of the cyclic sulphenamide form of oxidized PTP1B by TRX1²⁶³.

3.3 Phosphatases in Plasmodium

3.3.1 The Plasmodium phosphatome – *In silico* studies

Protein phosphatases in *Plasmodium* have been annotated in three independent studies^{264–266}. To sum up the current state of knowledge and taking into account all three cited phosphatome studies, *P. falciparum* encodes potentially 10-16 PPPs, 10-13 PP2C phosphatases, four NIFs and four PTPs^{240,264–266}. One of the PTPs is a PTP-like protein (PTPLA), member of a catalytically inactive PP group^{240,267}. Figure 46 shows an overview of *Plasmodium* PPs and the groups they belong to, as annotated by Guttery, *et al.*²⁶⁶.

Wilkes and Doerig screened the predicted proteomes of *Plasmodium* and other eukaryotic organisms for the presence of PP catalytic domains²⁶⁴. The retrieved PP sequences were then clustered by the major PP groups which was used to reconstruct the phylogeny in each PP group. The *P. falciparum* phosphatome was the smallest among the model organisms studied (plant, animal, algae, Kinetoplastida, Excavata). However, *Plasmodium* shows a high diversity of PPs: all four PP classes are represented by one member from almost every subtype. Yet, *Plasmodium* does not encode any PP of the Cdc25, the Cdc14, the classical PTP and the LMW-PTP group. Thus the authors conclude that the parasite maintains a large functional capability despite a small phosphatome, and it can extend its phosphatase functional capacities by additional regulatory mechanisms²⁶⁴.

A later *in silico* screen by Guttery, *et al.* reported 29 and 30 phosphatases for *P. falciparum* and *P. berghei* respectively, out of which 28 genes are direct orthologues²⁶⁶. Compared to the previous screen, two additional PPs were described for both species, PPP8/EFPP and PTPLA. Comparison of the human and rodent phosphatome revealed that *P. berghei* lacks PPM10, but codes for two PPs absent from *P. falciparum*, PTP2 and NIF1.

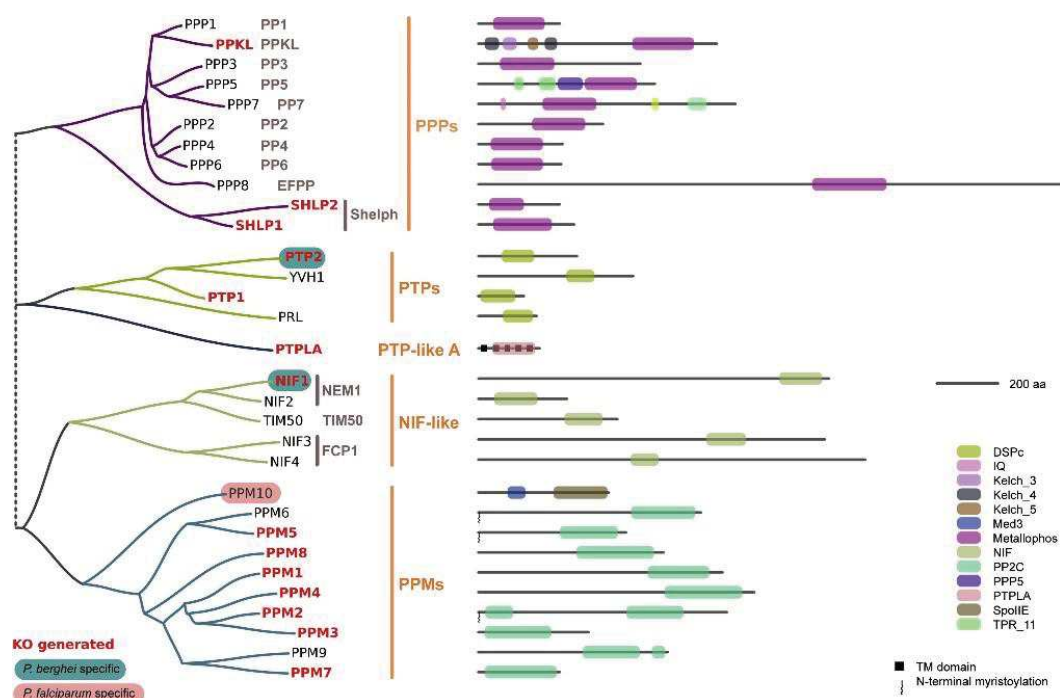


Figure 46: Schematic phylogenetic tree and domain architectures for the PPs of *P. berghei* ANKA and *P. falciparum* 3D7 showing family and subfamily classification²⁶⁶. Knockout mutants obtained are shown in red.

Pandey *et al.* performed another bioinformatics screen of *Plasmodium* PPs, but they searched phosphatase families based on broader selection criteria regarding substrate specificity: they included PP families that not only dephosphorylate proteins, but that also can accept lipids, phosphoinositides, DNA, mRNA, carbohydrates or inorganic moieties^{265,268}. Some examples of broad-activity Tyr phosphatase groups present in *Plasmodium* are rhodanese homology domain (RHOD), haloacid dehalogenase (HAD) and His phosphatase (HP) families.

By this approach, 67 putative PP sequences were identified in *P. falciparum*. Apart from the new broad-specificity PP groups, this screen contained all classical PPs predicted by the two other phosphatome studies, and identified two additional putative PPPs (PF3D7_0918000 and PF3D7_0912400) and one new PPM (PPM11, PF3D7_1208900) sequence²⁶⁵.

The PPP family is divided into the PP1, PP2A, PP2B, PP4, PP5, PP6, PP7 and PPKL subfamilies (see Figure 31), and *Plasmodium* has exactly one member of each subtype²⁶⁹. The PPKL subfamily is widespread in plants, but also encoded by *P. falciparum*, *P. berghei* and *T. gondii*²⁷⁰. Additionally, two bacterial-like PPPs are present in *Plasmodium*: *Shewanella*-like phosphatase 1 (*PfShelph1*, PF3D7_1469200) and *PfShelph2* (PF3D7_1206000), which are homologues of *Shewanella* CAPTPase^{211,264}. *T. gondii* codes for only one Shelph gene (TGME49_2547700) which is most similar in sequence to *PfShelph1*.

Apart from orthologues of classical mammalian, plant and bacterial-like PPPs, Apicomplexans possess a unique group of pseudo-phosphatases termed EFPP²⁷¹, and the *Plasmodium* orthologue is called EFPP or PP8²⁶⁶. EFPPs possess EF-hand motifs in their long N-terminal domain, but are different from the PP7/EFPP group. These presumably Ca²⁺-binding proteins lack essential residues in their catalytic domain and probably are catalytically inactive²⁷¹.

Altogether, *Plasmodium* encodes four phosphatases absent from the rodent or human host, namely PPKL, EFPP as well as Shelph1 and Shelph2²⁶⁶. These PPs would be interesting candidates for future drug targets.

When comparing the *Plasmodium* phosphatome to the known kinome, it is obvious that *Plasmodium* kinases outnumber the phosphatases by two-to threefold: two independent genomic analyses

identified 86 or 99 putative protein kinases in *P. falciparum*, representing 1.1–1.6% of the coding genes^{116,117}. Out of these, 65 belong to the eukaryotic protein kinase (ePK) family¹²¹. The surplus of kinases can be explained by the fact that kinases have a high degree of substrate specificity while PPs, especially PPPs, augment their functional repertoire by regulatory mechanisms²²⁹.

Nearly half of the *Plasmodium* PPs have been the subject of further biochemical or functional studies. The functions of *Plasmodium* phosphatases have been mostly studied in the murine malaria model *P. berghei*²⁶⁶, while biochemical characterizations were conducted for the *P. falciparum* orthologues. Table 5 gives an overview of all PPs that have been the subject of detailed investigation.

Several *Plasmodium* phosphatase activities have been biochemically characterized, and most biochemical studies have investigated the respective *P. falciparum* enzyme. Among the PPP family, the following are confirmed active phosphatases: PP1, PP2A, Calcineurin, PP5, PP6, PP7, *PbShelph1* and *PfShelph2*. *Plasmodium* possesses 10 to 12 putative PPM sequences, out of which only PPM2 activity has been demonstrated and investigated^{273,274}. None of the four *Plasmodium* proteins possessing the conserved catalytic motifs of the FCP/SCP phosphatase family have been biochemically investigated to date. Four putative PTP genes were identified in *Plasmodium*, among which one sequence (PTP2, PF3D7_1127000) has an incomplete PTP motif and probably does not contain a catalytically active site²⁶⁵. YVH1 and PRL are two DSBs among the identified PTPs that have been biochemically characterized and shown to be active enzymes *in vitro*^{133,275}.

Table 5: Overview of characterized *Plasmodium* phosphatases (adapted from ²²⁷). Substrates used in the biochemical PP activity assays are the non-proteinaceous chromogenic substrate *p*-nitrophenylphosphate (pNPP) or proteinaceous *p*-histone (phospho-histone H1), *pS* (phosphor-serine peptide) or *pY* (phosphor-tyrosine peptide). OMFP (3-*O*-methylfluorescein phosphate) and MFP fluorogenic substrates are dephosphorylated by both STPs and PTPs. Orthovanadate is a specific inhibitor of PTP activities.

	Plasmodb accession nb of <i>P. falciparum</i> catalytic subunit	Biochemical characterization	Functional characterization studies (<i>P. berghei</i> or <i>P. falciparum</i>)
PPP group			
PP1	PF3D7_1414400	STP activity in presence of Mn ²⁺ , substrates pNPP and pS; inhibited by OA, tautomycin, I1, I2; N122D ablates activity ²⁷⁶	Putative role egress Putative role in cell cycle regulation ^{277–282}
PP2A	PF3D7_0925400	Activity on pNPP, pS; divalent ions required ; inhibited by OA, I1 ^{283,284} ; activated by PTP2A ²⁸⁵	²⁸⁵
PP2B/ Calcineurin	PF3D7_0802800	Activity on pNPP, pS; divalent ions and Ca ²⁺ /Calmodulin required; non-competitive inhibition by Cyclophilin and CyclosporinA ²⁸³	Parasite attachment to RBC; male gametogenesis, ookinete formation; sporozoite-to-liver stage transition ^{160,286,287}
PP5	PF3D7_1355500	Activated by unsaturated fatty acids; PP activity assay with p-histone and pNPP; inhibition by OA IC ₅₀ =5.1nM ²⁸⁸	
PP7	PF3D7_1423300	Mn ²⁺ -dependent STP activity; phosphorylase a and pNPP as substrate ²⁸⁹	
PPKL	PF3D7_1466100	PP activity using difluoro-4-methylumbelliferyl phosphate (DiFMUP) substrate, Mn ²⁺ and Mg ²⁺ ²⁹⁰	Ookinete development ^{270,290}
Shelph1	PF3D7_1469200	Activity towards MFP substrate in presence of Mn ²⁺ ²⁹¹	Microneme maturation and ookinete development ²⁹¹

Shelp2	PF3D7_1206000	PTP activity, requires Mn ²⁺ or Co ²⁺ ; D79N mutation ablates activity ¹⁸³	Possibly RBC invasion ^{183,292}
PPM group			
PPM1	PF3D7_0410300		Microgamete exflagellation ²⁶⁶
PPM2	PF3D7_1138500	STP activity, dependent on Mg ²⁺ ; dephosphorylates PEF1β ^{273,274}	Gametocyte sex allocation; ookinete differentiation ²⁶⁶
PPM5	PF3D7_0810300		Oocyst development ²⁶⁶
UIS2	PF3D7_1464600	STP activity towards PefF2α-P; inhibited by PPM-specific inhibitors EDTA and Cd; preference Mn ²⁺ over Mg ²⁺ ²⁹³	Sporozoite transformation into liver stage ²⁹³
DSP group			
PRL	PF3D7_1113100	Activity towards OMFP substrate; inhibition by orthovanadate and CAAX peptide; no inhibition by STP inhibitor cocktail ²⁷⁵	
YVH1	PF3D7_0309000	PTP activity, inhibited by orthovanadate; no requirement for divalent metal ions; residues C71, C168 and C222 necessary for activity ¹³³	

In the following sections current knowledge will be presented on the *Plasmodium* phosphatases for which a function in parasite development has been described (summarized in Figure 47).

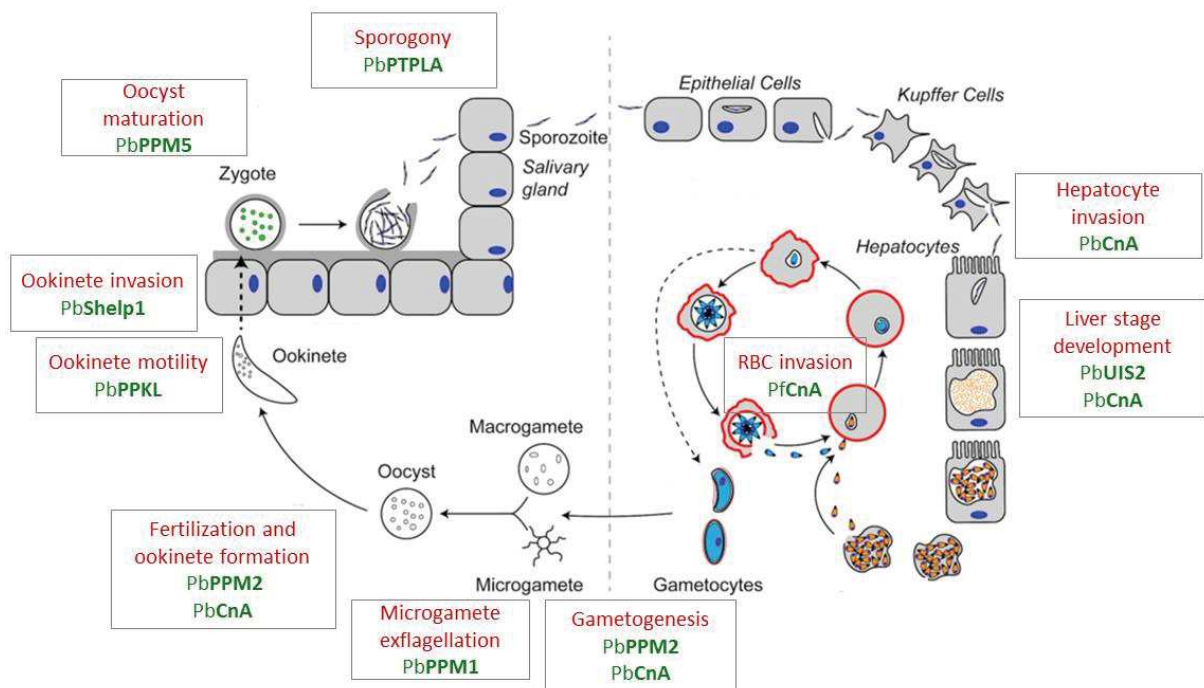


Figure 47: Overview of *Plasmodium* phosphatases functions in the parasite life cycle adapted from²⁹⁴

3.3.2 PPs which function in the mosquito stages

Several phosphatases have been shown to play a role at different points of the parasite development in the mosquito, and this work was mostly done in *P. berghei*. An important functional analysis systematically characterized the whole *P. berghei* phosphatome and found diverse phosphatases to be regulators in the parasite sexual stages²⁶⁶. Guttery *et al.* attempted to delete every phosphatase separately, and then analyzed the phenotypes of the phosphatase knockout strains obtained. Additionally, the subcellular localization of the phosphatases was determined by C-terminal GFP-tagging of the endogenous locus, in a single-homologous recombination event.

➤ Phosphatases involved in gametogenesis

The mosquito takes up male and female gametocytes via a blood meal from the human host. The first developmental step of the parasite in the mosquito is gametogenesis, the maturation of gametocytes into gametes. Gametogenesis is initiated by stimuli in the mosquito midgut environment¹⁷. Upon activation, both male and female gametocytes egress from erythrocytes, and female gametocytes mature to form macrogametes. Male gametocytes undergo three rounds of genomic DNA replication resulting in eight nuclei that are each packed into an axoneme-containing microgamete²⁹⁵.

PPM2 controls female gametogenesis in *P. berghei*, as gene knockout resulted in more than 70% reduced macrogamete numbers²⁶⁶. **PPM1** and Cn on the other hand, are required for male gametogenesis. PPM1-KO microgametes are completely blocked in exflagellation²⁶⁶. Philip and Waters (2015) demonstrated the importance of **Calcineurin** subunit A (CnA) in parasite sexual development in the *P. berghei in vivo* rodent model. Cn function was investigated via an auxin-inducible degron (AID) protein knockdown system, and CnA-depleted parasites showed a 50% decrease in male gametogenesis.

➤ Phosphatases in fertilization and ookinete development

The next step in parasite sexual development is the fusion of the macro- and microgamete to form a zygote, which develops into a motile ookinete within approximately 18 hours. The ookinete migrates to the luminal part of the midgut epithelium, and transgresses an epithelial cell. In the intracellular space between the epithelial cell basal side and the basal lamina, the ookinete develops into an oocyst that matures over 10 days to give rise to thousands of sporozoites¹⁸. Different steps of fertilization and ookinete development are regulated by *PbCn*, *PbPPM2*, *PbSHLP1* and *PbPPKL*.

PbCn is involved in the maturation of zygotes to ookinetes. In the CnA-KD, the majority of resulting zygotes were unable to develop into ookinetes. A separate phenotype is observed when CnA is depleted at ookinete stage, which leads to a defect in the ookinete-to-oocyst transition, demonstrating that CnA is also required for this developmental step²⁸⁶.

PbPPM2 is required for ookinete maturation into oocysts. Ookinete-to-oocyst conversion is drastically impaired in Δ PPM2 parasites, resulting in an almost complete block of parasite development at this stage. Ultrastructural characterization of the Δ PPM2 ookinetes showed that the majority featured a round morphology with cytoskeletal abnormalities, being clearly different from the typical crescent shape of wt ookinetes²⁶⁶.

PbShelph1 functional characterization also revealed a function in ookinete development²⁹¹. Tagging of the endogenous *PbShelph1* locus demonstrated protein expression in all parasite stages and its localization to the endoplasmic reticulum (ER). The deletion of *Shelph1* resulted in impaired ookinete formation and a complete arrest at the ookinete-to-oocyst conversion²⁹¹. An ultrastructural analysis of the *PbShelph1*-KO ookinetes showed that micronemes development was impaired, resulting in a

reduced number and mislocalization of micronemes. Nevertheless, ookinete motility was normal in the Shelph1-KO, suggesting that the Shelph1-KO ookinetes can cross the midgut epithelium, but are unable to develop into oocysts. *PbShelph1* is an active phosphatase with phospho-Tyr activity *in vitro*, which is coherent with its affiliation to the Shelph family of PPs²⁹¹.

Another PP implicated in ookinete development is **PPKL**. Two independent studies investigated PPKL function, localization and expression in *P. berghei*^{270,290}. PPKL is highly expressed in, female gametocytes and ookinetes, and immunoprecipitated PPKL displays phosphatase activity. Upon deletion of PPKL, ookinete development and differentiation were impaired. More specifically, the *ppkl*-KO ookinete showed an immotile phenotype, as the apical microtubules had dissociated from the inner membrane complex. The immotile ookinetes were unable to invade the mosquito mid-gut epithelium. Interestingly, PPKL activity itself is differentially phosphorylated. So PPKL is probably regulated by phosphorylation, as is the case for its plant orthologue *AtBSU1*^{270,296}. PPKL is an active phosphatase *in vitro*, and phosphatase activity is ablated when the PPP active site residues are mutated²⁹⁰.

➤ **Phosphatases important for oocyst maturation and sporogony**

Upon active egress from the oocyst, thousands of sporozoites are released into the open hemolymph circulation of the mosquito²⁹⁷. The sporozoites then migrate to and invade the salivary glands, traversing its basal lamina and epithelial cell layer to get into the central secretory cavity. From here, they can be transmitted to the mammalian host²⁹⁸. Oocyst maturation into sporozoites, is governed by another set of phosphatases, namely *PbPPM5* and *PbPTPLA* (PTP-like A homologue).

PbPPM5 deletion does not affect parasite development until the ookinete stage. However, PPM5-KO ookinetes are impaired in their maturation into oocysts, as seen by a reduced oocyst number and size. Although ookinete motility is normal, the mutant ookinetes have reduced numbers of micronemes. Maturation of PPM5-KO completely comes to a halt at a later stage: no sporozoites are generated in the PPM5-KO parasites, and the parasite development is stalled at this stage. PPM5 protein was found expressed in all sexual and asexual stages, and the protein localizes diffusely to cytoplasm, nucleus and to membranes. PPM5 could associate to membranes as it is predicted to be myristoylated at its N-terminus²⁶⁶.

PbPTPLA is another PP essential for sporozoite formation. PTPLA-KO parasites develop normally until the oocyst stage, but cannot produce sporozoites²⁶⁶.

Overall we can suppose, but not know for sure, that the *P. falciparum* orthologues of the PPs described likely fulfill the same functions in mosquito stages as do their *P. berghei* orthologues described in this chapter.

3.3.3 PPs important for liver stage development

Malaria transmission to the vertebrate occurs when an infected mosquito injects crescent-shape salivary gland sporozoites (Ssp) into the skin. From here, the parasites enter the blood circulation and invade hepatocytes. Inside the liver cells, the sporozoite differentiates into a spherical liver stage or exo-erythrocytic form (EEF) that matures to form several thousand of merozoites in a few days. The merozoites then egress from the hepatocyte and start to infect red blood cells²⁰.

3.3.3.1 UIS2

Sporozoites are a metabolically particular stage, as translation is globally repressed for most transcripts, and inactive mRNAs are stored inside stress granules and P-bodies²⁹⁹. However, approximately 30 genes are active and even upregulated in sporozoites, and this group of genes was termed UIS (upregulated in sporozoites)²⁰. Among these genes is the kinase UIS1 that phosphorylates the eukaryotic translation initiation factor eIF2 α ³⁰⁰.

eIF2-GTP together with eIF1, Met-tRNA_i, the 40S ribosomal subunit, mRNA and eIF5 form the 43S pre-initiation complex of translation. eIF2 GTPase activity leads to the recognition of the AUG start codon and release of eIF1. The subsequent dissociation of eIF2-GDP from the complex allows the recruitment of the 60S ribosomal subunit. eIF2-GDP then needs to be recycled for the next round of translation initiation and this process depends on the GTP-exchange factor eIF2B. eIF2 is a heterotrimer composed of α , β and γ subunits³⁰¹. eIF2 γ is the catalytic subunit and binds tRNA_i-Met, whereas eIF2 β recruits mRNA, eIF1, eIF5 and eIF2B. eIF2 α is the regulatory subunit and is regulated by phosphorylation of Ser₅₉ in *Plasmodium* (Ser₅₁ in yeast and mammals)^{300,302}. Phosphorylation turns eIF2 α into an inhibitor of the GTP exchange factor eIF2B and thereby into an inhibitor of translation initiation³⁰³.

eIF2 α phosphorylation is the mechanism by which translational quiescence of salivary gland sporozoites is regulated²⁹⁹. The eIF2 kinase UIS1 is essential and sufficient for translational repression in this stage³⁰⁰. Consequentially, eIF2 α must be dephosphorylated once parasites develop into liver stages in order to quit the quiescence and to allow translation of liver stage-specific transcripts. Therefore, Zhang *et al.* searched for an eIF2 α phosphatase and found UIS2 (PF3D7_1464600) to dephosphorylates eIF2 α among the UIS genes²⁹³. UIS2 had been retrieved among the PPPs in the phosphatome study by Wilkes & Doerig as well as by Pandey *et al.*, but not in the screen by Guttery *et al.*^{264–266}. In mammals, eIF2 α is dephosphorylated by PP1³⁰². In *Plasmodium* however, P_heIF2 α is lacking any PP1-binding motif. Zhang *et al.* showed that UIS2 dephosphorylates P_heIF2 α *in vitro*. Furthermore, they studied UIS2 function by generating a *P. berghei* conditional knockout line using the FlpL/FRT site-specific recombination system³⁰⁴. The *uis2* cKO parasites developed normally in the mosquito. However, when *uis2* cKO sporozoites invaded hepatocytes in culture, they were unable to develop into liver stages, and remained as crescent-shaped sporozoites. When transmitted to mice, these sporozoites were unable to establish an infection. Therefore, UIS2 is essential for *P. berghei* liver stage development. UIS2 works by dephosphorylating eIF2 α and thereby abolishes the global translational repression exerted by eIF2 α -P²⁹³. Although its role in translational control requires UIS2 localization in the parasite cytoplasm, a recent study employed the BioID technique and revealed an additional UIS2 localization in the PVM of intrahepatic cells, yet the function associated to this location remains to be investigated.

3.3.3.2 Calcineurin function in liver stages

Aside from its importance for other parasite stages, Calcineurin also plays a role in *Plasmodium* liver development. Calcineurin is involved, but not essential, for the transition of sporozoites to liver stages. Cn depletion using the AID strategy led to a minor decrease of sporozoite invasion into hepatocytes, but the sporozoites that managed to invade the hepatocytes were affected in their development into liver stages, as half of them failed to give rise to EEFs. Nevertheless, the remaining 50% of EEFs that had managed to form in absence of Cn proceeded normally in their development²⁸⁶.

3.3.4 PPs important in the parasite erythrocytic cycle

Reverse genetic studies have clearly demonstrated that Calcineurin regulates parasite invasion into RBCs. For PP1 and Shelph2 function however, the current scientific data are poor and only suggest a function in the parasite erythrocytic cycle, but the link needs to be confirmed.

3.3.4.1 Calcineurin

P. falciparum Cn function in the parasite asexual development has been demonstrated by reverse genetic studies, which found Cn essential for merozoite invasion into the red blood cell^{160,286}.

Indeed, Cn is indispensable in host-cell receptor-dependent merozoite attachment to the RBC prior to invasion¹⁶⁰. Using Cyclosporin A and FK506 inhibitors of Cn activity, it was also shown that inhibition of the enzyme impedes microneme secretion and reduces the invasion efficiency of merozoites²⁸⁷. Actin was identified as a substrate of Cn, with Cn inhibition leading to a reduced depolymerization of cortical actin in the apex of the merozoite. Actin dynamics are likely important for glideosome-dependent motility and could be part of the motor to drive invasion: actin polymerization is essential for gliding motility in *Toxoplasma*⁶⁹, and filaments in *Plasmodium* merozoites localize to the apical pellicle and to the MJ during merozoite and sporozoite invasion⁷⁰. Therefore Cn could be a major regulator of parasite motility.

3.3.4.2 Shelph2

Shelph2 was predicted to be part of the parasites protein repertoire involved in RBC invasion, as it was detected in a transcriptional profiling screen by Hu *et al*³⁰⁵. This genome-wide screen analyzed *P. falciparum* transcriptional profiles after inducing growth perturbations by different chemical compounds. From the expression data, proteins with similar expression profiles upon drug pressure were clustered together. Next, available protein interaction data and predictions helped to construct protein interaction networks from these gene expression clusters. Shelph2 was predicted to form part of the protein network responsible for merozoite invasion into the RBC³⁰⁵.

A phosphatome study in *P. berghei* showed that *Shelph2* deletion neither impairs red blood cell development nor the mosquito stages of the parasite²⁶⁶. In the *P. falciparum* RBC stages, Shelph2 protein is detectable only in schizonts and merozoites, which corresponds to its very late mRNA expression profile^{183,306}. It localizes to vesicular structures in the parasite cytoplasm which do not associate with any known rhoptry, microneme or dense granule markers¹⁸³. *In vitro*, PfShelph2 was shown to be an active Tyr-phosphatase, just as would be expected from its sequence orthology to *Shewanella* CAPTPase^{183,224}. Shelph2 dephosphorylates the red blood cell membrane protein Band 3 *in vitro*¹⁸³. Band 3 is a RBC trans-membrane protein that fulfills diverse functions: it is an anion transporter and serves as a major center for RBC membrane organization, as it is linked to the RBC sub-membrane skeleton via ankyrin and adducin¹⁷⁷. Band 3 Tyr phosphorylation by RBC Syk and Lyn kinases reduces Band 3 affinity for Ankyrin. This leads to its release from the spectrin/actin skeleton, thereby reducing membrane integrity¹⁸². Interestingly, *Plasmodium* infection stimulates Band 3 hyperphosphorylation in the early invaded RBC¹⁸⁵. Fernandez-Pol *et al.* therefore suggest a model in which Band 3 is phosphorylated upon parasite attachment and detaches from the submembrane cytoskeleton, thereby clearing the way for the parasite to enter. Reconstitution of Band 3 positioning must be initiated by its dephosphorylation, for example by Shelph2 if it is secreted into the RBC upon invasion¹⁸³.

3.3.4.3 PP1

The ubiquitous eukaryotic enzyme PP1 is also conserved in *P. falciparum*²⁷⁶. In *Plasmodium* parasite extracts from the intra-erythrocytic stages, PP1-like activity is more important than PP2a-like activity, whereas the erythrocyte demonstrates almost exclusively PP2A-activity³⁰⁷. Recombinant *Pf*PP1 has phosphatase activity, which can be inhibited by OA, tautomycin, phosphate, pyrophosphate and mammalian PP1-specific inhibitors I1 and I2³⁰⁸. *Pf*PP1 is also likely an active phosphatase *in vivo*, because its amino acid sequence is highly conserved with PP1 from other organisms containing all PPP catalytic motifs, and because PP1 inhibitors impair parasite growth³⁰⁷. Besides, *Pf*PP1 can take over the function of its yeast homologue Glc7p, as it rescued the *glc7p* low glycogen phenotype by complementation³⁰⁹.

PP1 shows a nucleo-cytoplasmic localization in asexual and intrahepatic *P. berghei* stages^{293,310}. Moreover, it was also reported to be located in the lumen of Maurer's clefts (MC) in *P. falciparum* using anti-human PP1 antibodies²⁷⁷. Maurer's clefts are parasite-derived membranous compartments in the RBC cytosol that the parasite employs for protein trafficking, sorting and export. In this compartment, PP1 would dephosphorylate skeleton-binding protein 1 (SBP1), a MC's transmembrane protein whose C-terminal tail interacts with RBC cytosolic protein Lantibiotic synthetase component C-like protein (LANCL 1)³¹¹. The phosphorylation status of SBP1 could modulate MC anchoring or function²⁷⁷.

PP1 is likely essential for parasite growth, as genetic deletion attempts failed so far in *P. berghei* and *P. falciparum*^{266,293}. PP1 is also likely an essential gene in *Toxoplasma*, as *Tg*PP1 (TGME49_310700) could not be knocked out in a genome-wide CRISPR screen³¹². As PP1 is indispensable for different Apicomplexa species, this suggests a conserved role of PP1 for similar functions in the parasite development. Till date, no conditional reverse genetic strategies have been applied for determining PP1 functions in parasite development. A possible *Pf*PP1 function in parasite egress came from the use of classical PPP inhibitors. Interestingly, the *calA* treatment rendered the merozoites incapable to egress from the host cell, thus suggesting a possible involvement of *Pf*PP1 in parasite egress. However, the molecular mechanism underlying the *calA*-mediated egress block are not known, and future studies need to investigate which PP activity inhibited by *calA* mediates egress²⁷⁷. Another way to help understand PP1 functions lies in the functional characterization of PIPs. So far, *in vivo* and *in vitro* experiments have validated the interaction of PP1 with five *Plasmodium* proteins, *Pf*LRR1, I2, I3, eIF2 β and RCC1, suggesting the involvement of the enzyme in the regulation of mitosis. In these studies, *Xenopus* oocytes were used as a model to test *in vivo* the functionality of PP1 inhibitors: *Xenopus* oocytes are physiologically arrested in G2/M meiotic prophase I, and it has been shown that inhibition of PP1 activity disrupts this meiotic arrest, leading to the so-called oocyte germinal breakdown (GVBD)²⁷⁸.

*Pf*LRR1 (Leucin-rich repeat protein 1) was identified as orthologue of yeast Sds22 protein, which is required for metaphase-to-anaphase transition in *Schizosaccharomyces pombe* by enhancing PP1 activity at this stage³¹³. *Pf*LRR1 is predicted to adopt a horse-shoe shaped structure made up by up to 16 LRR repeats, a structural feature that serves as PP1 binding motif in Sds22³¹⁴. *Pf*LRR1 was shown to bind to PP1 recombinant protein, and a PP1-*Pf*LRR complex could be immunoprecipitated from parasite cellular extracts. LRR1 acts as an inhibitor of *Pf*PP1 activity *in vitro*, just as was reported for the mammalian homologue. In the parasite asexual stages, LRR1 mRNA expression is highest in young trophozoites. Injection of *Pf*LRR1 capped mRNA into *Xenopus* oocytes disrupted meiotic arrest, showing that *Pf*LRR1 acts as PP1 inhibitor *in vivo*, and that LRR1-PP1 interaction regulates cell cycle progression^{278,315}.

Another PIP, inhibitor-2 (I2) is one of the most evolutionarily ancient PP1 regulators. I2 has a prominent role in the regulatory networks that assure the tight regulation of mitosis and cytokinesis in human cells, by balancing Aurora A, Aurora B and PP1 activities^{316,317}. Human I2 can act as PP1 inhibitor or activator, depending on its phosphorylation state. When I2 is phosphorylated on Ser₈₇ (by Greatwall kinase) and Ser₇₃, it activates PP1¹⁷³. One important downstream effect of the I2-PP1 complex is the deactivation of Aurora B kinase. Aurora B kinase has various prominent roles in mitosis, including the promotion of chromosome condensation and a checkpoint function for assuring the correct attachment of centromeres to the bipolar spindle³¹⁸. A *Plasmodium* I2 homologue was identified that inhibits PP1 activity *in vitro*. Mutation of the predicted PP1-docking motifs ablates inhibition. PfI2 localizes to the parasite nucleus and cytoplasm in all intraerythrocytic stages. As attempts to delete the gene failed, another approach was used to assess I2 function *in vivo*: iRBCs were treated with synthetic peptides that block I2 binding to PP1, which led to a 80% inhibition of parasite growth. Therefore, *Plasmodium* I2 is most likely essential for parasite survival. Injection of I2 recombinant protein into *Xenopus* oocytes resulted in GVBD, pointing at a possible function of I2 in cell cycle regulation²⁷⁹.

PP1 inhibitor 3 (I3) is also found in *P. falciparum*. In contrast to I3 inhibitory activity in other organisms, *in vitro* assays showed that PfI3 is a positive regulator of PP1 activity. Kinetics and affinity of PP1-I3 binding were characterized for the recombinant proteins. I3 probably forms a complex with PP1 *in vivo* in the parasite cytosol, as was shown using GST pull-down assays. PfI3 is likely essential for the parasite, as attempts to obtain knockout parasites were unsuccessful. I3 nuclear localization in asexual stages suggests that I3 regulates nuclear functions of PP1²⁸⁰.

Another PIP is the β -subunit of eukaryotic translation initiation factor 2 (eIF2 β). Although translation only takes place in the parasite cytoplasm, and to some degree in the mitochondria and apicoplast²⁹⁹, eIF2 β shows a nuclear as well as cytoplasmic localization. PfEIF2 β possesses two PP1-binding motifs, and by pull-down assay was shown to interact directly with PfPP1²⁸². In humans, it was demonstrated that eIF2 β and PP1 interact and that eIF2 β binding alters the substrate preference of PP1. Interestingly, HseIF2 β functions as an activator of its own dephosphorylation, but as an inhibitor of PP1-mediated dephosphorylation of eIF2 α and glycogen phosphorylase *in vitro*³⁰². As phosphorylation of the regulatory subunit eIF2 α can repress translation initiation²⁹⁹, it is possible that PP1 also interferes in translation regulation. Overall, eIF2 β has been validated as a PIP that might modulate PP1 substrate specificity in *Plasmodium*. A reverse effect of PP1 binding on eIF2 and on translation initiation has not been demonstrated so far *in vivo* in *Plasmodium* or humans³⁰².

An additional mechanism in which eIF2B is a key regulator in the eukaryotic cell integrated stress response (ISR), also called unfolded protein response (UPR). eIF2 α is phosphorylated by PERK and other kinases in response to unfolded proteins in the ER and other cellular stresses³¹⁹. Phosphorylated eIF2 α converts eIF2 into a competitive inhibitor of eIF2B. The reduced eIF2B activity will then repress translation initiation globally, but will favor translation of some mRNA, such as transcription factor ATF4 mRNA. ATF4 is a stress response regulator that will switch on cellular stress responses on the transcriptional level³⁰⁵. PP1 in complex with the PIP growth arrest and DNA damage-inducible protein 34 (GADD 34) mediates eIF2 α dephosphorylation³²⁰ and is therefore crucial for ISR signal termination to restore protein synthesis and normal cell functioning³²⁰. The cellular perturbations that induce the ISR pathway can be caused by intracellular pathogens such as *Plasmodium*. An experimental cerebral malaria model of *P. berghei* ANKA infection in mice showed that *Pb* infection induces the activation of the PERK-eIF2 α pathway in neuronal cells. Furthermore distinct increases of ATF4 and GADD34 levels and activation of caspase activity could be observed upon *Pb* infection. This demonstrates that *Plasmodium* infection can induce an ISR mechanism in neuronal host cell, activating apoptotic pathways that result in neuronal cell death³²¹. The ISR also gets activated in *Plasmodium*-infected

hepatocytes, and astonishingly, it promotes parasite survival and development at this stage by a yet unknown mechanism³²².

Beyond that, the Khalife group employed biochemical and bioinformatic approaches to identify new PIPs, and this study broadened the putative functions associated to PP1²⁸¹. Co-affinity purification using recombinant PP1 protein followed by mass spectrometry identified 6 new putative PIPs. Out of these only three targets, which function in protein, glucose and lipid metabolism, bear the RVxF motif. Next, a yeast-two-hybrid (Y2H) screening was performed to discover 134 PIP candidates, of which 30 possess the RVxF motif. Furthermore, the group performed an *in silico* screening for an extended highly specific RVxF motif, as described by²⁵⁰, to identify PP1-interacting candidates. By this strategy 55 putative PIPs were found. This use of this specific RVxF motif has the limitation that it will not detect all PIPs, as for example PflRR1 binds PP1 through LRR motifs, and Pfl2 and Pfl3 encompass only a short RVxF motif³²³. These already validated PIPs therefore couldn't be detected by this bioinformatic screen. In a subsequent step, the group could validate 35 of all putative PIPs by an ELISA-based assay demonstrating the interaction of recombinant PIPs with PP1c.

In total, 186 new putative PIPs were identified by Hollins *et al.*, but no candidate was found by all three approaches. Based on a previous protein interactome study³²⁴, these potential new PIPs were predicted to regulate transcription and DNA maintenance, as well as folding, proteolysis and pathogenicity²⁸¹. One of the putative PIPs found by Y2H as well as the *in silico* approach, was termed RCC-PIP due to the presence of RCC (Regulator of chromosome condensation) motifs, and was more thoroughly investigated³²⁵. RCC-PIP was confirmed to interact with PP1 *in vitro* and *in vivo*, and displayed a perinuclear cytoplasmic localization. Interestingly, a Y2H screen in search for other RCC-PIP interactors, revealed CDPK7 binding by RCC-PIP, which was validated *in vitro*. In conclusion, RCC-PIP might serve as scaffold anchoring PP1 and CDPK7 activities, or it might even balance PP1 and CDPK7 activity in a putative common function³²⁵.

It is clear that future studies are necessary in order to explore the potentially very diverse functions of PP1 and its interacting partners in *Plasmodium* development.

4. Objectives of this thesis

Plasmodium displays a complex life cycle during which the parasite undergoes drastic morphogenesis changes in asexual blood stages, sexual development, or transition to ookinete and sporozoite in the mosquito. These drastic morphological transitions require the timely regulated activation of different genetic programs³⁰⁶. Another layer of regulation is achieved at the post-translational level, which includes protein phosphorylation *via* the opposing enzymatic activities of kinases and PPs.

Protein phosphorylation is the major regulatory mechanism of eukaryotic cells to control their cellular processes³²⁶. This is increasingly becoming clear as well for *Plasmodium* development as described in the bibliography part. Egress and invasion are key steps in intraerythrocytic development, that take place within less than a minute and rely on a regulated sequence of protein secretion from diverse apical organelles, including exonemes, micronemes and rhoptries. The accurate coordination of these events requires phospho-signaling in the parasite triggered by the second messengers cGMP, cAMP and Ca²⁺^{327–330}. These signals activate the respective sensitive kinases, meaning *PfPKG*, *PfPKA* and CDPKs that will phosphorylate specific substrates acting as direct or indirect effectors in the respective molecular processes^{328,330–336}.

While many kinases have been functionally characterized, most parasite PPs are poorly studied so far. *P. falciparum* encodes 29 PPs that belong to the four main eukaryotic PP families^{348,349}: Among these, calcineurin (*PfPPP3*) is the only PP for which a role has been demonstrated by reverse genetic studies, during the attachment step of the merozoite to the RBC during invasion^{362,363}.

Given the scarcity of functional reverse genetics studies on *P. falciparum* PPs, the main objective of my thesis was to identify PPs involved in the egress and invasion steps, as many phosphorylation events are known to take place at these crucial stages of parasite development. The identification of candidate PPs was done in an *in silico* approach based on available transcriptomics data. For the selected candidate genes, the second step then was to employ reverse genetics for two major objectives:

1. Characterize the PPs expression dynamics and subcellular localization during the course of the RBC cycle. For this, we used the CRIPR-Cas9 gene edition strategy to insert a triple HA tag at the end of the endogenous coding sequence.
2. Explore the biological function of the PPs during the RBC cycle by engineering direct knockout or inducible knockdown/ knockout parasite lines using CRISPR-Cas9. In a next step, these strains would be phenotypically analyzed for their ability to complete the different steps of *P. falciparum* intra-erythrocytic development, i.e. invasion, intracellular development and schizogony, and egress.

For our *in silico* screen aiming at the identification of candidate PPs involved in egress and invasion we analyzed the transcription profile of the 29 *P. falciparum* PP genes: we searched for PP genes which display an expression peaks at the end of the erythrocytic cycle (40-48h schizonts), but which are low expressed in rings and trophozoites. So the genes fulfilling these differential expression criteria would be highly and specifically expressed at the time of egress and invasion.

We used PlasmoDB database (plasmodb.org) to interrogate the transcriptomic data for each PP over the 48h erythrocytic cycle as well as the MS evidence for protein expression. This search retrieved 9 PPs, among which 6 showed the desired expression profile (Figure 48): PF3D7_0802800 (Cn), PF3D7_1423300 (*PfPPP7*), PF3D7_1206000 (*PfShelph2*), PF3D7_1469200 (*PfShelph1*), PF3D7_1018200 (*PfPPP8*) and PF3D7_0810300 (*PfPPM5*). Two other PPs possess a slightly earlier expression peak,

between 35 and 40h, namely PF3D7_0927700 (*Pf*PP4) and PF3D7_1414400 (*Pf*PP1). The last candidate PF3D7_1309200 (*Pf*PPM6) has a pretty flat profile, yet with a late transcriptional peak around 40h.

Of these 9 candidates, we retrieved two unusual members of the PPP family, named Shelph PPs, which have bacterial origin and therefore no orthologue in humans^{348,368}. All classical eukaryotic PPPs as well as PPM6 and Shelph1 retrieved from our screen were reported to be likely essential for intraerythrocytic development in both *Pf* and *Pb*^{266,367}. In contrast, Shelph2 and PPM5 are likely dispensable (right panel of Figure 48).

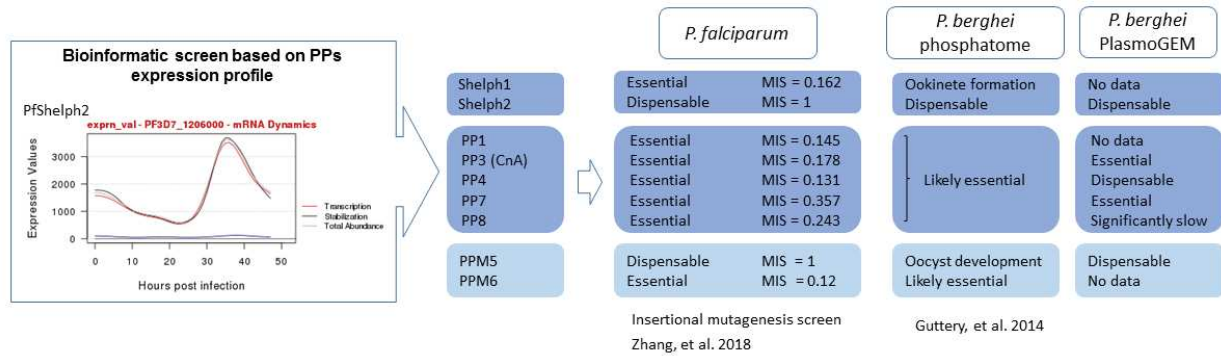


Figure 48: List of the *P. falciparum* PPs of interest. When possible, data regarding their essentiality in the murine malaria model *P. berghei*^{326,327} and in the related apicomplexan parasite *T. gondii*³²⁸ are shown. The left panel shows an exemplary transcriptional profile (depicted is *pfshelph2* mRNA abundance) that was used as criterium for this screen¹⁷⁰. Genome-wide screens in *P. falciparum* and *P. berghei* predicted essentiality among these genes, as shown in the blue boxes. An insertional mutagenesis screen in *Pf* analyzed if a gene can be disrupted in the CDS. This generated the MIS value = mutagenesis index score, which was calculated based on the susceptibility of the ORF in each transcriptional unit to being disrupted. MIS values ranging between 0 and 0.4 indicate gene essentiality, whereas MIS magnitudes between 0.6 and 1 point at a dispensable gene³²⁹. *P. berghei* gene disruption screens were done in two independent studies^{266,330}.

From this list of candidate PPs, we chose four genes, namely Shelph2, PP1, PP4 and PP7, for the reasons described below.

The first project of my thesis consisted in the functional characterization of Shelph2, a PP of bacterial origin absent from the human host. Previous studies indicated a possible role of Shelph2 in invasion: a genome-wide screen using co-transcriptional profiling and protein-protein-interaction data predicted Shelph2 to be part of the protein network necessary for merozoite invasion³⁰⁵. Furthermore, Fernandez-Pol *et al.* published video microscopy data suggesting that Shelph2 was secreted into the RBC upon invasion, and reported Band 3 dephosphorylation by Shelph2 *in vitro*. This conducted them to propose a model in which Shelph2 might serve Band 3 dephosphorylation at the time of merozoite invasion to promote RBC cytoskeleton reconstruction once the merozoite has completed its internalization¹⁸³. However, direct proof of Shelph2 function during invasion was not provided by reverse genetic studies. This is why we generated Shelph2-KO parasites and investigated their capacity to fulfill the entire asexual RBC development.

We also selected 3 classical PPP members PP1, PP4 and PP7 for in-depth analysis. PP1 and PP4 were chosen due to their possible involvement in egress, as treatment of schizonts with the PP1 and PP2A-family inhibitor calA abrogates egress²⁷⁷. In spite of the broad inhibitory activity of calA, PP1 and PP4 are the 2 members of the PP1- and PP2A-family that seem to be expressed in blood stages^{308,331}. Finally, PP7 was also an interesting candidate because of the presence of an N-terminal Calmodulin-binding domain and C-terminal Ca²⁺ binding EF hand motifs, suggesting a possible regulation by Ca²⁺. As Ca²⁺ signaling and CDPKs are crucial in both invasion and egress, the presence of these domains may be relevant to a function during these steps.

As PP1, PP4 and PP7 might be essential, our goal was to engineer inducible KD parasites to investigate the role of these enzymes^{266,329}. We first used the glmS ribozyme strategy to knock-down PP4 and PP7 and were successful in obtaining genomic loci that were edited by introduction of a HA₃ tag and a glmS ribozyme sequence in 3' of the respective genes³⁷². Unfortunately, the mRNA destabilization upon glucosamine treatment did not induce any PP4 protein depletion. Therefore we changed our strategy, and used the inducible DiCre recombinase system to engineer inducible KO of PP1 and PP7^{102,373,374}. We obtained iKO-PP1 parasites that led to the functional description of PP1 phosphatase. Besides describing PP1 expression timing and localization using a PP1-HA₃ line, we aimed at identifying PP1 functions in the parasite cycle. The DiCre-loxP system was used to deplete PP1 at different time points of the intraerythrocytic cycle, with the objective to define functions of this phosphatase at different stages of parasite development.

This thesis will contribute to the understanding of the role of phosphatases in *P. falciparum* development in RBCs. The work on phosphatases by us and other groups should allow to reveal the distinct cellular phosphosignalling modules in the parasite, their activation and dynamics, their substrates and finally their downstream effects.

RESULTS

Chapter 1: Functional characterization of the phosphatase Shelph2

1.1 Introduction

Plasmodium does not only encode classical eukaryotic PPP homologues, but also two enzymes with high similarity to CAPTPase from the psychrophilic bacteria belonging to *Shewanella* genus, namely Shelph1 and Shelph2. Biochemical studies of *Shewanella* CAPTPase pointed out two remarkable characteristics: first, this enzyme maintains a high catalytic activity at cold temperatures²²⁴, and second, it has exclusive Tyr PP activity, although it bears the conserved catalytic center of PPP Ser/Thr PPs²²².

Both *Plasmodium* Shelph1 and Shelph2 enzymes were biochemically characterized, showing that they are active Tyr PPs whose activities were not sensitive to classical PPP inhibitors, consistent with the reported PP activity of their bacterial homologue^{183,291}. Shelph1 is dispensable in *Pb* blood stage as it seems to be mainly important for ookinete maturation, in particular micronemes biogenesis^{266,291}, but was reported to be likely essential for *Pf* intraerythrocytic development³²⁹. In contrast, *shelph2* gene could be successfully disrupted both in *Pb* and *Pf*^{266,329}, yet the mutants were not further investigated. Using a *Pf*Shelph2-GFP tagged parasite line, Shelph2 was localized in vesicles apical to the nuclei of the forming daughter cells in schizonts. Interestingly, the secretion of Shelph2 into the RBC upon merozoite invasion was observed using live video microscopy. *Plasmodium* infection is known to induce hyperphosphorylation of Tyr residues of the major RBC membrane protein Band 3¹⁸⁵ and Shelph2 has the potential to dephosphorylate Band 3 *in vitro*¹⁸³. As this modification is known to control its association with the RBC sub-membrane cytoskeleton¹⁸², it was hypothesized that Shelph2 may mediate dephosphorylation of Tyr-phosphorylated Band 3 during the course of invasion but this putative role of Shelph2 has to be confirmed.

Given its late transcriptional profile in *Pf* asexual blood stages, and its apical localization associated with a potential secretion in the RBC during invasion, the first aim of my thesis was to investigate the function of PfShelph2. Direct knockout of *shelph2* gene was attained in the laboratory before my arrival. A major part of my work on Shelph2 consisted in the phenotypical characterization of these Shelph2-KO parasites, as described in the following section.

1.2 Shelph2, a bacterial-like phosphatase of the malaria parasite *Plasmodium falciparum*, is dispensable during asexual blood stage.

RESEARCH ARTICLE

Shelph2, a bacterial-like phosphatase of the malaria parasite *Plasmodium falciparum*, is dispensable during asexual blood stage

Alexandra Miliu, Maryse Lebrun, Catherine Braun-Breton, Mauld H. Lamarque*

DIMNP, CNRS, Université de Montpellier, Montpellier, France

* mauld.lamarque@umontpellier.fr



OPEN ACCESS

Citation: Miliu A, Lebrun M, Braun-Breton C, Lamarque MH (2017) Shelph2, a bacterial-like phosphatase of the malaria parasite *Plasmodium falciparum*, is dispensable during asexual blood stage. PLoS ONE 12(10): e0187073. <https://doi.org/10.1371/journal.pone.0187073>

Editor: Olivier Silvie, INSERM, FRANCE

Received: August 8, 2017

Accepted: October 12, 2017

Published: October 26, 2017

Copyright: © 2017 Miliu et al. This is an open access article distributed under the terms of the Creative Commons Attribution License, which permits unrestricted use, distribution, and reproduction in any medium, provided the original author and source are credited.

Data Availability Statement: All relevant data are within the paper and its Supporting Information files.

Funding: This research was supported by the Laboratoire d'Excellence (LabEx) (ParaFrap ANR-11-LABX-0024 and ANR-10-LABX-12-01)-ML and CBB received the funding. The funders had no role in study design, data collection and analysis, decision to publish, or preparation of the manuscript.

Competing interests: The authors have declared that no competing interests exist.

Abstract

During the erythrocytic cycle of the malaria parasite *Plasmodium falciparum*, egress and invasion are essential steps finely controlled by reversible phosphorylation. In contrast to the growing number of kinases identified as key regulators, phosphatases have been poorly studied, and calcineurin is the only one identified so far to play a role in invasion. *PfShelph2*, a bacterial-like phosphatase, is a promising candidate to participate in the invasion process, as it was reported to be expressed late during the asexual blood stage and to reside within an apical compartment, yet distinct from rhoptry bulb, micronemes, or dense granules. It was also proposed to play a role in the control of the red blood cell membrane deformability at the end of the invasion process. However, genetic studies are still lacking to support this hypothesis. Here, we take advantage of the CRISPR-Cas9 technology to tag *shelph2* genomic locus while retaining its endogenous regulatory regions. This new strain allows us to follow the endogenous *PfShelph2* protein expression and location during asexual blood stages. We show that *PfShelph2* apical location is also distinct from the rhoptry neck or exo-nemes. We further demonstrate *PfShelph2* dispensability during the asexual blood stage by generating *PfShelph2*-KO parasites using CRISPR-Cas9 machinery. Analyses of the mutant during the course of the erythrocytic development indicate that there are no detectable phenotypic consequences of *Pfshelph2* genomic deletion. As this lack of phenotype might be due to functional redundancy, we also explore the likelihood of *PfShelph1* (*PfShelph2* paralog) being a compensatory phosphatase. We conclude that despite its cyclic expression profile, *PfShelph2* is a dispensable phosphatase during the *Plasmodium falciparum* asexual blood stage, whose function is unlikely substituted by *PfShelph1*.

Introduction

Apicomplexan parasites represent tremendous issues in terms of economy and public health concerns. *Plasmodium falciparum*, the etiologic agent of the deadliest form of malaria, is responsible for almost 500000 deaths every year, mostly affecting children in sub-Saharan Africa [1]. The lack of vaccine and the emergence of drug-resistant parasites highlight the urge to find new therapeutic targets.

P. falciparum life cycle alternates between its definitive host, the *Anopheles* mosquito, and the human host where it replicates asexually first in the liver, and then repetitively in the red blood cells (RBCs). The 48 hours (h) asexual blood cycle can be divided into several steps: RBC invasion, intracellular development within a vacuole, followed by several rounds of DNA replication that culminate in the individualization of new daughter cells named merozoites. Finally, these merozoites egress from the host cell and a new erythrocytic cycle can be initiated. Each one of these steps must be tightly regulated to ensure the release of mature merozoites fully competent for the next invasion step.

Egress and invasion take place within less than a minute and rely on a rapid burst of protein discharge from several apical organelles, including exonemes, micronemes and rhoptries. To orchestrate these finely tuned events, the parasite uses complex signaling pathways relying mainly on cyclic nucleotides, namely cyclic guanosine monophosphate (cGMP) and cyclic adenosine monophosphate (cAMP), and calcium as signaling molecules [2–5]. These signals activate their dedicated kinases, i.e. *Pf*PKG, *Pf*PKA and calcium-dependent protein kinases (CDPKs), that will in turn phosphorylate their respective substrates thought to be direct or indirect effectors required for these steps to proceed [3,5–11].

In sharp contrast to kinases, phosphatases (PPs) have received much less attention so far. Yet, a recent functional analysis of the murine malaria model *P. berghei* phosphatome revealed that out of 30 PPs, 16 of them are likely essential during asexual stages while another 6 are required for full sexual development in the mosquito, thus highlighting the crucial importance of these enzymes for parasite survival [12]. No such analysis has been conducted yet in *P. falciparum*, and calcineurin is the only PP reported to be involved in invasion based on reverse genetic studies [13].

In a search for *P. falciparum* PPs potentially involved in egress/invasion, we focused our interest on two bacterial-like PPs on the basis of their transcriptomic profile [14]. They are more closely related to PPs from bacteria of the *Schewanella* genus and therefore named *Pf*Shelph1 (PF3D7_1469200) and *Pf*Shelph2 (PF3D7_1206000) for “*Schewanella*-like phosphatase” [15,16]. Apart from bacteria, Shelphs are only found in Chromoalveolata, Fungi, Plantae and parasites belonging to Excavata, making them attractive putative targets for drug development [15,17]. Both *shelph* genes have been independently knocked-out in *P. berghei*: the loss of *Pb*Shelph2 did not disturb the parasite life cycle neither in mice nor in mosquitoes, while the absence of *Pb*Shelph1 affected ookinete development and consequently parasite transmission [12,17]. In *P. falciparum*, Fernandez-Pol *et al.* reported a perinuclear localization of *Pf*Shelph2 in schizonts and merozoites, distinct from microneme, rhoptry and dense granule markers [18]. They also determined that *Pf*Shelph2 displays a restricted tyrosine phosphatase activity *in vitro*, as was reported for *Pb*Shelph1 [17,18]. Therefore, despite being grouped within the serine/threonine PhosphoProtein Phosphatase (PPP) group, based on the presence of consensus signature motifs in their protein sequences [16,17], *Plasmodium* Shelphs exhibit the same specificity as their bacterial ortholog which is a strict tyrosine phosphatase [19]. Although reverse genetic studies are still lacking for *P. falciparum* Shelphs, two functional association studies, based primarily on co-transcriptional profile analyses, identified *Pf*Shelph2 as a protein that might be involved in invasion because of its co-expression with known “invasome” genes [20,21]. Furthermore, the enzyme was shown to dephosphorylate Band3 *in vitro*, one of the major surface protein of red blood cells [18]. As Band3 tyrosine phosphorylation status is known to control its association/disassociation from the RBC sub-membranous cytoskeleton [22], it has been hypothesized that *Pf*Shelph2 might modulate band3 phosphorylation during the course of invasion. Yet, so far no direct evidence of *Pf*Shelph2 function during the asexual blood stage has been established.

In this study, we undertook the functional characterization of *Pf*Shelph2 during the RBC cycle using reverse genetics. We tagged the endogenous gene using CRISPR-Cas9 technology

to characterize *PfShelph2* expression at the protein level and showed that it was strictly restrained to late schizonts and merozoites. Its location at the merozoite apex did not colocalize with rhoptry neck or exoneme markers. We also successfully generated a *Shelph2*-KO line, thereby demonstrating that this PP is dispensable during asexual development. The phenotypic characterization of the mutant revealed that the absence of *Shelph2* did not induce any significant defect during the erythrocytic cycle, suggesting possible functional redundancy. Finally, we explored whether *PfShelph1* might be a compensatory PP for *PfShelph2* loss and conclude that this hypothesis is very unlikely.

Materials and methods

Parasite culture and transfection

P. falciparum 3D7 strain, obtained from the Malaria Research and Reference Reagent Resource Center (MR4-BEI resources, MRA-102), was cultured in human erythrocytes obtained as donations from anonymized individuals from the french Bloodbank (Etablissement Français du Sang, Pyrénées Méditerranée, France) at 5% hematocrit in RPMI 1640 medium (Gibco), supplemented with gentamycin at 20 µg/ml and 10% human serum [23]. The cultures were kept at 37°C under a controlled trigaz atmosphere (5% CO₂, 5% O₂ and 90% NO₂). For synchronization, mature parasites were isolated using gelatin floatation [24]. Alternatively, late schizonts were collected on cushions of 70% (v/v) Percoll adjusted to isotonicity [25]. To restrict the invasion time-frame, parasites were subsequently synchronized in ring stages using 5% sorbitol [26].

For *Pf3D7* transfections, 5–10% ring stages were transfected with 60–80 µg of circular or linear plasmid DNA as described previously [27,28]. Transgenic parasites were grown in agitation (200 rpm) and selected by addition of 2.5 nM WR99210 (for pL7-*Shelph2**-HA₃, pL7-*Shelph2*-KO or pARL2-*Shelph1*-GFP), and 1.5 µM DSM1 (for pUF1-Cas9). Drug pressure was removed after parasite genotyping, except for the maintenance of pARL2-*Shelph1*-GFP.

Molecular biology

All the primers used in this study are listed in S1 Table. All the PCR products have been verified by sequencing (Eurofins).

The PCR reactions were performed using the Phusion or Q5 DNA polymerase (NEB Biolabs). Bacterial colonies were screened using the GoTaq G2 Green master mix (Promega).

RNA extraction was performed using the NucleoSpin® RNAII kit (Macherey-Nagel). cDNA preparations were obtained by reverse transcription using Superscript III First-Strand Synthesis SuperMix for RT-PCR (Invitrogen) and 500 ng–1 µg of total RNA.

For qRT-PCR, two independent RNA samples from *Pf3D7* and the three *PfShelph2*-KO lines were prepared. Each cDNA was diluted 1/20 before measuring by qPCR. *shelph1* (PF3D7_1469200), *PPKL* (protein phosphatase containing kelch-like domains; PF3D7_1466100), and *shelph2* mRNA expression were quantified using the LightCycler 480 Sybr Green I system (Roche) using primers listed in S1 Table. Fructose-biphosphate aldolase (FBA; PF3D7_1444800) was used as the reference gene. LightCycler 480 Software version 1.5 was used for relative quantification analysis. The expression of each target gene in *PfShelph2*-KO was then normalized to *Pf3D7* expression level.

Plasmid constructs

To generate pL7-*Shelph2**-HA₃ vector, we first amplified the triple HA tag from pLIC-DHFR [29] using primers MLa33/MLa32 and cloned it SpeI/AscI into pL6_BsgI_V3 (modified

version of pL6_eGFP, gift from Jose-Juan Lopez-Rubio). This generated pL6_BsgI-HA₃ plasmid. Next, we amplified 646 bp of *shelph2* 3'UTR from Pf3D7 gDNA using primers MLa40/MLa41 and cloned it AscI/SacII into pL6_BsgI-HA₃ to generate pL6_BsgI-HA₃-3'UTR. The 3'UTR was designed 207 bp downstream of *shelph2* stop codon due to a very rich A/T richness that prevented the design of a specific primer. The full *shelph2* coding sequence (CDS) amplified using primers MLa3/MLa4 was first subcloned into the pCR-BluntII-TOPO vector (Invitrogen). Shield mutations in *shelph2* CDS were introduced by mutagenesis with primers MLa79/MLa80 using the QuickChange Site-directed Mutagenesis kit (Stratagene) according to the manufacturer instructions. The resulting mutated *shelph2*^{*} was again subcloned into the pCR-BluntII-TOPO and verified by sequencing. 712 bp of *shelph2*^{*} was re-amplified using primers MLa59 and MLa45 and cloned into pL6_BsgI-HA₃-3'UTR using SpeI, yielding pL6_BsgI-*shelph2*^{*}-HA₃-3'UTR. From this vector, the whole *shelph2*^{*}-HA₃-3'UTR cassette was re-amplified using primers MLa59/MLa60 and cloned InFusion (Clontech) SpeI/AflII into pL6-eGFP [28]. The resulting vector pL6-*shelph2*^{*}-HA₃-3'UTR was digested BtgZI to allow the insertion of *shelph2* gRNA corresponding to hybridized primers MLa63/MLa64. The final plasmid named pL7-Shelph2^{*}-HA₃ was used for transfection.

To generate pL7-Shelph2-KO vector, 388 bp fragment encompassing the 5'UTR and the first 219 bp of *shelph2* CDS was amplified by PCR as homology region 1 using primers MLa54/MLa53. The fragment was cloned NcoI/EcoRI by InFusion into the pL6-eGFP vector, downstream of hDHFR cassette, giving pL6-3'UTR. Similarly, a 760 bp fragment corresponding to *Pfshelph2* 3'UTR was amplified using primers MLa50/MLa51 and cloned AflII/SpeI by InFusion into pL6-3'UTR plasmid, upstream of hDHFR cassette. Finally, gRNA MLa63/MLa64 was inserted into the plasmid in BtgZI as described above. The resulting vector was named pL7-Shelph2-KO and used to transfect parasites.

To generate pARL2-Shelph1-GFP plasmid, the entire *shelph1* coding sequence without the stop codon was PCR amplified using primers MLa1 and MLa2 and cloned XhoI/KpnI in frame with a GFP tag into pARL2-GFP vector [30].

*Pf*Shelph2-KO phenotypic assays in asexual blood stage

All the experiments described below have been performed on tightly synchronized parasites with a 2 hours re-invasion time frame.

To follow *P. falciparum* intra-erythrocytic development, synchronized parasite cultures were smeared in triplicate from 2h post-invasion until 48h. The ratio of ring, trophozoite and schizont was evaluated for 200 infected RBCs at each time point.

For determining the number of merozoites per segmenter, late schizonts of about 40h were purified on a Percoll gradient, and parasites were left maturing for an additional 4h in the presence of 1.5 μM compound 2 to block egress [6,31]. After one wash in complete medium, blood smears were done in triplicate and analyzed by counting 50 segmenters per smear.

Proliferation rate assays were set up at 1% parasitemia in ring stage. Samples were taken up in ring stage 6h post-invasion during the first cycle. 48h later, ring stage samples of the next cycle were again collected and fixed in 4% paraformaldehyde (PFA) for 4h at room temperature (RT). Flow cytometry (FACS) was then used to determine the parasitemia. Fixed cells were washed twice in phosphate buffer saline (PBS), followed by 30 minutes (min) incubation with 1X SybrGreen (Invitrogen) in the dark. Cells were washed, resuspended in 700 μl PBS and analyzed by BD FACS Canto I flow cytometer using FACS Diva software (BD Biosciences). SYBR green was excited with a blue laser at 488 nm, and fluorescence was detected by a 530/30 nm filter.

Immunoblot and immunofluorescence assays

Immuno-fluorescence assays (IFAs) were performed on smeared infected RBCs. Cells were fixed with 4% PFA for 30 min at RT before a 10 min permeabilization step in PBS-0,1% Triton X100. Following 30 min saturation in PBS-1.5% bovine serum albumin (BSA), cells were incubated 45 min with primary antibodies diluted in PBS-BSA. After 3 washes in PBS, cells were incubated 45 min with secondary Alexa-488- or Alexa-594-conjugated secondary antibodies highly cross-adsorbed (Invitrogen) diluted in PBS-BSA as recommended by the manufacturer. Nuclei were stained with Hoechst. Images were taken on a Zeiss Axioimager Z2 equipped with an apotome, at the Montpellier RIO imaging facility. Images were processed by Zen Blue edition software (Zeiss) for optical sectioning, luminosity and contrast adjustment. Antibody dilutions were rat anti-HA 1/100 (Roche Diagnostics), mouse anti-MSP1 19kDa 1/1000 (gift from M. Blackman), mouse anti-PfRON4 1/100 [32] and mouse anti-SUB1 pure (gift from M. Blackman).

Proteins were analyzed by SDS-PAGE and immunoblot. When required, parasites were separated from RBC by 0.01% saponin treatment for 5 min at 4°C prior to resuspension in Laemmli sample buffer in reduced conditions. Antibody dilutions were rat anti-HA 1/100 (Roche Diagnostics), rabbit anti-Histone H3 1/10000 (Abcam). Secondary antibodies conjugated to alkaline phosphatase (Promega) were diluted according to the manufacturer's instructions and used with NBT/BCIP reagents (Promega).

Results and discussion

PfShelph2 biosynthesis starts during late schizogony, and its apical positioning is distinct from rhoptries or exonemes

We were interested in identifying PPs potentially involved in *P. falciparum* egress or invasion. In this context, *PfShelph2* was selected as a candidate based on its transcriptional profile [14] and its putative role as an invasion protein [18,20,21]. To determine its protein expression profile in its native genomic context, we engineered a triple hemagglutinin (HA₃) epitope tagged line using CRISPR-Cas9 technology [28] (Fig 1A). Following *Pf3D7* transfection, parasites were selected using WR and DSM1, before cloning by limiting dilution. Two *PfShelph2*-HA₃ clonal lines were analyzed by PCR for *shelph2* editing (Fig 1B). Integrative PCR (INT) confirmed the tag insertion in the two edited clones (A5 and E6), while the presence of wild type *shelph2* locus was detected with PCR WT in the parental line but not in *PfShelph2*-HA₃ parasites. Sequencing of the *shelph2* locus confirmed the presence of the shield mutations in *shelph2* CDS and the in frame fusion of the HA₃ tag at the C-terminus (S1 Fig).

We used *PfShelph2*-HA₃ parasites to investigate *PfShelph2* expression during the 48h erythrocytic cycle. Parasites were synchronized and samples were collected at ring, trophozoite and schizont stage for immunoblot (Fig 1C). Our results show that *PfShelph2*-HA₃ migrated as a 37 kDa fusion protein, consistent with its predicted molecular mass after cleavage of its putative N-terminal signal peptide. Concordant with the transcriptomic data and previous immunofluorescence studies [14,18], the protein is only expressed in schizonts. Interestingly, a very recent ChIP-seq analysis identified *Pfshelph2* promoter region as a putative target of *PfAP2-I* transcription factor [33]. *PfAP2-I* is only expressed in trophozoites and schizonts and binds gene promoters that are predominantly invasion-related, chromatin-related and cell-cycle-related. This suggests that *PfShelph2* late expression profile might rely on *PfAP2-I* activity.

We also investigated *PfShelph2* stage-specific expression by IFA, using Merozoite Surface Protein 1 (MSP1) staining as a marker of parasite maturation. MSP1 is one of the major merozoite surface components and is cleaved at a juxtamembrane position by a protease named

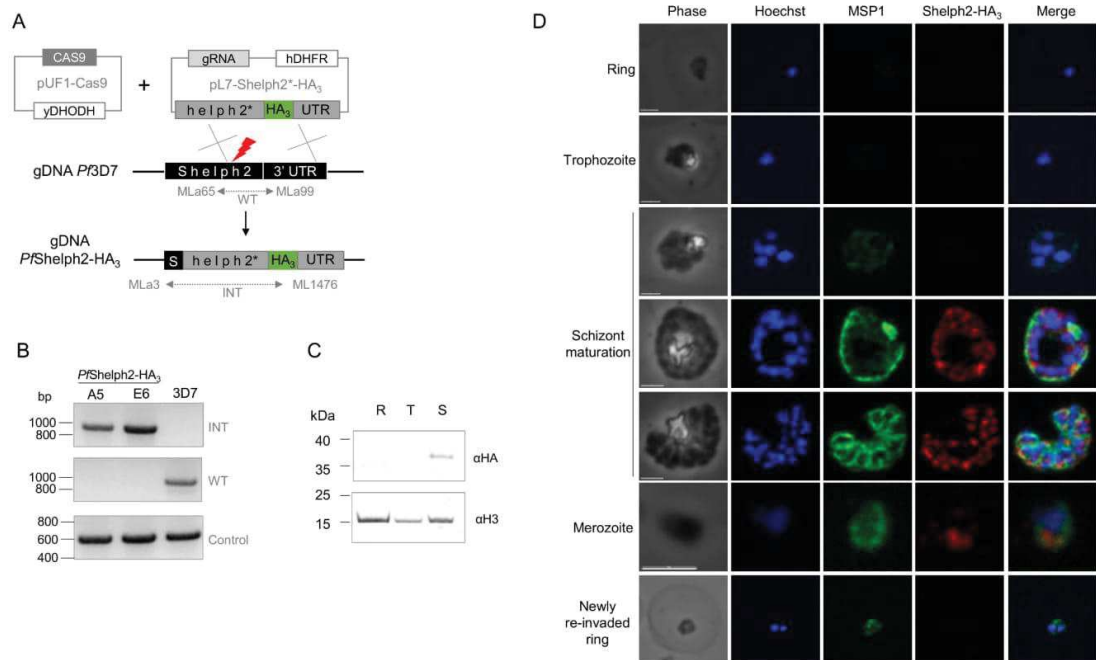


Fig 1. Transgenic *PfShelph2-HA₃* characterization. (A) Scheme depicting the strategy used to engineer *PfShelph2-HA₃* parasites. Plasmids pUF1-Cas9 and pL7-Shelph2*-HA₃ were transfected in *Pf3D7* and selected by addition of DSM1 and WR drugs respectively. The red thunder represents Cas9 double strand break. Parasites were genotyped by PCR (WT and INT) using primers depicted as arrows in the figure. (B) PCR genotyping of two edited *PfShelph2-HA₃* lines versus *Pf3D7* parental strain. Control PCRs were performed on *PfPRL* gene (PF3D7_1113100) using primers MLa11 and MLa12. (C) Immunoblot of *PfShelph2-HA₃* parasites on rings (R), trophozoites (T) or schizonts (S) extracts using anti-HA antibodies. Equivalent amounts of proteins were loaded per lane and verified using anti-Histone H3 antibodies. (D) IFA of *PfShelph2-HA₃* parasites using anti-HA and anti-MSP1₁₉ antibodies at different stages of the RBC cycle, i.e. ring, trophozoite, schizont and merozoite. Scale bar, 2 μm.

<https://doi.org/10.1371/journal.pone.0187073.g001>

PfSUB2 [34], shedding the bulk of the protein while a 19 kDa fragment (MSP1₁₉) is carried into the newly invaded parasite before being degraded [35]. As shown in Fig 1D, *PfShelph2-HA₃* is not detected from ring stage to young schizont. Then, during late schizogony, when MSP1₁₉ gives either a peripheral schizont staining or labels the periphery of each merozoite during budding, *PfShelph2-HA₃* is found in discrete apical foci and remains detectable in free merozoites. In contrast, in newly re-invaded ring, evidenced by the persistent parasite membrane staining with MSP1₁₉, *PfShelph2-HA₃* staining disappears. Our observations are consistent with the reported localization of *PfShelph2* [18,20] and confirm the late biosynthesis profile seen by western-blot. The fact that the protein is detected in the same structure in late schizonts and in free merozoites, but not in newly invaded parasites, suggests that the protein might be secreted post-merozoite release, i.e. likely during invasion. This observation is in agreement with previous findings regarding *PfShelph2* dynamics of release during the course of invasion, which showed using live video microscopy that its apical pattern was retained during the invasion step until the parasite was approximately halfway through the invasion process [18].

Given its apical localization in merozoites and its possible secretion during invasion, dual labeling with microneme, rhoptry or dense granule markers has been previously tested but failed to assign *PfShelph2* to any of these organelles [18]. In the same study, *PfRON3*, the

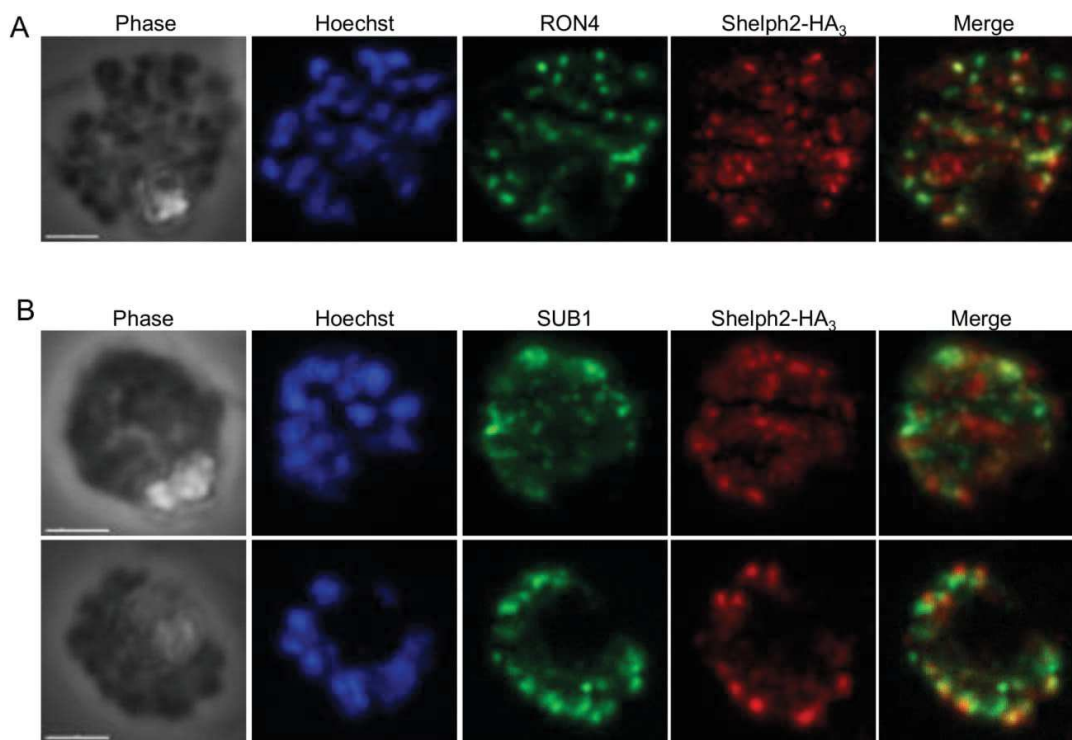


Fig 2. Dual labeling of *PfShelph2*-HA₃ with rhoptry neck and exoneme markers. IFA of *PfShelph2*-HA₃ parasites using anti-HA and (A) anti-*PfRON4* or (B) anti-*PfSUB1* antibodies on schizonts. Scale bar, 2 μm.

<https://doi.org/10.1371/journal.pone.0187073.g002>

ortholog of *Toxoplasma gondii* rhoptry neck protein 3, was used as a rhoptry neck marker. Yet, *PfRON3* was shown to be a rhoptry bulb protein in *P. falciparum* [36,37]. This prompted us to re-analyze the possible association of *PfShelph2* with this rhoptry sub-compartment using anti-*PfRON4* antibodies [32], but we found no obvious overlap between *PfShelph2* and *PfRON4* signals in schizonts (Fig 2A). We then investigated whether *PfShelph2* could be stored in exonemes. Exonemes resemble dense granules but are slightly more elongated organelles [38]. They have been identified by immuno-electron microscopy while investigating the sub-cellular localization of the serine protease *PfSUB1*. *PfSUB1* is discharged in the parasitophorous vacuole just prior egress, and therefore, exonemes are considered as secretory organelles. We observed a very distinct pattern between *PfSUB1* and *PfShelph2*-HA₃, leading us to conclude that *PfShelph2* is not contained within exonemes (Fig 2B). Therefore, *PfShelph2* displays an expression profile similar to many invasion-related proteins, and is located in an apical compartment in the invasive merozoite that is different from the rhoptry neck or exonemes. Unfortunately, *PfShelph2* expression level by IFA was too low to explore its localization further by immuno-electron microscopy.

PfShelph2 is a dispensable PP during asexual blood stage

Next, we investigated *PfShelph2* function during the red blood cell cycle by a direct knock-out strategy where we aimed to replace most of *shelph2* CDS with the selectable hDHFR marker (Fig 3A). We isolated three *PfShelph2*-KO clonal lines (B2, D3 and E1) that were genotyped by

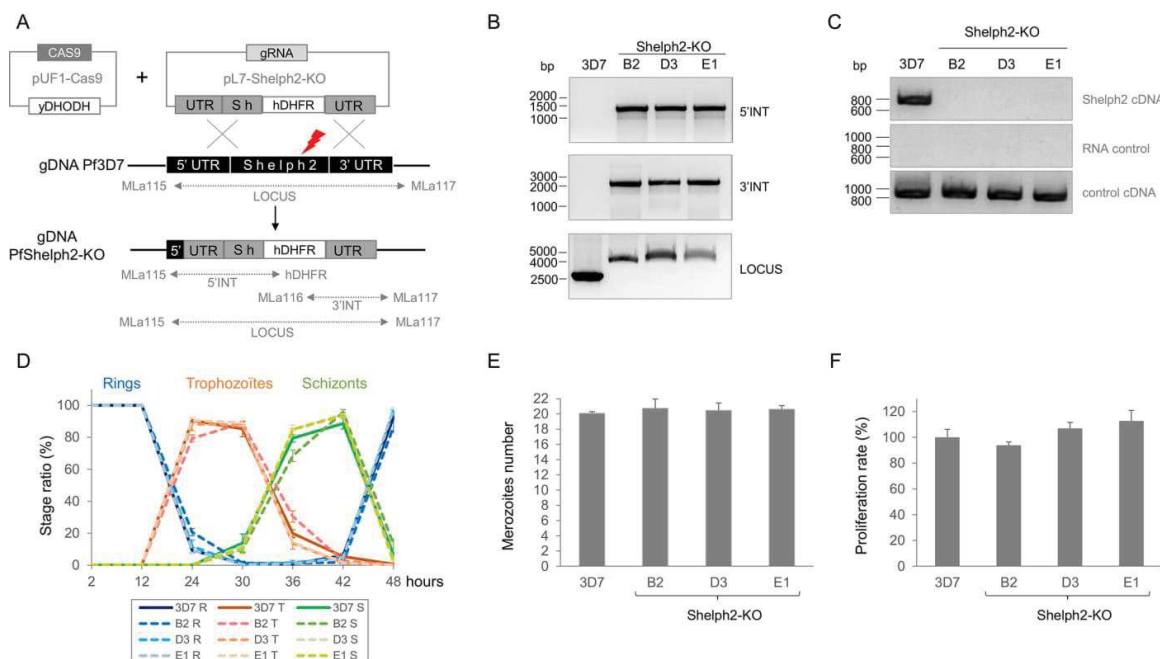


Fig 3. Successful disruption of *Pfs shelph2* gene and phenotypic characterization of *Pfs Shelph2-KO* parasites in asexual blood stage. (A) Scheme depicting the strategy used to generate *Pfs Shelph2-KO* parasites. Plasmids pUF1-Cas9 and pL7-Shelph2-KO were transfected in *Pf3D7* and selected by addition of DSM1 and WR drugs respectively. The red thunder represents Cas9 double strand break. Three clonal lines, namely B2, D3 and E1, were genotyped by PCR (LOCUS, 5'INT and 3'INT) using primers depicted as arrows in the figure. (B) PCR genotyping of three *Pfs Shelph2-KO* lines versus *Pf3D7*. PCR 5'INT refers to 5' integration, PCR 3'INT to the 3' integration, while PCR LOCUS shows the amplification of the whole *shelph2* genomic locus. (C) RT-PCR of *shelph2* mRNA in *Pfs Shelph2-KO* lines versus *Pf3D7*. RNA samples were also used as PCR templates to verify the absence of contaminating genomic DNA. Control cDNA corresponds to the 880 bp amplification of PF3D7_1127000 from cDNA using primers MLa13 and MLa14, while PCR from gDNA is expected to amplify a 1850 bp fragment. (D) The intra-erythrocytic development of *Pfs Shelph2-KO* lines B2, D3 and E1 was followed in comparison with *Pf3D7*. For each time point, smears were done in triplicate and 200 infected RBCs were counted per smear. The graph shows the ratio of each stage (R for ring, T for trophozoite and S for schizont) as a function of time post-invasion. Error bars represent standard deviation. This experiment was repeated 2 times independently. (E) The graph represents the number of merozoites produced per schizont in *Pf3D7* or *Pfs Shelph2-KO* lines. Tightly synchronized schizonts of about 40h were allowed to mature in presence of compound 2 for 4h. After one wash in complete medium, smears were done in triplicate and 50 infected RBCs were counted per smear. Error bars represent standard deviation. This experiment was repeated 3 times independently. (F) Parasite proliferation rate was measured in ring stage by FACS from one cycle to the next one. Results are shown as a percentage of *Pf3D7* proliferation rate. Error bars represent standard deviation. This experiment was repeated 3 times independently.

<https://doi.org/10.1371/journal.pone.0187073.g003>

PCR for hDHFR cassette integration (Fig 3B). We also confirmed the absence of *shelph2* mRNA by RT-PCR (Fig 3C).

Having established *Pfs Shelph2-KO* lines, we next assessed the possible phenotypic consequences of *Pfs Shelph2* loss during the asexual blood stage. First, we followed their intracellular development. To do this, parasites were tightly synchronized within a 2 hours window and ring-stage parasites were monitored through the cell cycle (Fig 3D). Progression from ring to trophozoite, evidenced by the detection of the hemozoin pigment, occurred around 24h, then followed by DNA replication during schizogony between 30-36h. Merozoites egress from host cell started from 42h and allowed the next cycle to take place as evidenced by the concomitant increase in rings. Thus, maturation of *Pfs Shelph2-KO* parasites within the erythrocyte is not significantly altered compared to *Pf3D7*.

To assess for specific defects during schizogony, we next evaluated the parasite replication by counting the number of merozoites produced per schizont (Fig 3E). Again, synchronized

cultures were allowed to progress until 40–42 h, at which time, parasites egress was blocked for 4h by *Pf*PKG inhibition in presence of compound 2 while not affecting schizonts maturation to segmenters [6]. All the strains produced an average of 20 merozoites per schizont, demonstrating that the absence of *Pf*Shelph2 does not affect mitosis or daughter cells formation. We then tested the mutant for possible subtle defects in egress/invasion. For this, newly re-invaded ring stages were allowed to progress to the next erythrocytic cycle and parasitemia was measured by FACS (Fig 3F). The results show that *Pf*Shelph2-KO growth rate is very similar to that of *Pf*βD7, suggesting that *Pf*Shelph2 does not play a prominent role neither in egress nor in invasion.

Despite its tightly controlled expression, our results demonstrate that *shelph2* knock-out does not affect *P. falciparum* intra-erythrocytic cycle as parasites maturation, daughter cell formation and proliferation rate were comparable to those of *Pf*βD7. These results are consistent with data obtained in *P. berghei*, where *Pb*Shelph2-KO did not impair neither asexual blood stage in mice, nor sexual development in mosquitoes [12]. Therefore, Shelph2 is a dispensable PP in *Plasmodium* species that can be explained either by a non-critical function, or by compensation by another PP. Functional redundancy during asexual blood stage was suggested in *P. berghei*, as 14 independent PP knock-outs, including *Pb*Shelph2-KO, did not induce any growth phenotype of the mutants in mice [12]. The most obvious compensatory PP for *Pf*Shelph2-KO line would be *Pf*Shelph1 that shares 29.5% similarity at the protein level and the same *in vitro* phosphatase specificity [17]. Although its function has never been investigated in *P. falciparum*, its ortholog *Pb*Shelph1 is critical for ookinete development and differentiation, thus demonstrating that at least in the mosquito, *Pb*Shelph2 cannot compensate for *Pb*Shelph1 loss [17].

To evaluate whether *Pf*Shelph1 might counterbalance the absence of *Pf*Shelph2, we first assessed its location by expressing a *Pf*Shelph1-GFP fusion ectopically in *Pf*βD7 parasites. By western-blot, the fusion protein is detected around 65 kDa, which corresponds to its expected molecular mass (Fig 4A). By fluorescence microscopy, we detected a perinuclear labeling during schizogony, suggestive of an endoplasmic reticulum positioning (Fig 4B). Although further co-localization studies should be done to properly refine this cellular location, our results would be concordant with the reported localization of *Pb*Shelph1 [17]. While the different locations of the two *P. falciparum* Shelphs do not point towards functional compensatory mechanism between the two enzymes, we ascertained this hypothesis by comparing *Pfshelph1* mRNA expression in *Pf*Shelph2-KO versus *Pf*βD7 by qRT-PCR. We used *Pfshelph2* mRNA as a negative control for the mutant, and *PfPPKL* phosphatase mRNA as a putative steady control based on the gene dispensability during asexual proliferation in *P. berghei* [39]. As anticipated, *Pfshelph2* mRNA becomes undetectable in *Pf*Shelph2-KO while *PfPPKL* expression is not significantly changed (Fig 4C). Likewise, we do not observe any major transcriptional regulation of *Pfshelph1*. Altogether, our results do not argue in favor of *Pf*Shelph1 being a compensatory PP in *Pf*Shelph2-KO, although further experiments should be done to properly assess this possibility.

*Pf*Shelph2 enzymatic activity as a tyrosine phosphatase is intriguing, as no canonical tyrosine kinase family has been described in *P. falciparum* [40]. Nevertheless, trace amounts of phospho-tyrosine phosphorylations (about 0.5%) have been detected in global phosphoproteomic studies [41,42]. These are thought to be mainly due to auto-phosphorylation of some parasite protein kinases within their activation loop [42]. Whether *Pf*Shelph2 might help regulate the enzymatic activity of some of these kinases remains to be explored. *Pf*Shelph2 could also dephosphorylate host cell proteins. Indeed, it has been well described that *P. falciparum* induces vast tyrosine and serine phosphorylation changes of RBCs proteins during its intracellular growth [43]. Moreover, mounting evidence supports the view where the interaction

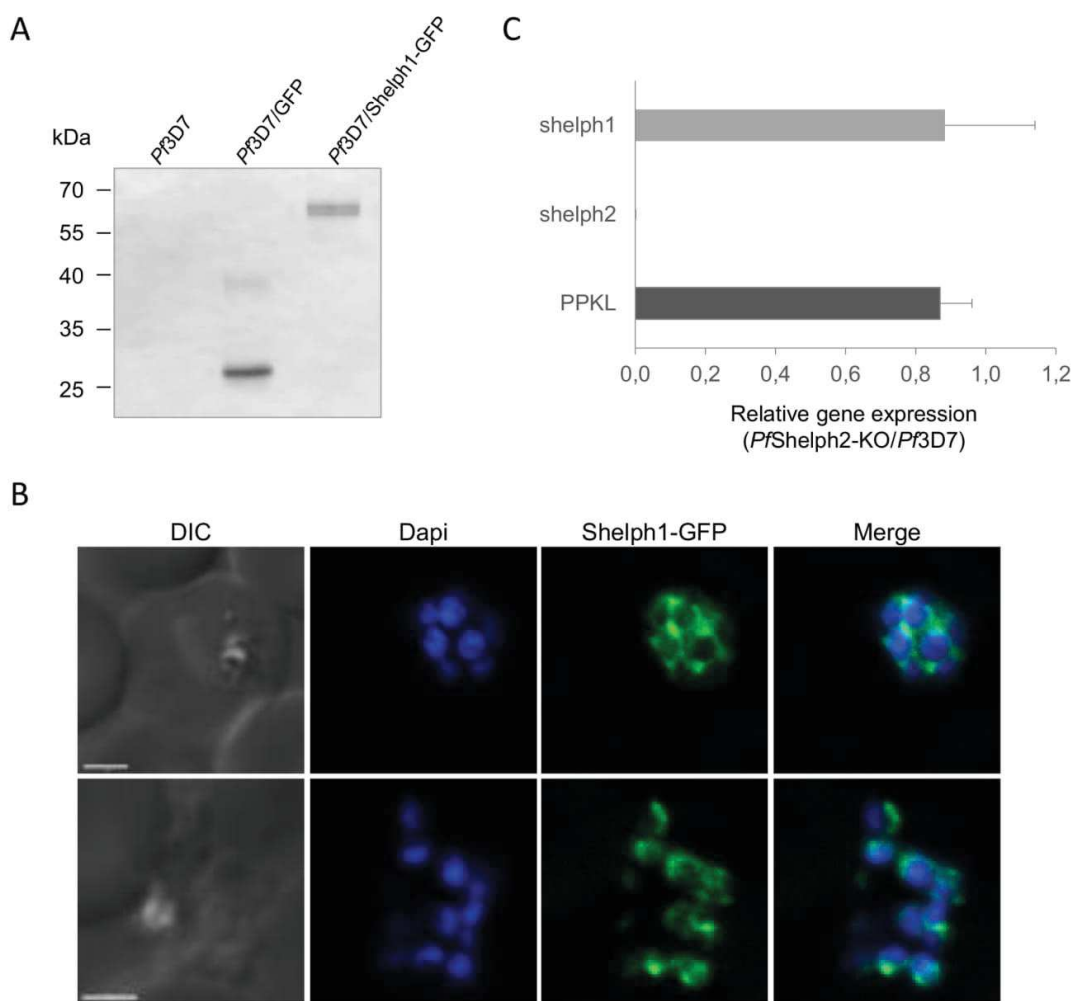


Fig 4. *PfShelph1* localization and gene transcript levels. (A) Western-blot of *Pf3D7*, *Pf3D7/GFP* (empty vector) and *Pf3D7/Shelph1-GFP* parasite extracts. GFP alone is observed at 27 kDa, while *Shelph1-GFP* is expressed as a 66 kDa fusion protein. (B) Fluorescence microscopy of *Pf3D7/Shelph1-GFP* line. Scale bar, 2 μ m. (C) Quantitative RT-PCR analysis was performed on cDNA from *Pf3D7* and *PfShelph2-KO* parasites. The gene relative expression in *PfShelph2-KO* parasites is given following normalization to *Pf3D7*. *PfPPKL* and *Pfshelph2* transcript levels were used as controls. Fructose biphosphate aldolase was used as the reference gene. The graph represents the mean of two independent experiments, for which the data of the three *PfShelph2-KO* lines were pooled. Error bars represent standard deviation.

<https://doi.org/10.1371/journal.pone.0187073.g004>

between free merozoite and erythrocyte triggers phosphorylation changes of RBC proteins [44–47] that may directly or indirectly modify the biophysical properties of the RBC membrane, as the phosphorylative status of RBC skeletal proteins affects erythrocyte deformability [48]. For instance, binding of *PfEBA175* to its RBC receptor glycoprotein A was recently shown to induce significant modifications of the erythrocyte membrane deformability, essential for invasion [44,47]. Similarly, interaction between the adhesin *PfRh5* and its host receptor Basigin triggers phosphorylations of numerous RBC cytoskeletal proteins including dematin, band 4.1, Ankyrin and spectrin [45]. Fernandez-Pol *et al.* already postulated that *PfShelph2*

may participate in the association/disassociation of Band3 from the underlying cytoskeleton during invasion based on its capacity to dephosphorylate Band 3 *in vitro* [18], but direct proof of *PfShelph2* discharge in the RBC is still missing. The lack of detectable invasion defect in absence of *PfShelph2* suggests that its putative function in dephosphorylating RBC substrates might not be of primary importance for invasion, although compensatory PPs of parasitic or erythrocytic origin might also substitute for *PfShelph2*.

Understanding the complex interplay between parasite kinases and PPs during *Plasmodium* life cycle still remains a challenge. To achieve this goal, we need to undertake a systematic functional characterization of its PPs but this task might be complicated by functional redundancy. In this context, the advent of CRISPR-Cas9 technology will be an invaluable tool to generate multi-knock-out or multi-edited parasite lines.

Supporting information

S1 Table. Primers used in this study.
(PDF)

S1 Fig. Verification of *PfShelph2*-HA₃ edition by sequencing. (A) Sequencing showing *Pf*3D7 sequence (top) that corresponds to the guide RNA sequence followed by the PAM, and the related sequence in *PfShelph2**-HA₃ parasites (bottom) carrying the desired shield mutations without affecting the protein sequence. (B) Sequencing showing the 3' end of *shelph2* CDS in *Pf*3D7 (top), and the related sequence in *PfShelph2*-HA₃ parasites (bottom) showing the successful in frame integration of the linker and HA₃ tag.
(TIF)

Acknowledgments

We thank J.J. Lopez-Rubio for pL6-eGFP and pUF1-Cas9 plasmids; M. Blackman for anti-MSP1₁₉ and anti-SUB1 antibodies. We thank the “Montpellier Ressources Imagerie” (MRI) platform for imaging, Yann Bordat from the MRI-Cytometry platform, and Philippe Clair from the qPCR Haut Debit Montpellier GenomiX platform.

Author Contributions

Conceptualization: Maryse Lebrun, Catherine Braun-Breton, Mauld H. Lamarque.

Funding acquisition: Maryse Lebrun, Catherine Braun-Breton.

Investigation: Alexandra Miliu, Mauld H. Lamarque.

Project administration: Mauld H. Lamarque.

Supervision: Catherine Braun-Breton, Mauld H. Lamarque.

Validation: Alexandra Miliu, Mauld H. Lamarque.

Visualization: Alexandra Miliu, Mauld H. Lamarque.

Writing – original draft: Maryse Lebrun, Catherine Braun-Breton, Mauld H. Lamarque.

References

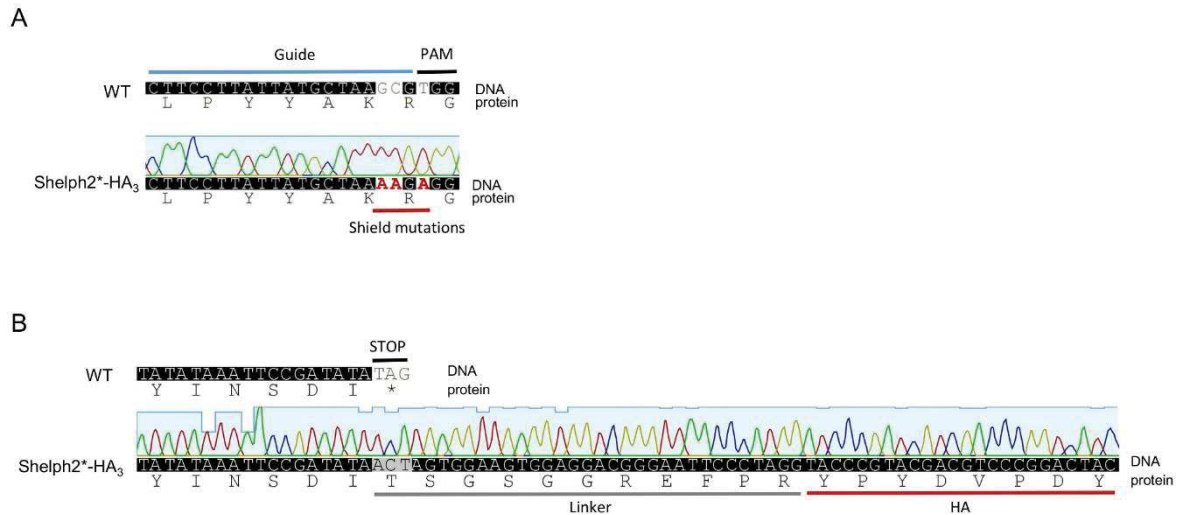
1. World Malaria Report 2016.
2. Hopp CS, Bowyer PW, Baker DA. The role of cGMP signalling in regulating life cycle progression of *Plasmodium*. *Microbes Infect.* 2012; 14: 831–837. <https://doi.org/10.1016/j.micinf.2012.04.011> PMID: 22613210

3. Dawn A, Singh S, More KR, Siddiqui FA, Pachikara N, Ramdani G, et al. The Central Role of cAMP in Regulating Plasmodium falciparum Merozoite Invasion of Human Erythrocytes. *PLoS Pathog.* 2014; 10: e1004520. <https://doi.org/10.1371/journal.ppat.1004520> PMID: 25522250
4. Doerig C, Baker D, Billker O, Blackman MJ, Chitnis C, Kumar Dhar S, et al. Signalling in malaria parasites. The MALSIG consortium. *Parasite.* 2009; 16: 169–182. <https://doi.org/10.1051/parasite/2009163169> PMID: 19839262
5. Billker O, Lourido S, Sibley LD. Calcium-Dependent Signaling and Kinases in Apicomplexan Parasites. *Cell Host Microbe.* 2009; 5: 612–622. <https://doi.org/10.1016/j.chom.2009.05.017> PMID: 19527888
6. Taylor HM, McRobert L, Grainger M, Sicard A, Dluzewski AR, Hopp CS, et al. The Malaria Parasite Cyclic GMP-Dependent Protein Kinase Plays a Central Role in Blood-Stage Schizogony. *Eukaryot Cell.* 2010; 9: 37–45. <https://doi.org/10.1128/EC.00186-09> PMID: 19915077
7. Brochet M, Collins MO, Smith TK, Thompson E, Sebastian S, Volkman K, et al. Phosphoinositide Metabolism Links cGMP-Dependent Protein Kinase G to Essential Ca²⁺ Signals at Key Decision Points in the Life Cycle of Malaria Parasites. *PLoS Biol.* 2014; 12: e1001806. <https://doi.org/10.1371/journal.pbio.1001806> PMID: 24594931
8. Alam MM, Solyakov L, Bottrill AR, Flueck C, Siddiqui FA, Singh S, et al. Phosphoproteomics reveals malaria parasite Protein Kinase G as a signalling hub regulating egress and invasion. *Nat Commun.* 2015; 6: 7285. <https://doi.org/10.1038/ncomms8285> PMID: 26149123
9. Lasonder E, Green JL, Camarda G, Talabani H, Holder AA, Langsley G, et al. The *Plasmodium falciparum* Schizont Phosphoproteome Reveals Extensive Phosphatidylinositol and cAMP-Protein Kinase A Signaling. *J Proteome Res.* 2012; 11: 5323–5337. <https://doi.org/10.1021/pr300557m> PMID: 23025827
10. Kato N, Sakata T, Breton G, Le Roch KG, Nagle A, Andersen C, et al. Gene expression signatures and small-molecule compounds link a protein kinase to Plasmodium falciparum motility. *Nat Chem Biol.* 2008; 4: 347–356. <https://doi.org/10.1038/nchembio.87> PMID: 18454143
11. Dvorin JD, Martyn DC, Patel SD, Grimley JS, Collins CR, Hopp CS, et al. A Plant-Like Kinase in Plasmodium falciparum Regulates Parasite Egress from Erythrocytes. *Science.* 2010; 328: 910–912. <https://doi.org/10.1126/science.1188191> PMID: 20466936
12. Guttery D, Poulin B, Ramaprasad A, Wall R, Ferguson DP, Brady D, et al. Genome-wide Functional Analysis of Plasmodium Protein Phosphatases Reveals Key Regulators of Parasite Development and Differentiation. *Cell Host Microbe.* 2014; 16: 128–140. <https://doi.org/10.1016/j.chom.2014.05.020> PMID: 25011111
13. Paul A, Saha S, Engelberg K, Jiang RY, Coleman B, Kosber A, et al. Parasite Calcineurin Regulates Host Cell Recognition and Attachment by Apicomplexans. *Cell Host Microbe.* 2015; 18: 49–60. <https://doi.org/10.1016/j.chom.2015.06.003> PMID: 26118996
14. Bozdech Z, Linás M, Pulliam BL, Wong ED, Zhu J, DeRisi JL. The Transcriptome of the Intraerythrocytic Developmental Cycle of Plasmodium falciparum. *PLoS Biol.* 2003; 1: e5. <https://doi.org/10.1371/journal.pbio.0000005> PMID: 12929205
15. Andreeva AV, Kutuzov MA. Widespread presence of “bacterial-like” PPP phosphatases in eukaryotes. *BMC Evol Biol.* 2004; 4: 47. <https://doi.org/10.1186/1471-2148-4-47> PMID: 15555063
16. Wilkes JM, Doerig C. The protein-phosphatome of the human malaria parasite Plasmodium falciparum. *BMC Genomics.* 2008; 9: 412. <https://doi.org/10.1186/1471-2164-9-412> PMID: 18793411
17. Patzewitz E-M, Guttery D, Poulin B, Ramakrishnan C, Ferguson DP, Wall R, et al. An Ancient Protein Phosphatase, SHLP1, Is Critical to Microneme Development in Plasmodium Ookinets and Parasite Transmission. *Cell Rep.* 2013; 3: 622–629. <https://doi.org/10.1016/j.celrep.2013.01.032> PMID: 23434509
18. Fernandez-Pol S, Slouka Z, Bhattacharjee S, Fedotova Y, Freed S, An X, et al. A Bacterial Phosphatase-Like Enzyme of the Malaria Parasite Plasmodium falciparum Possesses Tyrosine Phosphatase Activity and Is Implicated in the Regulation of Band 3 Dynamics during Parasite Invasion. *Eukaryot Cell.* 2013; 12: 1179–1191. <https://doi.org/10.1128/EC.00027-13> PMID: 23825180
19. Tsuruta H, Aizono Y. Enzymatical properties of psychrophilic phosphatase I. *J Biochem (Tokyo).* 1999; 125: 690–695.
20. Hu G, Cabrera A, Kono M, Mok S, Chaal BK, Haase S, et al. Transcriptional profiling of growth perturbations of the human malaria parasite Plasmodium falciparum. *Nat Biotechnol.* 2010; 28: 91–98. <https://doi.org/10.1038/nbt.1597> PMID: 20037583
21. Kutuzov MA, Andreeva AV. Prediction of biological functions of Shewanella-like protein phosphatases (Shelphs) across different domains of life. *Funct Integr Genomics.* 2012; 12: 11–23. <https://doi.org/10.1007/s10142-011-0254-z> PMID: 21960277
22. Ferru E, Giger K, Pantaleo A, Campanella E, Grey J, Ritchie K, et al. Regulation of membrane-cytoskeletal interactions by tyrosine phosphorylation of erythrocyte band 3. *Blood.* 2011; 117: 5998–6006. <https://doi.org/10.1182/blood-2010-11-317024> PMID: 21474668

23. Trager W, Jensen JB. Human malaria parasites in continuous culture. *Science*. 1976; 193: 673–675. PMID: 781840
24. Pasvol G, Wilson RJ, Smalley ME, Brown J. Separation of viable schizont-infected red cells of *Plasmodium falciparum* from human blood. *Ann Trop Med Parasitol*. 1978; 72: 87–88. PMID: 350172
25. Saul A, Myler P, Elliott T, Kidson C. Purification of mature schizonts of *Plasmodium falciparum* on colloidal silica gradients. *Bull World Health Organ*. 1982; 60: 755–759. PMID: 6758971
26. Lambros C, Vanderberg JP. Synchronization of *Plasmodium falciparum* erythrocytic stages in culture. *J Parasitol*. 1979; 65: 418–420. PMID: 383936
27. Crabb BS, Cowman AF. Characterization of promoters and stable transfection by homologous and non-homologous recombination in *Plasmodium falciparum*. *Proc Natl Acad Sci U S A*. 1996; 93: 7289–7294. PMID: 8692985
28. Ghorbal M, Gorman M, Macpherson CR, Martins RM, Scherf A, Lopez-Rubio J-J. Genome editing in the human malaria parasite *Plasmodium falciparum* using the CRISPR-Cas9 system. *Nat Biotechnol*. 2014; 32: 819–821. <https://doi.org/10.1038/nbt.2925> PMID: 24880488
29. Huynh M-H, Carruthers VB. Tagging of endogenous genes in a *Toxoplasma gondii* strain lacking Ku80. *Eukaryot Cell*. 2009; 8: 530–539. <https://doi.org/10.1128/EC.00358-08> PMID: 19218426
30. Przyborski JM, Miller SK, Pfahler JM, Henrich PP, Rohrbach P, Crabb BS, et al. Trafficking of STEVOR to the Maurer's clefts in *Plasmodium falciparum*-infected erythrocytes. *EMBO J*. 2005; 24: 2306–2317. <https://doi.org/10.1038/sj.emboj.7600720> PMID: 15961998
31. Collins CR, Hackett F, Strath M, Penzo M, Withers-Martinez C, Baker DA, et al. Malaria Parasite cGMP-dependent Protein Kinase Regulates Blood Stage Merozoite Secretory Organellar Discharge and Egress. *PLoS Pathog*. 2013; 9: e1003344. <https://doi.org/10.1371/journal.ppat.1003344> PMID: 23675297
32. Roger N, Dubremetz J-F, Delplace P, Fortier B, Tronchin G, Vernes A. Characterization of a 225 kilodalton rhoptry protein of *Plasmodium falciparum*. *Mol Biochem Parasitol*. 1988; 27: 135–141. [https://doi.org/10.1016/0166-6851\(88\)90033-3](https://doi.org/10.1016/0166-6851(88)90033-3) PMID: 3278223
33. Santos JM, Josling G, Ross P, Joshi P, Orchard L, Campbell T, et al. Red Blood Cell Invasion by the Malaria Parasite Is Coordinated by the PfAP2-I Transcription Factor. *Cell Host Microbe*. 2017; 21: 731–741.e10. <https://doi.org/10.1016/j.chom.2017.05.006> PMID: 28618269
34. Harris PK, Yeoh S, Dluzewski AR, O'Donnell RA, Withers-Martinez C, Hackett F, et al. Molecular Identification of a Malaria Merozoite Surface Sheddase. *PLoS Pathog*. 2005; 1: e29. <https://doi.org/10.1371/journal.ppat.0010029> PMID: 16322767
35. Blackman MJ, Heidrich HG, Donachie S, McBride JS, Holder AA. A single fragment of a malaria merozoite surface protein remains on the parasite during red cell invasion and is the target of invasion-inhibiting antibodies. *J Exp Med*. 1990; 172: 379–382. PMID: 1694225
36. Ito D, Han E-T, Takeo S, Thongkukiatkul A, Otsuki H, Torii M, et al. Plasmodial ortholog of *Toxoplasma gondii* rhoptry neck protein 3 is localized to the rhoptry body. *Parasitol Int*. 2011; 60: 132–138. <https://doi.org/10.1016/j.parint.2011.01.001> PMID: 21237287
37. Zhao X, Chang Z, Tu Z, Yu S, Wei X, Zhou J, et al. PFRON3 is an erythrocyte-binding protein and a potential blood-stage vaccine candidate antigen. *Malar J*. 2014; 13: 490. <https://doi.org/10.1186/1475-2875-13-490> PMID: 25495792
38. Yeoh S, O'Donnell RA, Koussis K, Dluzewski AR, Ansell KH, Osborne SA, et al. Subcellular Discharge of a Serine Protease Mediates Release of Invasive Malaria Parasites from Host Erythrocytes. *Cell*. 2007; 131: 1072–1083. <https://doi.org/10.1016/j.cell.2007.10.049> PMID: 18083098
39. Guttery DS, Poulin B, Ferguson DJP, Szöör B, Wickstead B, Carroll PL, et al. A Unique Protein Phosphatase with Kelch-Like Domains (PPKL) in *Plasmodium* Modulates Ookinete Differentiation, Motility and Invasion. *PLoS Pathog*. 2012; 8: e1002948. <https://doi.org/10.1371/journal.ppat.1002948> PMID: 23028336
40. Ward P, Equinet L, Packer J, Doerig C. Protein kinases of the human malaria parasite *Plasmodium falciparum*: the kinome of a divergent eukaryote. *BMC Genomics*. 2004; 5: 79. <https://doi.org/10.1186/1471-2164-5-79> PMID: 15479470
41. Treeck M, Sanders J, Elias J, Boothroyd J. The Phosphoproteomes of *Plasmodium falciparum* and *Toxoplasma gondii* Reveal Unusual Adaptations Within and Beyond the Parasites' Boundaries. *Cell Host Microbe*. 2011; 10: 410–419. <https://doi.org/10.1016/j.chom.2011.09.004> PMID: 22018241
42. Solyakov L, Halbert J, Alam MM, Semblat J-P, Dorin-Semblat D, Reiningger L, et al. Global kinomic and phospho-proteomic analyses of the human malaria parasite *Plasmodium falciparum*. *Nat Commun*. 2011; 2: 565. <https://doi.org/10.1038/ncomms1558> PMID: 22127061

43. Pantaleo A, Ferru E, Carta F, Mannu F, Giribaldi G, Vono R, et al. Analysis of changes in tyrosine and serine phosphorylation of red cell membrane proteins induced by *P. falciparum* growth. *PROTEOMICS*. 2010; 10: 3469–3479. <https://doi.org/10.1002/pmic.201000269> PMID: 20799346
44. Koch M, Wright KE, Otto O, Herbig M, Salinas ND, Tolia NH, et al. *Plasmodium falciparum* erythrocyte-binding antigen 175 triggers a biophysical change in the red blood cell that facilitates invasion. *Proc Natl Acad Sci*. 2017; 114: 4225–4230. <https://doi.org/10.1073/pnas.1620843114> PMID: 28373555
45. Aniwah Y, Gao X, Hao P, Meng W, Lai SK, Gunalan K, et al. *P. falciparum* RH5-Basigin interaction induces changes in the cytoskeleton of the host RBC. *Cell Microbiol*. 2017; e12747. <https://doi.org/10.1111/cmi.12747> PMID: 28409866
46. Zuccala ES, Satchwell TJ, Angrisano F, Tan YH, Wilson MC, Heesom KJ, et al. Quantitative phosphoproteomics reveals the *Plasmodium* merozoite triggers pre-invasion host kinase modification of the red cell cytoskeleton. *Sci Rep*. 2016; 6. <https://doi.org/10.1038/srep19766> PMID: 26830761
47. Sisqueira X, Nebl T, Thompson JK, Whitehead L, Malpede BM, Salinas ND, et al. *Plasmodium falciparum* ligand binding to erythrocytes induce alterations in deformability essential for invasion. *eLife*. 2017; 6. <https://doi.org/10.7554/eLife.21083> PMID: 28226242
48. Pantaleo A, De Franceschi L, Ferru E, Vono R, Turrini F. Current knowledge about the functional roles of phosphorylative changes of membrane proteins in normal and diseased red cells. *J Proteomics*. 2010; 73: 445–455. <https://doi.org/10.1016/j.jprot.2009.08.011> PMID: 19758581

S1 Figure: Verification of Shelph2-HA₃ edition by sequencing. (A) Sequencing showing Pf3D7 sequence (top) that corresponds to the guide RNA sequence followed by the PAM, and the related sequence in PfShelph2*-HA₃ parasites (bottom) carrying the desired shield mutations without affecting the protein sequence. (B) Sequencing showing the 3' end of shelph2 CDS in Pf3D7 (top), and the related sequence in PfShelph2-HA₃ parasites (bottom) showing the successful in frame integration of the linker and HA₃ tag.



S1 table: Primers used in this study.

Primer name	Sequence (5'-3') – Restriction site in bold	Restriction Site
MLa33	TAAGTCCTCC ACTAGT GGAAGTGGAGGACGGGAATT	SpeI
MLa32	CGGAAGATAG GGCGCGC CTTAGGCATAATCTGGAACATCG	AscI
MLa40	TATGCCTAAG GGCGCGC CTACCTTTATCATTAAAAGGTCTC	AscI
MLa41	CAATGGCCCTTT CCGCGG AGTAAAGCTTACATATTCATTA AAAAG	SacII
MLa3	CGCCTCGAGATGAATATATCATATTTAAGGAATTTTTT	
MLa4	CGCGGTACCTATATCGGAATTTATATAATTTACTTTATATG	
MLa79	CTTCCTTATTATGCTAAAAGAGGTATTGATTATATAAATGATG	
MLa80	CATCATTTATATAATCAATACCTCTTTTAGCATAATAAGGAAG	
MLa59	CGCGGGGAGG ACTAGT CATTAGGGAAAATGTGTTCTGTG	SpeI
MLa45	CTCCACTCC ACTAGT TATATCGGAATTTATATAATTTACTTTATATG	SpeI
MLa60	TTACAAAATG CCTAAG AGTAAAGCTTACATATTCATTA AAAAG	AflIII
MLa63	TAAGTATATAATATTCTTCCTTATTATGCTAAGCGTTTTAGAGCTAGAA	
MLa64	TTCTAGCTCTAAAACCGCTTAGCATAATAAGGAAGAATATTATATACTTA	
MLa54	TTTTACGTT CCATGG GTTGAAAATTTATTATTTTATGGTG	NcoI
MLa53	ATTAAATCTAG AATTC TTAGAACACATTTTCCCTAATGG	EcoRI
MLa50	TTACAAAATG CCTAAG TACCTTTTATCATTAAAAGGTCTC	AflIII
MLa51	AGCCGAAGAT ACTAGT GGAATAGTATAATGCCCATGAAGTC	SpeI
MLa1	CG CCTCGAG ATGAATGTAGACAAAATACTTTGG	XhoI
MLa2	CG CGGTAC CAAATCTTTAATTTTATGACTTAGAC	KpnI
MLa11	CGCCTCGAGATGAAGAGTTTGGAGAATAACG	
MLa12	CGCGGTACCCATAAAAATGACATTTCTAAGAC	
MLa13	CGCCTCGAGATGTGGAATAAATTAATGATGC	
MLa14	CGCGGTACCTAAAAATTA AACATTTAACATTAGG	

Mla65	CTTCCTTATTATGCTAAGCG	
MLa99	CCTTTTAAATGATGAAAGGTATTTGATATCC	
ML1476	CAGCGTAGTCCGGGACGTCGTAC	
MLa115	CAAGTTTATTATACATCCTATACATTTACTTTAAACC	
MLa116	ACGATGCAGTTTAGCGAACC	
MLa117	TCCAATACTTTCCAATGTTTCATGG	
hDHFR	CCAGGTGTTCTCTCTGATGTCC	
qPCR primers		
Primer name	Sequence (5' - 3')	Gene
MLa218	TGGCTAACCATAATTACCTTTTTGG	<i>shelph1</i>
MLa219	CTCTCTACGTCCCATGGAT	<i>shelph1</i>
MLa224	AAGTGCCACCTCAAAGAGTG	<i>PPKL</i>
MLa225	GCTTCTGGTGGACTTCCTTT	<i>PPKL</i>
MLa226	TGTACCACCAGCCTTACCAG	<i>FBA</i>
MLa227	TTCCTTGCCATGTGTTCAAT	<i>FBA</i>
Shlp2_F	TGCTAAGCGTGGTATTGATT	<i>shelph2</i>
Shlp2_R	CTGCAGCACGAGAAAAGTAT	<i>shelph2</i>

1.3 Conclusion and perspectives

In this study, we described Shelph2 protein expression and localization over the erythrocytic cycle of *P. falciparum*. We found the protein to be mostly expressed in schizonts and merozoites, and confirmed by IFA the previously reported localization of Shelph2 to apical organelles that do not coincide with known rhoptry, microneme and exoneme markers. Unfortunately, our study could not identify the role of Shelph2 in parasite intraerythrocytic development, as gene deletion did not have any measurable phenotype. This made us hypothesize that other PPs could have redundant functions with Shelph2. Shelph1 would be the most obvious compensatory enzyme, but we showed that its parasite localization differed from the one observed for Shelph2 in Pf3D7 parasites, making it unlikely that it might sustain the same function. As Shelph1-GFP was episomally expressed under the control of CRT promoter, one has to be cautious with this result. Therefore, to properly assess Shelph1 localization, it would be interesting to endogenously tag *shelph1* using CRISPR-Cas9, both in wild-type and *PfShelph2*-KO parasites, to investigate whether the absence of Shelph2 induces Shelph1 relocation in the parasite. Possible redundancy between the Shelphs could also be assessed by generating a single Shelph1-KO and a double Shelph2-Shelph1-KO. We attempted to disrupt *shelph1* gene by a direct knockout approach but repeatedly failed to obtain these parasites, suggesting that *PfShelph1* may be essential. Therefore, a conditional approach will be necessary in future to investigate *PfShelph1* function.

If not Shelph1, Shelph2 function could still be compensated by another Tyr-PP. There are 4 reported PTP in *Pf* genome, namely YVH1, PRL, PTP1 and PTPLA^{265,332,333}, of which only the first two enzymes were shown experimentally to display phospho-Tyr PP activity *in vitro*^{332,333}. For PTP1, biochemical data are missing, while PTPLA lacks important catalytic residues suggesting that it is not an active enzyme^{240,267}. To test for possible compensatory mechanisms between these PTPs and Shelph2, the mRNA expression level of these PTPs could be compared in the wild-type and Shelph2-KO lines. However, it is to be noted that unlike the Shelphs, these PTPs do not harbor an N-terminal signal peptide, making it unlikely to be secreted PPs.

Shelph2 was reported to be secreted during invasion using live-video microscopy¹⁸³, suggesting that its main role might occur in the host RBC and not in the parasite. We tried to confirm this secretion by performing subcellular fractionation assays on invading merozoites. However, these assays are experimentally difficult to perform as (i) parasites need to be very tightly synchronized; (ii) the number of invading merozoites is low compared to the number of fresh red blood cells used in the assay, which dilutes the signal with non invaded RBCs. Using this assay, we could not confirm Shelph2 secretion at the time of invasion, but the experiments could be tried again. Alternatively, it would be interesting to use a FRET-based β -lactamase (BLA) strategy first adapted to *T. gondii*³³⁴. In this assay, BLA-fusion proteins can be detected in the host cells treated with a BLA substrate, coumarin cephalosporin fluorescein (CCF2). When the substrate is intact, excitation at 407 nm results in FRET to the fluorescein emission at 520 nm. In the presence of BLA, cleavage of the substrate dissociates the fluorophores and excitation at 407 nm results in emission at 447 nm. A change in fluorescence from green to blue therefore indicates secretion of the protein. In our case, fresh RBCs could be incubated with CCF2, prior to mixing with late schizonts stages blocked in egress by Compound 2 treatment. Following release of the inhibitor, invasion would be allowed to take place and the newly re-invaded RBCs fixed for fluorescence analysis.

Finally, we also tried to look at Shelph2 secretion by comparing the Tyr phosphorylation pattern of RBCs proteins in the WT and Shelph2-KO line using anti-phosphoTyr antibodies, but we did not evidence any obvious phosphorylation changes. This technic is not very sensitive and it may be more appropriate to perform a RBC phosphoproteome at the time of merozoites invasion, keeping in mind that again most of the RBCs will not be re-invaded.

As Shelph2 is dispensable in *Plasmodium* RBC development, it might have a role in other stages of the parasite life cycle. Although Shelph2 in *P. berghei* was found neither to be required for blood stages nor for sexual parasite development in mosquitoes³¹⁰, discrepancies between *Pf* and *Pb* have already been reported. Such studies in *Pf* would probably require to initiate a collaboration.

Chapter 2: GlmS ribozyme strategy and characterization of PP4 and PP7

2.1 Introduction

Among the PPs that were retrieved in our *in silico* screen, were PP1, PP4 and PP7 (Figure 48). They belong to the PPP subfamily, and as such possess Ser/Thr PP activity.

PP4, along with PP2A and PP6 share structural features³³⁵ and form a separate subcluster among PPP (Figure 32) that shares structural features³³⁵. *Pf*PP4 has never been studied, but an endogenous PP4-GFP fusion in *P. berghei* showed that the protein was expressed during asexual blood stages with a cytoplasmic localization, in gametocytes, and also in mosquito stages such as the ookinete and the oocyst³¹⁰. *Pb*PP4 was refractory to genetic deletion²⁶⁶, and *Pf*PP4 could not be disrupted by insertional mutagenesis³²⁹, thereby suggesting that *pp4* is an essential gene for the erythrocytic cycle. This characteristic and the regulated expression of the gene during the 48h cycle (Figure 49), incited us to investigate *Pf*PP4 function.

Despite its nomenclature, *Plasmodium* PP7 is a PPEF member of the PPEF/PP7 clade of PPPs. *Pf*PP7 shows the same conserved domains as described for the PPEF family: the N-terminal part encodes an IQ motif that functions in binding EF-hand containing proteins, such as Calmodulin. The central part of

Pfpp7 gene is the conserved PP catalytic domain, whereas the C-terminus harbours three Ca²⁺-binding EF hand motifs. The catalytic domain of *PfPP7* was initially called “PPJ” and biochemically characterized, showing Mn²⁺-dependent Ser/Thr PP activity and insensitivity to PP2A- (microcystin, OA) or PP1-inhibitors²⁸⁹. The protein was shown to localize to the parasite cytoplasm²⁸⁹. Still, *PfPP7* function has not been investigated so far.

Several biological processes of *Plasmodium* are regulated by Ca²⁺ and its effector proteins, among others invasion, microneme secretion, gliding motility and egress^{111,336–338}. The possible regulation of *PfPP7* by Ca²⁺ associated with a peak of expression in late schizont stage^{289,306} (Figure 49) therefore make this PP an interesting candidate for a function in egress or invasion. Attempts to knockout *pp7* in *P. berghei*³¹⁰ and *P. falciparum* failed³²⁹, indicating an essential role for this PP late during the erythrocytic cycle.

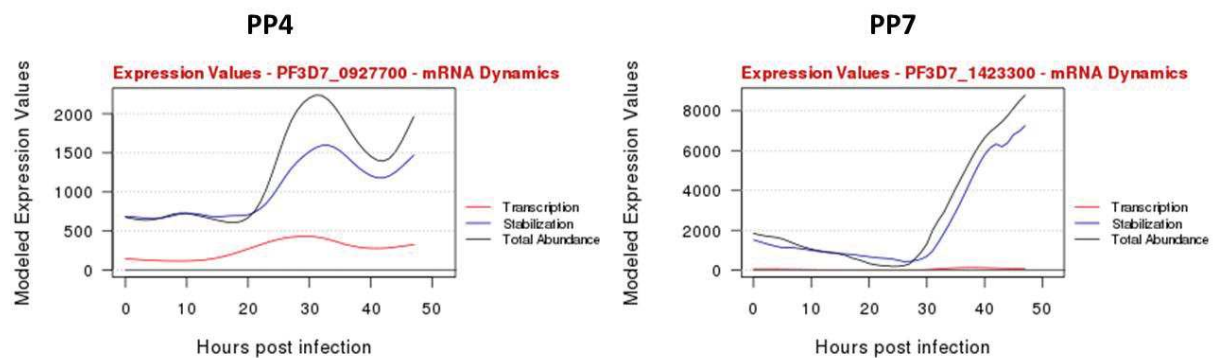


Figure 49: *PfPP4* and *PP7* expression over the intraerythrocytic cycle. Real-time transcription and decay data. Biosynthetic pyrimidine labeling was used for the calculation of real-time, whole-genome analysis of transcription and stability throughout asexual development of *P. falciparum* 3D7 strain. On the y-axis the “modeled expression values” represent transcript abundance values normalized to the total mRNA abundance¹⁷⁰.

PP1 is a highly conserved enzyme in eukaryotes, involved in transcription, splicing, mitosis and many other cellular processes^{192,339}. PP1 is the major PP activity both in mammalian cells as well as in blood stage *Pf*³⁴⁰, and biochemical characterization of *PfPP1* recombinant enzyme demonstrated PP activity sensitive to PP1 inhibitors³⁴¹. Specificity and regulation of PP1 are achieved by assembly with different regulatory partner proteins, so-called PIPs²⁴⁷. In *Pf*, four PIPs have been described, and many others have been predicted^{279,281,342,343}, but the functions of PP1 for parasite development remain unknown.

Given the likely essentiality of PP1, PP4 and PP7, we chose an inducible knockdown approach for the functional study of these genes, namely the *glmS* ribozyme strategy that has been recently adapted to *P. falciparum*³⁴⁴.

The *glmS* gene codes for the enzyme glutamine-fructose-6-phosphate-amidotransferase that catalyzes the formation of glucosamine-6-phosphate, an intermediate in cell wall biogenesis, from fructose-6-phosphate and glutamine³⁴⁵. The *glmS* ribozyme lies in the intergenic region preceding the *glmS* gene and forms an RNA secondary structure that displays self-cleavage activity specifically in response to glucosamine-6-phosphate (GlcN6P), thus providing a specific negative feedback mechanism for regulating the enzyme expression³⁴⁶.

The *glmS* ribozyme from *Bacillus anthracis* has been adapted as a genetic tool to control yeast reporter gene expression³⁴⁷. Due to differences in the metabolism of yeast and bacteria, exogenous addition of 5mM glucosamine (GlcN) was sufficient to induce cleavage of the *glmS* ribozyme, which was placed in 3' of a reporter gene. Prommana *et al.* adapted this *glmS* ribozyme to *P. falciparum* (Figure 50A)³⁴⁴. The *glmS* sequence was integrated in 3' of the genomic *dihydrofolate reductase-thymidylate synthase* (DHFR-TS) locus (Figure 50B). Treating this edited parasite line with 1 mM GlcN achieved 90%

downregulation of the endogenous DHFR-TS gene, which could be reversed after GlcN removal (Figure 50 C-D). Importantly, GlcN toxicity to the parasites started at a concentration of 5mM after 48h of treatment (Figure 50E). Therefore, the *glmS* ribozyme is a powerful tool to down-regulate endogenous gene expression, within the effective range of 0 to 5 mM GlcN.

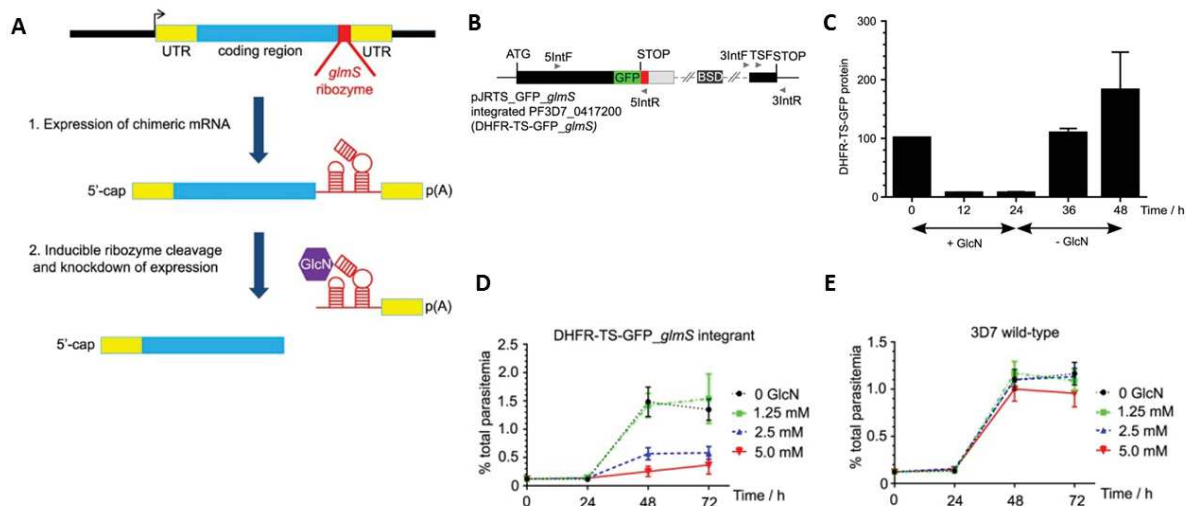


Figure 50: The *glmS* ribozyme as reverse genetic tool for *Plasmodium*. (A) Schematic of the *glmS* ribozyme as reverse genetic tool. (B) Integration of the *glmS* sequence in 3' of the essential DHFR-TS gene. The gDNA of edited parasites is shown. (C) GlcN induces reversible protein depletion in the DHFR-TS-GFP-*glmS* parasites. Parasites were treated with 2.5 mM GlcN at 0hpi, and GFP fusion protein was quantified using FACS. GlcN was removed at 24hpi, showing recovery of target protein expression. (D) and (E) Growth of DHFR-TS-GFP-*glmS* integrant and 3D7 wt parasites in presence of different GlcN concentrations³⁴⁴.

2.2 Setting up the *glmS* ribozyme system for getting inducible PP knockdown parasites

Testing reporter gene KD using the *glmS* ribozyme

First, we wanted to check if ribozyme induction of an episomally expressed GFP-reporter gene works in our hands. For this purpose we used the same construct encoding a *Pb*DHFR-TS-GFP fusion protein as described and kindly provided by the group of P. Shaw³⁴⁴. In this construct, *Pb*DHFR-TS-GFP expression is placed under the control of *Pf* heat shock protein 86 (*hsp86*) promoter, and is fused with a mitochondrial targeting peptide from *Pf**hsp60* (Figure 51A). GlcN was added to early ring stage parasites, and parasites were allowed to progress till late schizonts (43 hpi). Parasites were then fixed and GFP fluorescence was measured by flow cytometry. We found that 1mM GlcN was sufficient to induce almost complete GFP down-regulation within 34 hours of GlcN treatment (Figure 51B). IFAs confirmed the downregulation of a mitochondrial-localized GFP upon exposure to GlcN (Figure 51C).

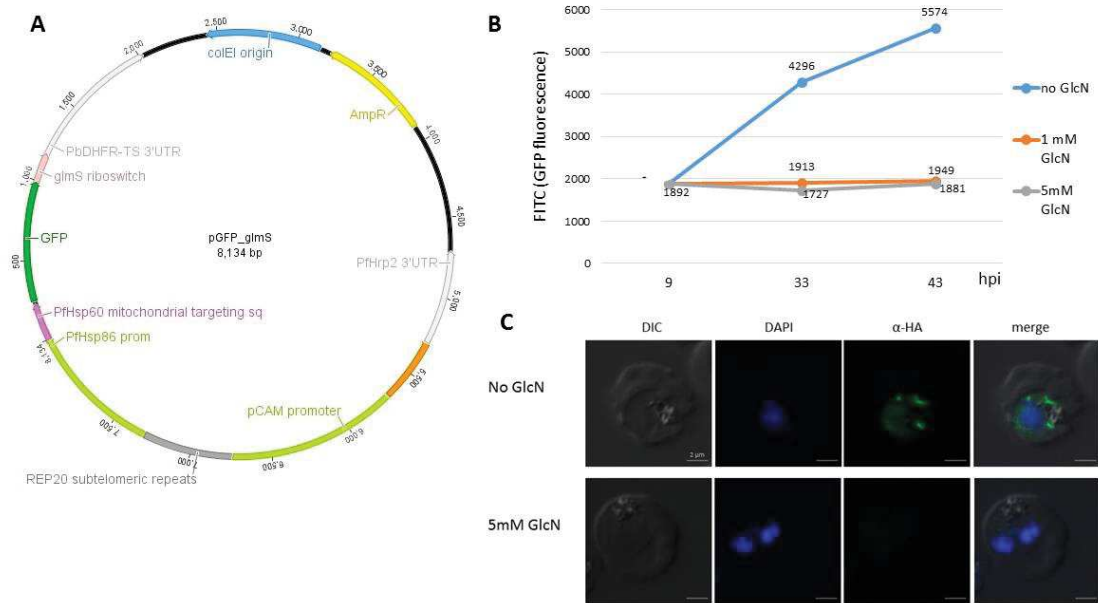


Figure 51: GlcN regulation of an episomally expressed GFP-glmS. (A) Plasmid encoding a mitochondrial-targeted GFP, under control of the Hsp86 promoter, and fused to the *glmS* ribozyme with 3' regulatory elements of *PbDHFR-TS*. This plasmid was transfected into 3D7 wt parasites. (B) Ring stage parasites were exposed to different GlcN concentrations for 34 h. Parasitized red blood cells expressing *pPbDHFR-TS-GFP_glmS* were enumerated by flow cytometry based on the level of GFP-fusion protein. (C) IFA of the same experiment showing the GFP fluorescence in presence or absence of GlcN. Scale bar 2 μ m.

So as the episomal *glmS* ribozyme was working efficiently in our hands, we proceeded in integrating this sequence downstream of *Plasmodium* PP loci, in order to generate inducible PP-KD parasites.

Generating PP4-*glmS* and PP7-*glmS* knockdown parasites

Our strategy was to insert at the 3' end of the PP4 and PP7 coding sequence a cassette comprising a HA₃ tag followed by the *glmS* ribozyme and the 3' regulatory region of the *P. berghei* DHFR-TS 3'UTR (*PbDT* 3'). The main advantage of this strategy resides in the capacity to tag and insert a regulatable motif to the PP of interest with a single recombination event. This cassette was ordered as a synthetic fragment (iDT DNA), named HA₃-*glmS*-*PbDT* 3' and cloned into a pLN vector (Figure 52). To modify the genomic locus of PP4 and PP7 using CRISPR-Cas9³⁴⁸, we then cloned on either side of the cassette two homology regions (HR) that could be used by the parasite to repair the double strand break induced by the Cas9 nuclease. HR1 corresponds to a fragment of the PP 3' genomic DNA, while HR2 matches a sequence of the respective 3'UTR. When necessary, a part of the 3' coding sequence was recodonized to insert shield mutations. These are additional silent mutations in the Cas9 binding site that would protect the DNA sequence from Cas9-mediated cleavage³⁴⁸. On the other hand, the Cas9 nuclease was provided by the pDC2 vector (gift from M. Lee), in which we also cloned the single guide RNA (sgRNA). Constructs as shown in Figure 52 were generated for the purpose of PP4 and PP7 locus editing.

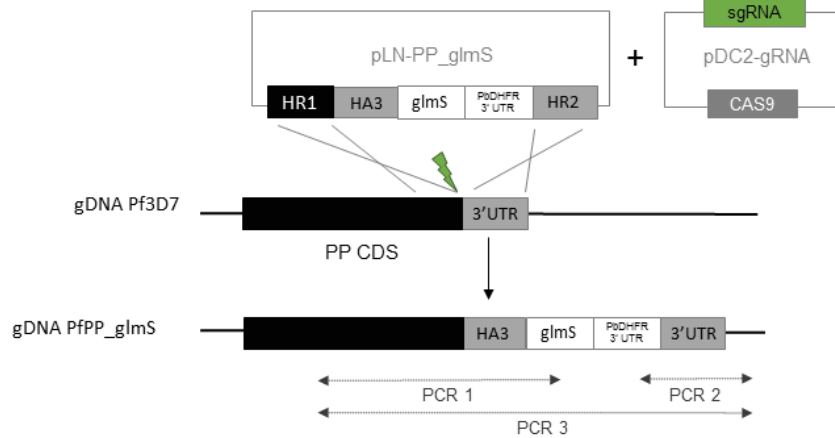


Figure 52: Cloning strategy for generating PP-glmS ribozyme-inducible KD parasites. Homology region 1 (HR1) matching the PP CDS, and HR2 corresponding to the 3'UTR were cloned on either side of the HA₃-glmS-PbDT 3' cassette into pLN vector. A double strand-break (green arrow) is induced by Cas9 at the 3' end of the CDS and repaired by the parasites via double homologous recombination using HR1 and HR2 as donor DNA sequence. The gRNA-targeted part of the PP sequence was recodonomized or mutated.

Pf3D7 parasites were co-transfected with the pLN-PP-glmS and pDC2 modified vectors. After 2 weeks of plasmid selection with 2.5 µg/ml of BSD and 2.5 nM of WR99210, parasites transfected with PP4-glmS and PP7-glmS came back. It is to be noted that similar constructs were made to obtain PP1-glmS edited parasites, but following transfection, parasites bearing the expected modification never came back. We hypothesize that adding a ribozyme sequence in 3' of PP1 mRNA may interfere with its stability and therefore could be lethal to the parasites. Alternatively, the *PbDT* 3' used in the construct might be inappropriate to regulate PP1 expression.

PP4-glmS and PP7-glmS parasites were genotyped by PCRs to check for HA₃-glmS-PbDT3' integration (Figure 53). The five clones of PP4-glmS were positive for the 5' (PCR1) and the 3' (PCR2) integrative PCRs (localization of the primers shown in Figure 52). The amplification of the whole PP4 locus (PCR3) gave the expected 3160 bp band, as compared to the 1800 bp amplification in the parental line (Figure 53A). For PP7-glmS we performed two transfections, T13 and T14, corresponding to two different sgRNAs. By integrative PCR we found that only T14 had the desired 5' and 3' integration (Figure 53B). The amplification of the whole locus showed that the parasite population within T14 culture was a mix of edited and wt parasites.

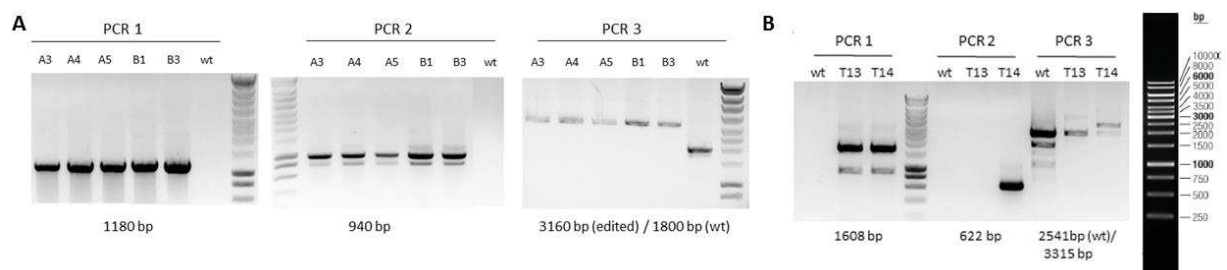


Figure 53: Genotyping of PP4-HA₃-glmS and PP7-HA₃-glmS parasites. (A) Integrative PCRs for five clonal lines bearing the PP4-HA₃-glmS DNA edition. (B) Integrative PCRs of the transfected populations of PP7-HA₃-glmS parasites. Two different gRNAs were used for transfections T13 and T14. Only the T14 parasites demonstrate the expected integration. The PP7-glmS transfectant parasites were not submitted to cloning by limiting dilution. Gene Ruler 1kb DNA ladder was used as marker.

Using CRISPR-Cas9, we successfully obtained PP4-glmS and PP7-glmS edited parasites, as shown by integrative PCRs. The efficiency of PP4 edition was very good as 5 clones out of 5 had the expected genomic modification. As for PP7-glmS, the transfected parasites now need to be cloned by limiting dilution.

Test GlcN-mediated glmS downregulation

We first tested GlcN toxicity on the *P. falciparum* strain (Pf3D7) that we have in the lab. Parasites were exposed to GlcN concentrations ranging from 1 mM to 5 mM over two intraerythrocytic cycles, and their proliferation rate was measured by FACS. We observed that GlcN concentrations of up to 3.5 mM did not affect parasite development, whereas higher concentrations led to a 50% decrease in parasite growth (Figure 54A). Our results are quite similar to those previously reported³⁴⁴, and highlight the fact that in our lab, GlcN above 3.5 mM is detrimental to the parasite.

We next tested PP4 down-regulation on PP4-glmS clone B1. Synchronized ring stage parasites were exposed to GlcN concentrations ranging from 0 to 5 mM. After 48 hours of GlcN exposure, we measured the protein expression levels by WB. As shown in Figure 54B, we could not evidence any major down-regulation of PP4, even at the toxic concentration of 5 mM GlcN, thus preventing any further phenotyping of this PP4 knockdown line.

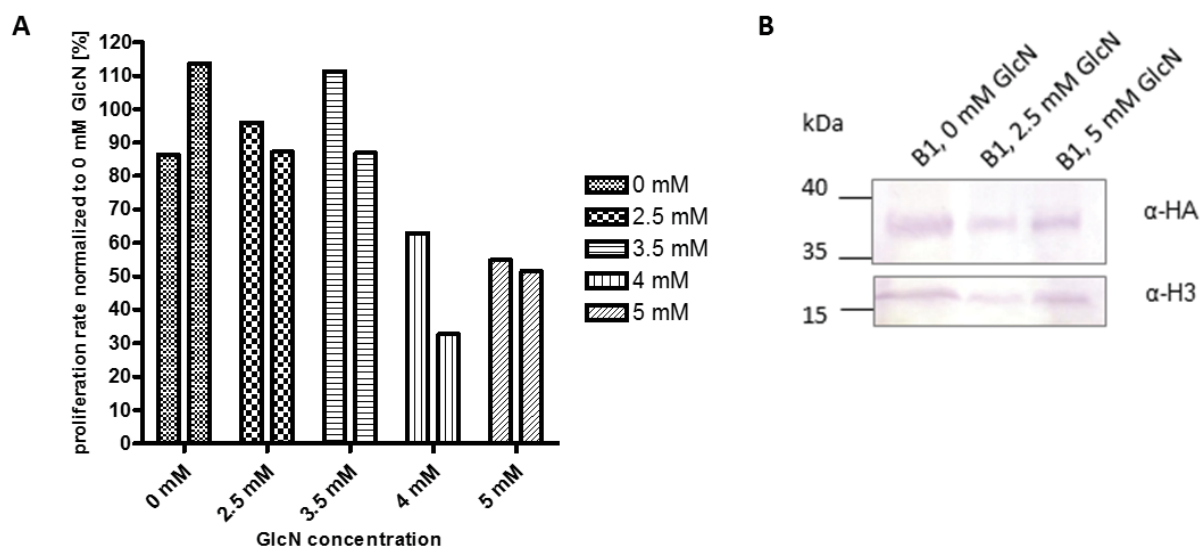


Figure 54: Test of GlcN dose-dependent toxicity and induction of glmS-mediated PP4 down-regulation. (A) 3D7 wt ring parasites were treated with varying levels of GlcN for 2 cycles. The proliferation rate over one cycle of GlcN exposure (48h till 96h post-GlcN) was measured by flow cytometry and normalized to the proliferation rate in absence of GlcN. Two separate experiments are shown as separate bars. (B) Testing the GlcN regulation of endogenous PP4-glmS expression. Parasite extracts of late stage parasites after 48h treatment with 0, 2.5 and 5 mM GlcN were loaded on gel. Histone H3 served as a loading control.

Depending on the gene of interest, knockdown of gene expression using the glmS strategy can be achieved with GlcN concentrations below its toxicity level^{344,349}. Unfortunately, in the case of PP4, protein depletion could not be achieved in this concentration range. Yet, we used the PP4-glmS and PP7-glmS parasites to investigate their subcellular location in asexual blood stages.

2.3 Subcellular localization of PP4 and PP7

We took advantage of the HA₃-tagging of PP4 and PP7 in the engineered PP4-glmS and PP7-glmS lines to check their expression and localization by IFA and WB.

By WB, PP4- HA₃ was detected as a 39 kDa fusion protein, as expected, using an asynchronous parasite lysate (Figure 55B). However, the protein was barely detectable by IFA (Figure 55A), and gave a weak and diffuse cytoplasmic pattern. This weak fluorescence could reflect a genuine low level of expression

of the protein as suggested by transcriptomic data¹⁷⁰, or could be due to an inaccessibility of the tag to the antibodies. In contrast, PP7 was found mostly associated to the parasite nucleus (Figure 55A), which is in disagreement with its previous reported location that was mostly cytoplasmic²⁸⁹. However, in this study, the localization was performed using an antibody directed against a PP7 peptide that could recognize both the full length and a truncated version of the protein. In our PP7-*glmS* line, we modified the endogenous 3'UTR for PbDT3' and therefore we cannot exclude that we are disturbing the protein timing of expression and hence, localization.

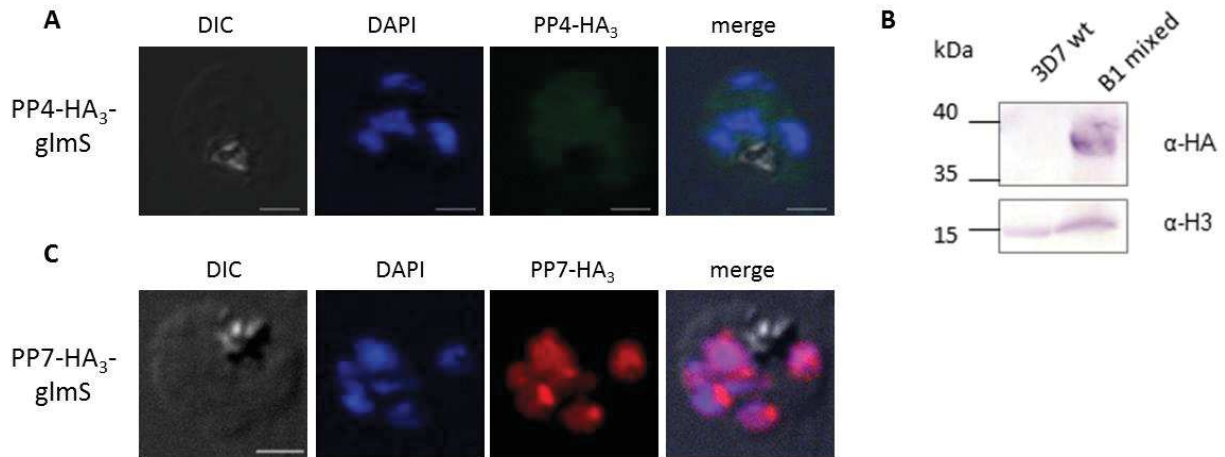


Figure 55: Expression and localization of PP4-HA₃ and PP7-HA₃ protein in the *glmS*-edited parasites (A) IFAs of PP4-HA₃-*glmS*, clone B1, using anti-HA antibodies. Scale bar 2 μ m. (B) Western Blot of mixed stage parasite extracts of 3D7 wt and PP4-HA₃-*glmS*, clone B1, using anti-HA antibodies. Equivalent amounts of proteins were loaded per lane and verified using anti-Histone H3 antibodies. (C) IFAs of PP7-HA₃-*glmS* parasites.

2.4 Generating inducible knockout (iKO) of PP7

Given the lack of sufficient down-regulation using the *glmS* ribozyme and the toxicity of GlcN, we then opted for an inducible knockout strategy using the DiCre system¹⁰². Constructs for PP1 and PP7 were generated; iKO-PP7 is described below, while the iKO-PP1 will be described in the next chapter.

The strategy used relies on the insertion of two *loxP* sites at the PP endogenous locus. The first one is placed after the stop codon (3' *loxP*), and the second introduced in a synthetic intron (*loxPint*)³⁵⁰ in place of a native intron located at the beginning of the gene if possible, so as to delete most of the gene upon recombination between the two *loxP* sequences by the Cre recombinase (Figure 56A). Additionally, an HA₃ tag was inserted at the end of the coding sequence to help track the proteins. The two *loxP* sites were introduced by two independent transfections, enabling first to engineer a PP-HA₃-*loxP* line, and then the desired iKO-PP strain. To insert the 3' *loxP* site, we modified the pLN-PP7-*glmS* plasmid containing the HR, by substituting the *glmS*-PbDT 3' sequence by a HA₃-stop-*loxP* cassette. Following transfection of this plasmid along with the pDC2-sgRNA vector, parasites came back and were cloned by limiting dilution, enabling to obtain a clonal line of PP7-HA₃-*loxP* (clone 3C) that was verified by PCR and sequencing for genomic edition (Figure 56B). The *loxPint* was then inserted in a second step in place of intron 2, using HR located on both sides of this intron and another sgRNA. Successful integration was confirmed by PCR on the parasite population that re-appeared in the culture following transfection (Figure 56C), thus showing that we obtained iKO-PP7 parasites. In future, this population will be cloned and analyzed for PP7 gene excision upon rapamycin treatment followed by phenotypic characterization.

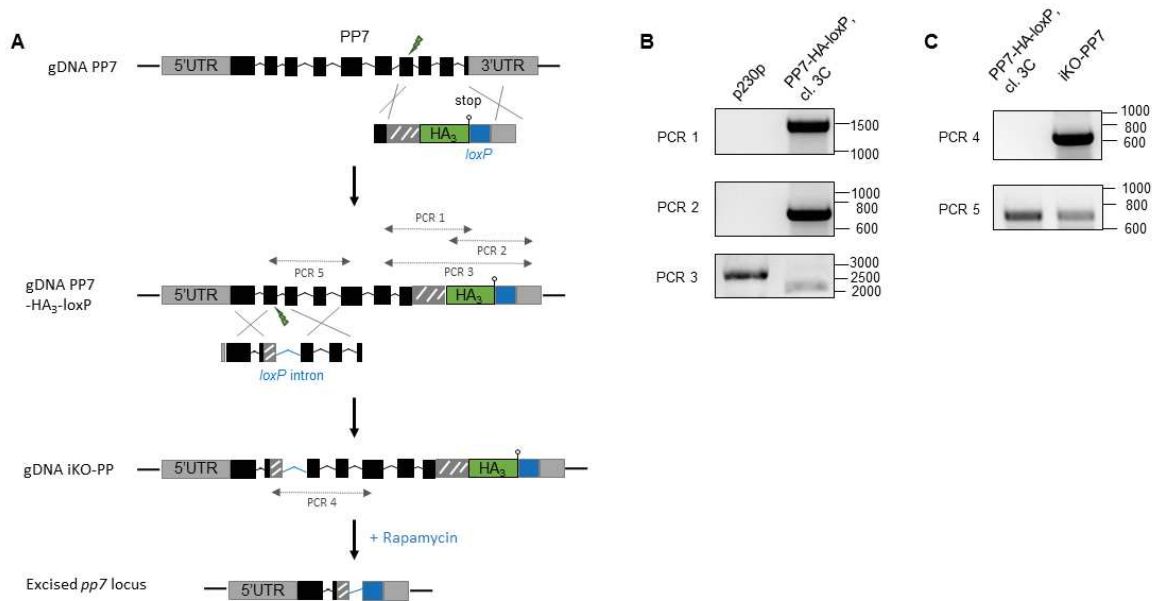


Figure 56: Generating iKO-PP7 parasites by insertion of two loxP sites. (A) Scheme showing the two homologous recombination events leading to iKO-PP7 parasites. The PP7 gene is composed of 16 exons and 15 introns, which are only depicted schematically. The green flash indicates Cas9 cleavage site, and the grey striped boxes are recodoned sequences. (B) PCRs confirming the HA₃-loxP insertion in 3' of pp7 gene. (B) loxPint was inserted substituting for intron 2 of pp7. PCR 4 detected gene edition, but also remaining unedited parasites in the transfectant population (PCR 5). As a next step, single positive clones need to be obtained from these transfectants.

The PP7-HA₃-loxP parasites were used for characterizing PP7 protein localization and expression. A protein of approximately 115 kDa was expressed in the parasites, corresponding to the expected molecular mass for PP7-HA₃ (Figure 57B). Surprisingly, the localization of PP7-HA₃ was different in the glmS and loxP lines: while in the glmS parasites PP7 was exclusively found in the nuclear and perinuclear space (Figure 55A), in the loxP line PP7 demonstrated a partially cytoplasmic soluble and partially dotted, possibly vesicular, pattern (Figure 57A). The localization in the loxP line corresponds to the previously reported cytoplasmic and vesicular localization using antibodies raised against the catalytic domain of PP7²⁸⁹, and is likely the correct localization of the endogenous protein²⁸⁹.

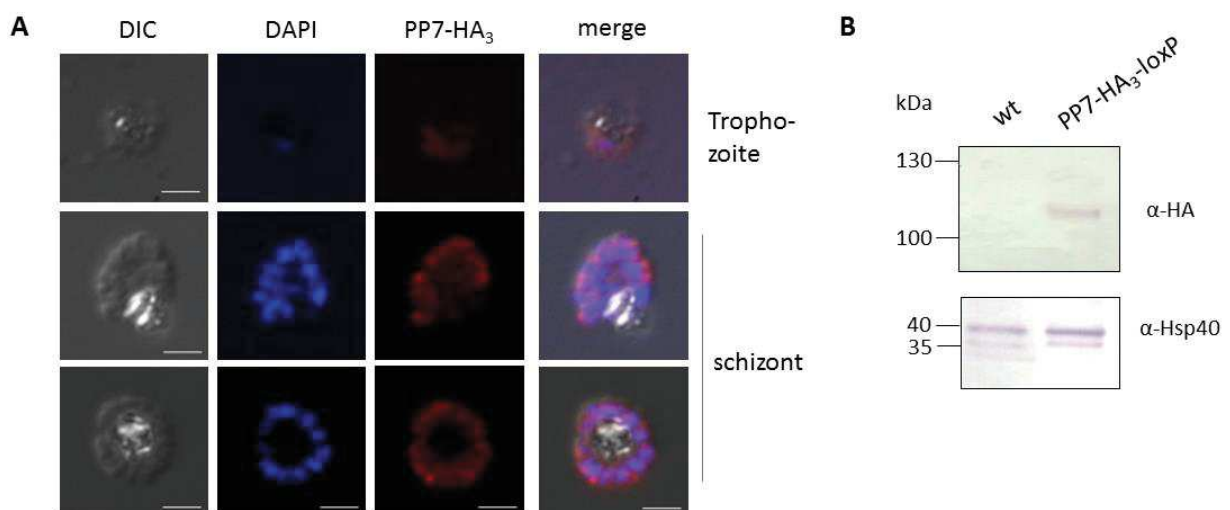


Figure 57: Characterization of PP7 using PP7-HA₃-loxP parasites. (A) The IFAs show PP7-HA₃-loxP, clone 3C parasites at different stages, using anti-HA antibodies. Scale bars, 2 μm. (B) Western Blot of PP7-HA₃-loxP, cl. 3C detects PP7-HA₃ at the expected size of ~116kDa. Hsp40 was checked as loading control.

2.5 Conclusion and perspectives

We aimed at characterizing the function of two putative essential PPs during *P. falciparum* asexual blood stage, namely, PP4 and PP7, for which no study in this parasite is currently available.

We first set up the *glmS* ribozyme strategy, to engineer PP knockdown lines. Although we succeeded in introducing a HA₃-*glmS* sequence at the 3' of the genomic locus for both genes, examination of PP4-*glmS* line revealed that the protein level did not change significantly upon GlcN treatment, preventing further functional characterization. We hypothesize that *glmS* knockdown efficiency is likely gene-dependent, like most of the conditional systems. Indeed, the ribozyme needs to form a correct secondary structure in order to be active in the presence of a metabolite, and possible secondary structures on the pre-mRNA could hinder proper ribozyme folding. As an alternative, we generated PP7 inducible knockout parasites (iKO-PP7) based on the DiCre system. We now need to test whether introduction of the *loxP* sites in PP7 genomic DNA allows for proper gene excision, which will be a prerequisite for understanding PP7 function during the erythrocytic cycle. If such an excision occurs upon rapamycin treatment, we will first monitor the parasites growth by FACS and monitor their morphology at different time points by blood smears. Based on the late expression profile of PP7, we expect a phenotype late in the RBC cycle, i.e. in late schizonts stages that could be linked to schizonts maturation, merozoites egress, motility and/or host cell invasion. According to the phenotype observed, we will monitor individually each of these steps by combining IFAs, egress/invasion assays, video-microscopy and EM. This future work will be the first step in deciphering the function of PP7, the second calcium-regulated PP besides calcineurin.

While engineering conditional knockdown or knockout lines, we achieved to introduce a C-terminal tag into PP4 and PP7. PP4 was very faintly detected by IFA, preventing us to assign a clear subcellular localization of this PP, although it seemed to be mostly cytoplasmic. PP4 orthologues from other organisms have a dual localization, cytoplasmic and nuclear depending on the respective regulatory subunits of the PP4 trimeric holoenzyme^{351,352}. So in future we should optimize the IFA preparation of PP4-HA₃ to better define the localization of *Pf*PP4 at different time points of the erythrocytic cycle, in order to advance in the understanding of this protein for which expression peaks in early schizogony.

Surprisingly, we observed 2 distinct locations for PP7 depending of the parasite line used. In the PP7-*glmS* strain, PP7 was found in the nuclear and perinuclear zone, while in the PP7-HA3-*loxP* line, the protein was cytoplasmic, which corresponds to its previously described location using antibodies²⁸⁹. The real time mRNA transcription and decay profile of PP7 is very peculiar¹⁷⁰, showing that it is mainly regulated by its mRNA stability, and not by transcriptional regulation. In eukaryotes, the mRNAs 3'UTR plays an essential role in the binding of proteins that regulate translation efficiency, as well as RNA stability³⁵³. Therefore, we hypothesize that replacing the endogenous PP7 3'UTR by a *glmS*-PbDT3' led to PP7 dysregulation of its timing of expression that resulted in protein mislocalization. Yet we do not explain how PP7 could be targeted to the nucleus. It is possible that under normal conditions a few amount of the PP shuttles to the nucleus via its interaction with regulators, and that this shuttling was enhanced by its misregulation of expression. In this study, we engineered an iKO-PP7 line that represents the first step towards the elucidation of its function in the malaria parasite *P. falciparum*.

We do not know which functions *Pf*PP7, a very late expressed PP that is activated by Ca²⁺, could have in *Plasmodium*. For PPEF family members in other organisms mostly metazoan-specific functions were described. PPEF expression is restricted to the central nervous system and primary sensory structures in metazoans³⁵⁴. One important PPEF function is illustrated by *Drosophila* PPEF orthologue RdgC

(Retinal degradation C). RdgC was found to act as Rhodopsin PP in the signal transduction via G protein coupled receptor in photoreceptor cells, a role that might be conserved in mammals³⁵⁵.

Among unicellular organisms, PPEF orthologues were described in Kinetoplastida³⁵⁶. Kinetoplastida PPEF proteins were shown to be N-terminally acylated *in vivo*, which likely explains the observed localization of *Leishmania* PPEF to the parasite endomembrane system. Gene disturbance of *Trypanosoma brucei* PPEF using RNA interference resulted in a partial growth defect³⁵⁶, but the exact role of kinetoplastid PPEFs has not been understood yet.

For *PfPP7* no acylation has been reported yet, but using *in silico* tools, two possible palmytoylation sites are predicted^{357,358}. Our and a previous study found a dotted localization in the cytoplasm, which could imply PP7 association to apical merozoite organelles. This possibility and PP7 localization should be further investigated in future.

Chapter 3: Characterization of *PfPP1* phosphatase

3.1 Introduction and Strategy

Among our list of lately expressed PPs was *PfPP1*, the mRNA expression of which already peaks in early schizogony at ca. 34hpi (Figure 58). PP1 is a highly conserved enzyme among eukaryotes, that exerts diverse functions in nuclear events such as transcription, splicing and mitosis, but also participates in glycogen metabolism, protein synthesis and apoptosis¹⁹². Although PP1 catalytic subunit (PP1c) has low substrate specificity *in vitro*, *in vivo* the enzyme is specifically targeted to the correct substrate at the correct subcellular localization and time by means of regulatory partner proteins, so-called PIPs. PP1 can associate with one or two regulatory domains to form a whole array of distinct multimeric PP1 holoenzymes specialized in different functions²⁴⁷.

P. falciparum PP1 has 82% sequence identity with human PP1, and was shown to be an active PP *in vitro*, sensitive to classical PP1 inhibitors (tautomycin, OA, and mammalian I1 and I2)³⁴¹. *PfPP1* was of special interest to us, as the use of its inhibitor, calyculin A (calA) suggested a possible role of this enzyme in egress²⁷⁷. Five PP1 regulatory proteins have been identified so far, being *PfLRR1*, RCC-PIP, eIF2 β , and homologues to eukaryotic I2 and I3, suggesting possible PP1 functions in cell cycle progression^{278,279,325,342,343}. Additionally, 186 new putative PIPs were identified in a screen by Y2H, *in silico* analyses and co-IP. These putative PIPs were predicted to be involved in many cellular functions, such as DNA maintenance (5% of proteins), transcription, RNA metabolism (3%) or translation (6%)²⁸¹. Other eukaryotic PP1 orthologues were shown to possess multiple roles in transcription, DNA processing and mitosis, as reviewed in¹⁹².

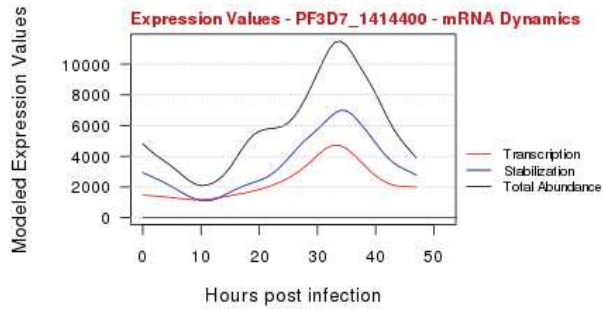


Figure 58: PP1 mRNA abundance as determined by real-time transcription and decay¹⁷⁰

In this chapter, we analyzed the function of *Pf*PP1 in the intraerythrocytic stages by generating an inducible PP1 KO line. PP1 protein was down-regulated at different stages of parasite development, and the resulting phenotype was characterized.

3.2 Article: PP1 has essential functions in *P. falciparum* erythrocytic schizogony and egress

Introduction

Plasmodium falciparum (*P. falciparum*), the etiologic agent of human malaria, is an obligate intracellular Apicomplexan parasite that is still responsible for 445 000 deaths in 2017, mostly children in sub-Saharan Africa⁵. Following its transmission by a mosquito bite, the parasite develops asymptotically in the liver before being released in the blood circulation where it will repeatedly invade red blood cells (RBCs). Within this niche, the parasite multiplies asexually by a process named schizogony to form new invasive forms, the merozoites that, once released from the host cell (egress), will repeat another erythrocytic cycle. All the symptoms of malaria are due to this RBC cycle and therefore these parasite stages have been the focus of most of the studies.

Protein phosphorylation is a conserved mechanism that allows to finely regulate many aspects of proteins, including their stability, activity, or subcellular localization and is involved in varied biological processes. It is regulated by the antagonist actions of kinases and phosphatases. *P. falciparum* is no exception and uses protein phosphorylation to regulate key events of its intracellular life cycle, including schizogony^{169,359}, egress^{99,111,142} and RBCs invasion^{150,155,160}.

Protein phosphorylation probably takes part in controlling parasite schizogony, which consists in repetitive rounds of DNA replication and mitosis, followed by one final cytokinesis step. Several parasite kinases are candidates for regulating this atypical cell cycle^{138,168,169,171,360}. *Plasmodium* encodes homologues to known eukaryotic cell cycle regulating kinases, with six CDK homologues (*pk5*, *pk6*, *crk1*, *crk3*, *crk4*, *mrk*) and additionally Ark and Nek kinases^{78,168}. *Plasmodium* schizogony starts with the duplication of the parasite genome. In eukaryotes, replication starts at origins of DNA replication, which get activated only during S phase, a process regulated by the stepwise assembly and activation of replicative complexes³⁶¹. The action of kinases and several activation factors lead to the assembly of the final replicative complex CMG (Cdc45/MCM2-7/GINS), which initiates DNA replication and is the dynamic platform for the recruitment of DNA polymerases to the advancing replication fork^{77,362}. *Plasmodium* encodes the basic components of this eukaryotic DNA replication machinery,

including MCM 2-7^{80,363}, PCNA³⁶⁴, DNA polymerases³⁶⁵ and ORC components *PfORC1*, *PfORC2* and *PfORC5*^{79,366,367}. Recent studies demonstrate that the *Plasmodium* DNA replication machinery is regulated by phosphorylation: *PfORC1* phosphorylation by PK5 leads to ORC1 dissociation from the DNA and promotes its export to the cytoplasm where it is degraded in late stages of schizogony⁷⁹. Another kinase, *PfCRK4* likely also controls DNA replication¹⁶⁹.

Following the replication of the parasite genome, the chromosomes get segregated in a “closed” mitosis, in which the nuclear envelope stays intact over the whole mitosis. Centriolar plaques (CPs) duplicate, migrate apart and stay anchored to the inner leaflet of the nuclear membrane where they anchor microtubules of the forming nuclear spindle^{89,368}. Then *Plasmodium* mitosis proceeds in the classical phases metaphase, anaphase and telophase, at the end of which the nuclear envelope divides⁸⁴. Phosphorylation might play a role in controlling parasite mitosis. The kinase *PfArk1* is a candidate regulator of chromosome segregation in mitosis, as such a role was reported for its *T. gondii* homologue^{138,174}.

After the segregation of nuclear genomes by mitosis, the last step of schizogony is the formation and budding of daughter cells. The IMC is thought to play key role in cytokinesis, providing a scaffold to which new organelles are trafficked and onto which merozoites are built^{88,89,369}. Phosphorylation events are critical for proper cytokinesis, as the absence of a complex of MRK, Cyclin1 and MAT1 impaired final enclosure on the merozoite basal part, and the merozoite cytoplasm remained connected to the common cytoplasm¹³⁹.

The role of protein phosphorylation for merozoite egress is illustrated by the essentiality of protein kinase G (PKG) and CDPK5 for this process. Apart from kinases, the coordinated action of Ca²⁺ and proteases are required for egress^{95,96,336}. Merozoites egress from the host RBC by first rupturing the parasitophorous vacuole membrane (PVM), and later the RBC membrane (RBCM). PVM rupture requires the secretion of egress-specific apical organelles: SUB1 protease is discharged from exonemes in a PKG-dependent manner^{95,99}, followed by PKG and CDPK5-controlled release of micronemal proteins AMA1 and EBA175 that are deposited on the merozoite surface^{99,111}. RBCM rupture then requires the action of proteases from the serine-rich antigen family, SERA5 and SERA6, that get activated in the PV by SUB1^{96,97}.

While the identification and characterization of *Plasmodium* kinases responsible for all these events have been thoroughly investigated, their counterparts, the phosphatases (PPs), received much less attention. Yet, a genome-wide functional analysis of the rodent malaria model *Plasmodium berghei* (*P. berghei*) phosphatome revealed that half of them might be essential during asexual stages²⁶⁶, and a recent genome-wide transposon mutagenesis study in *P. falciparum* uncovered 21 non-mutable PPs out of 34³²⁹, thus highlighting the crucial role of these enzymes for parasite survival.

The PPP (phosphoprotein phosphatases) family of Serine/Threonine PPs are highly conserved among organisms. In eukaryotic cells, PP1 and PP2A are the major PP activities, comprising 90% of all PP activity, and this holds also true in *P. falciparum*, with PP1 activity reported to be the major Ser/Thr PP in the parasite³⁰⁷. Treatment of *P. falciparum* asexual stages with PP1- and PP2A inhibitors has a strong detrimental effect on blood stage parasitemia, thus suggesting that one or several PPs of the PPP family are likely essential for the completion of the erythrocytic cycle³⁰⁷. *P. falciparum* encodes a conserved PP1 enzyme (*PfPP1*), which was shown to have catalytic activity *in vitro* that can be inhibited by the classical PP1 inhibitors tautomycin, okadaic acid, mammalian I2 and I3³⁰⁸. But besides its biochemical characterization, the role of *PfPP1* for the parasite life cycle has not been revealed so far. Mutagenesis and knockout attempts of PP1 in *P. falciparum* or *P. berghei* failed, suggesting that it is essential for both *Plasmodium* species^{266,329}. To better understand *PfPP1* biological function, one can characterize PP1-interacting proteins, or PIPs, that in mammals are known to act as substrate specifiers,

endogenous inhibitors or targeting subunits. So PIPs are responsible for directing PP1 to the correct substrate at the correct location and timing *in vivo*. PIPs contain consensus PP1 docking motifs allowing their *in silico* prediction. Four *Plasmodium* PIPs were characterized and shown to bind PfPP1 *in vitro*. These include Pf Leucine Rich Repeat 1 (PfLRR1), Pf Inhibitor 2 (Pfl2), Pf Inhibitor 3 (Pfl3) and the β -subunit of eukaryotic translation initiation factor 2 (eIF2 β)^{278,282}. The homology of PfLRR1, Pfl2 and Pfl3 to mammalian PIPs described as mitosis regulators suggests that PfPP1 may also be involved in the same cellular process. Indeed, PfLRR1 and Pfl2 microinjection overcame the G2/M checkpoint in the *Xenopus* oocyte model²⁷⁸, suggesting that like their mammalian homologues, they are involved in the control of the cell cycle, likely *via* their interaction with PP1. *In vitro* Pfl2 and PfLRR1 displayed inhibition of PP1 activity, whereas Pfl3 binding to PP1 increased phosphatase activity^{279,342}. Besides these 4 PIPs, 186 new PIPs were predicted based on a yeast-two-hybrid screen and *in silico* screening, out of which 35 were confirmed to interact *in vitro* with PP1 protein by ELISA²⁸¹. All these putative PIPs still await validation in the parasite.

It was also suggested that PfPP1 takes part in the egress process. Indeed, treatment of schizonts with calyculin A (calA), a well described PP1 and PP2A inhibitor, prevented merozoites re-invasion and led to the accumulation of stalled segmenters²⁷⁷. This phenotype might be related to the phosphorylation status of the Maurer's clefts (MCs) resident protein skeleton-binding protein 1 (SBP1) that would modulate the interaction between MCs and the RBC membrane. In spite of the accumulating evidence that PfPP1 may be essential for parasite survival during *P. falciparum* asexual stages, direct proofs are still missing and its functions are still unresolved.

Here, we have used reverse genetics to study PfPP1 protein expression, subcellular localization and biological function over the erythrocytic cycle. Our results provide for the first time evidence that PfPP1 is an essential enzyme for asexual stages, due to its dual function in parasite multiplication and egress.

Results

Generation of a PP1 inducible knockout line

Previous studies using Ser/Thr inhibitors pointed towards an essential role of PP1³⁰⁷. These results were further corroborated by the likely essentiality of *PP1* gene as direct knockout could not be obtained in Pf and *P. berghei*^{266,329}. Thus, we adopted an inducible knockout strategy based on the Cre/lox system that was recently improved by expressing the dimerizable Cre recombinase (DiCre) in the p230p locus of Pf3D7³⁷⁰. To engineer a floxed *PP1* gene, we first inserted a triple hemagglutinin (HA₃) tag followed by a stop codon and a loxP site at the 3' end of the gene, giving rise to PP1-HA₃-loxP line (Figure 59A-B). We then introduced an artificial loxP intron (loxPint) in place of the native first intron of *PP1* genomic sequence (Figure 59A), leading to the desired floxed *pp1* locus. Two independent clones of the inducible knockout line (iKO-PP1), namely 5E and 9C were obtained. PP1 editions were verified by integrative PCRs (Figure 59C) and sequencing. The proper excision of the loxPint during mRNA maturation was verified by RT-PCR (Suppl Figure 1).

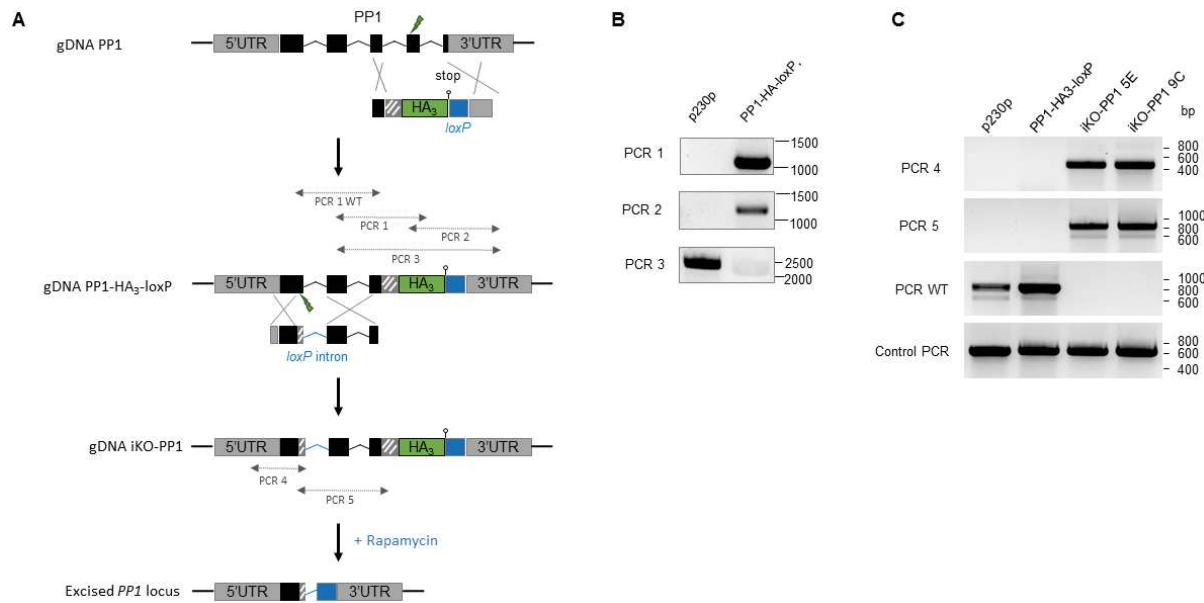


Figure 59 : Generation of the *PfPP1-HA₃* and *iKO-PfPP1* lines. (A) Schematic showing that the two *loxP* sites were introduced in separated transfections and recombination events. The first recombination is the integration of *HA₃-loxP*, which led to the clone 12H that was used for characterizing *PP1* expression. The second recombination exchanged *PfPP1* intron 1 by *loxP*int. (B) Integrative PCRs confirm the successful gene edition leading to *PfPP1-HA₃-loxP* parasites. (C) 5' and 3' integrative PCRs show successful introduction of the *loxP*int site for *PfPP1-iKO* clones 5E and 9C.

***PfPP1* is expressed late and shows a predominantly cytoplasmic localization**

The expression of *PfPP1* phosphatase has been previously analyzed by northern-blot from mixed erythrocytic stages or using a monoclonal antibody against human *PP1*^{277,308,309}. Therefore, to re-analyze *P. falciparum* endogenous *PP1* expression and localization, we took advantage of the *PfPP1-HA₃-loxP* line previously generated. By Western-blot, we show that *PfPP1* protein is expressed from 24 hours post-infection (hpi) but is mostly expressed during schizogony with a peak at 40 hpi (Figure 60A). This pattern of expression is in agreement with the cycling pattern of *PfPP1* mRNA abundance¹⁷⁰, with *PP1* transcript peaking at 34 hpi for decreasing again afterwards. So *PfPP1* protein level follows the curve of mRNA abundance with more or less 6 hours of delay.

Next, *PfPP1* subcellular localization was investigated by immunofluorescence assays (IFA). *PfPP1* was detected in all parasite stages, including merozoites, and shows a pattern mostly distinct from the nuclear DAPI staining, suggestive of a cytoplasmic localization (Figure 60B). Moreover, no colocalization was found with parasite apical organelles such as micronemes and rhoptries (Suppl. Figure 2). Taken together, our results demonstrate that *PfPP1* phosphatase is expressed as a cytoplasmic protein in *P. falciparum* asexual stages, mostly during schizogony.

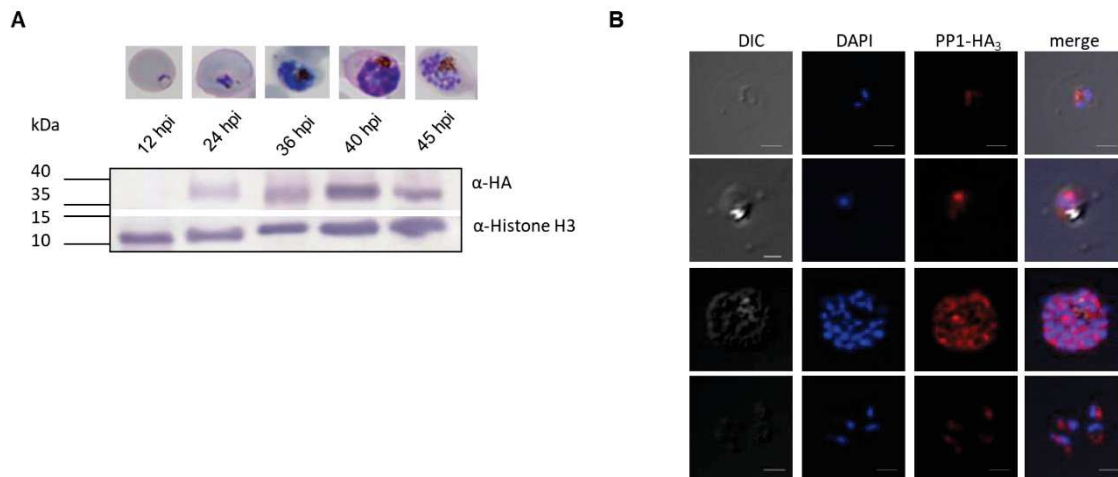


Figure 60 : Characterization of *PfPP1* expression using the HA₃-tagged line. (A) Western-blot of PP1-HA₃ expression over the erythrocytic cycle using anti-HA antibodies. Histone H3 was used as a loading control. (B) Subcellular localization of PP1 as verified by IFA. PP1 is a cytoplasmic soluble protein.

***PfPP1* is essential for erythrocytic schizogony**

Based on *PfPP1* timing of expression described above, we first decided to uncover its role at the onset of schizogony by inducing gene excision at ring stage. For this, parasites were treated with 10nM Rapamycin at 5 hpi. As shown in Figure 61A, 20 hours post-treatment, full length *Pfpp1* locus was amplified in the controls treated with DMSO, while the excised locus was only detected after rapamycin treatment. As a result, *PfPP1* protein was depleted by 90 % as shown by Western-blot (Figure 61B). To assess the phenotypic consequence of *PfPP1* depletion, the parasites were cultured until the next RBC cycle and parasitemia was evaluated by FACS analysis (Figure 61C). We observed a complete block in parasite growth as compared to the control, thus showing for the first time that *PfPP1* is essential for *P. falciparum* to complete the erythrocytic cycle. Scrutinizing the parasites by blood smears indicated that like the control parasites, the rapamycin-treated ones were able to differentiate in mature trophozoites of 30 hpi and to begin their multiplication by schizogony as evidenced by the presence of several nuclei at 38 hpi (Figure 61D). However, they were unable to form mature schizonts containing new invasive daughter cells and instead formed degenerate schizonts at 45 hpi while 90% of the control parasites had already re-invaded new RBCs. This block during schizogony was reflected by a decrease in the parasite mean DNA content that was already detectable at 38 hpi and became more prominent at 45 hpi when compared to the DNA content of the remaining segmenters in the control cultures. This observation was reflected in the DNA quantification we performed for each condition to determine at which time point schizogony started to be affected (Figure 61E). In the DMSO-treated cultures, the parasites displayed a DNA content that evolved from 3-7N at 30 hpi, to mainly 3-7N and 8-16N at 38 hpi, and dropped to 1N at 45 hpi following re-invasion. In contrast, *PfPP1* depletion led to a majority of parasites harbouring primarily 3-7N at 38 hpi and a mix of 3-7N and 8-16N at 45 hpi, reflecting the schizogony arrest (Figure 61F).

Altogether, our results clearly demonstrate an essential role of *PfPP1* phosphatase during *P. falciparum* asexual multiplication by schizogony.

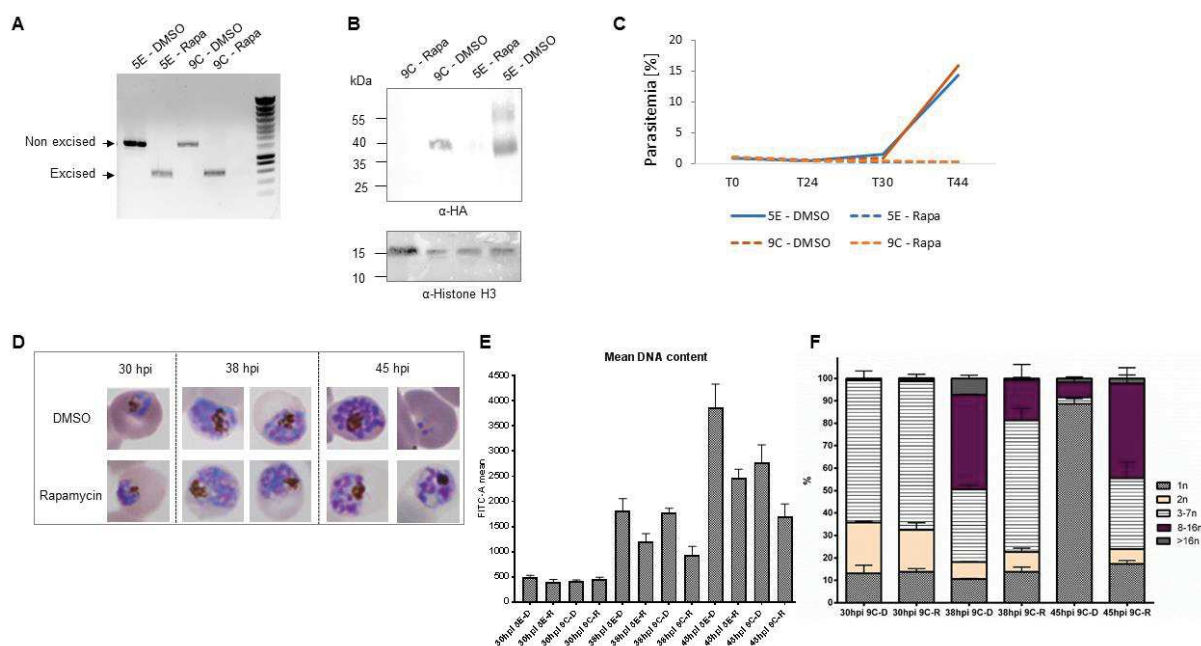


Figure 61: Conditional PP1 knockout at ring stage reveals PfPP1 function in schizogony. (A) Rapamycin induces DiCre activation. Complete excision of the PfPP1 locus was detected at 24h post treatment. (B) Rapamycin treatment in rings leads to 90% PfPP1 protein depletion by 38hpi, as verified by Western Blot. Histone H3 is used as loading control. (C) PfPP1-depleted parasites do not re-invade. The parasitemia were measured by FACS. (D) Giemsa blood smears of representative Rapa- or DMSO-treated PfPP1-iKO parasites. (E) DNA content of the PfPP1-iKO parasites was quantified by flow cytometry. The mean FITC-A value representing the mean DNA content of the whole parasite population for every time point and condition is depicted here. Samples were taken at 30hpi, 38hpi and 45hpi, for both PfPP1-iKO strains 5E and 9C. (F) FACS data were gated, assigning every range of FITC-A to a number of nuclei, as confirmed by Giemsa smears. Exemplarily, measurements of clone 9C are shown, but the same results were found for clone 5E.

PfPP1 depletion in trophozoite stage prevents the next re-invasion step while allowing proper schizont maturation

Our previous work suggested that PfPP1 might be involved in egress, as increasing concentrations of calyculin A (calA), a well characterized Ser/Thr phosphatase inhibitor of PP1 and PP2A activities, induced an increase in the number of stalled schizonts and concomitantly a reduced number of re-invaded ring stages²⁷⁷. To assess the possible contribution of PfPP1 in egress, we treated the iKO-PfPP1 parasites with rapamycin at 30 hpi. As shown by Western-blot, the treatment induced 90% of PfPP1 protein depletion by 44 hpi, allowing us to determine the enzyme contribution later during the erythrocytic cycle (Figure 62A). PfPP1 depletion led to a complete block in RBCs re-invasion in the next cycle as determined by FACS, while the control parasites showed a 6 fold increase in parasitemia (Figure 62B). Analysis of the parasites by blood smears indicated that iKO-PfPP1 parasites depleted of PP1 were blocked in late schizont stage, in contrast to DMSO treated parasites that were in ring stage (Figure 62C).

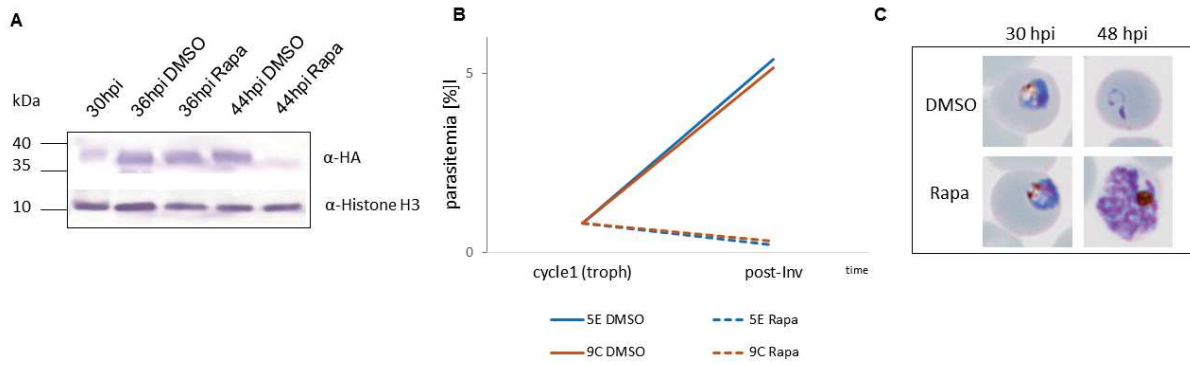


Figure 62: Rapamycin treatment at 30hpi allows for normal schizont maturation, but prevents egress. (A) PfPP1 protein depletion following Rapamycin treatment at 30hpi, exemplarily shown for PfPP1-iKO cl. 5E. At 36hpi, PfPP1 protein is still present in almost normal amounts, but gets almost completely depleted until 44hpi. (B) Giemsa smears show that Rapamycin-treated PfPP1-iKO trophozoites mature normally till segmented schizont stage, but do not re-invade. (C) FACS measurement of the parasitaemia at 30hpi and 50hpi shows that Rapa-treated PfPP1-iKO parasites do not re-invade. P230P is the DiCre expressing 3D7 wt strain, and serves as control together with PfPP1-HA₃-loxP cl. 12H. 12H is the parental strain of the PfPP1-iKO clones.

Parasites multiplication by schizogony consists of multiple and asynchronous nuclear multiplication and mitosis that end up by merozoites individualization known as segmentation or budding. To determine whether the iKO-PfPP1 stalled schizonts were able to bud, we performed IFA using anti-MTIP and anti-MSP1 antibodies to visualize the IMC and the parasite plasma membrane respectively. The inner membrane complex (IMC) consists of flat vesicles underlying the merozoite plasma membrane and is rebuilt in the daughter cells at the end of schizogony, while MSP1 is one of the major merozoite protein displayed at the parasite surface. In both DMSO and rapamycin treated parasites, we observed the formation of the IMC and plasma membrane around each daughter cell, thus demonstrating that depletion of PfPP1 does not impact on merozoite budding (Figure 63A and B, Suppl. Figure 3).

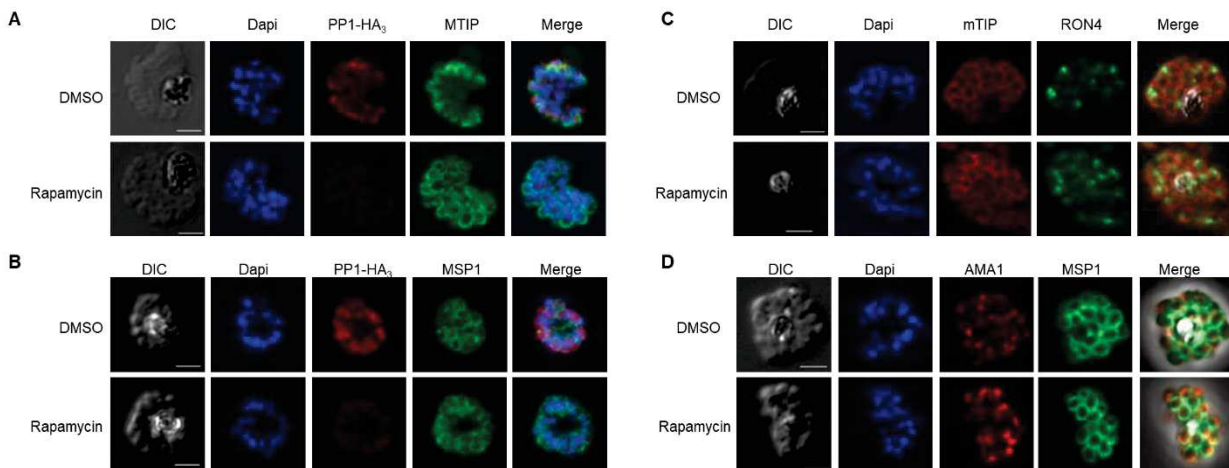


Figure 63: Normal parasite segmentation and secretory organelle synthesis following PfPP1 depletion. iKO-PfPP1 parasites were treated with Rapamycin/DMSO at 30hpi. Schizonts of 42hpi were allowed to mature until segmentation for 4h in C2, followed by a wash, before the iRBCs were smeared for IFAs. (A) and (B) Schizont segmentation was checked using anti-MTIP and anti-MSP1 antibodies. (C) and (D) The biosynthesis and location of roptries and micronemes was checked by the detection of their respective markers RON4 and AMA1 using specific antibodies.

Furthermore we did not observe any defect in the biogenesis of apical secretory organelles in the nascent merozoites (Figure 63C and D). Taken together, our data suggest that PfPP1 depletion does not prevent merozoites segmentation or *de novo* apical organelles synthesis, thereby suggesting that schizonts are blocked in a step downstream of these events, which likely corresponds to egress.

PfPP1 is essential for merozoites egress from the RBC

Merozoites egress from the RBCs is a tightly orchestrated process leading to the rupture of both the PV and the host cell membranes. Following PVM poration by an unknown mechanism³⁷¹, specific organelles named exonemes are discharged in a PKG-dependent manner to notably release the protease SUB1 in the PV where it will process its substrates, among which the SERAs protease family⁹⁹. Subsequently, micronemes are secreted as exemplified by the merozoite surface relocation of AMA1 or EBA175, this discharge being PKG- and CDPK5-dependent^{99,111}. To understand at which step egress was blocked, we first assessed for SUB1 secretion. For this, parasites were tightly synchronized in a 2 hours window. At 42 hpi, they were treated with Compound 2 (C2) for 4 hours to let them mature, released from this inhibition by washes to allow for exoneme secretion, and treated for 2 hours with E64 to prevent RBCM rupture¹⁰⁸. The iKO-PP1 parasites treated with DMSO or rapamycin were then stained with anti-SUB1 antibodies. When stored in exonemes, SUB1 gives a strong dotted pattern, while the fluorescence becomes weak and diffuse following exocytosis⁹⁹. Our preliminary data show that in the time of this experiment, 60% of the control parasites had undergone SUB1 secretion while 40% still retained the protein in exonemes. In sharp contrast, 95% of the iKO-PP1 treated rapamycin had an exonemal pattern, suggesting that *PfPP1*-depleted parasites are unable to secrete exonemes (Figure 64A). We next checked for micronemal secretion as a downstream event following exonemal release. Late schizonts were allowed first to mature for 4h in C2, followed by 2h of further maturation in E64, and were used for IFAs using anti-AMA1 antibodies. In the DMSO-treated control, up to 40 % of schizonts had undergone AMA1 secretion during the course of the experiment (Figure 64B). In the rapamycin-treated parasites however, AMA1 displayed an exclusively micronemal localization, suggesting that PP1 depleted parasites are deficient in microneme secretion.

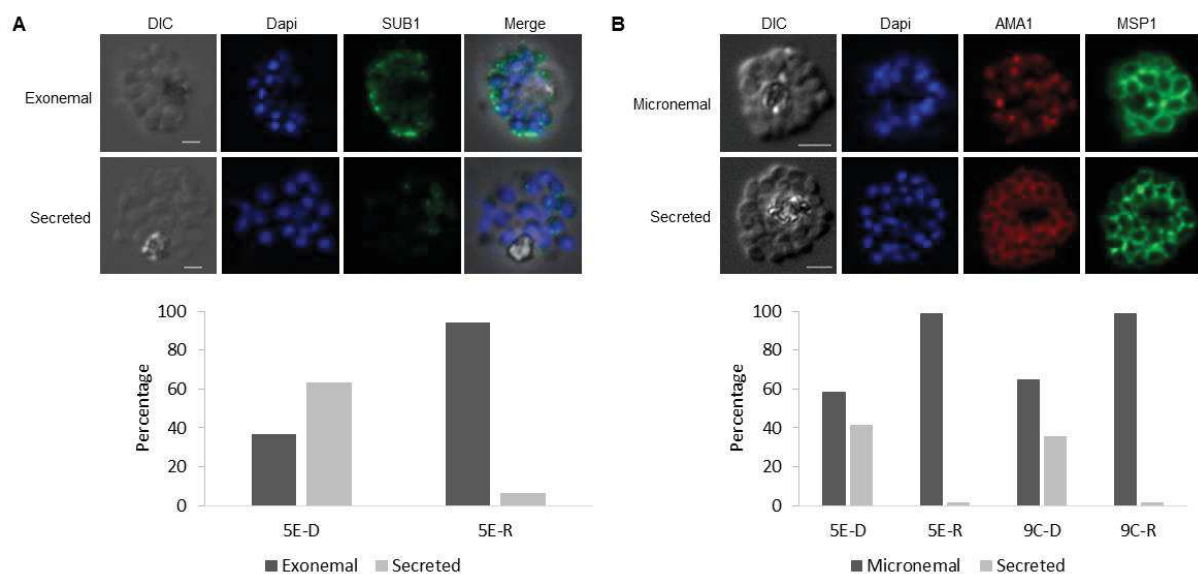


Figure 64: Induced *PfPP1* knockout prevents exoneme and microneme secretion prior to egress. (A) SUB1 secretion from exonemes was assayed in iKO-*PfPP1* parasites. Following Rapamycin/DMSO treatment at 30hpi, 42hpi schizonts were matured in C2 for 4h, following by two washes and 2hrs of E64 treatment. The IFAs show exemplary parasites where SUB1 is exonemal, or secreted. The panel below presents the quantification of SUB1 secretion in both DMSO and Rapamycin-treated iKO-*PfPP1* strain 5E. (B) IFAs showing the dotted staining of micronemal AMA1. AMA1 secretion leads to its deposition on the surface of the intracellular daughter merozoites. The graph below depicts the percentage of micronemal versus secreted AMA1 staining in *PfPP1*-iKO clones 5E and 9C, treated with DMSO (D) or Rapamycin (R) at 30hpi. 42hpi schizonts were matured in C2 for 4h, following by two washes and 1.4h of E64 treatment. At the end of this incubation, smears were made for IFAs and counted for every condition and strain.

Collectively, our results demonstrate that PP1 depletion late in schizogony (44 hpi) induces a drastic block in egress, likely due to a severe defect in exoneme and microneme secretion.

Discussion

PP1-like enzymatic activity has been described 20 years ago as the major phosphatase activity in the parasite *P. falciparum*³⁰⁷, but the refractoriness of the gene for genetic deletion has prevented further functional studies^{266,293,329}. This work provides for the first time a detailed characterization of the role of PP1 phosphatase during the asexual blood cycle. Using the conditional DiCre system, we generated an inducible PP1 knockout that revealed two essential functions of this enzyme, the first during the course of schizogony and the second for merozoites egress.

By tagging the endogenous PP1 locus, we followed PP1 expression by Western-blot, and showed that it increased from rings to schizonts (24 hpi to 40 hpi), and decreased in late schizont stage (45 hpi) (Figure 60A). We took advantage of this timing of expression to induce PP1 gene deletion before the start of its biosynthesis, i.e. early ring stage, with the idea that we may thereby achieve a complete protein depletion. By doing so, we observed a complete block in parasite growth associated to a severe defect in schizogony, evidenced by the presence of arrested schizonts in the culture by blood smears (Figure 61D), and supported by the decrease in the parasite DNA content following PP1 depletion. The schizogonic cell cycle of *Plasmodium* is atypical compared to the classical view of eukaryotic cell cycle. It consists of multiple and asynchronous rounds of S-M phases without cytokinesis, resulting in the formation of a syncytial schizont. Therefore, the observed impairment in schizogony could reflect a defect in DNA replication, segregation or both.

In yeast and mammals, it is well documented that PP1 takes part in the DNA replication process. For instance, the ORC complex binds the origin of replication in early G1 to initiate a new DNA replication cycle and disassociates from the chromatin in S phase by CDK-dependent phosphorylation^{372–374}. Dephosphorylation of ORC2 by the phosphatase PP1 has been shown to promote the re-association of ORC to DNA and therefore to initiate the next round of replication^{374,375}. ORC2 can directly interact with PP1 via a conserved KSVSF motif. In *P. falciparum*, a putative ORC2 homologue is found in the genome (PF3D7_0705300) showing 36% and 42% homology with the yeast and human ORC2 respectively³⁷⁶. Interestingly, *PfORC2* is reported to be phosphorylated by global phosphoproteomic studies^{121,130,136,137}, and has also been identified as a putative substrate of the cyclin-related kinase CRK4¹⁶⁹. As CRK4 conditional depletion induces a block in nuclear division, it is possible that in *P. falciparum* as well, initiation of replication may rely partly on the phosphorylation status of the ORC helicase¹⁶⁹. Consistent with this idea, it has been shown that the nucleo-cytoplasmic translocation and DNA binding activity of another subunit of the ORC complex, *PfORC1*, was regulated by phosphorylation, likely by the CDK-like kinase *PfPK5*⁷⁹. So far, the identity of the phosphatase(s) involved in the balance of ORC phosphorylation is unknown. *PfORC2* has not been identified as a PP1 interacting protein neither by yeast-two-hybrid nor by *in silico* analysis²⁸¹. Therefore, whether PP1 plays a role in the control of S phase via the ORC complex regulation remains to be determined.

Another mechanism associated to DNA replication and regulated by PP1 in mammals is the activation of the MCM helicase complex. The pre-replicative complex (pre-RC) comprising the ORC, Cdt1, Cdc6 and the MCM proteins is activated through the recruitment of 2 additional initiation factors, namely Cdc45 and the GINS complex⁷⁷. This recruitment takes place via the concerted action of CDK and DDK to form the pre-initiation complex and leads to the formation of an active helicase that can unwind the DNA to establish the replication fork. In this model, PP1 counterbalances DDK-dependent phosphorylation of MCM4, thereby preventing the activation of the pre-RC and blocking the initiation of replication^{377–380}. According to this model, PP1 depletion in *P. falciparum* would result in a premature entry of the parasite into S phase, which does not correspond to the observed phenotype. However, the lack of clear homologues of Cdc45, GINS complex, CDK and DDK in *Plasmodium* likely points toward

a different mechanism for MCM helicase regulation, if such a regulation exists in the parasite. It is noteworthy that MCM2 and MCM4 proteins are indeed subject to post-translational modifications by phosphorylation in *P. falciparum* (plasmoDB), and that their phosphorylation status is modulated by CRK4 activity¹⁶⁹.

Apart from a direct role of PP1 in DNA replication, we cannot exclude that the defect in DNA replication following PP1 depletion may also arise from chromosomes mis-segregation leading to cell cycle arrest. In mammalian cells, PP1 is a well described regulator of mitosis progression and mitotic exit (for review see ¹⁹²), and in particular, its role in chromosome segregation has been well documented. To ensure faithful chromosome segregation, attachment of kinetochores to the opposite sides of the mitotic spindle is regulated by the opposing activities of Aurora B kinase and PP1 phosphatase. To fulfill this function, PP1 is regulated by its interaction with endogenous PIPs, in particular Inhibitor-2 (I2), Inhibitor-3 (I3) and Sds22 (also named PP1R7)^{316,381,382}. Interestingly, these 3 PIPs are conserved in *P. falciparum*, with Sds22 being named LRR1 because of the presence of a leucine rich repeat in the protein. They were shown to bind PP1 *in vitro* and to modulate its activity upon binding via a conserved RVxF motif^{278,279,342}. Importantly, all of them were refractory to genetic deletion suggesting that their function, in relation to PP1 modulation, might be essential for the parasite. Therefore, the conservation of PIPs involved in chromosome segregation suggests that at least part of the mammalian PP1 functions might be conserved in the malaria parasite during mitosis.

In light of its presumptive functions in the nucleus, it is puzzling that we did not find PP1 in this compartment by IFA (Figure 60A). Besides, previous subcellular fractionation experiments reported the presence of the enzyme in both parasite cytoplasm and nucleus²⁷⁸. There are several reasons that may explain this discrepancy: first, only a few amount of protein may undergo this nucleo-cytoplasmic shuttling, and second this transport might be cell-cycle regulated. Given the asynchronous nature of nuclear division, only a subset of nuclei would thus contain PP1, making it difficult to visualize. Our next goal will be to understand better the schizogony defect of the iKO-PP1 parasites, but discriminating between impairment in DNA replication and mitosis poses technical challenges in the malaria parasite because of (i) the size of the cell and consequently of the nuclei, (ii) the scarcity in the number of *P. falciparum* cell cycle markers and (iii) the asynchronous nature of schizogony. To gain further insight in the cellular mechanisms affected during schizogony, we plan to analyze the cell cycle of the iKO-PP1 parasites by IFA using available markers (anti-tubulin, anti-centrin), by EM to look at the ultrastructure of the arrested schizonts, and by co-immunoprecipitation studies to identify PP1 regulators and substrates that may be involved in these events.

Importantly, by depleting PP1 later during the erythrocytic cycle, we were also able to point out a critical function of this phosphatase during the egress step. This result is supported by the absence of re-invasion of the iKO-PP1 parasites and the concomitant accumulation of segmenters in the culture (Figure 62B and C).

The discharge of the exonemal protein SUB1 in the PV is the first molecular event described in the multistep process of merozoites release, shortly followed by micronemes secretion^{95,111}. Our preliminary data suggest that PP1-depleted parasites are strongly affected in their capacity to secrete both exonemes and AMA1-containing micronemes (Figure 64), which would explain the observed egress defect. To confirm that the main deficiency of PP1-depleted parasites relates to exonemal release, we will monitor by WB the SUB1-dependent processing of some of its substrates, i.e. MSP1 and SERA6. Moreover, we will check for PVM integrity (i) by using an ectocopy EXP1-mCherry reporter as a marker for PVM⁹⁶ and (ii) by looking at the ultrastructure of the egress-blocked schizonts by EM. We expect to observe an intact PVM in the parasites, as SUB1 discharge occurs prior to PVM fragmentation. It is striking that the phenotype observed upon PP1 depletion is reminiscent of the one observed when parasites are treated with PKG inhibitors¹⁰³. PKG is the first enzyme in the egress

signaling known to date, and its activity is necessary for both exoneme and microneme secretion⁹⁹. It is therefore tempting to speculate that PKG and PP1 might coordinate the same signaling pathways by a fine balance of (de)phosphorylation events. Unfortunately, despite the identification of some of PKG-cellular targets³⁸³, the question remains open as to how PKG activity triggers organelles secretion. Another possibility would be that PP1 acts upstream of PKG signaling. Two events have been reported to occur prior to PKG activation: PVM rounding, which is followed by PVM poration. The first morphological change in egress is when the irregularly shaped PVM rounds up, as was shown by video microscopy. This rounding up is dependent on intracellular Ca^{2+} , but the exact mechanisms leading the membrane rounding have not been elucidated yet⁹⁸. The rounding is followed by PVM poration that has been revealed by electron tomography³⁷¹, but the effector molecules underlying this step are currently unknown. Future experiments will help to define if PP1 is involved in PVM rounding. For this, the morphology of the iKO-PP1 segmenters blocked in egress should be scrutinized more in detail using soluble PV and PVM markers in order to see if rounding happens in the iKO-PP1. Furthermore, an experiment should be performed for treating iKO-PP1 parasites with a Ca^{2+} ionophore, to verify if an increased Ca^{2+} level could maybe overcome the egress block in the iKO-PP1.

In the same line, we also intent to verify if the defect in egress of the iKO-PP1 can be phenocopied by calA treatment of wt parasites. Since calA is a PP1- and PP2A inhibitor, it is highly interesting to specify in which step of egress calA-inhibited parasites are blocked in order to understand PP function in egress. Furthermore we intend to edit the PP1 genomic locus by introducing a single point mutation (Y270F) reported in mammals to render the enzyme less sensitive to the inhibitor while retaining most of its activity²⁰⁸. This edition could result in parasites resistant to calA. If the Y270F mutation renders *Pf*PP1 less sensitive to calA, the PP1_{Y270F}- strain would be a very useful tool to determine if *Pf*PP1 is involved in egress.

This work unraveled for the first time pleiotropic functions of PP1 phosphatase from the malaria parasite. The characterization at the molecular level of *P. falciparum* schizogony and egress is key to the better understanding of the red blood cell cycle. Therefore it will become crucial to define PP1 interactome for each of these events to describe the fine interplay between kinases and phosphatases as a major regulator of *P. falciparum* life cycle.

Experimental procedures

Molecular biology

The primers used in this work are listed in Table 6. All The PCR amplifications were obtained using the Q5 DNA polymerase (NEB) and verified by sequencing (Eurofins).

To generate the pLN-PP1-HA₃-loxP vector, we cloned the *PP1* homology regions (HR) into a pLN plasmid carrying a Blasticidin (Bsd) resistance cassette. Since our initial strategy was to generate PP1-HA₃-glmS regulatable parasites, we first generated a pLN-PP1-*glmS* vector containing the *pp1* HRs. In this plasmid, *pp1* HR1 was produced by overlapping PCR and cloned XmaI/AfeI: the first fragment amplified using MLa118 and MLa119 corresponds to exon 3 and the second to a recodonized region encompassing exons 4 and 5 and amplified with MLa120 and MLa121. HR2 representing the 440bp fragment of the 3'UTR directly downstream of the stop codon was amplified with MLa178 and MLa179 and cloned into the vector using PstI and HpaI restriction sites. As we did not obtain PP1-HA₃-glmS edited parasites, and the glmS strategy was little efficient for PP4, we adopted the DiCre strategy for PP1, and replaced the glmS-PbDT3' cassette by a synthetic HA₃-loxP cassette (synthesized by idtdna) by InFusion (Clontech) cloning. This gave rise to pLN-PP1-HA₃-loxP.

For generating the pLN-*loxPint*-PP1 vector, HR1 was designed as an overlapping PCR, with the first PCR fragment amplified using MLa264 and MLa265 and corresponding to *PP1* 5'UTR and exon 1, and the second fragment to a synthetic DNA fragment containing the recodonized 3' part of *PP1* exon1 followed by a *loxPint* artificial intron sequence³⁵⁰, and amplified with primers MLa268 and MLa269. HR2 corresponding to the 3' UTR was amplified using MLa266 and MLa267. Both HRs were cloned by a single InFusion reaction in *Xma*I/*Pst*I.

The gRNAs were cloned in *Bbs*I into the pDC2-cam-co-Cas9-U62-hDHFR vector provided by Marcus Lee.

For introducing the Y270F single point mutation into PP1, a pLN-PP1-Y270F-HA₃-*loxP* vector was generated in which the TAT codon was mutated to TTT. pLN-PP1-HA₃-*loxP* vector was used as template for site-directed mutagenesis PCR using MLa304 and MLa305 and the Quik change lightning Multi-site-directed mutagenesis kit (Agilent).

Table 6: Primers used for cloning. Listed in (chronological) order of usage, as described in the methods. F- forward, R-reverse

Primer name	Amplicon F (forward), R (reverse)	5' → 3' sequence
	HA ₃ - <i>loxP</i> cloning	
MLa 118	PP1 HR1 genomic part (F)	ctgCCCGGGGATTATGTGGATAGAGGAAAACAAAG
MLa 119	PP1 HR1 genomic part (R)	CTGATGTGCCTGCATATTAATC
MLa 120	PP1 HR1 recodonized part (F)	ATATGCAGGGCACATCAGG
MLa 121	PP1 HR1 recodonized part (R)	tgtAGCGCTATTGGCCGCTTTCTTTTTTC
MLa 178	PP1 HR2 (F)	cgcCTGCAGTATATTACAAACTTAGGATCCTAATATATTAAT TG
MLa 179	PP1 HR2 (R)	ctgGTTAACGAAAAATACTACTTTTATAGATAATATTTGTTTTG TTC
MLa 206	gRNA HA ₃ - <i>loxP</i> (F)	TATTGTCAACACTCATCATTGCAC
MLa 207	gRNA HA ₃ - <i>loxP</i> (R)	AAACGTGCAATGATGAGTGTTGAC
MLa 187	check 5' integration of HA ₃ - <i>loxP</i> (F)	CATGGACAGTTTTATGATTTGTTAAGG
MLa 188	check 3' integration of HA ₃ - <i>loxP</i> (R)	GAAATATATGGCTAAATTAATATAAATAGC
MLa 244	InFusion cloning of HA ₃ - <i>loxP</i> into pLN (F)	AGAAAGCGCCAATAGCTACCCGTACGACGTCC
MLa 245	InFusion cloning of HA ₃ - <i>loxP</i> into pLN (R)	CCTAAGTTTTGTAATATACTTAATAAATTCGTATAATGT ATGC
	<i>loxPint</i> cloning	
MLa 268	Recodon- <i>loxPint</i> (F)	GAATATGGTGGATTTCCACCAG
MLa 269	Recodon- <i>loxPint</i> (R)	CTCTATCCACATAATCACCTAAAAG
MLa 264	HR1 (F)	CTCAAGCTTGGGGGGATCCATATCAAATAAAATAAATTCATT CTC
MLa 265	HR1 (R)	TGGAAATCCACCATATTCAAATAAC
MLa 266	HR2 (F)	GTGATTATGTGGATAGAGGAAAACAAAG
MLa 267	HR2 (R)	GAATTAGCTAAGCATGCGCTCGATCATTTTCTCCCCACC
MLa 287	gRNA <i>loxPint</i> (F)	TATTAATAATAGATAATTTGCATC
MLa 288	gRNA <i>loxPint</i> (R)	AAACGATGCAAATTATCTATTTTT

	Check DiCre-mediated PP1 excision	
MLa 187	F	CATGGACAGTTTTATGATTTGTTAAGG
MLa 179	R	ctgGTTAACGAAAAATACTACTTTTATAGATAATATTTGTTTTG TTC
	Y270F mutagenesis	
MLa 304	Mutagenesis Y270F PP1 (F)	AGCGCCCCTAATTTTTGTGGTGAATTTGATAATGC
MLa 305	Mutagenesis Y270F PP1 (R)	GCATTATCAAATTCACCACAAAAATTAGGGGCGCT

Parasite culture, transfection and synchronization

For transfections, 60 to 80 µg of each plasmid were transfected into 5-10% young ring stage parasites, and parasites were kept in agitation. Transgenic parasites were selected for in presence of 2.5 nM WR99210 and 2.5 µg/ml Bsd. For *PP1* gene excision, rapamycin was used from LC Laboratories (Cat.-No. R-5000). Stocks were stored in DMSO (10 mM) at -20°C and used at a final concentration of 10 nM for 4h, and then washed away. Gene excision was confirmed by PCR amplification, using primers MLa187 and MLa179. For the timely synchronization of parasite populations, late schizonts were selectively recovered on cushions of 70% (v/v) Percoll adjusted to isotonicity³⁸⁴. These late schizonts were allowed to invade for a certain time-frame, followed by the selection for ring stages using 5% sorbitol³⁸⁵.

For experiments that required a high number of synchronous segmented schizonts, 40 – 42 hpi schizonts were treated for up to 5h with 1.5 µM of C2, followed by two washes. To permit PVM rupture, but prevent final merozoite egress, the c2-treated and washed segmenters were treated for up to 2h with 50 µM of E64.

Flow cytometry

Flow cytometry was used both to determine parasitemia in growth assays, as well as to determine the DNA content during schizogony. Infected erythrocytes were fixed in 4% paraformaldehyde (PAF) for 4h at room temperature, and then stored at 4°C. Cells were washed twice in phosphate buffered saline (PBS), and stained with 1X SYBR green (Invitrogen) for 30min, followed by one wash in PBS. Fluorescence was measured with a BD FACS Canto I cytometer, and analyzed with BD FACS Diva software. For the exact determination of DNA content, a very tightly synchronized parasite population at different maturation stages was used as control FACS samples.

Immunoblot and Immunofluorescence Assays

Immuno-fluorescence assays (IFAs) were performed on smears of infected RBCs. The smears were fixed with 4% PAF for 20min, followed by 5min of neutralization with 0.1M glycine/PBS. Cells were permeabilized with 0.2% Triton/PBS for 20min, and incubated for 20min with 2% bovine serum albumin (BSA) to block unspecific binding. Primary antibody incubation ensued for 1h at RT, with either rat α-HA (1:1000, Roche Diagnostics), rabbit α-MTIP (1:500, gift from Tony Holder), mouse α-MSP1.19 (1:1000, gift from M. Blackman), mouse α-RON4 (1:200,), α-SUB1 (1:2, gift from M. Blackman) and rabbit α-SERA6 (1:1000, gift from M. Blackman), rabbit α-AMA1 (1:1000). Primary antibodies were detected using Alexa-488 or Alexa-594-coupled secondary antibodies. Cells were stained with Hoechst for 5min, and mounted using Immumount (Thermo Scientific) solution. Images were taken using Zeiss Axioimager Z2 and processed using Zen blue edition (Zeiss) software.

Immunoblot samples were prepared by lysing the RBCs using 0.01% Saponin in PBS and protease inhibitors (cOmplete™ EDTA-free Protease Inhibitor Cocktail, Sigma) for 5min. Following washes, parasite DNA was digested by Benzonase (EDM Millipore 70746-3) and parasites were lysed in Laemmli sample buffer with DTT. Minimum 5×10^6 parasites per sample were loaded in a 12% SDS PAGE and proteins separated in gel were blotted onto a nitrocellulose membrane. Proteins were detected using primary antibodies α -HA (1:1000) and α -histone H3 (1:15 000, Abcam), and alkaline phosphatase-conjugated secondary antibodies (Promega).

Supplementary Data

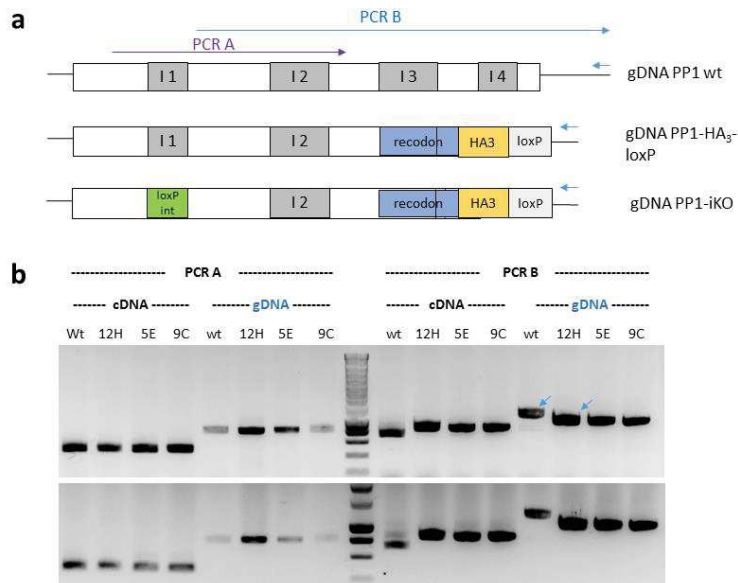


Figure S1: The proper excision of the *loxPint* during mRNA maturation was verified by RT-PCR => The spliceosome recognizes the intron-exon boundaries of *loxPint*

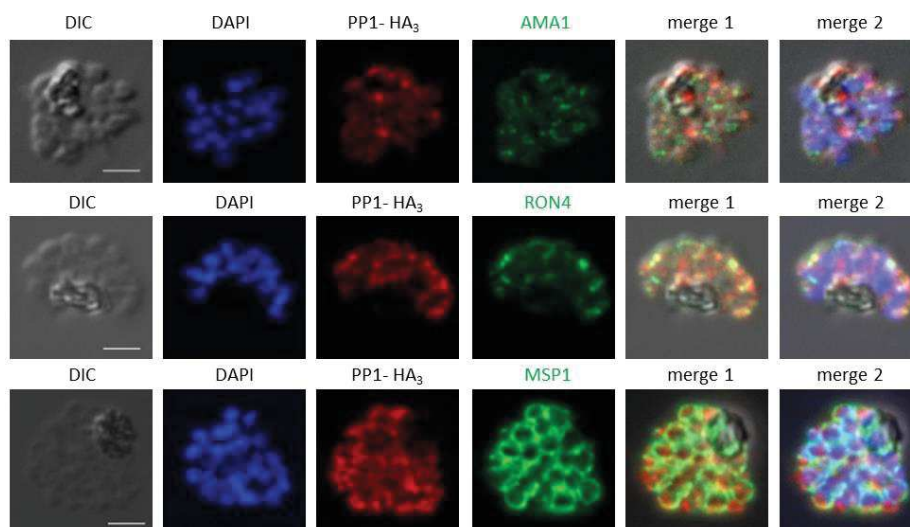


Figure S2: Subcellular localization of PP1: PP1 does not localize to micronemes and rhoptries. IFAs were made using rhoptry marker RON4 and micronemal protein AMA1, showing no colocalization of PP1-HA₃ with these organelles. MSP1 stains the merozoite surface.

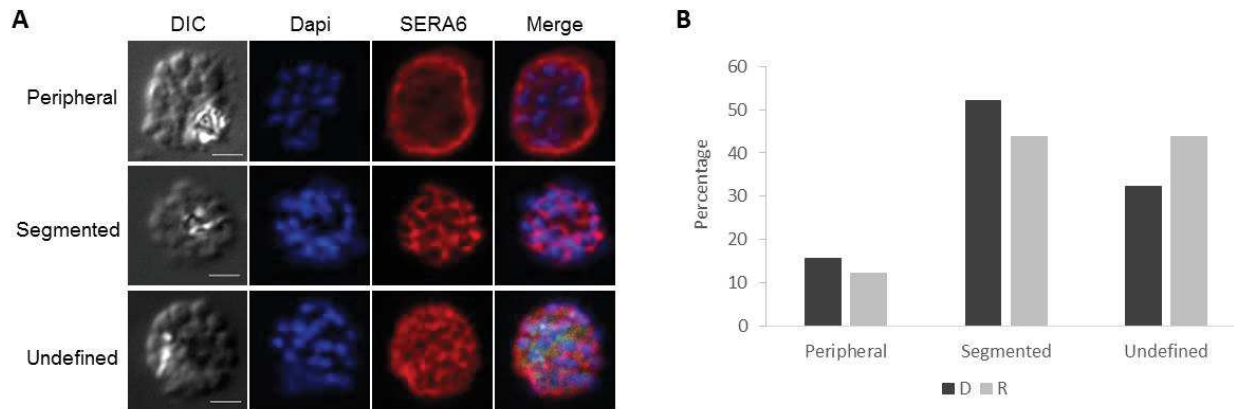


Figure S3: PP1 depletion in schizont stage does not affect segmentation. After Rapa treatment at 30hpi, at 42hpi schizonts were matured in C2 for 4h. (A) IFAs to check segmentation with the PV soluble protein SERA6. (B) Quantification of patterns of SERA6 staining observed from (A)

3.3 Conclusions and perspectives

In this work we demonstrate for the first time a dual function of *P. falciparum* PP1 phosphatase in schizogony as well as in egress.

Depletion of *PfPP1* in early ring stage results in a schizogony defect evidenced by a delay and halt of DNA replication, while protein depletion in late schizonts induces a block of merozoites egress from the RBC. It is interesting to note that *PfPP1* functions during the cell cycle seem to be conserved throughout the eukaryotic kingdom, while others became specific to the obligatory intracellular lifestyle of this parasite. Consistent with this idea, some of the PIPs related to the cell cycle control are probably conserved with regards to mammals or yeast and indeed could be identified on the base of their homology with their mammalian counterparts (Pfl2, Pfl3...), while one can expect to identify Apicomplexa specific PIPs related to egress. Given the conservation of PP1 in the Apicomplexa phylum²²⁷, it would be interesting to verify whether the biological functions of *PfPP1* highlighted by our results might also be conserved in other parasites such as *T. gondii*. The conservation of the I2 inhibitor in *T. gondii* (*TgI2*) and its modulation of *TgPP1* activity *via* its interaction with several conserved motifs suggest that this might indeed be the case³⁸⁶. Moreover, it was reported that *T. gondii* extracellular tachyzoites were sensitive to the PP1/PP2A inhibitor OA, resulting in a reduction of invasiveness of the parasites³⁸⁷, suggesting an additional role of PP1 during invasion, that we could not explore using our iKO-PP1 mutant as it was blocked at an earlier step. This effect is likely due to inhibition of *TgPP1*, as *TgPP2A* activity was not detected in the parasite. Therefore, PP1 is a very well conserved eukaryotic PP, whose role in parasitic-specific steps of their life cycle deserves further investigation.

A PP1 interactome is available but has been generated using Y2H and *in silico* screening, which do not consider the dynamics and protein environment that *PfPP1* encounters in the parasite²⁸¹. Therefore, in order to advance in the understanding of PP1 function in schizogony and egress, we propose to co-IP PP1 partner proteins at two different parasite stages, mature trophozoite/early schizont to fish partners involved in schizogony, and late schizonts (segmenters) to identify proteins required for egress. To do this, iKO-PP1 line (that displays a PP1 C-terminal HA₃ tag) will be cultured in presence of DMSO or rapamycin and parasites will be collected at the time points indicated above. Immunoprecipitation experiments will be performed using anti-HA antibodies, followed by mass-spectrometry analyses. Partners for which the number of identified peptides will be reduced in the

condition of PP1 depletion will be taken into consideration. It will also be interesting to perform a phosphoproteomic study in the same conditions as cited above. These results, in comparison with the proteomic data might help identify direct PP1 substrates.

Out of all *Pf* kinases highly expressed in schizogony, only PK5 and CRK4 were found to function in DNA replication^{79,169}. PK5 acts as negative regulator of *Pf*ORC1 association to DNA, and likely promotes *Pf*ORC1 export, followed by degradation in the cytoplasm once DNA replication is complete in late schizogony⁷⁹. For CRK4 on the other hand, the mechanism of action is unclear, but absence of this kinase resulted in a halt in DNA replication¹⁶⁹. As a first step to identify CRK4 functions, CRK4 phosphoproteomic data were generated at two time points during schizogony, at 29 and 37h, comparing parasites expressing CRK4 (+Shield) and parasite depleted of the enzyme (-Shield). Interestingly, components of the DNA replication machinery were strongly enriched among the putative CRK4 substrates, such as ORC, MCM and DNA polymerases¹⁶⁹. We then used this CRK4 phosphoproteomic data sets, to compare it with the published PP1 interactome.

14 proteins were found both in the PP1 and CRK4 datasets, and are presented in Table 7. Besides many proteins of unknown function, a putative Zinc finger protein (PF3D7_1008100), a structural maintenance of chromosomes protein 6 (SMC6, PF3D7_0525200) and a putative pre-mRNA-splicing factor ATP-dependent RNA helicase (PRP2, PF3D7_1231600) were retrieved. These proteins are likely involved in DNA and RNA biology, but due to the absence of functional studies it is unclear whether they have a specific role in parasite DNA replication or mitosis. Available real-time transcription data imply that some of these genes are highly expressed at the timing of the first round of DNA replication (~28-30hpi³⁸⁸) until the end of schizogony, and are co-expressed with PP1 and CRK4 (Table 7, right column)¹⁷⁰. So it needs to be validated if these proteins truly interact with PP1 and CRK4, and second, if they function in parasite schizogony.

In summary, the common interactors of PP1 and CRK4 might be interesting candidates for future research.

Table 7: List of proteins predicted to be both PP1 interactors and CRK4 substrates. The predicted PIP interactome was taken from²⁸¹. From the CRK4 phosphoproteomic data set, only those proteins were selected for which phosphorylation was more than 2 times decreased in absence of Shield at both 29 and 37hpi¹⁶⁹. The functional annotation of these 14 genes, as well as the mRNA expression profiles¹⁷⁰ and predicted protein domains, if present, are described in the middle and left column, respectively (data retrieved from plasmodb.org).

Gene ID	Annotation on PlasmoDB	mRNA expression data + presence of conserved protein domains (plasmodb.org)
PF3D7_1008100	putative zinc finger protein	Expressed throughout the cycle, slight mRNA peak at 40hpi
PF3D7_0307700	unknown function	
PF3D7_0525200	structural maintenance of chromosomes protein 6, putative	Expressed throughout the cycle, mRNA peak in late schizonts
PF3D7_0526500	unknown function	mRNA expression peaks in ring stage (12hpi)
PF3D7_1210600	unknown function	mRNA peaks at 20hpi
PF3D7_1227700	unknown function	Rather homogenous mRNA expression over the cycle; Possibly actin binding properties (blast)
PF3D7_0530000	unknown function	mRNA peaks at 20-30hpi
PF3D7_1357400	unknown function	Slight expression peak at 20hpi
PF3D7_1231600	putative pre-mRNA-splicing factor ATP-dependent RNA helicase	mRNA expressed throughout the cycle, lowest expression at 38hpi
PF3D7_1348400	conserved <i>Plasmodium</i> membrane protein	expressed throughout the cycle; 4 predicted TM domains,
PF3D7_1308400	unknown function	slightly higher expression at 20-30hpi; 2-3 putative TM domains
PF3D7_0611800	unknown function	mRNA expressed throughout the cycle; Pentapeptide-like domain of unknown function
PF3D7_0723800	unknown function	mRNA peaks at 40hpi
PF3D7_1238500	unknown function	mRNA peaks at 20hpi

Having established the involvement of PP1 in merozoite egress, we interrogated the predicted PP1 interactome for proteins that could function in egress. Interestingly, SERA6 is a putative PIP, as it was found by Y2H screen and bears two PP1-binding motifs²⁸¹. Indeed, SERA6 was reported to be phosphorylated on S₁₈₃ in schizonts by Solyakov *et al.*¹²¹, but this phosphosite was not confirmed by other phosphoproteome studies. Henceforward it would be interesting to validate if SERA6 acts as PP1 regulatory protein or substrate *in vivo*. However, SERA6 is exported to the PV³⁸⁹, whereas PP1 has no SP and resides inside the parasite cytosol, which is in disagreement with a possible interaction of these proteins.

Another putative PIP is the merozoite adhesin MSP9, which is part of the MSP1/6/7 adhesion complex^{29,30,390}, and which was retrieved from the Y2H screen, but which doesn't bear a classical PP1 binding motif²⁸¹. The role of the MSP1/6/7 complex in invasion is well established as it binds to RBC receptors Band 3 and GPA^{29,30}, with MSP9 contributing to Band 3 binding during RBC invasion *in vivo*³⁹¹, but it has not been investigated if this complex also is involved in egress. Processed MSP1 was reported to promote egress by binding to RBC spectrin¹⁰⁴, but it remains unclear whether other components of the MSP1/6/7 complex also actively participate in egress. PP1 is localized in the parasite cytosol, whereas MSP9 is exported and accumulates in the PV and on the merozoite surface^{391,392}. So if MSP9 is a PP1 substrate, then this interaction between the two proteins would have to take place inside the parasite secretory pathway before MSP9 export. Given the absence of a SP in PP1, it is unlikely that PP1 comes into contact with MSP9 *in vivo*.

Next, we inquired if there might be a crosstalk between parasite PP1 and PKG, a major player in egress. Thus, we compared the predicted PP1 interactome with the phosphoproteome of PKG³⁸³, retrieving five common proteins: histone H2B, a putative member of the LEM3/CDC50 family involved in phospholipid transport in yeast and *Leishmania*, a DBL-like antigen A332 and a putative nuclear polyadenylated RNA-binding protein (NAB2). None of these proteins is expected to function in egress. In any case, a future PP1 phosphoproteome study is essential to verify if PP1 and PKG regulate common targets.

In conclusion, our work provided valuable insights into the expression and functions of *Pf*PP1 phosphatase. The understanding of *Pf*PP1 function will advance by the future identification of regulators and substrates of this phosphatase, in order to define a *P. falciparum* interactome that will help in the better understanding of essential steps of this parasite life cycle, i.e. schizogony and egress.

MATERIAL & METHODS

1. Molecular biology

The primers used in this work are listed in Table 8, **Fehler! Verweisquelle konnte nicht gefunden werden.** Table 9 and Table 10Table 6 for Shelph2, PP4/PP7 and PP1 characterization, respectively. All PCR amplifications for molecular cloning were done using the Q5 DNA polymerase (NEB) and verified by sequencing (Eurofins). Bacterial colonies were screened using the GoTaq G2 Green master mix (Promega).

1.1 Molecular cloning Shelph2

All the primers used for our study of Shelph2 are listed in Table 8.

To generate pL7-Shelph2*-HA₃ vector, we first amplified triple HA tag from pLIC-DHFR³⁹³ using primers MLa33/MLa32 and cloned it SpeI/Ascl in pL6_BsgI_V3 (modified version of pL6_eGFP, gift from Jose-Juan Lopez-Rubio). This generated pL6_BsgI-HA₃ plasmid. Next, we amplified 646 bp of *shelph2* 3'UTR from Pf3D7 gDNA using primers MLa40/MLa41 and cloned it Ascl/SacII in pL6_BsgI-HA₃ to generate pL6_BsgI-HA₃-3'UTR. The 3'UTR was designed 207 bp after *shelph2* stop codon due to a very rich A/T richness that prevented the design of a specific primer. The full *shelph2* coding sequence (CDS) amplified using primers MLa3/MLa4 was first subcloned in the pCR-BluntII-TOPO vector (Invitrogen). Shield mutations in *shelph2* CDS were introduced by mutagenesis with primers MLa79/MLa80 using the QuickChange Site-directed Mutagenesis kit (Stratagene) according to the manufacturer instructions. The resulting mutated *shelph2** was again subcloned in the pCR-BluntII-TOPO and verified by sequencing. 712 bp of *shelph2** was re-amplified using primers MLa59 and MLa45 and cloned in pL6_BsgI-HA₃-3'UTR using SpeI, yielding pL6_BsgI-*shelph2**-HA₃-3'UTR. From this vector, the whole *shelph2**-HA₃-3'UTR cassette was re-amplified using primers MLa59/MLa60 and cloned InFusion (Clontech) SpeI/AflIII in pL6-eGFP³⁹⁴. The resulting vector pL6-*shelph2**-HA₃-3'UTR was digested BtgZI to allow the insertion of *shelph2* gRNA corresponding to hybridized primers MLa63/MLa64. The final plasmid named pL7-Shelph2*-HA₃ was used for transfection.

To generate pL7-Shelph2-KO vector, 388 bp fragment encompassing the 5'UTR and the first 219 bp of *shelph2* CDS was amplified by PCR as homology region 1 using primers MLa54/MLa53. The fragment was cloned NcoI/EcoRI by InFusion in the pL6-eGFP vector, downstream of hDHFR cassette, giving pL6-3'UTR. Similarly, a 760 bp fragment corresponding to *Pfshelph2* 3'UTR was amplified using primers MLa50/MLa51 and cloned AflIII/SpeI by InFusion in pL6-3'UTR plasmid, upstream of hDHFR cassette. Finally, gRNA MLa63/MLa64 was inserted in the plasmid in BtgZI as described above. The resulting vector was named pL7-Shelph2-KO and used to transfect parasites.

To generate pARL2-Shelph1-GFP plasmid, the entire *shelph1* coding sequence without the stop codon was PCR amplified using primers MLa1 and MLa2 and cloned XhoI/KpnI in frame with a GFP tag in pARL2-GFP vector³⁹⁵.

Table 8: Primers used for the work on Shelph2.

Primer name	Sequence (5'-3') – Restriction site in bold	Restriction Site
MLa33	TAAGTCCTCC ACTAGT GGAAGTGGAGGACGGGAATT	SpeI
MLa32	CGGAAGATAG GGCGCGCCTT AGGCATAATCTGGAACATCG	Ascl
MLa40	TATGCCTAAG GGCGCGCCT ACCTTTTCATCATTTAAAGGTCTC	Ascl
MLa41	CAATGGCCCTTT CCGCGG AGTAAAGCTTTACATATTCATTA ³⁹⁵ AAG	SacII
MLa3	CGCCTCGAGATGAATATATCATATTTAAGGAATTTTC	

MLa4	CGCGGTACCTATATCGGAATTTATATAATTTACTTTATATG	
MLa79	CTTCCTTATTATGCTAAAAGAGGTATTGATTATATAAATGATG	
MLa80	CATCATTTATATAATCAATACCTCTTTTAGCATAATAAGGAAG	
MLa59	CGCGGGGAGG ACTAGT CATTAGGGAAAATGTGTTCTGTG	SpeI
MLa45	CTCCACTTCC ACTAGT TATATCGGAATTTATATAATTTACTTTATATG	SpeI
MLa60	TTACAAAATG CTTAAG AGTAAAGCTTTACATATTCATTA AAAAAG	AflIII
MLa63	TAAGTATATAATATTCTTCCTTATTATGCTAAGCGGTTTTAGAGCTAGAA	
MLa64	TTCTAGCTCTAAAACCGCTTAGCATAATAAGGAAGAATATTATATACTTA	
MLa54	TTTTACCGTTC CCATGG GTTGAAAAATTATTATTATTTTATGGTG	NcoI
MLa53	ATTAAATCTAG AATTC TTAGAACACATTTTCCCTAATGG	EcoRI
MLa50	TTACAAAATG CTTAAG TACCTTTTCATCATTTAAAAGGTCTC	AflIII
MLa51	AGCCGAAGAT ACTAGT GGAATTAGTATAATGCCCATGAAGTC	SpeI
MLa1	CG CTCGAG ATGAATGTAGACAAAATACTTTGG	XhoI
MLa2	CG GGTAC CCAAATCTTTAATTTTATGACTTAGAC	KpnI
MLa11	CGCCTCGAGATGAAGAGTTTGGAGAATAACG	
MLa12	CGCGGTACCCATAAAAATGACATTTCTAAGAC	
MLa13	CGCCTCGAGATGTGGAATAAATTAATGATGC	
MLa14	CGCGGTACCTAAAAAATTA AACATTTAACATTAGG	
MLa65	CTTCCTTATTATGCTAAGCG	
MLa99	CCTTTAAATGATGAAAGGTATTTGATATCC	
ML1476	CAGCGTAGTCCGGGACGTCGTAC	
MLa115	CAAGTTTATTATACATCCTATACATTTACTTTAAACC	
MLa116	ACGATGCAGTTTAGCGAACC	
MLa117	TCCAATACTTTCCAATGTTTCATGG	
hDHFR	CCAGGTGTTCTCTCTGATGTCC	
qPCR primers		
Primer name	Sequence (5' - 3')	Gene
MLa218	TGGCTAACCATAATTACCTTTTTGG	<i>shelph1</i>
MLa219	CTCTCTACGTCCTCATGGAT	<i>shelph1</i>
MLa224	AAGTGCCACCTCAAAGAGTG	<i>PPKL</i>
MLa225	GCTTCTGGTGGACTTCCTTT	<i>PPKL</i>
MLa226	TGTACCACCAGCCTTACCAG	<i>FBA</i>
MLa227	TTCCTTGCCATGTGTTCAAT	<i>FBA</i>
Shlp2_F	TGCTAAGCGTGGTATTGATT	<i>shelph2</i>
Shlp2_R	CTGCAGCACGAGAAAAGTAT	<i>shelph2</i>

1.2 Molecular cloning PP4 and PP7

The primers specifically used for the cloning of PP4 and PP7 homologous recombination constructs are listed in Table 9. For cloning the pLN-PP-HA₃-*glmS* constructs, two homology regions HR1 and HR2 were cloned into a pLN vector.

For PP4, the 631bp homologous region HR1 was amplified with MLa130 and MLa131, and cloned into the vector by XmaI and AfeI sites. The reverse primer MLa131 was designed to introduce shield mutations and to recodonize the 3' 29bp of PP4 CDS.

For PP7, the HR1 encoding a fragment of the PP coding sequence was followed by a recodonized fragment that represents the 3' part of the gene. These two fragments, the original and the

recodonized sequence, were amplified by overlapping PCR. The 740bp HR1 was amplified with MLa 151 and MLa 152, and, together with the recodonized fragment amplified with MLa 153 and MLa 154, was cloned into BamHI and AfeI restriction sites.

HR2 matches 580 bp (PP4) or 478 bp (PP7) of the respective 3'UTR directly downstream of the stop codon. The PP4 HR2 fragment was amplified with MLa184 and MLa185 and cloned into the vector using Bgl II and Pst I restriction sites. PP7 HR2 was amplified with MLa 182 and MLa183 (PP7), and cloned into PstI and Hpa I restriction sites.

The pLN-PP4/PP7-HA₃-glmS constructs were then used to generate pLN-PP4/PP7-HA₃-loxP plasmids. For this, the HA₃-loxP sequence was amplified using primers MLa244 and MLa245, and pasted InFusion into the AfeI and PstI linearized pLN-PP4/PP7-HA₃-glmS. Transfections for obtaining HA₃-loxP parasite lines were done using the same gRNAs as for HA₃-glmS transfections (Table 9).

For generating the pLN-loxPint-PP7 vector, HR1 was designed as an overlapping PCR, with the first PCR fragment amplified using MLa251 and MLa252 and corresponding to PP1 5'UTR and exon 1, and the second fragment to a synthetic DNA fragment containing the recodonized 3' part of PP1 exon1 followed by a loxPint artificial intron sequence³⁵⁰, and amplified with primers MLa249 and MLa250. HR2 corresponding to the 3' UTR was amplified using MLa253 and MLa254. Both HRs were cloned by a single InFusion reaction in XmaI/PstI.

Table 9: Primers used for cloning of PP4 and PP7 constructs. F-forward, R- reverse.

Primer name	Amplicon F (forward), R (reverse)	5' → 3' sequence
PP4 HA ₃ -glmS cloning		
MLa 130	PP4 HR1 (F)	ctt <u>CCC</u> GGGTATCCATTACATTTAACGTTAATACGAG
MLa 131	PP4 HR1 (R)	gtgAGCGCTGGAGAAATACACTGGTGGAAATTTTCTAAGTT CAGTCGTATTATTATTG
MLa 184	PP4 3'UTR (HR2) (F)	cgcAGATCTTGCAATGACCCACATCATATC
MLa 185	PP4 3'UTR (HR2) (R)	tgtCTGCAGTTTTTTTCTCCTCTGAAATGAC
MLa 137	gRNA 2 (F)	TAAGTATATAATATTGTTAGGAGAAATACACTGGTGTTTTA GAGCTAGAA
MLa 138	gRNA 2 (R)	TTCTAGCTCTAAAACACCAGTGTATTTCTCCTAACAAATATTA TATACTTA
MLa 18	5' integrative PCR (F)	cgc <u>CTCGAGATGA</u> ACCCTAAAGATTTAGATAAAG
ML 2880	5' integrative PCR (R)	TAACCTCCATCCTCGTCAACTAAG
ML 2881	3' integrative PCR (R)	TGAACCGCATCGAGCTGA
MLa 189	3' integrative PCR (R)	CATGTGGATCATATTTTCTTAACAGC
PP7 HA ₃ -glmS cloning		
MLa 151	PP7 HR1 (F)	ctgGGATCCTTAGTCAGATTGATAAATAGCAATTCC
MLa 152	PP7 HR1 (R)	TTCCATAAGAATATCGTCGTC AAC
MLa 153	PP7 recodonized (F)	CGACGATATTCTTATGGAAGTAGC
MLa 154	PP7 recodonized (R)	cgcAGCGCTATTATTGCTGTATATATAGGTTGGCTTG
MLa 182	PP7 3'UTR (HR2) (F)	cgcCTGCAGCCATTCTAAATATATCGTTTTTAATG
MLa 183	PP7 3'UTR (HR2) (R)	ctgGTTAACCTTATTAGGTTTATATGATAACAACAGG
MLa 208	gRNA 1 (F)	TATTGACGATATTCTTATGGAAGT
MLa 209	gRNA 1 (R)	AAACACTTCCATAAGAATATCGTC
MLa 210	gRNA 2 (F)	TATTTGTCTATCGATTTGGCTAGC
MLa 211	gRNA 2 (R)	AAACGCTAGCCAAATCGATAGACA
MLa 212	5' integrative PCR (F)	CTGAATTTGAGCAGGTTTACG
MLa 213	3' integrative PCR (R)	TTTCAACTCATCTATAATCCTAGACATC

	Replace glmS by loxP	
Mla 244	HA ₃ -loxP (F)	AGAAAGCGGCCAATAGCTACCCGTACGACGTCC
Mla 245	HA ₃ -loxP (R)	CCTAAGTTTTGTAATATACTTAACTAATAACTTCGTATAATG TATGC
	PP7 loxPint cloning	
MLa 249	Recodon-loxPint (F)	TTTCATTCTTTTGTGTTGTTGTAAGT
MLa 250	Recodon-loxPint (R)	AAGGGTTTATAAATTTCACTAAAA
MLa 251	HR1 (F)	CTCAAGCTTGGGGGATCGGAAGAAGAATGGAAAATTAC AAC
MLa 252	HR1 (R)	ACAAACAAAAGAATGAAAACCTTTTTCTTC
MLa 253	HR2 (F)	TGAAATTTATAAACCCCTTAATAAAAAC
MLa 254	HR2 (R)	GAATTAGCTAAGCATGCGCAAACCTTTGTGAACCAAGTTG TATG
MLa 291	gRNA 1 (F)	TATTCTTTTGTGTTGCACCGTG
MLa 292	gRNA 1 (R)	AAACCACGGTGCAACAAACAAAAG
MLa 308	Integrative PCR 4 (F)	CTGTATGGAGGAAGTTCGACC
MLa 312	Integrative PCR 5 (detect unedited locus) (F)	CGATCACATACACGAATATATAACC

1.3 Molecular cloning PP1

Since our initial strategy was to generate PP1-HA₃-glmS regulatable parasites, we first generated a pLN-PP1-*glmS* vector containing the *pp1* HRs. In this plasmid, *pp1* HR1 was produced by overlapping PCR and cloned XmaI/AfeI: the first fragment amplified using MLa118 and MLa119 corresponds to exon 3 and the second to a recodonized region encompassing exons 4 and 5 and amplified with MLa120 and MLa121. HR2 representing the 440bp fragment of the 3' UTR directly downstream of the stop codon was amplified with MLa178 and MLa179 and cloned into the vector using PstI and HpaI restriction sites. As we did not obtain PP1-HA₃-glmS edited parasites, and the *glmS* strategy was little efficient for PP4, we adopted the DiCre strategy for PP1, and replaced the *glmS*-PbDT3' cassette by a synthetic HA₃-loxP cassette (synthesized by idtdna) by InFusion (Clontech) cloning. To generate the pLN-PP1-HA₃-loxP vector, we cloned the *PP1* homology regions (HR) into a pLN plasmid carrying a Blasticidin (Bsd) resistance cassette. This gave rise to pLN-PP1-HA₃-loxP.

For generating the pLN-loxPint-PP1 vector, HR1 was designed as an overlapping PCR, with the first PCR fragment amplified using MLa264 and MLa265 and corresponding to *PP1* 5' UTR and exon 1, and the second fragment to a synthetic DNA fragment containing the recodonized 3' part of *PP1* exon1 followed by a loxPint artificial intron sequence³⁵⁰, and amplified with primers MLa268 and MLa269. HR2 corresponding to the 3' UTR was amplified using MLa266 and MLa267. Both HRs were cloned by a single InFusion reaction in XmaI/PstI.

The gRNAs were cloned in BbsI into the pDC2-cam-co-Cas9-U62-hDHFR vector provided by Marcus Lee.

For introducing the Y270F single point mutation into PP1, a pLN-PP1-Y270F-HA₃-loxP vector was generated in which the TAT codon was mutated to TTT. pLN-PP1-HA₃-loxP vector was used as template for site-directed mutagenesis PCR using MLa304 and MLa305 and the Quik change lightning Multi-site-directed mutagenesis kit (Agilent).

Table 10: Primers used for PP1 cloning. Listed in (chronological) order of usage, as described in the methods text .F- forward, R-reverse

Primer name	Amplicon F (forward), R (reverse)	5' → 3' sequence
	HA ₃ -loxP cloning	
MLa 118	PP1 HR1 genomic part (F)	ctgCCCGGGGATTATGTGGATAGAGGAAAACAAAG
MLa 119	PP1 HR1 genomic part (R)	CTGATGTGCCCTGCATATTAATC
MLa 120	PP1 HR1 recodonized part (F)	ATATGCAGGGCACATCAGG
MLa 121	PP1 HR1 recodonized part (R)	tgtAGCGCTATTGGCCGCTTCTTTTTTTC
MLa 178	PP1 HR2 (F)	cgcCTGCAGTATATTACAAAACCTTAGGATCCTAATATATTAAT TG
MLa 179	PP1 HR2 (R)	ctgGTTAACGAAAAATACTACTTTTATAGATAATATTTGTTTTG TTC
MLa 206	gRNA HA ₃ -loxP (F)	TATTGTCAACACTCATCATTGCAC
MLa 207	gRNA HA ₃ -loxP (R)	AAACGTGCAATGATGAGTGTTGAC
MLa 187	check 5' integration of HA ₃ -loxP (F)	CATGGACAGTTTTATGATTTGTTAAGG
MLa 188	check 3' integration of HA ₃ -loxP (R)	GAAATATATGGCTAAATTAATATAAATAGC
MLa 244	InFusion cloning of HA ₃ -loxP into pLN (F)	AGAAAGCGGCCAATAGCTACCCGTACGACGTCC
MLa 245	InFusion cloning of HA ₃ -loxP into pLN (R)	CCTAAGTTTTGTAATATACTTAACTAATAACTTCGTATAATGT ATGC
	loxPint cloning	
MLa 268	Recodon-loxPint (F)	GAATATGGTGGATTCCACCAG
MLa 269	Recodon-loxPint (R)	CTCTATCCACATAATCACCTAAAAG
MLa 264	HR1 (F)	CTCAAGCTTGGGGGGATCCATATCAAATAAAATAAATTCATT CTTC
MLa 265	HR1 (R)	TGGAAATCCACCATATTCAAATAAC
MLa 266	HR2 (F)	GTGATTATGTGGATAGAGGAAAACAAAG
MLa 267	HR2 (R)	GAATTAGCTAAGCATGCGCTCGATCATTCTCCCCACC
MLa 287	gRNA loxPint (F)	TATTAATAATAGATAATTTGCATC
MLa 288	gRNA loxPint (R)	AAACGATGCAAATTATCTATTTTT
	Check DiCre-mediated PP1 excision	
MLa 187	F	CATGGACAGTTTTATGATTTGTTAAGG
MLa 179	R	ctgGTTAACGAAAAATACTACTTTTATAGATAATATTTGTTTTG TTC
	Y270F mutagenesis	
MLa 304	Mutagenesis Y270F PP1 (F)	AGCGCCCCTAATTTTTGTGGTGAATTTGATAATGC
MLa 305	Mutagenesis Y270F PP1 (R)	GCATTATCAAATTCACCACAAAATTAGGGGCGCT

1.4 qRT-PCR

RNA was extracted from infected erythrocytes via the NucleoSpin RNA extraction kit (Macherey-Nagel). 500 ng of RNA were used as template for the Reverse transcription reaction, using the SuperScript III First-Strand Synthesis SuperMix for qPCR (Invitrogen). The cDNA generated in this reaction was diluted 1/20 before measuring by qPCR.

Shlp1 expression (PF3D7_1469200) was assessed comparing the 3D7 wt strain with three Shlp2-KO clones. In contrast to Shlp1 and Shlp2, PPKL (protein phosphatase containing kelch-like domains; PF3D7_1466100) exhibits Ser/ Thr PP activity (Guttery, et al. 2012), and was therefore chosen as phosphatase control in the qRT-PCR.

For quantifying the expression of Shlp1, Shlp2 and PPKL phosphatases, the LightCycler 480 Sybr Green I system (Roche) was employed. Fructose-biphosphate aldolase (PF3D7_1444800) was used as reference gene.

For determining the exact amplification efficiency for each gene, Standard curves were generated. LightCycler 480 Software, Version 1.5 was used for “Relative advanced quantification” data analysis. The expression of each target gene in the Shlp2-KO clones was then normalized to the wt expression level.

2. Parasite culture and transfection

Culture

P. falciparum 3D7 strain and transgenic daughter lines were cultured in human erythrocytes at 5% hematocrit in RPMI 1640 (Gibco), supplemented with 10% Albumax and gentamycin at 20 µg/ml. The cultures were kept at 37°C under a controlled trigaz atmosphere (5% CO₂, 5% O₂ and 90% NO₂).

For the inducible depletion of PP1 protein, PP1-iKO parasites were treated with rapamycin from LC Laboratories (Cat.-No. R-5000). Stocks were stored in DMSO (10 mM) at -20°C and used at a final concentration of 10 nM for 4h, and then washed away.

For the timely synchronization of parasite populations, mature parasites were isolated using gelatin floatation³⁹⁶. Alternatively, late schizonts were selectively recovered from cushions of 70% (v/v) Percoll adjusted to isotonicity³⁸⁴. These late schizonts were allowed to invade for a certain time-frame, followed by the selection for ring stages using 5% sorbitol³⁸⁵. PP-HA₃-loxP and PP1-iKO parasite lines that were derived from the DiCre expressing strain p230pDiCre provided by E. Knuepfer³⁷⁰ were synchronized exclusively by Percoll and Sorbitol treatment. For experiments that required a high number of synchronous segmented schizonts, 40 – 42 hpi schizonts were treated for up to 5h with 1.5 µM of c2, followed by two washes. To phenotype the iKO-PP1 parasites during egress and prevent the DMSO control parasites to egress, parasites were treated for up to 2h with 50 µM of E64.

Transfection

For parasite transfections, 5-10% ring stages were transfected with 60-80 µg of circular or linear plasmid DNA as described previously^{394,397}. Transgenic parasites were grown in agitation (200 rpm) and selected by addition of 2.5 nM WR99210 (for pL7-Shelph2*-HA₃, pL7-Shelph2-KO, pARL2-Shelph1-GFP and pDC2-gRNA), 1.5 µM DSM1 (for pUF1-Cas9) and 2.5 µg/ml blasticidin S (for pLN-PP). Drug pressure was removed after parasite genotyping, except for episomes maintenance.

3. Parasite phenotypic assays

The phenotypic analysis of Shelph2-KO and PP1-iKO parasites were performed on tightly synchronized parasites with a 2 to 4 hours re-invasion time frame.

To follow *P. falciparum* intra-erythrocytic development, synchronized parasite cultures were smeared in triplicate from 2h post-invasion until 48h. The ratio of ring, trophozoite and schizont was evaluated for 200 infected RBCs at each time point.

For determining the number of merozoites per segmenter, late schizonts of about 40h were purified on a Percoll gradient, and parasites were left maturing for an additional 4h in the presence of 1.5 μ M compound 2 or E64 (50 μ M) to block egress^{398,399}. After one wash in complete medium, blood smears were done in triplicate, Giemsa-stained and analyzed by counting 50 segmenters per smear. Alternatively the smears were stained with Hoechst and nuclei counted by fluorescence.

Proliferation rate assays were set up at 1 % parasitemia in ring stage. Samples were taken in ring stage 6h post-invasion during the first cycle. 48h later, ring stage samples of the next cycle were again collected and fixed in 4% PFA for 4h at room temperature (RT). Flow cytometry (FACS) was then used to determine the parasitemia.

Exoneme and microneme secretion was examined by IFA staining of SUB1 and AMA1, respectively. PP1-iKO parasites were treated with 10nM Rapamycin at 30hpi for 4 hours, and left to mature till schizont stage. At 40-42hpi, schizonts were purified using Percoll, and incubated with E64 until 48hpi, when smears were made and processed for IFAs.

4. Flow cytometry

Flow cytometry was used both to determine parasitemia in growth assays, as well as to determine the DNA content during schizogony. Infected erythrocytes were fixed in 4% paraformaldehyde (PFA) for 4h at room temperature, and then stored at 4°C. Cells were washed twice in phosphate buffered saline (PBS), and stained with 1X SYBR green (Invitrogen) for 30min, followed by one wash in PBS. Cells were resuspended in 700 μ l PBS and analyzed by BD FACS Canto I flow cytometer using FACS Diva software (BD Biosciences). SYBR green was excited with a blue laser at 488 nm, and fluorescence was detected by a 530/30 nm filter.

For the exact determination of DNA content of the PP1-iKO parasites, these parasites were very tightly synchronized (1h re-invasion time frame). PP1-iKO parasites were treated 10nM Rapamycin at 6hpi for 4h. At 30hpi, 38hpi and 45hpi infected RBCs were fixed PFA for FACS analysis, and blood smears were made for counting the nuclei. FACS Diva software and nuclei counts of the parasite smears were used to set up the gates for 1n, 2n, 3n, 4n, etc.

5. Immunoblot and Immunofluorescence Assays

Immuno-fluorescence assays (IFAs) were performed on smears of infected RBCs. The smears were fixed with 4% PAF for 20min, followed by 5min of neutralization with 0.1M glycine/PBS. Cells were permeabilized with 0.2% Triton/PBS for 20min. Following saturation in PBS-2% bovine serum albumin (BSA) for 20min, cells were incubated 45 min with primary antibodies diluted in PBS-BSA. After 3

washes in PBS, cells were incubated 45 min with secondary Alexa-488- or Alexa-594-conjugated secondary antibodies highly cross-adsorbed (Invitrogen) diluted in PBS-BSA as recommended by the manufacturer. Nuclei were stained with Hoechst. Images were taken on a Zeiss Axioimager Z2 equipped with an apotome, at the Montpellier RIO imaging facility. Images were processed by Zen Blue edition software (Zeiss) for optical sectioning, luminosity and contrast adjustment.

Primary antibody dilutions were rat anti-HA 1/1000 (Roche Diagnostics), rabbit α -MTIP 1/500 (gift from Tony Holder), mouse α -MSP1 19kDa 1/1000 (gift from M. Blackman), mouse α -RON4 (1/200), mouse α -SUB1 (1/2, gift from M. Blackman) and rabbit α -SERA6 1/1000 (gift from M. Blackman), rabbit α -AMA1 1/1000).

Proteins were analyzed by SDS-PAGE and immunoblot. Immunoblot samples were prepared by lysing the RBCs using 0.01% Saponin in PBS and protease inhibitors (cOmplete™ EDTA-free Protease Inhibitor Cocktail, Sigma) for 5min. Following washes, parasite DNA was digested by Benzonase (EDM Millipore 70746-3) and parasites were lysed in Laemmli sample buffer with DTT. Minimum 5×10^6 parasites per sample were loaded in a 12% SDS PAGE and proteins separated in gel were blotted onto a nitrocellulose membrane. Proteins were detected using primary antibodies α -HA (1:1000) and α -histone H3 (1:15 000, Abcam), and alkaline phosphatase-conjugated secondary antibodies (Promega). Secondary antibodies conjugated to alkaline phosphatase (Promega) were diluted according to the manufacturer's instructions and used with NBT/BCIP reagents (Promega).

DISCUSSION

The initial aim of our project was to find PPs possibly involved in egress and invasion. For that purpose, we used differential gene expression as a criterion to find candidate genes. The presence of a signal peptide for possible secretion into the host cell upon invasion was an additional characteristic we took into consideration. Our screening strategy retrieved 9 PPs, of which Cn is the only one for which reverse genetic studies have been conducted in *P. falciparum*, demonstrating a crucial role in invasion⁴⁰⁰. Interestingly, this screen also identified Shelph2 and PPM5 that were previously categorized by an *in silico* approach in a “merozoite invasion network” defined by co-transcriptional expression pattern³⁰⁵.

We undertook the characterization of Shelph2, PP1, PP4 and PP7. These PPs are conserved in Apicomplexa but the clear lack of studies on PPs make it difficult to predict whether their function might be conserved. The diversity of life style of Apicomplexan parasites, the nature of their host and the way they multiply within host cells varies a lot, with mechanisms so different such as schizogony, endodyogeny and endopolygeny⁸³. Therefore there might be PP functions conserved in eukaryotes, PP functions specific to Apicomplexa, and finally PPs that adopted species-specific functions. Such a speciation is exemplified by PP1, for which we demonstrated a conserved role in the control of *P. falciparum* cell cycle and a parasite-specific function in host cell exit. Regarding the Shelphs PPs, we could not assign any biological function to PfShelph2, presumably because of functional redundancy. However, the unique orthologue in *Toxoplasma*, namely TgShelph, shares 30% identity to PfShelph1 and is required for *T. gondii* virulence *in vivo* (Mauld Lamarque, personal communication), suggesting that these bacterial-like PPs might be functionally important at one stage of these parasites life cycle.

Given the spread of malaria-resistant lines to the existing drugs, one can wonder whether PPs might represent good drug targets in future. PPs are emerging as novel drug targets for different diseases, including cancers^{241,401}. In the case of treatment of malaria infection, the high conservation between human and *Plasmodium* PPs might complicate the design of specific inhibitors, but proper biochemical and structural studies of Pf enzymes are missing to evaluate that risk. However, it has been shown in the case of PfPP1 that interfering with PfPP1 and its interaction with PIPs using peptides was detrimental to parasite growth²⁷⁹. Thus, preventing the binding of PPs to their regulatory subunits and/or targets might be a promising strategy for the development of antimalarials. In this regard, the identification of PIPs involved in parasite-specific cellular mechanisms will be crucial.

In this work we showed that PfPP1 is essential for parasite intraerythrocytic development by at least two different mechanisms. Given the need for novel antimalarials, the question arises if parasite PP1 could be a good drug target.

It is problematical for druggability that PP1 is extremely well conserved among eukaryotes¹⁹³, which is also the case for Plasmodium PP1: PfPP1 protein sequence is highly similar to human PP1 showing 83% identity (Figure 65). Despite this high similarity, some drugs attain specificity by differences in the protein three-dimensional structure. The question of PfPP1 and HsPP1 adopt different tertiary structure elements which could be specifically targeted by drug design, needs to be evaluated by a biochemist. However, given the high conservation of PP1, it is more convenient to search for putative drug targets among the PP1 interacting proteins: future research will likely discover PIPs that are parasite-specific and essential, making them suitable drug targets.

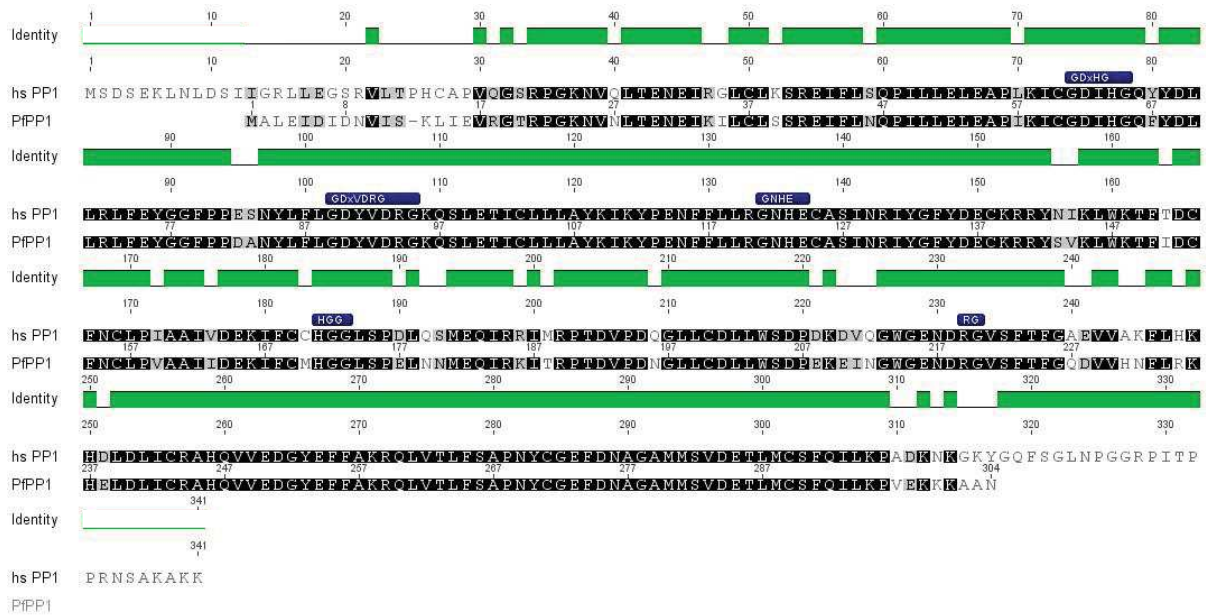


Figure 65: Protein alignment of human and *Pf* PP1c. Alignment was done using geneious blast tool. The conserved metal- and phosphate-binding motifs of eukaryotic PPPs are annotated with blue boxes. Amino acids labeled with black boxes indicates identity, grey labeling indicates chemical similarity.

In this work we analyzed *Plasmodium* PPs, but orthologues of these enzymes likely also play important roles in other Apicomplexans. For instance, the use of PP1 inhibitors in *T. gondii* showed a role of PP1-like enzymes in host cell invasion³⁸⁷. Most of the *Plasmodium* PPs have orthologues in other Apicomplexans²²⁷, as seen in Table 11. However, the *Plasmodium* phosphatome is the best characterized among all Apicomplexans²⁷¹.

Therefore the knowledge that is and will be generated for *Plasmodium* PPs, might in future transferred to understand PP functions in other Apicomplexans. However, the life style of Apicomplexans, the nature of their host and the way they multiply within host cells varies a lot, with mechanisms so different such as schizogony, endodyogony and endopolygony⁸³. Therefore there might be PP functions conserved in eukaryotes, PP functions specific to Apicomplexans, and finally PPs that adopted species-specific functions. As can be seen from Table 11, Apicomplexan PPs of the PPKL, EFPP and Shelph group have no orthologues in their vertebrate hosts, thus making them potentially suitable drug targets.

Orthologues to *Plasmodium* PPs are also found in other parasitic protozoa than Apicomplexans (Table 11). Interestingly, Shelphs are present in Kinetoplastida. Contrary to the current annotations on toxodb and a previous genomic and phylogenetic analysis of bacterial-like PPs in eukaryotes²¹¹, we identified a Shelph orthologue in *T. gondii* (TGME49_254770) that has highest similarity with *Pf*Shelph1 (30 % identity).

Table 11: Ser/Thr phosphatases of Apicomplexans and other parasitic protozoa. *Theileria parva*, *Babesia bovis*, *Cryptosporidium parvum*²⁷¹. Adapted from ^{211,240,271,402}

	PPP total	PP1	PP2A, PP4, PP6	Cn	PP5	PPEF (PP7)	PPKL	EFPP	Shelphs	PPM total	PTPs
Apicomplexa											
<i>P. falciparum</i>	11	1	3	1	1	1	1	1	2	10	4
<i>T. parva</i>	7	1	2	-	1	1	1	1	-	4	2
<i>B. bovis</i>	7	1	2	-	1	1	1	1	-	4	3
<i>T. gondii</i>	2	1	-	1	-	-	-	-	1	2	1
<i>C. parvum</i>	8	1	2	1	1	-	1	1	1	10	6
Kinetoplastida											
<i>T. brucei</i>	41	8	3	2	1	2	-	-	2	13	25
<i>T. cruzi</i>	42	7	4	2	1	2	-	-	3	14	32
<i>L. major</i>	43	8	4	2	1	1	-	-	3	15	32
<i>H. sapiens</i>	13	3	4	3	1	2	-	-	-	16	107 ⁴⁰²

In contrast to findings in *Pf* and most eukaryotes, PPM activity was reported to be the major PP activity in *T. gondii* extracellular and intracellular parasites⁴⁰³. For *T. gondii* whole phosphatome studies have not been undertaken, but several PPs have been found important for parasite biology, among others *TgHAD2*⁴⁰⁴, *TgCn*⁴⁰⁰ and *TgPP1* in host cell invasion³⁸⁷ and a PP2C that likely regulates *T. gondii* actin dynamics by means of its substrate toxofilin, an actin-depolymerizing protein⁴⁰⁵. In conclusion, reversible protein phosphorylation is a common means to regulate protein function, and is integrated in complex cellular signaling networks in *Plasmodium* and in other eukaryotes. Future directives in understanding PP function will therefore contribute to the understanding of essential mechanisms in parasite biology. The essentiality of most PPs emphasizes the need to better characterize these enzymes as they (or some of their partners) might represent targets for future clinical intervention.

This thesis has widened the knowledge about *P. falciparum* phosphatases: in addition to Cn that had previously been reported to be involved in the attachment step of invasion⁴⁰⁰, we described that PP1 functions in schizogony as well as in egress. However, the understanding of PP function in *Plasmodium* biology is still at the very beginning. The identification of PP substrates *in vivo* will be essential for revealing the action of each PP holoenzyme at the molecular level and for identifying the signaling pathways and phosphorylation networks a PP is integrated in. Only a few methods are currently available to discover PP substrates *in vivo*. The classical approach to identify the substrates of a kinase or PP is phosphoproteomics, which requires KD/KO strains or enzyme-specific inhibitors for proof of the concept. Alternative approaches for *in vivo* substrate identification are substrate trapping, which has successfully been applied to human PTPs⁴⁰⁶. Substrate trapping consists in the expression of an enzymatically dead PP that will form covalent complexes with the substrates that can be immunoprecipitated from the cell. The range of methods for identifying kinase substrates is larger, because artificial ATP analogues can be used to tag the phosphorylated substrates. One example is selective thiophosphorylation using an ATPγS analogue that was established in *T. gondii* to identify of *TgCDPK1* substrates⁴⁰⁷. With the actual advances in *P. falciparum* genetics, these kinds of experiments can be performed.

Although the methods for substrate identification are available for *Plasmodium*, phosphoproteomic studies have only been conducted very recently, for *Plasmodium* kinases *PfPKG*, *PfCRK4*, *PfPK7*, *PfCDKP1* and *PbCDPK4*^{150,169,360,383,408}. The complete absence of phosphoproteomic datasets for any *Plasmodium* PP highlights that there is work to do in this direction. Our PP1-iKO parasites are a valuable strain for a future phosphoproteomic analysis.

It is important to keep in mind that phosphatases are not isolated proteins involved in a single function in *Plasmodium* biology. On the contrary, PPs must be considered as players inside a phosphorylation system that includes one or more kinases, the antagonizing phosphatase (s), their numerous protein substrates, and phosphoprotein-binding players that deliver the downstream signaling (see Figure 66)⁴⁰⁹. That is why the identification of substrates is the necessary next step in our understanding of PP function. The ultimate aim will therefore be to integrate future data on kinases, PPs, their substrates and phosphoprotein-binding proteins in order to reconstruct the different phosphorylation modules underlying all aspects of *Plasmodium* biology.

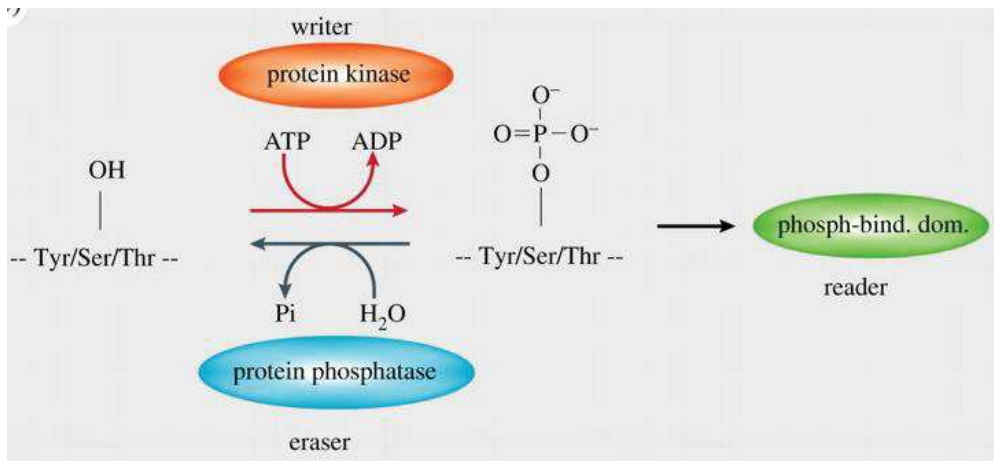


Figure 66: Scheme of an eukaryotic kinase-phosphatase-interaction domain system in protein phosphorylation. *Phosph-bind. Dom.*- phosphate-binding domain⁴⁰⁹.

References

1. Arisue, N. & Hashimoto, T. Phylogeny and evolution of apicoplasts and apicomplexan parasites. *Parasitol. Int.* **64**, 254–259 (2015).
2. Fréchal, K., Dubremetz, J.-F., Lebrun, M. & Soldati-Favre, D. Gliding motility powers invasion and egress in Apicomplexa. *Nat. Rev. Microbiol.* **15**, 645–660 (2017).
3. McFadden, G. I. & Roos, D. S. Apicomplexan plastids as drug targets. *Trends Microbiol.* **7**, 328–333 (1999).
4. Prevention, C.-C. for D. C. and. CDC - Malaria - Malaria Worldwide - Impact of Malaria. (2018). Available at: https://www.cdc.gov/malaria/malaria_worldwide/impact.html. (Accessed: 2nd August 2018)
5. WHO | World malaria report 2017. WHO Available at: <http://www.who.int/malaria/publications/world-malaria-report-2017/report/en/>. (Accessed: 7th February 2018)
6. Ashley, E. A., Phyo, A. P. & Woodrow, C. J. Malaria. *The Lancet* **391**, 1608–1621 (2018).
7. Liu, W. *et al.* Origin of the human malaria parasite *Plasmodium falciparum* in gorillas. *Nature* **467**, 420–425 (2010).
8. Rodrigues, P. T. *et al.* Human migration and the spread of malaria parasites to the New World. *Sci. Rep.* **8**, 1993 (2018).
9. Gething, P. W. *et al.* A new world malaria map: *Plasmodium falciparum* endemicity in 2010. *Malar. J.* **10**, 378 (2011).
10. Dunst, J., Kamena, F. & Matuschewski, K. Cytokines and Chemokines in Cerebral Malaria Pathogenesis. *Front. Cell. Infect. Microbiol.* **7**, (2017).
11. Dayananda, K. K., Achur, R. N. & Gowda, D. C. Epidemiology, drug resistance, and pathophysiology of *Plasmodium vivax* malaria. *J. Vector Borne Dis.* **55**, 1 (2018).
12. WHO | World Malaria Report 2016. WHO Available at: <http://www.who.int/malaria/publications/world-malaria-report-2016/report/en/>. (Accessed: 31st July 2018)
13. Graves, P. R. *et al.* Discovery of Novel Targets of Quinoline Drugs in the Human Purine Binding Proteome. *Mol. Pharmacol.* **62**, 1364–1372 (2002).
14. von Seidlein, L. & Dondorp, A. Fighting fire with fire: mass antimalarial drug administrations in an era of antimalarial resistance. *Expert Rev. Anti Infect. Ther.* **13**, 715–730 (2015).
15. Mahmoudi, S. & Keshavarz, H. Malaria Vaccine Development: The Need for Novel Approaches: A Review Article. *Iran. J. Parasitol.* **13**, 1–10 (2018).
16. Cowman, A. F., Berry, D. & Baum, J. The cellular and molecular basis for malaria parasite invasion of the human red blood cell. *J. Cell Biol.* **198**, 961–971 (2012).
17. Billker, O. *et al.* Calcium and a calcium-dependent protein kinase regulate gamete formation and mosquito transmission in a malaria parasite. *Cell* **117**, 503–514 (2004).
18. Cirimotich, C. M., Dong, Y., Garver, L. S., Sim, S. & Dimopoulos, G. Mosquito immune defenses against *Plasmodium* infection. *Dev. Comp. Immunol.* **34**, 387–395 (2010).
19. Kori, L. D., Valecha, N. & Anvikar, A. R. Insights into the early liver stage biology of *Plasmodium*. *J. Vector Borne Dis.* **55**, 9–13 (2018).
20. Matuschewski, K. *et al.* Infectivity-associated changes in the transcriptional repertoire of the malaria parasite sporozoite stage. *J. Biol. Chem.* **277**, 41948–41953 (2002).
21. Spielmann, T., Montagna, G. N., Hecht, L. & Matuschewski, K. Molecular make-up of the *Plasmodium* parasitophorous vacuolar membrane. *Int. J. Med. Microbiol. IJMM* **302**, 179–186 (2012).
22. Lanzer, M., Wickert, H., Krohne, G., Vincensini, L. & Braun Breton, C. Maurer's clefts: a novel multi-functional organelle in the cytoplasm of *Plasmodium falciparum*-infected erythrocytes. *Int. J. Parasitol.* **36**, 23–36 (2006).

23. Arnot, D. E., Ronander, E. & Bengtsson, D. C. The progression of the intra-erythrocytic cell cycle of *Plasmodium falciparum* and the role of the centriolar plaques in asynchronous mitotic division during schizogony. *Int. J. Parasitol.* **41**, 71–80 (2011).
24. Josling, G. A. & Llinás, M. Sexual development in *Plasmodium* parasites: knowing when it's time to commit. *Nat. Rev. Microbiol.* **13**, 573–587 (2015).
25. Harvey, K. L., Gilson, P. R. & Crabb, B. S. A model for the progression of receptor-ligand interactions during erythrocyte invasion by *Plasmodium falciparum*. *Int. J. Parasitol.* **42**, 567–573 (2012).
26. Cowman, A. F., Tonkin, C. J., Tham, W.-H. & Duraisingh, M. T. The Molecular Basis of Erythrocyte Invasion by Malaria Parasites. *Cell Host Microbe* **22**, 232–245 (2017).
27. O'Donnell, R. A., Saul, A., Cowman, A. F. & Crabb, B. S. Functional conservation of the malaria vaccine antigen MSP-119 across distantly related *Plasmodium* species. *Nat. Med.* **6**, 91–95 (2000).
28. Koussis, K. *et al.* A multifunctional serine protease primes the malaria parasite for red blood cell invasion. *EMBO J.* **28**, 725–735 (2009).
29. Goel, V. K. *et al.* Band 3 is a host receptor binding merozoite surface protein 1 during the *Plasmodium falciparum* invasion of erythrocytes. *Proc. Natl. Acad. Sci. U. S. A.* **100**, 5164–5169 (2003).
30. Baldwin, M. R., Li, X., Hanada, T., Liu, S.-C. & Chishti, A. H. Merozoite surface protein 1 recognition of host glycophorin A mediates malaria parasite invasion of red blood cells. *Blood* **125**, 2704–2711 (2015).
31. Boyle, M. J., Richards, J. S., Gilson, P. R., Chai, W. & Beeson, J. G. Interactions with heparin-like molecules during erythrocyte invasion by *Plasmodium falciparum* merozoites. *Blood* **115**, 4559–4568 (2010).
32. Harris, P. K. *et al.* Molecular identification of a malaria merozoite surface sheddase. *PLoS Pathog.* **1**, 241–251 (2005).
33. Arredondo, S. A. *et al.* Structure of the *Plasmodium* 6-cysteine s48/45 domain. *Proc. Natl. Acad. Sci. U. S. A.* **109**, 6692–6697 (2012).
34. Velge-Roussel, F. *et al.* Epitopic analysis of the *Toxoplasma gondii* major surface antigen SAG1. *Mol. Biochem. Parasitol.* **66**, 31–38 (1994).
35. Sanders, P. R. *et al.* Distinct Protein Classes Including Novel Merozoite Surface Antigens in Raft-like Membranes of *Plasmodium falciparum*. *J. Biol. Chem.* **280**, 40169–40176 (2005).
36. Kaneko, O., Mu, J., Tsuboi, T., Su, X. & Torii, M. Gene structure and expression of a *Plasmodium falciparum* 220-kDa protein homologous to the *Plasmodium vivax* reticulocyte binding proteins. *Mol. Biochem. Parasitol.* **121**, 275–278 (2002).
37. Adams, J. H., Blair, P. L., Kaneko, O. & Peterson, D. S. An expanding ebl family of *Plasmodium falciparum*. *Trends Parasitol.* **17**, 297–299 (2001).
38. Gilberger, T.-W., Thompson, J. K., Reed, M. B., Good, R. T. & Cowman, A. F. The cytoplasmic domain of the *Plasmodium falciparum* ligand EBA-175 is essential for invasion but not protein trafficking. *J. Cell Biol.* **162**, 317–327 (2003).
39. Sim, B. K., Chitnis, C. E., Wasniowska, K., Hadley, T. J. & Miller, L. H. Receptor and ligand domains for invasion of erythrocytes by *Plasmodium falciparum*. *Science* **264**, 1941–1944 (1994).
40. Tham, W.-H. *et al.* Complement receptor 1 is the host erythrocyte receptor for *Plasmodium falciparum* Pfrh4 invasion ligand. *Proc. Natl. Acad. Sci. U. S. A.* **107**, 17327–17332 (2010).
41. Crosnier, C. *et al.* Basigin is a receptor essential for erythrocyte invasion by *Plasmodium falciparum*. *Nature* **480**, 534–537 (2011).
42. Bei, A. K. & Duraisingh, M. T. Functional analysis of erythrocyte determinants of *Plasmodium* infection. *Int. J. Parasitol.* **42**, 575–582 (2012).
43. Cowman, A. F. & Crabb, B. S. Invasion of red blood cells by malaria parasites. *Cell* **124**, 755–766 (2006).
44. Baum, J. *et al.* Reticulocyte-binding protein homologue 5 - an essential adhesin involved in invasion of human erythrocytes by *Plasmodium falciparum*. *Int. J. Parasitol.* **39**, 371–380 (2009).
45. Douglas, A. D. *et al.* A Pfrh5-based vaccine is efficacious against heterologous strain blood-stage *Plasmodium falciparum* infection in aotus monkeys. *Cell Host Microbe* **17**, 130–139 (2015).

46. Hayton, K. *et al.* Various PfrH5 polymorphisms can support Plasmodium falciparum invasion into the erythrocytes of owl monkeys and rats. *Mol. Biochem. Parasitol.* **187**, 103–110 (2013).
47. Wanaguru, M., Liu, W., Hahn, B. H., Rayner, J. C. & Wright, G. J. RH5-Basigin interaction plays a major role in the host tropism of Plasmodium falciparum. *Proc. Natl. Acad. Sci. U. S. A.* **110**, 20735–20740 (2013).
48. Singh, S., Alam, M. M., Pal-Bhowmick, I., Brzostowski, J. A. & Chitnis, C. E. Distinct external signals trigger sequential release of apical organelles during erythrocyte invasion by malaria parasites. *PLoS Pathog.* **6**, e1000746 (2010).
49. Alexander, D. L., Mital, J., Ward, G. E., Bradley, P. & Boothroyd, J. C. Identification of the moving junction complex of Toxoplasma gondii: a collaboration between distinct secretory organelles. *PLoS Pathog.* **1**, e17 (2005).
50. Lebrun, M. *et al.* The rhoptry neck protein RON4 re-localizes at the moving junction during Toxoplasma gondii invasion. *Cell. Microbiol.* **7**, 1823–1833 (2005).
51. Straub, K. W., Cheng, S. J., Sohn, C. S. & Bradley, P. J. Novel components of the Apicomplexan moving junction reveal conserved and coccidia-restricted elements. *Cell. Microbiol.* **11**, 590–603 (2009).
52. Besteiro, S., Michelin, A., Poncet, J., Dubremetz, J.-F. & Lebrun, M. Export of a Toxoplasma gondii rhoptry neck protein complex at the host cell membrane to form the moving junction during invasion. *PLoS Pathog.* **5**, e1000309 (2009).
53. Alexander, D. L., Arastu-Kapur, S., Dubremetz, J.-F. & Boothroyd, J. C. Plasmodium falciparum AMA1 binds a rhoptry neck protein homologous to TgRON4, a component of the moving junction in Toxoplasma gondii. *Eukaryot. Cell* **5**, 1169–1173 (2006).
54. Cao, J. *et al.* Rhoptry neck protein RON2 forms a complex with microneme protein AMA1 in Plasmodium falciparum merozoites. *Parasitol. Int.* **58**, 29–35 (2009).
55. Hehl, A. B. *et al.* Toxoplasma gondii homologue of plasmodium apical membrane antigen 1 is involved in invasion of host cells. *Infect. Immun.* **68**, 7078–7086 (2000).
56. Mital, J., Meissner, M., Soldati, D. & Ward, G. E. Conditional expression of Toxoplasma gondii apical membrane antigen-1 (TgAMA1) demonstrates that TgAMA1 plays a critical role in host cell invasion. *Mol. Biol. Cell* **16**, 4341–4349 (2005).
57. Lamarque, M. H. *et al.* Plasticity and redundancy among AMA-RON pairs ensure host cell entry of Toxoplasma parasites. *Nat. Commun.* **5**, 4098 (2014).
58. Aikawa, M., Miller, L. H., Johnson, J. & Rabbege, J. Erythrocyte entry by malarial parasites. A moving junction between erythrocyte and parasite. *J. Cell Biol.* **77**, 72–82 (1978).
59. Mordue, D. G., Desai, N., Dustin, M. & Sibley, L. D. Invasion by Toxoplasma gondii establishes a moving junction that selectively excludes host cell plasma membrane proteins on the basis of their membrane anchoring. *J. Exp. Med.* **190**, 1783–1792 (1999).
60. Muniz-Feliciano, L. *et al.* Toxoplasma gondii-induced activation of EGFR prevents autophagy protein-mediated killing of the parasite. *PLoS Pathog.* **9**, e1003809 (2013).
61. Frénal, K. & Soldati-Favre, D. Plasticity and Redundancy in Proteins Important for Toxoplasma Invasion. *PLoS Pathog.* **11**, e1005069 (2015).
62. Gaskins, E. *et al.* Identification of the membrane receptor of a class XIV myosin in Toxoplasma gondii. *J. Cell Biol.* **165**, 383–393 (2004).
63. Baum, J. *et al.* A conserved molecular motor drives cell invasion and gliding motility across malaria life cycle stages and other apicomplexan parasites. *J. Biol. Chem.* **281**, 5197–5208 (2006).
64. Jones, M. L., Kitson, E. L. & Rayner, J. C. Plasmodium falciparum erythrocyte invasion: a conserved myosin associated complex. *Mol. Biochem. Parasitol.* **147**, 74–84 (2006).
65. Frénal, K. *et al.* Functional dissection of the apicomplexan glideosome molecular architecture. *Cell Host Microbe* **8**, 343–357 (2010).
66. Egartner, S. *et al.* The toxoplasma Acto-MyoA motor complex is important but not essential for gliding motility and host cell invasion. *PLoS One* **9**, e91819 (2014).
67. Meissner, M., Schlüter, D. & Soldati, D. Role of Toxoplasma gondii myosin A in powering parasite gliding and host cell invasion. *Science* **298**, 837–840 (2002).

68. Siden-Kiamos, I. *et al.* Stage-specific depletion of myosin A supports an essential role in motility of malarial ookinetes. *Cell. Microbiol.* **13**, 1996–2006 (2011).
69. Håkansson, S., Morisaki, H., Heuser, J. & Sibley, L. D. Time-lapse video microscopy of gliding motility in *Toxoplasma gondii* reveals a novel, biphasic mechanism of cell locomotion. *Mol. Biol. Cell* **10**, 3539–3547 (1999).
70. Angrisano, F. *et al.* Spatial localisation of actin filaments across developmental stages of the malaria parasite. *PLoS One* **7**, e32188 (2012).
71. Jacot, D. *et al.* An Apicomplexan Actin-Binding Protein Serves as a Connector and Lipid Sensor to Coordinate Motility and Invasion. *Cell Host Microbe* **20**, 731–743 (2016).
72. Riglar, D. T. *et al.* Super-resolution dissection of coordinated events during malaria parasite invasion of the human erythrocyte. *Cell Host Microbe* **9**, 9–20 (2011).
73. Frénal, K., Marq, J.-B., Jacot, D., Polonais, V. & Soldati-Favre, D. Plasticity between MyoC- and MyoA-glideosomes: an example of functional compensation in *Toxoplasma gondii* invasion. *PLoS Pathog.* **10**, e1004504 (2014).
74. Tardieux, I. & Baum, J. Reassessing the mechanics of parasite motility and host-cell invasion. *J. Cell Biol.* **214**, 507–515 (2016).
75. Behnke, M. S. *et al.* Coordinated Progression through Two Subtranscriptomes Underlies the Tachyzoite Cycle of *Toxoplasma gondii*. *PLoS ONE* **5**, e12354 (2010).
76. White, M. W. & Suvorova, E. S. Apicomplexa Cell Cycles: Something Old, Borrowed, Lost, and New. *Trends Parasitol.* (2018). doi:10.1016/j.pt.2018.07.006
77. Riera, A. *et al.* From structure to mechanism-understanding initiation of DNA replication. *Genes Dev.* **31**, 1073–1088 (2017).
78. Matthews, H., Duffy, C. W. & Merrick, C. J. Checks and balances? DNA replication and the cell cycle in *Plasmodium*. *Parasit. Vectors* **11**, 216 (2018).
79. Deshmukh, A. S. *et al.* Regulation of *Plasmodium falciparum* Origin Recognition Complex subunit 1 (PfORC1) function through phosphorylation mediated by CDK-like kinase PK5. *Mol. Microbiol.* **98**, 17–33 (2015).
80. Patterson, S. *et al.* Pre-replication complex organization in the atypical DNA replication cycle of *Plasmodium falciparum*: characterization of the mini-chromosome maintenance (MCM) complex formation. *Mol. Biochem. Parasitol.* **145**, 50–59 (2006).
81. Stanojcic, S., Kuk, N., Ullah, I., Sterkers, Y. & Merrick, C. J. Single-molecule analysis reveals that DNA replication dynamics vary across the course of schizogony in the malaria parasite *Plasmodium falciparum*. *Sci. Rep.* **7**, 4003 (2017).
82. Aikawa, M. & Beaudoin, R. L. Studies on nuclear division of a malarial parasite under pyrimethamine treatment. *J. Cell Biol.* **39**, 749–754 (1968).
83. Francia, M. E. & Striepen, B. Cell division in apicomplexan parasites. *Nat. Rev. Microbiol.* **12**, 125–136 (2014).
84. Gerald, N., Mahajan, B. & Kumar, S. Mitosis in the Human Malaria Parasite *Plasmodium falciparum*. *Eukaryot. Cell* **10**, 474–482 (2011).
85. Mahajan, B. *et al.* Centrins, cell cycle regulation proteins in human malaria parasite *Plasmodium falciparum*. *J. Biol. Chem.* **283**, 31871–31883 (2008).
86. Prensier, G. & Slomianny, C. The karyotype of *Plasmodium falciparum* determined by ultrastructural serial sectioning and 3D reconstruction. *J. Parasitol.* **72**, 731–736 (1986).
87. Sinou, V., Boulard, Y., Grellier, P. & Schrevel, J. Host cell and malarial targets for docetaxel (Taxotere) during the erythrocytic development of *Plasmodium falciparum*. *J. Eukaryot. Microbiol.* **45**, 171–183 (1998).
88. Striepen, B., Jordan, C. N., Reiff, S. & van Dooren, G. G. Building the Perfect Parasite: Cell Division in Apicomplexa. *PLoS Pathog.* **3**, (2007).
89. Bannister, L. H., Hopkins, J. M., Fowler, R. E., Krishna, S. & Mitchell, G. H. Ultrastructure of rhoptry development in *Plasmodium falciparum* erythrocytic schizonts. *Parasitology* **121** (Pt 3), 273–287 (2000).
90. Das, S., Lemgruber, L., Tay, C. L., Baum, J. & Meissner, M. Multiple essential functions of *Plasmodium falciparum* actin-1 during malaria blood-stage development. *BMC Biol.* **15**, 70 (2017).

91. Agop-Nersesian, C. *et al.* Rab11A-controlled assembly of the inner membrane complex is required for completion of apicomplexan cytokinesis. *PLoS Pathog.* **5**, e1000270 (2009).
92. Absalon, S., Robbins, J. A. & Dvorin, J. D. An essential malaria protein defines the architecture of blood-stage and transmission-stage parasites. *Nat. Commun.* **7**, 11449 (2016).
93. Kono, M. *et al.* Pellicle formation in the malaria parasite. *J. Cell Sci.* **129**, 673–680 (2016).
94. Ferguson, D. J. P. *et al.* MORN1 has a conserved role in asexual and sexual development across the apicomplexa. *Eukaryot. Cell* **7**, 698–711 (2008).
95. Yeoh, S. *et al.* Subcellular Discharge of a Serine Protease Mediates Release of Invasive Malaria Parasites from Host Erythrocytes. *Cell* **131**, 1072–1083 (2007).
96. Thomas, J. A. *et al.* A protease cascade regulates release of the human malaria parasite *Plasmodium falciparum* from host red blood cells. *Nat. Microbiol.* **3**, 447–455 (2018).
97. Collins, C. R., Hackett, F., Atid, J., Tan, M. S. Y. & Blackman, M. J. The *Plasmodium falciparum* pseudoprotease SERA5 regulates the kinetics and efficiency of malaria parasite egress from host erythrocytes. *PLoS Pathog.* **13**, e1006453 (2017).
98. Glushakova, S. *et al.* Rounding precedes rupture and breakdown of vacuolar membranes minutes before malaria parasite egress from erythrocytes. *Cell. Microbiol.* e12868 (2018). doi:10.1111/cmi.12868
99. Collins, C. R. *et al.* Malaria Parasite cGMP-dependent Protein Kinase Regulates Blood Stage Merozoite Secretory Organelle Discharge and Egress. *PLoS Pathog.* **9**, e1003344 (2013).
100. Hale, V. L. *et al.* Parasitophorous vacuole poration precedes its rupture and rapid host erythrocyte cytoskeleton collapse in *Plasmodium falciparum* egress. *Proc. Natl. Acad. Sci.* 201619441 (2017). doi:10.1073/pnas.1619441114
101. Abkarian, M., Massiera, G., Berry, L., Roques, M. & Braun-Breton, C. A novel mechanism for egress of malarial parasites from red blood cells. *Blood* **117**, 4118–4124 (2011).
102. Collins, C. R. *et al.* Robust inducible Cre recombinase activity in the human malaria parasite *Plasmodium falciparum* enables efficient gene deletion within a single asexual erythrocytic growth cycle. *Mol. Microbiol.* **88**, 687–701 (2013).
103. Taylor, H. M. *et al.* The Malaria Parasite Cyclic GMP-Dependent Protein Kinase Plays a Central Role in Blood-Stage Schizogony. *Eukaryot. Cell* **9**, 37–45 (2010).
104. Das, S. *et al.* Processing of *Plasmodium falciparum* Merozoite Surface Protein MSP1 Activates a Spectrin-Binding Function Enabling Parasite Egress from RBCs. *Cell Host Microbe* **18**, 433–444 (2015).
105. Kafsack, B. F. C. & Carruthers, V. B. Apicomplexan perforin-like proteins. *Commun. Integr. Biol.* **3**, 18–23 (2010).
106. Garg, S. *et al.* Calcium-dependent permeabilization of erythrocytes by a perforin-like protein during egress of malaria parasites. *Nat. Commun.* **4**, 1736 (2013).
107. Braun-Breton, C. & Abkarian, M. Red Blood Cell Spectrin Skeleton in the Spotlight. *Trends Parasitol.* **32**, 90–92 (2016).
108. Glushakova, S., Mazar, J., Hohmann-Marriott, M. F., Hama, E. & Zimmerberg, J. Irreversible effect of cysteine protease inhibitors on the release of malaria parasites from infected erythrocytes. *Cell. Microbiol.* **11**, 95–105 (2009).
109. Blackman, M. J., Chappel, J. A., Shai, S. & Holder, A. A. A conserved parasite serine protease processes the *Plasmodium falciparum* merozoite surface protein-1. *Mol. Biochem. Parasitol.* **62**, 103–114 (1993).
110. Kafsack, B. F. C. *et al.* Rapid membrane disruption by a perforin-like protein facilitates parasite exit from host cells. *Science* **323**, 530–533 (2009).
111. Absalon, S. *et al.* Calcium-Dependent Protein Kinase 5 Is Required for Release of Egress-Specific Organelles in *Plasmodium falciparum*. *mBio* **9**, (2018).
112. Wirth, C. C. *et al.* Perforin-like protein PPLP2 permeabilizes the red blood cell membrane during egress of *Plasmodium falciparum* gametocytes. *Cell. Microbiol.* **16**, 709–733 (2014).
113. Oregon State University | Oregon State University. Available at: <http://oregonstate.edu/>. (Accessed: 1st March 2018)

114. Olsen, J. V. *et al.* Global, in vivo, and site-specific phosphorylation dynamics in signaling networks. *Cell* **127**, 635–648 (2006).
115. Cieřła, J., Frączyk, T. & Rode, W. Phosphorylation of basic amino acid residues in proteins: important but easily missed. *Acta Biochim. Pol.* **58**, 137–148 (2011).
116. Ward, P., Equinet, L., Packer, J. & Doerig, C. Protein kinases of the human malaria parasite *Plasmodium falciparum*: the kinome of a divergent eukaryote. *BMC Genomics* **5**, 79 (2004).
117. Anamika, null, Srinivasan, N. & Krupa, A. A genomic perspective of protein kinases in *Plasmodium falciparum*. *Proteins* **58**, 180–189 (2005).
118. Hanks, S. K. & Hunter, T. Protein kinases 6. The eukaryotic protein kinase superfamily: kinase (catalytic) domain structure and classification. *FASEB J. Off. Publ. Fed. Am. Soc. Exp. Biol.* **9**, 576–596 (1995).
119. Tong, K., Wang, Y. & Su, Z. Phosphotyrosine signalling and the origin of animal multicellularity. *Proc. Biol. Sci.* **284**, (2017).
120. Tewari, R. *et al.* The Systematic Functional Analysis of Plasmodium Protein Kinases Identifies Essential Regulators of Mosquito Transmission. *Cell Host Microbe* **8**, 377–387 (2010).
121. Solyakov, L. *et al.* Global kinomic and phospho-proteomic analyses of the human malaria parasite *Plasmodium falciparum*. *Nat. Commun.* **2**, 565 (2011).
122. Schneider, A. G. & Mercereau-Puijalon, O. A new Apicomplexa-specific protein kinase family: multiple members in *Plasmodium falciparum*, all with an export signature. *BMC Genomics* **6**, 30 (2005).
123. Nunes, M. C., Goldring, J. P. D., Doerig, C. & Scherf, A. A novel protein kinase family in *Plasmodium falciparum* is differentially transcribed and secreted to various cellular compartments of the host cell. *Mol. Microbiol.* **63**, 391–403 (2007).
124. Kats, L. M. *et al.* An exported kinase (FIKK4.2) that mediates virulence-associated changes in *Plasmodium falciparum*-infected red blood cells. *Int. J. Parasitol.* **44**, 319–328 (2014).
125. Harmon, A. C. *et al.* CDPKs – a kinase for every Ca²⁺ signal? *Trends Plant Sci.* **5**, 154–159 (2000).
126. Harper, J. F., Breton, G. & Harmon, A. Decoding Ca(2+) signals through plant protein kinases. *Annu. Rev. Plant Biol.* **55**, 263–288 (2004).
127. Dvorin, J. D. *et al.* A Plant-Like Kinase in *Plasmodium falciparum* Regulates Parasite Egress from Erythrocytes. *Science* **328**, 910–912 (2010).
128. Carvalho, T. G. *et al.* The ins and outs of phosphosignalling in *Plasmodium*: Parasite regulation and host cell manipulation. *Mol. Biochem. Parasitol.* **208**, 2–15 (2016).
129. Lasonder, E., Treeck, M., Alam, M. & Tobin, A. B. Insights into the *Plasmodium falciparum* schizont phospho-proteome. *Microbes Infect.* **14**, 811–819 (2012).
130. Pease, B. N. *et al.* Global analysis of protein expression and phosphorylation of three stages of *Plasmodium falciparum* intraerythrocytic development. *J. Proteome Res.* **12**, 4028–4045 (2013).
131. Aranda, S., Laguna, A. & de la Luna, S. DYRK family of protein kinases: evolutionary relationships, biochemical properties, and functional roles. *FASEB J. Off. Publ. Fed. Am. Soc. Exp. Biol.* **25**, 449–462 (2011).
132. Sharma, A. Protein tyrosine kinase activity in human malaria parasite *Plasmodium falciparum*. *Indian J. Exp. Biol.* **38**, 1222–1226 (2000).
133. Kumar, R. *et al.* A zinc-binding dual-specificity YVH1 phosphatase in the malaria parasite, *Plasmodium falciparum*, and its interaction with the nuclear protein, pescadillo. *Mol. Biochem. Parasitol.* **133**, 297–310 (2004).
134. Lasonder, E., Green, J. L., Grainger, M., Langsley, G. & Holder, A. A. Extensive differential protein phosphorylation as intraerythrocytic *Plasmodium falciparum* schizonts develop into extracellular invasive merozoites. *Proteomics* **15**, 2716–2729 (2015).
135. Treeck, M., Sanders, J. L., Elias, J. E. & Boothroyd, J. C. The phosphoproteomes of *Plasmodium falciparum* and *Toxoplasma gondii* reveal unusual adaptations within and beyond the parasites' boundaries. *Cell Host Microbe* **10**, 410–419 (2011).
136. Lasonder, E. *et al.* The *Plasmodium falciparum* Schizont Phosphoproteome Reveals Extensive Phosphatidylinositol and cAMP-Protein Kinase A Signaling. *J. Proteome Res.* **11**, 5323–5337 (2012).

137. Treeck, M., Sanders, J., Elias, J. & Boothroyd, J. The Phosphoproteomes of *Plasmodium falciparum* and *Toxoplasma gondii* Reveal Unusual Adaptations Within and Beyond the Parasites' Boundaries. *Cell Host Microbe* **10**, 410–419 (2011).
138. Reininger, L., Wilkes, J. M., Bourgade, H., Miranda-Saavedra, D. & Doerig, C. An essential Aurora-related kinase transiently associates with spindle pole bodies during *Plasmodium falciparum* erythrocytic schizogony. *Mol. Microbiol.* **79**, 205–221 (2011).
139. Robbins, J. A., Absalon, S., Streva, V. A. & Dvorin, J. D. The Malaria Parasite Cyclin H Homolog PfCyc1 Is Required for Efficient Cytokinesis in Blood-Stage *Plasmodium falciparum*. *mBio* **8**, (2017).
140. Donald, R. G. K. *et al.* Anticoccidial kinase inhibitors: Identification of protein kinase targets secondary to cGMP-dependent protein kinase. *Mol. Biochem. Parasitol.* **149**, 86–98 (2006).
141. Brochet, M. *et al.* Phosphoinositide Metabolism Links cGMP-Dependent Protein Kinase G to Essential Ca²⁺ Signals at Key Decision Points in the Life Cycle of Malaria Parasites. *PLoS Biol.* **12**, e1001806 (2014).
142. Iyer, G. R. *et al.* Calcium-dependent phosphorylation of *Plasmodium falciparum* serine repeat antigen 5 triggers merozoite egress. *J. Biol. Chem.* **293**, 9736–9746 (2018).
143. Moudy, R., Manning, T. J. & Beckers, C. J. The loss of cytoplasmic potassium upon host cell breakdown triggers egress of *Toxoplasma gondii*. *J. Biol. Chem.* **276**, 41492–41501 (2001).
144. Carruthers, V. B. & Sibley, L. D. Mobilization of intracellular calcium stimulates microneme discharge in *Toxoplasma gondii*. *Mol. Microbiol.* **31**, 421–428 (1999).
145. Lourido, S., Tang, K. & Sibley, L. D. Distinct signalling pathways control *Toxoplasma* egress and host-cell invasion. *EMBO J.* **31**, 4524–4534 (2012).
146. Dawn, A. *et al.* The Central Role of cAMP in Regulating *Plasmodium falciparum* Merozoite Invasion of Human Erythrocytes. *PLoS Pathog.* **10**, e1004520 (2014).
147. Brochet, M. *et al.* Phosphoinositide metabolism links cGMP-dependent protein kinase G to essential Ca²⁺ signals at key decision points in the life cycle of malaria parasites. *PLoS Biol.* **12**, e1001806 (2014).
148. Brochet, M. & Billker, O. Calcium signalling in malaria parasites. *Mol. Microbiol.* **100**, 397–408 (2016).
149. Bansal, A. *et al.* Characterization of *Plasmodium falciparum* Calcium-dependent Protein Kinase 1 (PfCDPK1) and Its Role in Microneme Secretion during Erythrocyte Invasion. *J. Biol. Chem.* **288**, 1590–1602 (2013).
150. Kumar, S. *et al.* PfCDPK1 mediated signaling in erythrocytic stages of *Plasmodium falciparum*. *Nat. Commun.* **8**, (2017).
151. Bullen, H. E. *et al.* Phosphatidic Acid-Mediated Signaling Regulates Microneme Secretion in *Toxoplasma*. *Cell Host Microbe* **19**, 349–360 (2016).
152. Ono, T. *et al.* Adenylyl Cyclase ? and cAMP Signaling Mediate *Plasmodium* Sporozoite Apical Regulated Exocytosis and Hepatocyte Infection. *PLoS Pathog.* **4**, e1000008 (2008).
153. Gilson, P. R. & Crabb, B. S. Morphology and kinetics of the three distinct phases of red blood cell invasion by *Plasmodium falciparum* merozoites. *Int. J. Parasitol.* **39**, 91–96 (2009).
154. Treeck, M. *et al.* Functional Analysis of the Leading Malaria Vaccine Candidate AMA-1 Reveals an Essential Role for the Cytoplasmic Domain in the Invasion Process. *PLoS Pathog.* **5**, e1000322 (2009).
155. Leykauf, K. *et al.* Protein Kinase A Dependent Phosphorylation of Apical Membrane Antigen 1 Plays an Important Role in Erythrocyte Invasion by the Malaria Parasite. *PLoS Pathog.* **6**, e1000941 (2010).
156. Prinz, B. *et al.* Hierarchical phosphorylation of apical membrane antigen 1 is required for efficient red blood cell invasion by malaria parasites. *Sci. Rep.* **6**, 34479 (2016).
157. Krishnamurthy, S. *et al.* Not a Simple Tether: Binding of *Toxoplasma gondii* AMA1 to RON2 during Invasion Protects AMA1 from Rhomboid-Mediated Cleavage and Leads to Dephosphorylation of Its Cytosolic Tail. *mBio* **7**, (2016).
158. Tham, W.-H. *et al.* *Plasmodium falciparum* Adhesins Play an Essential Role in Signalling and Activation of Invasion into Human Erythrocytes. *PLoS Pathog.* **11**, e1005343 (2015).

159. Engelberg, K. *et al.* Specific phosphorylation of the PfRh2b invasion ligand of Plasmodium falciparum. *Biochem. J.* **452**, 457–466 (2013).
160. Paul, A. S. *et al.* Parasite Calcineurin Regulates Host Cell Recognition and Attachment by Apicomplexans. *Cell Host Microbe* **18**, 49–60 (2015).
161. Lourido, S. & Moreno, S. N. J. The calcium signaling toolkit of the Apicomplexan parasites Toxoplasma gondii and Plasmodium spp. *Cell Calcium* **57**, 186–193 (2015).
162. Thomas, D. C., Ahmed, A., Gilberger, T. W. & Sharma, P. Regulation of Plasmodium falciparum glideosome associated protein 45 (PfGAP45) phosphorylation. *PLoS One* **7**, e35855 (2012).
163. Jacot, D., Fréna, K., Marq, J.-B., Sharma, P. & Soldati-Favre, D. Assessment of phosphorylation in Toxoplasma glideosome assembly and function. *Cell. Microbiol.* **16**, 1518–1532 (2014).
164. Vaid, A., Thomas, D. C. & Sharma, P. Role of Ca²⁺/calmodulin-PfPKB signaling pathway in erythrocyte invasion by Plasmodium falciparum. *J. Biol. Chem.* **283**, 5589–5597 (2008).
165. Alam, M. M. *et al.* Phosphoproteomics reveals malaria parasite Protein Kinase G as a signalling hub regulating egress and invasion. *Nat. Commun.* **6**, 7285 (2015).
166. Douse, C. H. *et al.* Regulation of the Plasmodium motor complex: phosphorylation of myosin A tail-interacting protein (MTIP) loosens its grip on MyoA. *J. Biol. Chem.* **287**, 36968–36977 (2012).
167. Green, J. L. *et al.* The motor complex of Plasmodium falciparum: phosphorylation by a calcium-dependent protein kinase. *J. Biol. Chem.* **283**, 30980–30989 (2008).
168. Doerig, C., Endicott, J. & Chakrabarti, D. Cyclin-dependent kinase homologues of Plasmodium falciparum. *Int. J. Parasitol.* **32**, 1575–1585 (2002).
169. Ganter, M. *et al.* Plasmodium falciparum CRK4 directs continuous rounds of DNA replication during schizogony. *Nat. Microbiol.* **2**, 17017 (2017).
170. Data Set Pfa3D7 real-time transcription and decay. Available at: http://plasmodb.org/plasmo/app/record/dataset/DS_0fa4237b4b. (Accessed: 16th August 2018)
171. Van Biljon, R. A. *et al.* Inducing controlled cell cycle arrest and re-entry during asexual proliferation of Plasmodium falciparum malaria parasites. (2018). doi:10.1101/368431
172. Balu, B. *et al.* Atypical mitogen-activated protein kinase phosphatase implicated in regulating transition from pre-S-Phase asexual intraerythrocytic development of Plasmodium falciparum. *Eukaryot. Cell* **12**, 1171–1178 (2013).
173. Vigneron, S. *et al.* The master Greatwall kinase, a critical regulator of mitosis and meiosis. *Int. J. Dev. Biol.* **60**, 245–254 (2016).
174. Berry, L. *et al.* Toxoplasma gondii chromosomal passenger complex is essential for the organization of a functional mitotic spindle: a prerequisite for productive endodyogeny. *Cell. Mol. Life Sci. CMLS* (2018). doi:10.1007/s00018-018-2889-6
175. Dorin-Semlat, D. *et al.* Plasmodium falciparum NIMA-related kinase Pfnek-1: sex specificity and assessment of essentiality for the erythrocytic asexual cycle. *Microbiol. Read. Engl.* **157**, 2785–2794 (2011).
176. Reininger, L. *et al.* An essential role for the Plasmodium Nek-2 Nima-related protein kinase in the sexual development of malaria parasites. *J. Biol. Chem.* **284**, 20858–20868 (2009).
177. Li, H. & Lykotrafitis, G. Erythrocyte membrane model with explicit description of the lipid bilayer and the spectrin network. *Biophys. J.* **107**, 642–653 (2014).
178. Fowler, V. M. The human erythrocyte plasma membrane: a Rosetta Stone for decoding membrane-cytoskeleton structure. *Curr. Top. Membr.* **72**, 39–88 (2013).
179. Manno, S., Takakuwa, Y. & Mohandas, N. Modulation of erythrocyte membrane mechanical function by protein 4.1 phosphorylation. *J. Biol. Chem.* **280**, 7581–7587 (2005).
180. Zuccala, E. S. *et al.* Quantitative phospho-proteomics reveals the Plasmodium merozoite triggers pre-invasion host kinase modification of the red cell cytoskeleton. *Sci. Rep.* **6**, (2016).
181. Bouyer, G. *et al.* Plasmodium falciparum infection induces dynamic changes in the erythrocyte phospho-proteome. *Blood Cells. Mol. Dis.* **58**, 35–44 (2016).
182. Ferru, E. *et al.* Regulation of membrane-cytoskeletal interactions by tyrosine phosphorylation of erythrocyte band 3. *Blood* **117**, 5998–6006 (2011).

183. Fernandez-Pol, S. *et al.* A bacterial phosphatase-like enzyme of the malaria parasite *Plasmodium falciparum* possesses tyrosine phosphatase activity and is implicated in the regulation of band 3 dynamics during parasite invasion. *Eukaryot. Cell* **12**, 1179–1191 (2013).
184. Chishti, A. H. *et al.* Phosphorylation of protein 4.1 in *Plasmodium falciparum*-infected human red blood cells. *Blood* **83**, 3339–3345 (1994).
185. Pantaleo, A. *et al.* Analysis of changes in tyrosine and serine phosphorylation of red cell membrane proteins induced by *P. falciparum* growth. *PROTEOMICS* **10**, 3469–3479 (2010).
186. Lasonder, E., Treeck, M., Alam, M. & Tobin, A. B. Insights into the *Plasmodium falciparum* schizont phospho-proteome. *Microbes Infect.* **14**, 811–819 (2012).
187. Brunati, A. M. *et al.* Sequential phosphorylation of protein band 3 by Syk and Lyn tyrosine kinases in intact human erythrocytes: identification of primary and secondary phosphorylation sites. *Blood* **96**, 1550–1557 (2000).
188. Pantaleo, A. *et al.* Syk Inhibitors interfere with erythrocyte membrane modification during *P. falciparum* growth and suppress parasite egress. *Blood* blood-2016-11-748053 (2017). doi:10.1182/blood-2016-11-748053
189. Sicard, A. *et al.* Activation of a PAK-MEK signalling pathway in malaria parasite-infected erythrocytes. *Cell. Microbiol.* **13**, 836–845 (2011).
190. Shi, Y. Serine/threonine phosphatases: mechanism through structure. *Cell* **139**, 468–484 (2009).
191. Lillo, C. *et al.* Protein phosphatases PP2A, PP4 and PP6: mediators and regulators in development and responses to environmental cues. *Plant Cell Environ.* **37**, 2631–2648 (2014).
192. Rebelo, S., Santos, M., Martins, F., da Cruz e Silva, E. F. & da Cruz e Silva, O. A. B. Protein phosphatase 1 is a key player in nuclear events. *Cell. Signal.* **27**, 2589–2598 (2015).
193. Moorhead, G. B. G., De Wever, V., Templeton, G. & Kerk, D. Evolution of protein phosphatases in plants and animals. *Biochem. J.* **417**, 401–409 (2009).
194. Mai, B., Frey, G., Swanson, R. V., Mathur, E. J. & Stetter, K. O. Molecular cloning and functional expression of a protein-serine/threonine phosphatase from the hyperthermophilic archaeon *Pyrodictium abyssi* TAG11. *J. Bacteriol.* **180**, 4030–4035 (1998).
195. Chu, Y., Williams, N. H. & Hengge, A. C. Transition States and Control of Substrate Preference in the Promiscuous Phosphatase PP1. *Biochemistry* **56**, 3923–3933 (2017).
196. Goldberg, J. *et al.* Three-dimensional structure of the catalytic subunit of protein serine/threonine phosphatase-1. *Nature* **376**, 745–753 (1995).
197. Klee, C. B., Crouch, T. H. & Krinks, M. H. Calcineurin: a calcium- and calmodulin-binding protein of the nervous system. *Proc. Natl. Acad. Sci. U. S. A.* **76**, 6270–6273 (1979).
198. Shen, X. *et al.* The secondary structure of calcineurin regulatory region and conformational change induced by calcium/calmodulin binding. *J. Biol. Chem.* **283**, 11407–11413 (2008).
199. Fagerholm, A. E., Habrant, D. & Koskinen, A. M. P. Calyculins and related marine natural products as serine-threonine protein phosphatase PP1 and PP2A inhibitors and total syntheses of calyculin A, B, and C. *Mar. Drugs* **8**, 122–172 (2010).
200. Dounay, A. B. & Forsyth, C. J. Okadaic acid: the archetypal serine/threonine protein phosphatase inhibitor. *Curr. Med. Chem.* **9**, 1939–1980 (2002).
201. Calyculins and related marine natural products as serine-threonine protein phosphatase PP1 and PP2A inhibitors and total syntheses of calyculin A, ... - PubMed - NCBI. Available at: <https://www.ncbi.nlm.nih.gov/pubmed/?term=calyculins+and+related+marine+products>. (Accessed: 30th September 2017)
202. Paul, V. J., Arthur, K. E., Ritson-Williams, R., Ross, C. & Sharp, K. Chemical defenses: from compounds to communities. *Biol. Bull.* **213**, 226–251 (2007).
203. Wakimoto, T. *et al.* Calyculin biogenesis from a pyrophosphate protoxin produced by a sponge symbiont. *Nat. Chem. Biol.* **10**, 648–655 (2014).
204. Kita, A. *et al.* Crystal structure of the complex between calyculin A and the catalytic subunit of protein phosphatase 1. *Struct. Lond. Engl.* **1993** **10**, 715–724 (2002).
205. Prickett, T. D. & Brautigan, D. L. The alpha4 regulatory subunit exerts opposing allosteric effects on protein phosphatases PP6 and PP2A. *J. Biol. Chem.* **281**, 30503–30511 (2006).

206. Hastie, C. J. & Cohen, P. T. W. Purification of protein phosphatase 4 catalytic subunit: inhibition by the antitumour drug fostriecin and other tumour suppressors and promoters. *FEBS Lett.* **431**, 357–361 (1998).
207. Lubert, E. J., Hong, Y. & Sarge, K. D. Interaction between Protein Phosphatase 5 and the A subunit of Protein Phosphatase 2A EVIDENCE FOR A HETEROTRIMERIC FORM OF PROTEIN PHOSPHATASE 5. *J. Biol. Chem.* **276**, 38582–38587 (2001).
208. Huang, H. B., Horiuchi, A., Goldberg, J., Greengard, P. & Nairn, A. C. Site-directed mutagenesis of amino acid residues of protein phosphatase 1 involved in catalysis and inhibitor binding. *Proc. Natl. Acad. Sci. U. S. A.* **94**, 3530–3535 (1997).
209. Kutuzov, M. A. & Andreeva, A. V. Protein Ser/Thr phosphatases with kelch-like repeat domains. *Cell. Signal.* **14**, 745–750 (2002).
210. Mora-García, S. *et al.* Nuclear protein phosphatases with Kelch-repeat domains modulate the response to brassinosteroids in Arabidopsis. *Genes Dev.* **18**, 448–460 (2004).
211. Andreeva, A. V. & Kutuzov, M. A. Widespread presence of ‘bacterial-like’ PPP phosphatases in eukaryotes. *BMC Evol. Biol.* **4**, 47 (2004).
212. Uhrig, R. G., Kerk, D. & Moorhead, G. B. Evolution of bacterial-like phosphoprotein phosphatases in photosynthetic eukaryotes features ancestral mitochondrial or archaeal origin and possible lateral gene transfer. *Plant Physiol.* **163**, 1829–1843 (2013).
213. Uhrig, R. G. & Moorhead, G. B. Two ancient bacterial-like PPP family phosphatases from Arabidopsis are highly conserved plant proteins that possess unique properties. *Plant Physiol.* **157**, 1778–1792 (2011).
214. Kerk, D., Uhrig, R. G. & Moorhead, G. B. Bacterial-like PPP protein phosphatases: novel sequence alterations in pathogenic eukaryotes and peculiar features of bacterial sequence similarity. *Plant Signal. Behav.* **8**, e27365 (2013).
215. Heiny, S. R., Pautz, S., Recker, M. & Przyborski, J. M. Protein Traffic to the Plasmodium falciparum apicoplast: evidence for a sorting branch point at the Golgi. *Traffic Cph. Den.* **15**, 1290–1304 (2014).
216. Herrmann, J. M. & Neupert, W. Protein transport into mitochondria. *Curr. Opin. Microbiol.* **3**, 210–214 (2000).
217. Tsuruta, H. *et al.* Purification and some characteristics of phosphatase of a psychrophile. *J. Biochem. (Tokyo)* **123**, 219–225 (1998).
218. Tsuruta, H., Mikami, B., Yamamoto, C. & Yamagata, H. The role of group bulkiness in the catalytic activity of psychrophile cold-active protein tyrosine phosphatase. *FEBS J.* **275**, 4317–4328 (2008).
219. Tsuruta, H., Mikami, B. & Aizono, Y. Crystal structure of cold-active protein-tyrosine phosphatase from a psychrophile, *Shewanella* sp. *J. Biochem. (Tokyo)* **137**, 69–77 (2005).
220. Tsuruta, H., Tamura, J., Yamagata, H. & Aizono, Y. Specification of amino acid residues essential for the catalytic reaction of cold-active protein-tyrosine phosphatase of a psychrophile, *Shewanella* sp. *Biosci. Biotechnol. Biochem.* **68**, 440–443 (2004).
221. Tsuruta, H., Mikami, B., Yamamoto, C. & Yamagata, H. The role of group bulkiness in the catalytic activity of psychrophile cold-active protein tyrosine phosphatase. *FEBS J.* **275**, 4317–4328 (2008).
222. Tsuruta, H. & Aizono, Y. Enzymatical properties of psychrophilic phosphatase I. *J. Biochem. (Tokyo)* **125**, 690–695 (1999).
223. Rusnak, F. & Mertz, P. Calcineurin: form and function. *Physiol. Rev.* **80**, 1483–1521 (2000).
224. Tsuruta, H. & Aizono, Y. Catalytic efficiency and some structural properties of cold-active protein-tyrosine-phosphatase. *J. Biochem. (Tokyo)* **133**, 225–230 (2003).
225. Walton, K. M. & Dixon, J. E. Protein tyrosine phosphatases. *Annu. Rev. Biochem.* **62**, 101–120 (1993).
226. Y, L. G. and W. Functional diversity of mammalian type 2C protein phosphatase isoforms: new tales from an old family. - PubMed - NCBI. Available at: <https://www.ncbi.nlm.nih.gov/pubmed/?term=Functional+diversity+of+mammalian+type+2C+proteins+phosphatase+isoforms%3A>. (Accessed: 25th January 2018)

227. Yang, C. & Arrizabalaga, G. The serine/threonine phosphatases of apicomplexan parasites. *Mol. Microbiol.* **106**, 1–21 (2017).
228. Das, A. K., Helps, N. R., Cohen, P. T. & Barford, D. Crystal structure of the protein serine/threonine phosphatase 2C at 2.0 Å resolution. *EMBO J.* **15**, 6798–6809 (1996).
229. Shi, Y. Serine/threonine phosphatases: mechanism through structure. *Cell* **139**, 468–484 (2009).
230. Pan, C. *et al.* The catalytic role of the M2 metal ion in PP2C α . *Sci. Rep.* **5**, (2015).
231. Tanoue, K. *et al.* Binding of a third metal ion by the human phosphatases PP2C α and Wip1 is required for phosphatase activity. *Biochemistry* **52**, 5830–5843 (2013).
232. Bellinzoni, M., Wehenkel, A., Shepard, W. & Alzari, P. M. Insights into the catalytic mechanism of PPM Ser/Thr phosphatases from the atomic resolution structures of a mycobacterial enzyme. *Struct. Lond. Engl.* **15**, 863–872 (2007).
233. Jackson, M. D., Fjeld, C. C. & Denu, J. M. Probing the function of conserved residues in the serine/threonine phosphatase PP2C α . *Biochemistry* **42**, 8513–8521 (2003).
234. Yeo, M. & Lin, P. S. Functional characterization of small CTD phosphatases. *Methods Mol. Biol. Clifton NJ* **365**, 335–346 (2007).
235. Hsin, J.-P. & Manley, J. L. The RNA polymerase II CTD coordinates transcription and RNA processing. *Genes Dev.* **26**, 2119–2137 (2012).
236. Yeo, M., Lin, P. S., Dahmus, M. E. & Gill, G. N. A novel RNA polymerase II C-terminal domain phosphatase that preferentially dephosphorylates serine 5. *J. Biol. Chem.* **278**, 26078–26085 (2003).
237. Anderson, S. F., Schlegel, B. P., Nakajima, T., Wolpin, E. S. & Parvin, J. D. BRCA1 protein is linked to the RNA polymerase II holoenzyme complex via RNA helicase A. *Nat. Genet.* **19**, 254–256 (1998).
238. Zhang, Y. *et al.* Determinants for Dephosphorylation of the RNA Polymerase II C-Terminal Domain by Scp1. *Mol. Cell* **24**, 759–770 (2006).
239. Hale, A. J., ter Steege, E. & den Hertog, J. Recent advances in understanding the role of protein-tyrosine phosphatases in development and disease. *Dev. Biol.* **428**, 283–292 (2017).
240. Andreeva, A. V. & Kutuzov, M. A. Protozoan protein tyrosine phosphatases. *Int. J. Parasitol.* **38**, 1279–1295 (2008).
241. Heneberg, P. Use of protein tyrosine phosphatase inhibitors as promising targeted therapeutic drugs. *Curr. Med. Chem.* **16**, 706–733 (2009).
242. Kuznetsov, V. I., Hengge, A. C. & Johnson, S. J. New aspects of the phosphatase VHZ revealed by a high-resolution structure with vanadate and substrate screening. *Biochemistry* **51**, 9869–9879 (2012).
243. Denu, J. M., Lohse, D. L., Vijayalakshmi, J., Saper, M. A. & Dixon, J. E. Visualization of intermediate and transition-state structures in protein-tyrosine phosphatase catalysis. *Proc. Natl. Acad. Sci. U. S. A.* **93**, 2493–2498 (1996).
244. Grzyska, P. K., Kim, Y., Jackson, M. D., Hengge, A. C. & Denu, J. M. Probing the transition-state structure of dual-specificity protein phosphatases using a physiological substrate mimic. *Biochemistry* **43**, 8807–8814 (2004).
245. Gallego, M. & Virshup, D. M. Protein serine/threonine phosphatases: life, death, and sleeping. *Curr. Opin. Cell Biol.* **17**, 197–202 (2005).
246. Ceulemans, H., Stalmans, W. & Bollen, M. Regulator-driven functional diversification of protein phosphatase-1 in eukaryotic evolution. *BioEssays News Rev. Mol. Cell. Dev. Biol.* **24**, 371–381 (2002).
247. Bollen, M., Peti, W., Ragusa, M. J. & Beullens, M. The extended PP1 toolkit: designed to create specificity. *Trends Biochem. Sci.* **35**, 450–458 (2010).
248. Peti, W., Nairn, A. C. & Page, R. Structural Basis for Protein Phosphatase 1 Regulation and Specificity. *FEBS J.* **280**, 596–611 (2013).
249. Hendrickx, A. *et al.* Docking motif-guided mapping of the interactome of protein phosphatase-1. *Chem. Biol.* **16**, 365–371 (2009).
250. Meiselbach, H., Sticht, H. & Enz, R. Structural analysis of the protein phosphatase 1 docking motif: molecular description of binding specificities identifies interacting proteins. *Chem. Biol.* **13**, 49–59 (2006).

251. Pinheiro, A. S., Marsh, J. A., Forman-Kay, J. D. & Peti, W. Structural signature of the MYPT1-PP1 interaction. *J. Am. Chem. Soc.* **133**, 73–80 (2011).
252. Xu, Y., Chen, Y., Zhang, P., Jeffrey, P. D. & Shi, Y. Structure of a protein phosphatase 2A holoenzyme: insights into B55-mediated Tau dephosphorylation. *Mol. Cell* **31**, 873–885 (2008).
253. Gong, C. X. *et al.* Phosphorylation of microtubule-associated protein tau is regulated by protein phosphatase 2A in mammalian brain. Implications for neurofibrillary degeneration in Alzheimer's disease. *J. Biol. Chem.* **275**, 5535–5544 (2000).
254. Bradshaw, N. *et al.* A widespread family of serine/threonine protein phosphatases shares a common regulatory switch with proteasomal proteases. *eLife* **6**,
255. Bradshaw, N. *et al.* A widespread family of serine/threonine protein phosphatases shares a common regulatory switch with proteasomal proteases. *eLife* **6**, (2017).
256. Tonks, N. K. Protein tyrosine phosphatases--from housekeeping enzymes to master regulators of signal transduction. *FEBS J.* **280**, 346–378 (2013).
257. Ostman, A., Frijhoff, J., Sandin, A. & Böhmer, F.-D. Regulation of protein tyrosine phosphatases by reversible oxidation. *J. Biochem. (Tokyo)* **150**, 345–356 (2011).
258. Frangioni, J. V., Beahm, P. H., Shifrin, V., Jost, C. A. & Neel, B. G. The nontransmembrane tyrosine phosphatase PTP-1B localizes to the endoplasmic reticulum via its 35 amino acid C-terminal sequence. *Cell* **68**, 545–560 (1992).
259. Tonks, N. K. PTP1B: from the sidelines to the front lines! *FEBS Lett.* **546**, 140–148 (2003).
260. Salmeen, A. *et al.* Redox regulation of protein tyrosine phosphatase 1B involves a sulphenylamide intermediate. *Nature* **423**, 769–773 (2003).
261. Mahadev, K., Zilbering, A., Zhu, L. & Goldstein, B. J. Insulin-stimulated hydrogen peroxide reversibly inhibits protein-tyrosine phosphatase 1b in vivo and enhances the early insulin action cascade. *J. Biol. Chem.* **276**, 21938–21942 (2001).
262. den Hertog, J., Ostman, A. & Böhmer, F.-D. Protein tyrosine phosphatases: regulatory mechanisms. *FEBS J.* **275**, 831–847 (2008).
263. Schwertassek, U. *et al.* Reactivation of oxidized PTP1B and PTEN by Thioredoxin 1. *FEBS J.* **281**, 3545–3558 (2014).
264. Wilkes, J. M. & Doerig, C. The protein-phosphatome of the human malaria parasite *Plasmodium falciparum*. *BMC Genomics* **9**, 412 (2008).
265. Pandey, R. *et al.* Genome wide in silico analysis of *Plasmodium falciparum* phosphatome. *BMC Genomics* **15**, 1024 (2014).
266. Guttery, D. S. *et al.* Genome-wide functional analysis of *Plasmodium* protein phosphatases reveals key regulators of parasite development and differentiation. *Cell Host Microbe* **16**, 128–140 (2014).
267. Uwanogho, D. A. *et al.* Molecular cloning, chromosomal mapping, and developmental expression of a novel protein tyrosine phosphatase-like gene. *Genomics* **62**, 406–416 (1999).
268. Alonso, A. & Pulido, R. The extended human PTPome: a growing tyrosine phosphatase family. *FEBS J.* **283**, 1404–1429 (2016).
269. Yang, C. & Arrizabalaga, G. The serine/threonine phosphatases of apicomplexan parasites. *Mol. Microbiol.* **106**, 1–21 (2017).
270. Guttery, D. S. *et al.* A Unique Protein Phosphatase with Kelch-Like Domains (PPKL) in *Plasmodium* Modulates Ookinete Differentiation, Motility and Invasion. *PLoS Pathog.* **8**, e1002948 (2012).
271. Kutuzov, M. A. & Andreeva, A. V. Protein Ser/Thr phosphatases of parasitic protozoa. *Mol. Biochem. Parasitol.* **161**, 81–90 (2008).
272. Ward, P., Equinet, L., Packer, J. & Doerig, C. Protein kinases of the human malaria parasite *Plasmodium falciparum*: the kinome of a divergent eukaryote. *BMC Genomics* **5**, 79 (2004).
273. Mamoun, C. B., Sullivan, D. J., Banerjee, R. & Goldberg, D. E. Identification and characterization of an unusual double serine/threonine protein phosphatase 2C in the malaria parasite *Plasmodium falciparum*. *J. Biol. Chem.* **273**, 11241–11247 (1998).

274. Mamoun, C. B. & Goldberg, D. E. Plasmodium protein phosphatase 2C dephosphorylates translation elongation factor 1beta and inhibits its PKC-mediated nucleotide exchange activity in vitro. *Mol. Microbiol.* **39**, 973–981 (2001).
275. Pendyala, P. R. *et al.* Characterization of a PRL protein tyrosine phosphatase from Plasmodium falciparum☆. *Mol. Biochem. Parasitol.* **158**, 1–10 (2008).
276. Kumar, R., Adams, B., Oldenburg, A., Musiyenko, A. & Barik, S. Characterisation and expression of a PP1 serine/threonine protein phosphatase (PfPP1) from the malaria parasite, Plasmodium falciparum: demonstration of its essential role using RNA interference. *Malar. J.* **1**, 5 (2002).
277. Blisnick, T., Vincensini, L., Fall, G. & Braun-Breton, C. Protein phosphatase 1, a Plasmodium falciparum essential enzyme, is exported to the host cell and implicated in the release of infectious merozoites. *Cell. Microbiol.* **8**, 591–601 (2006).
278. Daher, W. *et al.* Regulation of protein phosphatase type 1 and cell cycle progression by PfLRR1, a novel leucine-rich repeat protein of the human malaria parasite Plasmodium falciparum. *Mol. Microbiol.* **60**, 578–590 (2006).
279. Fréville, A. *et al.* Plasmodium falciparum encodes a conserved active inhibitor-2 for Protein Phosphatase type 1: perspectives for novel anti-plasmodial therapy. *BMC Biol.* **11**, 80 (2013).
280. Fréville, A. *et al.* Plasmodium falciparum inhibitor-3 homolog increases protein phosphatase type 1 activity and is essential for parasitic survival. *J. Biol. Chem.* **287**, 1306–1321 (2012).
281. Hollin, T., De Witte, C., Lenne, A., Pierrot, C. & Khalife, J. Analysis of the interactome of the Ser/Thr Protein Phosphatase type 1 in Plasmodium falciparum. *BMC Genomics* **17**, 246 (2016).
282. Tellier, G. *et al.* Identification of Plasmodium falciparum Translation Initiation eIF2β Subunit: Direct Interaction with Protein Phosphatase Type 1. *Front. Microbiol.* **7**, (2016).
283. Dobson, S. *et al.* Characterization of protein Ser/Thr phosphatases of the malaria parasite, Plasmodium falciparum: inhibition of the parasitic calcineurin by cyclophilin-cyclosporin complex. *Mol. Biochem. Parasitol.* **99**, 167–181 (1999).
284. Dobson, S. *et al.* Characterization of a unique aspartate-rich protein of the SET/TAF-family in the human malaria parasite, Plasmodium falciparum, which inhibits protein phosphatase 2A. *Mol. Biochem. Parasitol.* **126**, 239–250 (2003).
285. Vandomme, A. *et al.* PhosphoTyrosyl phosphatase activator of Plasmodium falciparum: identification of its residues involved in binding to and activation of PP2A. *Int. J. Mol. Sci.* **15**, 2431–2453 (2014).
286. Philip, N. & Waters, A. P. Conditional Degradation of Plasmodium Calcineurin Reveals Functions in Parasite Colonization of both Host and Vector. *Cell Host Microbe* **18**, 122–131 (2015).
287. Singh, S., More, K. R. & Chitnis, C. E. Role of calcineurin and actin dynamics in regulated secretion of microneme proteins in Plasmodium falciparum merozoites during erythrocyte invasion. *Cell. Microbiol.* **16**, 50–63 (2014).
288. Dobson, S., Kar, B., Kumar, R., Adams, B. & Barik, S. A novel tetratricopeptide repeat (TPR) containing PP5 serine/threonine protein phosphatase in the malaria parasite, Plasmodium falciparum. *BMC Microbiol.* **1**, 31 (2001).
289. Dobson, S., Bracchi, V., Chakrabarti, D. & Barik, S. Characterization of a novel serine/threonine protein phosphatase (PfPPJ) from the malaria parasite, Plasmodium falciparum. *Mol. Biochem. Parasitol.* **115**, 29–39 (2001).
290. Philip, N., Vaikkinen, H. J., Tetley, L. & Waters, A. P. A unique Kelch domain phosphatase in Plasmodium regulates ookinete morphology, motility and invasion. *PLoS One* **7**, e44617 (2012).
291. Patzewitz, E.-M. *et al.* An ancient protein phosphatase, SHLP1, is critical to microneme development in Plasmodium ookinetes and parasite transmission. *Cell Rep.* **3**, 622–629 (2013).
292. Miliu, A., Lebrun, M., Braun-Breton, C. & Lamarque, M. H. Shelph2, a bacterial-like phosphatase of the malaria parasite Plasmodium falciparum, is dispensable during asexual blood stage. *PLoS One* **12**, e0187073 (2017).
293. Zhang, M., Mishra, S., Sakthivel, R., Fontoura, B. M. A. & Nussenzweig, V. UIS2: A Unique Phosphatase Required for the Development of Plasmodium Liver Stages. *PLoS Pathog.* **12**, e1005370 (2016).

294. Guerra, A. J. & Carruthers, V. B. Structural Features of Apicomplexan Pore-Forming Proteins and Their Roles in Parasite Cell Traversal and Egress. *Toxins* **9**, (2017).
295. Janse, C. J., van der Klooster, P. F., van der Kaay, H. J., van der Ploeg, M. & Overdulve, J. P. DNA synthesis in *Plasmodium berghei* during asexual and sexual development. *Mol. Biochem. Parasitol.* **20**, 173–182 (1986).
296. Kim, T.-W., Guan, S., Burlingame, A. L. & Wang, Z.-Y. The CDG1 kinase mediates brassinosteroid signal transduction from BRI1 receptor kinase to BSU1 phosphatase and GSK3-like kinase BIN2. *Mol. Cell* **43**, 561–571 (2011).
297. Klug, D. & Frischknecht, F. Motility precedes egress of malaria parasites from oocysts. *eLife* **6**, (2017).
298. Ghosh, A. K. & Jacobs-Lorena, M. Plasmodium sporozoite invasion of the mosquito salivary gland. *Curr. Opin. Microbiol.* **12**, 394–400 (2009).
299. Zhang, M., Joyce, B. R., Sullivan, W. J. & Nussenzweig, V. Translational control in Plasmodium and toxoplasma parasites. *Eukaryot. Cell* **12**, 161–167 (2013).
300. Zhang, M. *et al.* The Plasmodium eukaryotic initiation factor-2 α kinase IK2 controls the latency of sporozoites in the mosquito salivary glands. *J. Exp. Med.* **207**, 1465–1474 (2010).
301. Wakula, P. *et al.* The translation initiation factor eIF2 β is an interactor of protein phosphatase-1. *Biochem. J.* **400**, 377–383 (2006).
302. Wakula, P., Beullens, M., Ceulemans, H., Stalmans, W. & Bollen, M. Degeneracy and function of the ubiquitous RVXF motif that mediates binding to protein phosphatase-1. *J. Biol. Chem.* **278**, 18817–18823 (2003).
303. Holcik, M. & Sonenberg, N. Translational control in stress and apoptosis. *Nat. Rev. Mol. Cell Biol.* **6**, 318–327 (2005).
304. Combe, A. *et al.* Clonal conditional mutagenesis in malaria parasites. *Cell Host Microbe* **5**, 386–396 (2009).
305. Hu, G. *et al.* Transcriptional profiling of growth perturbations of the human malaria parasite *Plasmodium falciparum*. *Nat. Biotechnol.* **28**, 91–98 (2010).
306. Bozdech, Z. *et al.* The Transcriptome of the Intraerythrocytic Developmental Cycle of *Plasmodium falciparum*. *PLoS Biol.* **1**, e5 (2003).
307. Yokoyama, D. *et al.* Modulation of the growth of *Plasmodium falciparum* in vitro by protein serine/threonine phosphatase inhibitors. *Biochem. Biophys. Res. Commun.* **247**, 18–23 (1998).
308. Kumar, R., Adams, B., Oldenburg, A., Musiyenko, A. & Barik, S. Characterisation and expression of a PP1 serine/threonine protein phosphatase (PfPP1) from the malaria parasite, *Plasmodium falciparum*: demonstration of its essential role using RNA interference. *Malar. J.* **1**, 5 (2002).
309. Bhattacharyya, M. K., Hong, Z., Kongkasuriyachai, D. & Kumar, N. *Plasmodium falciparum* protein phosphatase type 1 functionally complements a *glc7* mutant in *Saccharomyces cerevisiae*. *Int. J. Parasitol.* **32**, 739–747 (2002).
310. Guttery, D. *et al.* Genome-wide Functional Analysis of Plasmodium Protein Phosphatases Reveals Key Regulators of Parasite Development and Differentiation. *Cell Host Microbe* **16**, 128–140 (2014).
311. Blisnick, T., Vincensini, L., Barale, J. C., Namane, A. & Braun Breton, C. LANCL1, an erythrocyte protein recruited to the Maurer's clefts during *Plasmodium falciparum* development. *Mol. Biochem. Parasitol.* **141**, 39–47 (2005).
312. Sidik, S. M. *et al.* A Genome-wide CRISPR Screen in *Toxoplasma* Identifies Essential Apicomplexan Genes. *Cell* **166**, 1423–1435.e12 (2016).
313. Yanagida, M., Kinoshita, N., Stone, E. M. & Yamano, H. Protein phosphatases and cell division cycle control. *Ciba Found. Symp.* **170**, 130–140; discussion 140–146 (1992).
314. Ceulemans, H. *et al.* Binding of the concave surface of the Sds22 superhelix to the α 4/ α 5/ α 6-triangle of protein phosphatase-1. *J. Biol. Chem.* **277**, 47331–47337 (2002).
315. Pfeuty, B., Bodart, J.-F., Blossey, R. & Lefranc, M. A dynamical model of oocyte maturation unveils precisely orchestrated meiotic decisions. *PLoS Comput. Biol.* **8**, e1002329 (2012).

316. Wang, W., Stukenberg, P. T. & Brautigan, D. L. Phosphatase inhibitor-2 balances protein phosphatase 1 and aurora B kinase for chromosome segregation and cytokinesis in human retinal epithelial cells. *Mol. Biol. Cell* **19**, 4852–4862 (2008).
317. Li, M., Satinover, D. L. & Brautigan, D. L. Phosphorylation and functions of inhibitor-2 family of proteins. *Biochemistry* **46**, 2380–2389 (2007).
318. Wang, W., Cronmiller, C. & Brautigan, D. L. Maternal phosphatase inhibitor-2 is required for proper chromosome segregation and mitotic synchrony during *Drosophila* embryogenesis. *Genetics* **179**, 1823–1833 (2008).
319. Pakos-Zebrucka, K. *et al.* The integrated stress response. *EMBO Rep.* **17**, 1374–1395 (2016).
320. Novoa, I., Zeng, H., Harding, H. P. & Ron, D. Feedback inhibition of the unfolded protein response by GADD34-mediated dephosphorylation of eIF2alpha. *J. Cell Biol.* **153**, 1011–1022 (2001).
321. Anand, S. S. & Babu, P. P. Endoplasmic reticulum stress and neurodegeneration in experimental cerebral malaria. *Neurosignals* **21**, 99–111 (2013).
322. Inácio, P. *et al.* Parasite-induced ER stress response in hepatocytes facilitates *Plasmodium* liver stage infection. *EMBO Rep.* **16**, 955–964 (2015).
323. Hollin, T., De Witte, C., Lenne, A., Pierrot, C. & Khalife, J. Analysis of the interactome of the Ser/Thr Protein Phosphatase type 1 in *Plasmodium falciparum*. *BMC Genomics* **17**, (2016).
324. LaCount, D. J. *et al.* A protein interaction network of the malaria parasite *Plasmodium falciparum*. *Nature* **438**, 103–107 (2005).
325. Lenne, A. *et al.* Characterization of a Protein Phosphatase Type-1 and a Kinase Anchoring Protein in *Plasmodium falciparum*. *Front. Microbiol.* **9**, 2617 (2018).
326. Guttery, D. *et al.* Genome-wide Functional Analysis of *Plasmodium* Protein Phosphatases Reveals Key Regulators of Parasite Development and Differentiation. *Cell Host Microbe* **16**, 128–140 (2014).
327. Schwach, F. *et al.* PlasmoGEM, a database supporting a community resource for large-scale experimental genetics in malaria parasites. *Nucleic Acids Res.* **43**, D1176–D1182 (2015).
328. Sidik, S. M. *et al.* A Genome-wide CRISPR Screen in *Toxoplasma* Identifies Essential Apicomplexan Genes. *Cell* **166**, 1423–1435.e12 (2016).
329. Zhang, M. *et al.* Uncovering the essential genes of the human malaria parasite *Plasmodium falciparum* by saturation mutagenesis. *Science* **360**, eaap7847 (2018).
330. PlasmoGEM phenotypes. Available at: <https://plasmogem.sanger.ac.uk/phenotypes>. (Accessed: 6th September 2018)
331. PlasmoDB : The *Plasmodium* Genomics Resource. Available at: <http://plasmodb.org/plasmo/>. (Accessed: 22nd November 2018)
332. Kumar, R. *et al.* A zinc-binding dual-specificity YVH1 phosphatase in the malaria parasite, *Plasmodium falciparum*, and its interaction with the nuclear protein, pescadillo. *Mol. Biochem. Parasitol.* **133**, 297–310 (2004).
333. Pendyala, P. R. *et al.* Characterization of a PRL protein tyrosine phosphatase from *Plasmodium falciparum*☆. *Mol. Biochem. Parasitol.* **158**, 1–10 (2008).
334. Lodoen, M. B., Gerke, C. & Boothroyd, J. C. A highly sensitive FRET-based approach reveals secretion of the actin-binding protein toxofilin during *Toxoplasma gondii* infection. *Cell. Microbiol.* **12**, 55–66 (2010).
335. Garcia, A., Cayla, X., Barik, S. & Langsley, G. A family of PP2 phosphatases in *Plasmodium falciparum* and parasitic protozoa. *Parasitol. Today Pers. Ed* **15**, 90–92 (1999).
336. Glushakova, S. *et al.* Cytoplasmic free Ca²⁺ is essential for multiple steps in malaria parasite egress from infected erythrocytes. *Malar. J.* **12**, 41 (2013).
337. Singh, S., Alam, M. M., Pal-Bhowmick, I., Brzostowski, J. A. & Chitnis, C. E. Distinct external signals trigger sequential release of apical organelles during erythrocyte invasion by malaria parasites. *PLoS Pathog.* **6**, e1000746 (2010).
338. Brochet, M. *et al.* Phosphoinositide metabolism links cGMP-dependent protein kinase G to essential Ca²⁺ signals at key decision points in the life cycle of malaria parasites. *PLoS Biol.* **12**, e1001806 (2014).

339. Moorhead, G. B. G., De Wever, V., Templeton, G. & Kerk, D. Evolution of protein phosphatases in plants and animals. *Biochem. J.* **417**, 401–409 (2009).
340. Yokoyama, D. *et al.* Modulation of the Growth of *Plasmodium falciparum* in Vitro by Protein Serine/Threonine Phosphatase Inhibitors. *Biochem. Biophys. Res. Commun.* **247**, 18–23 (1998).
341. Kumar, R., Adams, B., Oldenburg, A., Musiyenko, A. & Barik, S. Characterisation and expression of a PP1 serine/threonine protein phosphatase (PfPP1) from the malaria parasite, *Plasmodium falciparum*: demonstration of its essential role using RNA interference. *Malar. J.* **1**, 5 (2002).
342. Fr?ville, A. *et al.* *Plasmodium falciparum* Inhibitor-3 Homolog Increases Protein Phosphatase Type 1 Activity and Is Essential for Parasitic Survival. *J. Biol. Chem.* **287**, 1306–1321 (2012).
343. Tellier, G. *et al.* Identification of *Plasmodium falciparum* Translation Initiation eIF2 β Subunit: Direct Interaction with Protein Phosphatase Type 1. *Front. Microbiol.* **7**, 777 (2016).
344. Prommana, P. *et al.* Inducible knockdown of *Plasmodium* gene expression using the glmS ribozyme. *PLoS One* **8**, e73783 (2013).
345. Milewski, S. Glucosamine-6-phosphate synthase--the multi-facets enzyme. *Biochim. Biophys. Acta* **1597**, 173–192 (2002).
346. Winkler, W. C., Nahvi, A., Roth, A., Collins, J. A. & Breaker, R. R. Control of gene expression by a natural metabolite-responsive ribozyme. *Nature* **428**, 281–286 (2004).
347. Watson, P. Y. & Fedor, M. J. The glmS riboswitch integrates signals from activating and inhibitory metabolites in vivo. *Nat. Struct. Mol. Biol.* **18**, 359–363 (2011).
348. Ghorbal, M. *et al.* Genome editing in the human malaria parasite *Plasmodium falciparum* using the CRISPR-Cas9 system. *Nat. Biotechnol.* **32**, 819–821 (2014).
349. Ito, D., Schureck, M. A. & Desai, S. A. An essential dual-function complex mediates erythrocyte invasion and channel-mediated nutrient uptake in malaria parasites. *eLife* **6**, (2017).
350. Jones, M. L. *et al.* A versatile strategy for rapid conditional genome engineering using loxP sites in a small synthetic intron in *Plasmodium falciparum*. *Sci. Rep.* **6**, (2016).
351. Helps, N. R. *et al.* Protein phosphatase 4 is an essential enzyme required for organisation of microtubules at centrosomes in *Drosophila* embryos. *J. Cell Sci.* **111 (Pt 10)**, 1331–1340 (1998).
352. Cohen, P. T. W., Philp, A. & Vázquez-Martin, C. Protein phosphatase 4--from obscurity to vital functions. *FEBS Lett.* **579**, 3278–3286 (2005).
353. Molecular Biology of the Cell – Bruce Alberts. Available at: <https://brucealberts.ucsf.edu/current-projects/molecular-biology-of-the-cell/>. (Accessed: 10th September 2018)
354. Andreeva, A. V. & Kutuzov, M. A. PPEF/PP7 protein Ser/Thr phosphatases. *Cell. Mol. Life Sci. CMLS* **66**, 3103–3110 (2009).
355. Vinós, J., Jalink, K., Hardy, R. W., Britt, S. G. & Zuker, C. S. A G protein-coupled receptor phosphatase required for rhodopsin function. *Science* **277**, 687–690 (1997).
356. Mills, E., Price, H. P., Johnner, A., Emerson, J. E. & Smith, D. F. Kinetoplastid PPEF phosphatases: dual acylated proteins expressed in the endomembrane system of *Leishmania*. *Mol. Biochem. Parasitol.* **152**, 22–34 (2007).
357. Xie, Y. *et al.* GPS-Lipid: a robust tool for the prediction of multiple lipid modification sites. *Sci. Rep.* **6**, 28249 (2016).
358. GPS-Lipid - Prediction of Lipid Modifications (S-Palmitoylation, N-Myristoylation, S-Farnesylation, S-Geranylgeranylation). Available at: <http://lipid.biocuckoo.org/>. (Accessed: 18th September 2018)
359. Kumar, P. *et al.* Regulation of *Plasmodium falciparum* development by calcium-dependent protein kinase 7 (PfCDPK7). *J. Biol. Chem.* **289**, 20386–20395 (2014).
360. Fang, H. *et al.* Multiple short windows of calcium-dependent protein kinase 4 activity coordinate distinct cell cycle events during *Plasmodium* gametogenesis. *eLife* **6**, (2017).
361. Labib, K. How do Cdc7 and cyclin-dependent kinases trigger the initiation of chromosome replication in eukaryotic cells? *Genes Dev.* **24**, 1208–1219 (2010).
362. Georgescu, R. *et al.* Structure of eukaryotic CMG helicase at a replication fork and implications to replisome architecture and origin initiation. *Proc. Natl. Acad. Sci. U. S. A.* **114**, E697–E706 (2017).

363. Ansari, A. & Tuteja, R. Genome wide comparative comprehensive analysis of Plasmodium falciparum MCM family with human host. *Commun. Integr. Biol.* **5**, 607–615 (2012).
364. Mitra, P., Banu, K., Deshmukh, A. S., Subbarao, N. & Dhar, S. K. Functional dissection of proliferating-cell nuclear antigens (1 and 2) in human malarial parasite Plasmodium falciparum: possible involvement in DNA replication and DNA damage response. *Biochem. J.* **470**, 115–129 (2015).
365. White, J. H. & Kilbey, B. J. DNA replication in the malaria parasite. *Parasitol. Today Pers. Ed* **12**, 151–155 (1996).
366. Gupta, A., Mehra, P. & Dhar, S. K. Plasmodium falciparum origin recognition complex subunit 5: functional characterization and role in DNA replication foci formation. *Mol. Microbiol.* **69**, 646–665 (2008).
367. Sharma, R., Sharma, B., Gupta, A. & Dhar, S. K. Identification of a novel trafficking pathway exporting a replication protein, Orc2 to nucleus via classical secretory pathway in Plasmodium falciparum. *Biochim. Biophys. Acta* **1865**, 817–829 (2018).
368. Schrével, J., Asfaux-Foucher, G. & Bafort, J. M. [Ultrastructural study of multiple mitoses during sporogony of Plasmodium b. berghei]. *J. Ultrastruct. Res.* **59**, 332–350 (1977).
369. Vickerman, K. & Cox, E. E. G. Merozoite formation in the erythrocytic stages of the malaria parasite plasmodium vinckei. *Trans. R. Soc. Trop. Med. Hyg.* **61**, 303–312 (1967).
370. Knuepfer, E., Napiorkowska, M., van Ooij, C. & Holder, A. A. Generating conditional gene knockouts in Plasmodium – a toolkit to produce stable DiCre recombinase-expressing parasite lines using CRISPR/Cas9. *Sci. Rep.* **7**, (2017).
371. Hale, V. L. *et al.* Parasitophorous vacuole poration precedes its rupture and rapid host erythrocyte cytoskeleton collapse in Plasmodium falciparum egress. *Proc. Natl. Acad. Sci. U. S. A.* **114**, 3439–3444 (2017).
372. DePamphilis, M. L. *et al.* Regulating the licensing of DNA replication origins in metazoa. *Curr. Opin. Cell Biol.* **18**, 231–239 (2006).
373. Méndez, J. *et al.* Human origin recognition complex large subunit is degraded by ubiquitin-mediated proteolysis after initiation of DNA replication. *Mol. Cell* **9**, 481–491 (2002).
374. Lee, K. Y. *et al.* Phosphorylation of ORC2 protein dissociates origin recognition complex from chromatin and replication origins. *J. Biol. Chem.* **287**, 11891–11898 (2012).
375. Lee, K. Y., Bae, J. S., Kim, G. S. & Hwang, D. S. Protein phosphatase 1 dephosphorylates Orc2. *Biochem. Biophys. Res. Commun.* **447**, 437–440 (2014).
376. Mehra, P. *et al.* Expression and characterization of human malaria parasite Plasmodium falciparum origin recognition complex subunit 1. *Biochem. Biophys. Res. Commun.* **337**, 955–966 (2005).
377. Poh, W. T., Chadha, G. S., Gillespie, P. J., Kaldis, P. & Blow, J. J. Xenopus Cdc7 executes its essential function early in S phase and is counteracted by checkpoint-regulated protein phosphatase 1. *Open Biol.* **4**, 130138 (2014).
378. Hiraga, S.-I. *et al.* Rif1 controls DNA replication by directing Protein Phosphatase 1 to reverse Cdc7-mediated phosphorylation of the MCM complex. *Genes Dev.* **28**, 372–383 (2014).
379. Mattarocci, S. *et al.* Rif1 Controls DNA Replication Timing in Yeast through the PP1 Phosphatase Glc7. *Cell Rep.* **7**, 62–69 (2014).
380. Hiraga, S.-I. *et al.* Human RIF1 and protein phosphatase 1 stimulate DNA replication origin licensing but suppress origin activation. *EMBO Rep.* **18**, 403–419 (2017).
381. Tung, H. Y., Wang, W. & Chan, C. S. Regulation of chromosome segregation by Glc8p, a structural homolog of mammalian inhibitor 2 that functions as both an activator and an inhibitor of yeast protein phosphatase 1. *Mol. Cell. Biol.* **15**, 6064–6074 (1995).
382. Wang, W., Cronmiller, C. & Brautigan, D. L. Maternal phosphatase inhibitor-2 is required for proper chromosome segregation and mitotic synchrony during Drosophila embryogenesis. *Genetics* **179**, 1823–1833 (2008).
383. Alam, M. M. *et al.* Phosphoproteomics reveals malaria parasite Protein Kinase G as a signalling hub regulating egress and invasion. *Nat. Commun.* **6**, 7285 (2015).

384. Saul, A., Myler, P., Elliott, T. & Kidson, C. Purification of mature schizonts of *Plasmodium falciparum* on colloidal silica gradients. *Bull. World Health Organ.* **60**, 755–759 (1982).
385. Lambros, C. & Vanderberg, J. P. Synchronization of *Plasmodium falciparum* erythrocytic stages in culture. *J. Parasitol.* **65**, 418–420 (1979).
386. Deveuve, Q., Lesage, K., Mouveaux, T. & Gissot, M. The *Toxoplasma gondii* inhibitor-2 regulates protein phosphatase 1 activity through multiple motifs. *Parasitol. Res.* **116**, 2417–2426 (2017).
387. Delorme, V., Garcia, A., Cayla, X. & Tardieux, I. A role for *Toxoplasma gondii* type 1 ser/thr protein phosphatase in host cell invasion. *Microbes Infect.* **4**, 271–278 (2002).
388. Inselburg, J. & Banyal, H. S. Synthesis of DNA during the asexual cycle of *Plasmodium falciparum* in culture. *Mol. Biochem. Parasitol.* (1984).
389. Ruecker, A. *et al.* Proteolytic activation of the essential parasitophorous vacuole cysteine protease SERA6 accompanies malaria parasite egress from its host erythrocyte. *J. Biol. Chem.* **287**, 37949–37963 (2012).
390. Kariuki, M. M., Li, X., Yamodo, I., Chishti, A. H. & Oh, S. S. Two *Plasmodium falciparum* merozoite proteins binding to erythrocyte band 3 form a direct complex. *Biochem. Biophys. Res. Commun.* **338**, 1690–1695 (2005).
391. Li, X. *et al.* A co-ligand complex anchors *Plasmodium falciparum* merozoites to the erythrocyte invasion receptor band 3. *J. Biol. Chem.* **279**, 5765–5771 (2004).
392. Weber, J. L. *et al.* Primary structure of a *Plasmodium falciparum* malaria antigen located at the merozoite surface and within the parasitophorous vacuole. *J. Biol. Chem.* **263**, 11421–11425 (1988).
393. Huynh, M.-H. & Carruthers, V. B. Tagging of endogenous genes in a *Toxoplasma gondii* strain lacking Ku80. *Eukaryot. Cell* **8**, 530–539 (2009).
394. Ghorbal, M. *et al.* Genome editing in the human malaria parasite *Plasmodium falciparum* using the CRISPR-Cas9 system. *Nat. Biotechnol.* **32**, 819–821 (2014).
395. Przyborski, J. M. *et al.* Trafficking of STEVOR to the Maurer’s clefts in *Plasmodium falciparum*-infected erythrocytes. *EMBO J.* **24**, 2306–2317 (2005).
396. Pasvol, G., Wilson, R. J., Smalley, M. E. & Brown, J. Separation of viable schizont-infected red cells of *Plasmodium falciparum* from human blood. *Ann. Trop. Med. Parasitol.* **72**, 87–88 (1978).
397. Crabb, B. S. & Cowman, A. F. Characterization of promoters and stable transfection by homologous and nonhomologous recombination in *Plasmodium falciparum*. *Proc. Natl. Acad. Sci. U. S. A.* **93**, 7289–7294 (1996).
398. Taylor, H. M. *et al.* The Malaria Parasite Cyclic GMP-Dependent Protein Kinase Plays a Central Role in Blood-Stage Schizogony. *Eukaryot. Cell* **9**, 37–45 (2010).
399. Collins, C. R. *et al.* Malaria Parasite cGMP-dependent Protein Kinase Regulates Blood Stage Merozoite Secretory Organelle Discharge and Egress. *PLoS Pathog.* **9**, e1003344 (2013).
400. Paul, A. *et al.* Parasite Calcineurin Regulates Host Cell Recognition and Attachment by Apicomplexans. *Cell Host Microbe* **18**, 49–60 (2015).
401. McConnell, J. L. & Wadzinski, B. E. Targeting protein serine/threonine phosphatases for drug development. *Mol. Pharmacol.* **75**, 1249–1261 (2009).
402. Alonso, A. *et al.* Protein tyrosine phosphatases in the human genome. *Cell* **117**, 699–711 (2004).
403. Jan, G. *et al.* A *Toxoplasma* type 2C serine-threonine phosphatase is involved in parasite growth in the mammalian host cell. *Microbes Infect.* **11**, 935–945 (2009).
404. Engelberg, K. *et al.* A MORN1-associated HAD phosphatase in the basal complex is essential for *Toxoplasma gondii* daughter budding. *Cell. Microbiol.* **18**, 1153–1171 (2016).
405. Delorme, V., Cayla, X., Faure, G., Garcia, A. & Tardieux, I. Actin dynamics is controlled by a casein kinase II and phosphatase 2C interplay on *Toxoplasma gondii* Toxofilin. *Mol. Biol. Cell* **14**, 1900–1912 (2003).
406. Blanchetot, C., Chagnon, M., Dubé, N., Hallé, M. & Tremblay, M. L. Substrate-trapping techniques in the identification of cellular PTP targets. *Methods San Diego Calif* **35**, 44–53 (2005).
407. Lourido, S., Jeschke, G. R., Turk, B. E. & Sibley, L. D. Exploiting the unique ATP-binding pocket of *toxoplasma* calcium-dependent protein kinase 1 to identify its substrates. *ACS Chem. Biol.* **8**, 1155–1162 (2013).

408. Pease, B. N. *et al.* Characterization of Plasmodium falciparum Atypical Kinase PfPK7-Dependent Phosphoproteome. *J. Proteome Res.* **17**, 2112–2123 (2018).
409. Jin, J. & Pawson, T. Modular evolution of phosphorylation-based signalling systems. *Philos. Trans. R. Soc. Lond. B. Biol. Sci.* **367**, 2540–2555 (2012).

Summary

Plasmodium falciparum, the etiologic agent of malaria, is an obligate intracellular parasite of the Apicomplexa phylum that is responsible for 445000 deaths annually. *Plasmodium* development in human red blood cells (RBCs) corresponds to the symptomatic phase of the disease. It starts by the active penetration of the host cell by the invasive form named merozoite, followed by the parasite multiplication in a process called schizogony to form 16-32 new merozoites that are released from the RBC (egress step) and start a new cycle. During its 48h intra-erythrocytic development, this parasite uses reversible protein phosphorylation to regulate invasion, schizogony as well as egress, but our current knowledge on the contribution of parasite phosphatases in these cellular events is still very poor.

The objective of my thesis was to identify and functionally characterize phosphatases potentially involved in egress or invasion during *P. falciparum* RBC cycle. I focused my work on 4 of them, namely PP1, PP4, PP7 and Shelph2, on the basis of their late transcriptional expression profile during the intra-erythrocytic cycle, as this profile matches the timing of these two essential events. The first part of this study is dedicated to the functional characterization of Shelph2, a phosphatase of bacterial origin. By reverse genetics using CRISPR-Cas9 strategy, we endogenously tagged the gene, and showed that Shelph2 is stored in apical vesicles in the developing merozoites. We also demonstrated that it is dispensable for parasite RBC development, as the deletion of the gene did not affect invasion, parasite multiplication nor egress, suggesting possible functional redundancy with other parasite phosphatases.

In the second part of this work, we aimed to describe the roles of PP1, PP4 and PP7. As they were described as likely essential, we set up in the laboratory a conditional knock-down strategy named the *glmS* ribozyme, with the idea of destabilizing the mRNA following self-cleavage of the ribozyme upon metabolite addition, here glucosamine. We successfully introduced the *glmS* sequence in 3' of the genes of interest for PP4 and PP7 but we did not observe any significant protein depletion upon glucosamine addition, thus preventing us to use these lines to study PP4 and PP7 functions. Yet, these engineered parasite lines were used to analyze the subcellular localization of these phosphatases. As an alternative to the ribozyme, we used an inducible knock-out (iKO) approach based on a dimerizable Cre recombinase (DiCre system) that excises DNA fragments located between two *loxP* sites. We established two parasite lines, the iKO-PP7 that has not been further characterized and the iKO-PP1 strain. Using the iKO-PP1 parasites, we showed that PP1 is predominantly a cytosolic phosphatase mostly expressed during schizogony. Furthermore, the inducible excision of PP1 gene at two different time points of *P. falciparum* RBC cycle permitted us to reveal that PP1 plays two essential roles, one during schizogony and the other one at the time of parasite egress. This is to our knowledge the first description of a parasite phosphatase required for these developmental steps.

Key words: Malaria, *Plasmodium falciparum*, phosphatases, egress, schizogony

Résumé

Plasmodium falciparum, l'agent étiologique du paludisme, est un parasite intracellulaire obligatoire du phylum des Apicomplexa, responsable de 445 000 décès par an. Le développement de *Plasmodium* dans les globules rouges (GRs) humains correspond à la phase symptomatique de la maladie. Il commence par la pénétration active de la cellule hôte par la forme invasive nommée mérozoïte, suivie par la multiplication du parasite dans un processus appelé schizogonie pour former 16 à 32 nouveaux mérozoïtes qui sont alors libérés des GRs (étape de sortie) et peuvent alors initier un nouveau cycle. Au cours de son développement intra-érythrocytaire de 48h, ce parasite utilise la phosphorylation réversible de protéines pour réguler les étapes d'invasion, de schizogonie et de sortie du GR, mais nos connaissances actuelles sur la contribution des phosphatases parasitaires dans ces mécanismes demeurent très incomplètes.

L'objectif de ma thèse était d'identifier et de caractériser des phosphatases potentiellement impliquées dans la sortie ou l'invasion des GRs par *P. falciparum*. J'ai centré mon travail sur 4 d'entre elles, à savoir PP1, PP4, PP7 et Shelph2, sur la base de leur profil d'expression transcriptionnelle tardive au cours du cycle intra-érythrocytaire, qui correspond à ces deux événements cellulaires. La première partie de cette étude est consacrée à la caractérisation fonctionnelle de Shelph2, une phosphatase d'origine bactérienne. Par génétique inverse utilisant la stratégie CRISPR-Cas9, nous avons étiqueté le gène au locus endogène et montré que Shelph2 est stockée dans des vésicules apicales des mérozoïtes en formation. Nous avons également démontré que cette phosphatase n'est pas essentielle pour le développement intra-érythrocytaire du parasite dans les GRs car la délétion du gène n'affecte pas les étapes d'invasion, de multiplication des parasites ou de leur sortie des GRs, ce qui suggère la possibilité d'une redondance fonctionnelle avec d'autres phosphatases parasitaires.

Dans la deuxième partie de ce travail, nous avons cherché à décrire les rôles de PP1, PP4 et PP7. Les gènes codant pour ces enzymes étant décrits comme probablement essentiels, nous avons mis en place au laboratoire une stratégie de knock-down conditionnel (ribozyme *glmS*), avec l'idée de déstabiliser l'ARNm après auto-clivage du ribozyme lors de l'addition d'un métabolite, ici la glucosamine. Nous avons introduit avec succès la séquence *glmS* en 3' des gènes d'intérêt pour PP4 et PP7, mais nous n'avons pas observé de déplétion protéique significative lors de l'addition de glucosamine, empêchant d'utiliser ces lignées pour étudier les fonctions de PP4 et PP7. Cependant, ces lignées parasitaires modifiées ont été utilisées pour analyser la localisation subcellulaire de ces phosphatases. Comme alternative au ribozyme, nous avons utilisé une approche de knock-out inducible (iKO) basée sur une recombinaise Cre dimérisable (système DiCre) qui excise des fragments d'ADN situés entre deux sites *loxP*. Nous avons établi deux lignées de parasites, iKO-PP7 qui n'a pas encore été caractérisée et la souche iKO-PP1. En utilisant les parasites iKO-PP1, nous avons montré que PP1 était principalement une phosphatase cytosolique majoritairement exprimée au stade schizontes. De plus, l'excision inducible du gène *PP1* à deux moments différents du cycle érythrocytaire de *P. falciparum* nous a permis de révéler que PP1 joue deux rôles essentiels, l'un pendant la schizogonie et l'autre au moment de la sortie du parasite. A notre connaissance, ce travail représente la première description d'une phosphatase parasitaire requise pour ces étapes du développement asexué de *P. falciparum*.

Mots clés : Paludisme, *Plasmodium falciparum*, phosphatases, egress, schizogonie